MODELLING AND OPTIMISATION

OF

MDF HOT PRESSING

A thesis

submitted in partial fulfilment

of the requirements for the degree

of

Doctor of Philosophy

in

Chemical and Process Engineering

by

Arun Gupta

UNIVERSITY OF CANTERBURY

2007

Addendum

Acknowledgement of Authorship: I confirm that there is work in this thesis, on pages 10-20; 30; 33-34; 67-68; 81-82; 105-106; 108; 158; 160; and 162 – 163, that has been copied from two other sources and the authorship of this work has not been adequately attributed to the appropriate author.

The two Authors of the excerpts outlined above and included in this work are:

- Professor Heiko Thoemen, in his own PHD Thesis entitled “Modelling the Physical Processes in Natural Fibre Composites During Batch and Continuous Pressing”; and
- Dr Balazs G Zombori’s PHD Thesis entitled “Modelling the Transient Effects during the Hot-Pressing of Wood-Based Composites”;

I would further like to formally apologise for this oversight in attribution at the time of submitting my PHD Thesis in 2007 and acknowledge the contribution of the abovenamed academics to the rationale employed in my own research.

I further confirm that any fault which resulted in this error lies solely with me, and my limited understanding of the referencing requirements which applied at the time of submission. It was not my intention at any point to claim credit for work I had not done and I would therefore acknowledge the valuable contributions of all the researchers referred to in my thesis and confirm my sincere appreciation of their contribution in developing the mathematical model employed.

Dr Arun Gupta.
April 2023

Abstract

There are four big medium density fibreboard (MDF) plants in New Zealand with a total production capacity of close to one million cubic meters per year. A significant quantity of boards (nearly 3% or about 30,000 cubic meters per year) is rejected due to defects such as weak core, low modulus of rupture and elasticity, low internal bonding and delamination. The main cause of these defects, is lack of complete understanding of the inter relationship during the hot-pressing stage between the initial inputs such as temperature, moisture content, platen pressure and its impact on the properties of boards. The best solution is to develop a mathematical model to assist in understanding these relationships and to solve the equations in the model by using advanced software. This will reduce the number of expensive experiments and will enable us to see some of the parameters, which are otherwise difficult to visualise.

Several earlier researchers have tried to model hot pressing of wood composites, mostly either for particle board or oriented strand board (OSB), and only a few are for MDF. The type of numerical methods used to solve the model equations and various assumptions, changes from one investigator to the other. The non-availability of source code to convert the mathematical equations into programme, is one of the reasons for this model development. To improve the productivity of MDF plants in New Zealand, there was a need to develop a computer programme which can include all the latest findings and can remove the defects which are present in earlier models.

This model attempts a more complete integration than in the previous models of all the components such as heat transfer, moisture movement and vertical density profile formation in a one-dimensional model of hot pressing of MDF. One of the important features added in the heat and mass transfer part of the model is that the equilibrium moisture content (EMC) equation given for solid wood was modified to be applicable for the MDF fibres. In addition, this EMC equation can cover the complete range of hot pressing temperature from 160ºC to 200ºC. The changes in fibre moisture content due to bound water diffusion, which was were earlier neglected, was considered. The resin curing reactions for phenol formaldehyde and urea formaldehyde resins are also incorporated into the model, with the energy and water released during the curing reaction being included in the energy and mass balances.

The validation of the heat and mass transfer model was done by comparing the values of core temperature and core pressure from the model and the experiments. The experimental value of core pressure and core temperature is obtained by putting a thermocouple and pressure transducer in the middle of the mat. The experimental core temperature results show qualitative agreement with the predicted results. In the beginning, the core temperatures from both experiment and model overlap each other. In the middle of the press cycle, the experimental core temperature is higher by 10ºC and by the end the difference decreases to 5ºC.

The vertical density profile (VDP) is a critical determining factor for the strength and quality of MDF panels. The earlier concept of ratio of modulus of elasticity of the layer to the sum of modulus of elasticity of all the layers in the previous time step, given by Suo and Bowyer (1994), is refined with the latest published findings. The equation given by Carvalho et al. (2001) is used to calculate the MOE of different layers of the mat. The differential equation of a Maxwell element given by Zombori (2001) is used to measure stress, nonlinear strain function and relaxation of fibres. The model gives good agreement of peak and core density at lower platen temperature at 160ºC but with the increase of platen temperature to 198ºC, the rise in peak density is comparatively higher. There is a distinct increase in predicted peak density by 150 kg/m^3 in comparison to the experimental result, where the increase is only by 10 kg/m^3. There is a large decline (50 kg/m^3) in core density in the experimental results in comparison to only a slight decline (13 kg/m^3) in the predicted results.

The use of Matlab provides a very convenient platform for producing graphical results. The time of computation at present is nearly 20 hrs in a personal computer with Pentium four processor and one GB RAM. The model can predict properties of a pressed board for the standard manufacturing conditions and also the new hot pressing technologies such as the use of steam injection or a cooling zone in the continuous press. A comparative study has been done to show the advantages of using new hot pressing technology. The present model will become an important tool in the hands of wood technologist, process engineers and MDF manufacturing personnel, to better understand the internal processes and to improve production and quality of MDF boards.

This theoretical model helped in developing better understanding of internal processes. By using it, we can analyse the impact of platen temperature, moisture content on the core temperature, core pressure and density profile. It gives better insight into the relationship between core pressure and delamination of the board. The model is also able to predict the internal changes in the new hot pressing technologies such as the steam injection pressing and the use of a cooling zone in a continuous press. Using the simulation results, the exact time needed for the complete curing of resin can be calculated and then these results can be applied in the commercial plants. If the pressing time is reduced, then the over all production of both batch press and continuous press will increase.

The second part of the project is the development of an empirical model to correlate the physical properties from the MDF board to the mean density. The empirical model is simple and straightforward, and thus can be applied in commercial operation for control and optimization. The empirical model can predict peak density, core density, and modulus of rupture, elasticity and internal bonding within the limits in which those relationships are derived. The model gives good results for thickness ranging from 10 to 13.5 mm and density ranging from 485 kg/m^3 to 718 kg/m^3.

.

Acknowledgements

I would like to thank my supervisor Dr Pat Jordan and co-supervisor Associate Professor Shusheng Pang for their valuable advice, constructive guidance and constant encouragement in this project. It was a great learning exercise.

Many thanks to Dr Kelvin Chapman for sharing his practical experience with me, to keep always focussed and to solve the industrial problems.

I am very thankful to the CAPE Technical staff, Mr Tony Allen, Mr Bob Gordon, Mr Frank Weerts, Mr Peter Jones and Mr David Brown, for all of the help they provided during this work.

I am thankful to Mr Nigel Pink and Mr Paul Fuller from the Forestry Department and to Carter Holt Harvey Pine Panels for supplying resinated fibres.

I am very thankful for the financial and technical supports received from the New Zealand Government, the University of Canterbury and the Department of Chemical & Process Engineering, University of Canterbury.

I am thankful to my wife Ritu, for the understanding of my long hours of absence from home and my son Aditya, who has to play alone, during my work.

Contents

Modelling the Heat and Mass Transfer during Hot Pressing of MDF

Chapter-5

Experimental Results and Validation of the Heat and Mass Transfer Model

Chapter- 6

Empirical Model to Predict Mechanical Properties from the Mean Density

LIST OF FIGURES

Figures Page

LIST OF TABLES

NOMENCLATURE

The following listed symbols are used in this thesis. Others defined in the appropriate locations in this thesis for one-off use are not included:

A	Reaction constant for phenol formaldehyde resin (s^{-1});
A_o	Initial concentration of methylol groups (mol kg^{-1});
a	Porosity of wood (-);
c	Specific heat of oven dry wood (J $kg^{-1}K^{-1}$);
c_u	Specific heat of wood at a given moisture content (J $kg^{-1}K^{-1}$);
d	Change in thickness in the MDF mat and layers (m);
D	Platen movement (m);
D_{eff}	Effective diffusion coefficient (m^2 s^{-1});
D_{va}	Binary diffusion coefficient in the mixture of water vapour - air (m^2 s^{-1});
D_m	Transverse diffusion coefficient for moisture movement (m^2 s^{-1});
D^j	External mass transfer coefficient at the edge (m s^{-1});
E	Young's modulus of wood (Pa);
E_{act}	Activation energy for urea formaldehyde resin (kJ mol^{-1});
E_{cw}	Young's modulus of the cell wall (Pa);
E_μ	Activation energy for urea formaldehyde viscous component (kJ mol^{-1});
F	Extent of resin curing for the MDF resin (-);
H_v	Latent heat of sorption from vapour state (J kg^{-1});
H_r	Heat evolved from resin curing (J kg^{-1})
i	Number of layer countered from the mat surface;
j	Net vapour flux (kg m^{-2} s^{-1}) ;
k	Reaction rate constant (s^{-1});
k_d	Obstruction factor for molecular diffusion (-);
k_p	Permeability coefficient (m^2);
k_t	Thermal conductivity (W m^{-1} K^{-1});
m	Mass of vapour (kg);
m_{ev}	Evaporation rate (kg m^{-3} s^{-1});
m_r	Rate of resin curing (kg m^{-3} s^{-1});
M	Thickness of mat (m);
M_a	Molecular weight of air (kg mol^{-1});
M_i	Molecular weight of component I (kg mol^{-1});
MC	Moisture content (kg kg^{-1} or *%*);
MC_f	Bound water content (kg kg^{-1} or %)
MMw	Molecular weight of water (kg mol-1);
n	Order of reaction (-);
n	Total number of layers in the MDF mat;
P_{amb}	Total pressure of air in the atmosphere (Pa);
P	Total gas pressure inside the board (Pa);
p_v	Vapour partial pressure (Pa);
p_{sat}	Saturated vapour pressure at given temperature (Pa);
p_{amb}	Vapour partial pressure in the atmosphere air (Pa);
p_a	Air partial pressure inside the board (Pa);
p	Palka constant in MOE modification (-);
p_i	Partial pressure of component i (Pa);
q	Conductive heat flux (J $m^{-2}s^{-1}$);

r	Reaction rate of resin polycondensation (s^{-1});
R	8.37 Gas constant (J mol-1 K-1);
S	Summation of inverse MOE (Pa-1);
t	Time (s);
t′	Reduced time(s);
T	Temperature (K or °C)
Tabs	Absolute temperature (K);
Texp	Temperature of the experiment (K);
u_i	Mass ratio of component i (-);
V	Volume of mat layer (m^{-3});
x	Distance in the mat thickness direction measured from the top mat surfaces (m);

Greek symbols

ε	strain (-)
ε_y	yield strain of the cell wall
η	viscosity (Pa s)
η_a	viscosity of air ($kg/m^2/s$)
κ	viscosity of air (kg/m2/s)
μ	ratio of lateral strain to compressive strain
μr	viscous component of wood resin model (Pa s)
ρ	density (kg m-3)
ρr	relative density
ρr(ε)	relative density function.
σ	stress (Pa)
φ	void fraction (-)
ψ	relative humidity (-)
ψ(ε)	non linear strain function
t̛	time constant (s)

Subscripts

a	air
b	bound water
f	fibre
r	resin
u	at given moisture content
v	vapour
o	initial condition in the beginning
w	wood
ev	evaporation
cond	condensation

Superscripts

a	air
d	diffusion
	convection
edg	edge loss

c

Abbreviations

EMC	equilibrium moisture content
MDF	medium density fibreboard
MOE	modulus of elasticity
MOR	modulus of rupture
IB	internal bonding
OSB	oriented strand board
VDP	vertical density profile

Chapter-1

Project Description

1.1 Introduction:

Since the beginning of industrial wood-based panel manufacture, most research and development efforts have focused on the technical and economical optimization of both processes and products. Performance demands on panels have increased steadily over this period, while minimization of manufacturing costs per unit output was sought simultaneously.

There is a need to optimize the manufacturing parameters. There are two ways to do this, either by experimenting or by developing models simulating the manufacturing process. The limitation of the experimental approach is that the results are valid for only a limited set of parameters and specified raw material. Due to technical advancement and easily available software, it is now possible to develop and solve models that will simulate the formation of the wood-based composite panel under a given set of conditions.

Regarding technological and economic optimization, two major goals of research can be identified. The first goal has been to achieve a better understanding of the factors that influence panel properties and to optimize the panel properties without increasing the pressing time or the production costs. The second goal has been to maximize production speed.

1.1.1 Medium Density Fibreboard (MDF):

MDF is a wood composite that is prepared by mixing wood fibres with thermosetting resin and then hot pressing. The main uses of MDF are in the furniture industry where it is used as a replacement for solid wood. The process of MDF manufacturing is shown in the Figure 1.1

The logs from the forest are first debarked, and then converted into small chips. After that, these chips are screened from sand, dust and other unwanted materials. These

chips are then passed to the preheater by the screw. The main work of the screw is to transfer the chips to the preheater and also to act as a plug to retain steam within the screw conveyor and preheater. In the preheater, the temperature is above 100 degrees Celsius to plasticize the lignin between the cell walls of the fibre. These heated chips then go through the refiner, where they are converted to thin fibres. Thermosetting resin such as Urea-formaldehyde (UF) or Phenol formaldehyde (PF) is added in the blowline. These resinated fibres are first dried to a moisture content of 10 percent and form a thick mat in the mat former area. These mats then enter into the hot press for a few minutes depending upon the thickness. The MDF boards after cooling, trimming and sanding are ready for the market. There are two types of hot pressing followed in the commercial plant, batch pressing and the continuous pressing. The focus of this project is the modelling and simulation of internal changes that are occurring inside the board during hot pressing.

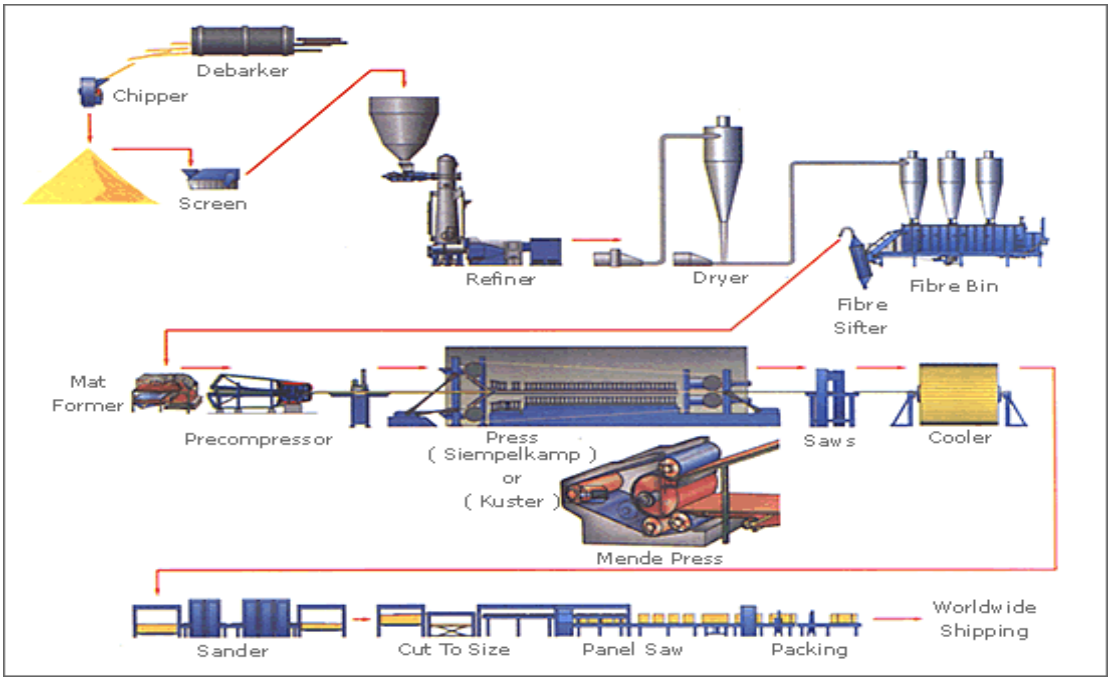

Figure 1.1: MDF manufacturing process (Courtesy- Simplekamp)

Figure 1.2 shows a commercial batch press and Figure 1.3 shows a continuous press.

Figure 1.2: Batch press (Courtesy- MTPL)

Figure 1.3: Continuous hot press (Courtesy- Metso Panel board)

1.1.2 Status of MDF in New Zealand: There are four large MDF plants in New Zealand and the total production capacity is 930 thousand cubic metres per year. The raw material used is radiata pine. New Zealand exports MDF to about 80 countries, and forms the major part of the revenue from the forest products. Forest and

forest based industries form the third major source of income of the New Zealand economy.

Table 1.1 MDF production in New Zealand

SN	Company	Location	Capacity m^3/ year
1	Carter Holt Harvey	Rangiora	220, 000
2	Fletcher Wood Panels Ltd	Taupo	165, 000
3	Nelson Pine Industries	Richmond, Nelson	375, 000
4	Rayonier New Zealand	Mataura	170, 000
	Total		**930,000**

(Source- Wood based Panels International Aug/Sept 2006)

In the competitive international market, it is very important for MDF industries to make high quality MDF board to sustain the export growth.

1.1.3 Main Quality Problems: In commercial production, it is difficult to determine the manufacturing parameters required to produce the desired quality of MDF, particularly when producing a new product or using new operating conditions. A small proportion of boards are rejected due to following defects:

1. Weak core
2. High surface density
3. Low modulus of elasticity (MOE) and rupture (MOR)
4. Low internal bonding
5. High chipping off
6. High water absorption and high dimensional swelling
7. Blisters in the sides and blowing
8. Warping

The primary cause of these defects is the lack of a full understanding of the manufacturing process. To develop a computer model by using advanced software is one of the best solutions, as it will not only decrease the number of expensive

experiments in the laboratory but will also allow us to see some of the parameters, which are otherwise difficult to observe.

1.2 Objectives of the Research:

This PhD project is aimed at developing two computer models to simulate the hot pressing process in the production of medium density fibreboard (MDF). Hot pressing is one of the critical operations during the manufacturing of medium density fibreboard (MDF). In the hot pressing, moisture, mass transfer, heat transfer and fibre densification interact, resulting in continuing changes in the mat physical, chemical and mechanical properties.

Two different approaches to model the hot pressing process of wood based composites can be found in the literature. The first is the empirical modelling approach, which employs statistical methods to link mean density to output parameters, such as mechanical properties of the final product. The second uses fundamental principles to describe the heat and mass transfer and density profile formation in a MDF board.. Both of these approaches are used in this thesis to develop better understanding of MDF hot pressing.

1.2.1 Fundamental Model:

The vertical density profile (VDP) has long been recognised as a critical determining factor for the strength and quality of MDF panels. This has led several previous workers to develop phenomenological models to predict the VDP during hot pressing. The models have included the processes of heat and mass transfer within the mat; rheology of the mat during pressing, including creep; kinetics of resin curing. The objective of this, as with previous models, is to assist in obtaining lower energy consumption, better quality pressed boards and more flexible operation in commercial plants.

This project attempts a more complete integration than hitherto of all these component processes in a one-dimensional model of pressing. The heat and mass

transfer part of the model predicts the moisture content changes, temperature profile, partial vapour pressure and total gas pressure across the thickness during closing of the press, as well as after the final platen position is reached. The correlation used for the calculation of equilibrium moisture content is an improvement over that used in previous models.

This model includes the mat mechanical and rheological properties, varying with moisture content and temperature under pressing force. The simulation will predict stress in the mat, strain and density across the thickness during pressing, using a Maxwell-element model for stress relaxation and visco-elastic properties. The rate of resin cure at the various temperatures in the panel dictates the relative compression at different points during the press closing. The polymerization kinetics of phenol-formaldehyde resin are included in the model to allow prediction of the rate of resin curing, in terms of the amount of polymerization during the hot pressing of MDF boards. The use of Matlab to solve the model equations gives a fast solution while providing a very convenient platform for producing graphical results.

The simulations results were validated by experimental measurements in a pilot press. Twenty two MDF boards were made with different pressing parameters and the data collected were compared with the simulation results from the model. The model could predict in an acceptable way the main variables that control the manufacturing of MDF boards. The simulation results for steam injection pressing and new cooling technology in continuous presses are also generated to increase the understanding of internal processes and to demonstrate the flexibility with which the model can be applied to other boundary conditions.

The fundamental model has incorporated the following behaviour:

(a) **Modelling of Heat and Mass Transfer Phenomena:** The heat and mass transfer part of the model predict the moisture content changes, temperature profile and gaseous pressure within the mat during the hot compression.

(b) **Modelling of Mat Rheology:** The model includes the mat mechanical and rheological properties varying with moisture content and temperature under

pressing force. Thus the model will help to understand the interrelationship between processing parameters and density profile. The mechanical properties of fibres show typical viscoelastic behaviour with time, temperature and moisture dependence.

(c) **Resin Cure:** The rate of resin cure at the various temperatures in the panel determines the amount of heat and water vapour released in the mat. Simulation of the resulting density profile requires incorporation of the temperature-sensitive resin cure rate with the heat and mass transfer and mat rheology equations.

1.2.1 Empirical Model:

The empirical model is used to determine the effects of mat material variables and pressing conditions on important panel properties. These properties include peak and core density, modulus of rupture (MOR), modulus of elasticity (MOE) and internal bonding (IB). The core temperature and internal pressure are also quantified. From the comparison, between the models, different modelling approaches in the field of wood composites are better understood and the advantages and disadvantages of each approach are analysed.

1.3 Research Procedure followed:

The main stages in the project were:

1. First to develop mathematical formulae to relate variables of internal conditions of the mat (temperature, moisture content, and gaseous pressure) to the processing parameters based on heat and mass transfer theories.

2. To model the degree of cure of the adhesive during hot pressing and include the effect of the exothermic reaction on the above mentioned internal conditions of the mat.

3. To calculate the development of the vertical density profile by comparing the viscoelastic behaviour of the mat with the Maxwell element and including the effect of temperature, moisture content and density on the modulus of elasticity of the mat layers.

4. Matlab software was used to solve the mathematical equations and to plot the simulation results.

5. The simulation results were then compared with the experimental results to validate the model

6. The model was then used to develop a better understanding of new pressing technology such as steam injection pressing and having a cooling zone in a continuous press.

1.4 Outcomes of the Project:

The principal outcome of the project is two mathematical models of the hot pressing of MDF that will offer the following benefits:

1. Better understanding of the relationship between the physical and chemical processes taking place during the pressing operation.

2. Understanding and quantification of the effects of process operating conditions on the properties of the MDF panels produced.

3. A flexible means of assessing new operating conditions by modifying the boundary conditions of the model. An example is the use of steam injection pressing and having a cooling zone in the continuous press.

1.5 Structure of the Thesis:

The thesis is divided into seven chapters. The first portion of the second chapter describes the development of the theoretical model of the density profile development before the second portion describes the development of the density profile using an empirical approach.

The third chapter is dedicated to describing the experimental work for validation of the vertical density profile formation. It provides information about the experimental technique such as γ- ray densitometry used to validate the model.

Chapter four discusses the development of the heat and mass transfer model. A one dimensional model is developed that is capable of describing changes of temperature, moisture content, total air pressure and resin curing within the mat. The last section of the chapter contains the simulation results to predict the internal changes inside the mat while following the latest technology of steam injection pressing and having a cooling zone in the continuous press.

Chapter five includes the analysis of experimental results under different pressing conditions and validation of the heat and mass transfer portion of the model.

Chapter six presents the empirical modelling approach. A set of correlation is developed on the basis of experimental results for the physical properties.

Chapter seven summarizes the entire research and discusses the conclusions from the experimental work and considers the future recommendations.

For quick identification, an overall list of figures, tables and symbols is provided at the beginning of this thesis.

1.6 Literature Review:

There are two different parts of modelling MDF pressing. The first part is to model the heat and mass transfer behaviour of the mat and the second is to model the viscoelastic behaviour of the mat. Even though both these operations are taking place simultaneously, they require different types of approach. In this literature review, first the development of heat and mass transfer section will be discussed and then the development of the viscoelastic behaviour; in the last the integration of both the models.

1.6.1 Moisture Movement and Heat Transfer:

Moisture movement and heat transfer within the wood-furnish mat during hot pressing are physical processes that interact with each other and with other mechanisms in a complex way. Even though the complete interactions of moisture movement and heat transfer are not fully understood, still there is a clear understanding of the general concepts involved in it. Many researchers have worked on it (Bolton and Humphrey 1988, Thomen Heiko 2000).

The hot platen is the main source of the heat supply, the water that is in the bound water form and that which is associated with the glue evaporates from the surface, as soon as the hot platen touches the mat surface. This evaporation causes an increase of the vapour pressure in the pore spaces of the outermost layer, and consequently a gas pressure gradient towards the central plane of the mat. A convective vapour flux occurs along this gradient. The vapour carries with it, its heat content. When the vapour reaches a cooler layer in the mat, some of the vapour condenses, and its latent heat is released. A relatively rapid temperature rise in this layer goes along with an increase of the moisture content. Once the moisture content has reached its maximum, the heat that is transferred from the surfaces to this zone by conduction starts to evaporate the moisture. By this sequence the zone of evaporation and condensation moves gradually towards the central plane.

Simultaneously with the described heat and moisture transfer from the surfaces

towards the central plane of the mat, temperature and gas pressure gradients develop within its horizontal plane, and this leads to the escape of heat, moisture and air through the edges.

The temperature development at different locations can be monitored by positioning thermocouples within the loose mat before pressing. This has been done frequently in the laboratory and in the industry for all kinds of press systems.

To determine the internal gas pressure, a thin steel tube that is attached to a pressure transducer can be inserted from the side into the mat. This technique was developed and first reported in the literature by Denisov and Sosnin (1967), and has been used by many researchers and in industrial applications.

1.6.2 Heat Conduction:

Conduction is the heat transfer mechanism in which energy exchange takes place in solids or in fluids at rest (i.e., no convective motion) from the region of high temperature to the region of low temperature. The relationship between heat flow and the temperature gradient is described by Fourier's law

The significance of conductive heat transfer varies with time and space within the mat throughout the pressing. Gefahrt (1977) distinguishes three zones where at least part of the transferred heat is driven by conduction. These zones are the heating platen-mat interface, the outer region between the surface and the vapour front and the inner region of the mat between the vapour front and the central plane.

Heat conduction at the heating platen-mat interface has been described as the major heat transfer by Bowen (1970). The role of radiation is believed to be negligible at the platen-mat interface (Strickler 1959, Humphrey and Bolton 1989a).

Strickler (1959) observed that the compaction pressure influences the temperature development in the central plane of the mat. He concluded from this that the higher compaction pressure increases the heat conduction rate at the interface. However, the effect of the compaction pressure on the core temperature may be conclusively

explained simply by the higher density (and consequently higher thermal conductivity) that was achieved when higher pressures were applied.

Gefahrt (1977) introduced an interfacial heat transfer coefficient to account for poor contact between heating platen and mat. He did not describe from which observation he concluded that the contact must be poor.

Von Haas (1998) pointed out that measurements of the surface temperature are usually done with common thermocouples. These are pressed somewhat into the mat surface, so that the temperature slightly below the surface is measured rather than the actual interfacial temperature.

Once the vapour front has proceeded towards the central plane, heat conduction becomes important again in the outer layers since heat has to be transferred through these layers to the zone of evaporation (Gefahrt 1977, Humphrey and Bolton 1989a).

Shao (1989) herself developed an unsteady-state technique to measure the thermal conductivity of un-resinated wood fibre networks as a function of density and moisture content. Haselein (1998) derived an equation from Shao's (1989) results that gives the thermal conductivity as a function of density and moisture content.

Avramidis and Lau (1992) determined the thermal conductivity of wood particle networks in the density range below 220 kg/m^3, using a modified unsteady-state method and confirmed that the thermal conductivity is usually influenced by density, moisture content and temperature in a positive way.

1.6.3 Gas Convection:

In general terms, convection is of its nature a bulk motion of a liquid or a gas. The transport of the vapour-air mixture as a whole through a wood-furnish mat can be regarded as forced convection, driven by total pressure gradients that develop during pressing.

As the mat is a capillary porous medium with the cell wall substance as matrix and the

inter-linked voids between and within the wood particles as pores, Darcy's law can be applied to describe the cross-sectional and in-plane convective flux. It states that the flux of a viscous fluid (which can be a liquid or a gas) in a porous medium is directly proportional to the pressure difference in the flow direction.

It is reasonable to assume that, on a microscopic level, almost all of the gas flows through the void spaces between the wood particles, rather than through the pore structure within the cell walls, Denisov et al. (1975).

Darcy's law is only valid if the flow is laminar. In the case of turbulent flow, the flow is not proportional to the pressure gradient. Denisov et al (1975) found a slight deviation from linearity for the transit of air through a flake mat. Von Haas et al (1998) confirmed this finding but concluded that this deviation is small enough to enable one to describe convective flow in the mat by Darcy's law. Humphrey and Bolton (1989a) pointed out that turbulent flow may be of some significance in steam injection pressing.

1.6.4 Gas Diffusion:

According to Fick's first law, the diffusive flux j^d is proportional to the concentration gradient *dc/dl* in the flow direction such that;

$$j^d = -D\,(dc/dl)$$

The concentration gradient can be expressed as a gradient of partial pressure, number of moles per unit volume, or moisture content. The obstruction factor for molecular diffusion through a porous material, k_d, introduced by Krischer (1963) can be obtained by dividing the diffusion coefficient of air by the measured diffusion coefficient of the material. It is a measure for the diffusion resistance the material offers to a diffusive flux.

Gas diffusion within the voids of the wood-furnish mat may be of some importance

during hot pressing, as considerable partial pressure gradients of air and water vapour develop, at least temporarily, between the surface and the core. Furthermore, gas diffusion may be a significant mechanism during conditioning of the panel after pressing, when convective gas flow ceases to play a major role within the panel.

1.6.5 Capillary Moisture Movement, Mat Porosity and Permeability :

Water vapour diffusion in a hygroscopic porous medium may go along with capillary water movement, which is a consequence of the surface tension of water condensed in fine pores. Krischer (1963), suggested that capillary water movement explains the observed moisture content dependency of water transfer through hygroscopic materials.

Dai.et.al (2005) have developed a theoretical model to predict the porosity and permeability of wood strand mats during consolidation. Their model can predict the formation of both inside and between strand void volumes. The inside void volume dominates the initial stage of pressing and between strand void volume the later stage of pressing. The permeability model shows that the mat permeability is mainly controlled by voids between strands instead of those inside strands. Mat density has significant impact on permeability. Strand thickness has a stronger impact than strand width and length.

The work of Hood.et.al (2005) and Dai.et.al (2005) has increased the understanding of void volume effects on internal environment conditions in wood composites during hot pressing.

1.6.6 Equilibrium Moisture Content:

Equilibrium Moisture content (EMC) is defined as the moisture content at which the wood neither gains nor loses moisture in a given condition. EMC is a function of a relative humidity and temperature. EMC is influenced by the previous exposure history of the wood (hysteresis effect) and varies within and between species.

The relationship between EMC, temperature and relative humidity below 100ºC has been studied by many researchers. In addition, empirical and theoretical models have been derived which provide equations to describe this relationship. Simpson (1973) compared predictions of theoretical models with data from literature and concluded that two-hydrate Hailwood and Horrobin model (1946) gives the most suitable results of the models tested. Simpson and Rosen (1981) tested the Hailwood and Horrobin model (1946) for temperatures up to 150ºC at atmospheric pressure and compared the estimated values with the experimental results. It was found the estimates deviates up to 250 % from the measurements around 150ºC. At room temperature, different EMC values are found depending upon whether equilibrium is approached from a higher (desorption) or lower (absorption) moisture content. This hysteresis effect is well described by Kollmann (1959).

Most of the experimental work mentioned above has been done for solid wood and EMC for MDF and particleboard can be expected to be somewhat different. Some of the investigations about the hygroscopicity of wood composites reported in the literature are qualitative rather than quantitative in nature.

For temperature above 150 °C, the equation of Day and Nelson (1965) is more stable and has the following form:

$$EMC = \left[\frac{1}{A}.In(1-\psi)\right]^{\frac{1}{B}}$$

ψ is relative humidity expressed in the form of ratio of present vapour pressure upon saturated vapour pressure.
The above equation is used in the model to calculate EMC.

The coefficients in the above equation can be fitted to experimental data for low temperature (USDA,1999; Ball et al.,2001) and for high temperatures (Resch et al.,1988; Striker,1968). The following fitted coefficients are for average EMC of desorption and adsorption (Pang,1997):

$$A = -0.34 \times 10^{-16} T^{5.98}$$

$B = 348T^{-0.946}$

T is temperature in Kelvin

1.6.7 Heat of Sorption:

As hygroscopic water in the cell wall material has a lower potential energy level than free water, absorption and desorption of water by wood is always accompanied by a corresponding release or consumption of energy. The latent heat of sorption H_l is the heat generated per unit mass of water absorbed by wood from the liquid state at given wood moisture content. Its value is almost zero at fibre saturation and increases towards lower moisture contents. If water is absorbed from the gaseous state, the latent heat of evaporation H_{evp}, which is the energy that is liberated when water vapour condenses to liquid water, has to be added to the latent heat of sorption H_l

Skaar (1972) described two basic methods for determining the latent heat of sorption H_l. The first one is a thermodynamic method that can be applied to derive the values of H_l from known sorption isotherms. The second method uses direct calorimetric measurements. Engelhart (1979) derives values for H_l from sorption isotherms in the temperature range between 100ºC and 170ºC. The findings that the latent heat of sorption is independent of the temperature at low moisture contents has been reported by Kelsey and Clarke(1956) for temperature below 100ºC .

1.6.8 Effect of Density Profile on Physical Properties:

The loose wood-furnish mat is densified in the hot press to its final thickness and density level. The visco-elastic behaviour of the wood-furnish material affects unwanted strain recovery processes (springback) upon press opening. The cross-sectional density profile of the final panel is a consequence of the non-uniformly distributed mechanical mat properties during pressing.

The study of time-dependent stress-strain behaviour of materials is called rheology (Bodig and Jayne, 1982). Rheology in it's narrower sense describes only the

phenomena such as viscous or delayed-elastic deformation. Stress relaxation and creep processes are consequences of such type of material behaviour. According to Ren (1991), the rheological behaviour of a material includes time-dependent as well as instantaneous deformation processes. Such usage of the term 'rheology' reflects the fact that both aspects of the material behaviour are interactive with each other, and that they are usually described simultaneously by so called rheological models.

Kunesh (1961) appears to be the first to emphasize the importance of the visco-elastic behaviour of wood-furnish materials for manufacture and usage of particleboard. Relaxation of overall and residual stresses affect the mat behaviour at press opening (springback) and the dimensional stability of the panel in use.

The strain developed when stress is applied to visco-elastic materials may be divided into elastic, a delayed-elastic and a viscous component. Elastic strain occurs instantaneously and is recoverable; delayed-elastic strain is time dependent and recoverable, and viscous strain is time dependent but not recoverable (Kunesh 1961, Kavvouras 1977). According to Raczkowski (1969), the Burger model can be used to describe a material that simultaneously experiences elastic, delayed-elastic and viscous deformation upon the application of stress. The Burger model is a series connection of a Maxwell model (spring and dashpot in series) and a Kelvin model (spring and dashpot in parallel). Each spring or dashpot may be described by rheological coefficients and the stress-strain relationship can be calculated once the rheological coefficients are known. Thomen (2000) had used the modified Burger model to describe the visco-elastic part of the MDF hot press model.

Wolcott (1989) modelled the nonlinear stress-strain behaviour of the cold compression process based on transverse compression theories of cellular materials. His model was capable of predicting the rapid increase of compression stresses during the consolidation process with varying degrees of accuracy.

Maku and Hamada (1955) were among the first to study the mechanical properties of single layer flakeboards. They showed that the relation of tensile, compressive, and shear strength, and modulus of elasticity to density can be described by exponential functions; the values of all these properties are positively correlated with density.

Strickler (1959) carried out an extensive and pioneering, though empirical, study to identify important factors that influence the panel properties.

The positive correlation between density of the surface layer and bending strength was confirmed by Kollmann (1957). However, Suchsland (1967) mentioned that such a shelling effect of the surface layers does not necessarily require higher surface densities. Factors such as particle geometry and ratio of panel density could also lead to a shelling effect, even if the core and surface densities are similar.

Harless et al. (1987) developed an early model to predict the density profile of particleboard. The model simulates the physical and mechanical processes that occur in the press and mat system. Heat conduction, gas transport, layer compaction and water phase changes were included in the model. Modelling of the compaction process currently terminates when the press platen reaches the final thickness. Changes in the density profile that might occur after press closure due to differential relaxation were ignored.

Suo and Bowyer (1994) simulated modelling of the particleboard density profile. Particleboard was modelled as a system consisting of a number of thin and uniform layers. The compression properties of these layers were determined as a function of the changing temperature and moisture content conditions. The strain of each layer was calculated during consolidation, and the changing thickness of the layers formed the density profile.

A modular finite-element computer simulation of the hot compression of wood based composites was developed by Hubert and Dai (1997). The model is one-dimensional and only final density profile predictions were reported, with no reference to the time-dependent formation of profile.

Dai and Steiner (1993) have given a model for the compression behaviour of a randomly formed flake mat. The model established a quantitative relationship between individual flake compression properties and over all mat response, as well as establishing the relationship between local compression and stresses and overall mat densification. Their model provides a basis for predicting vertical density profile,

spring back on press opening and even thickness swelling.

Lang and Wolcott (1995) developed a solid mechanics model to predict the static stress- strain behaviour of randomly formed wood-strand mats during pressing. Monte Carlo simulation is used for reconstructing the mat structure. Hooke's law, modified by non linear strain function, is used to calculate development of stress in the mat. Experimental results showed good agreement with the predicted stress response.

Dai (2001) developed a fundamental model of stress relaxation based on the compressive stress relaxation of wood flakes and a Poisson distribution of flake overlaps formed in the mat. His results showed that the stress relaxation of wood flakes at different levels of compression follows linear double logarithmic relationships with varying slopes or rates of stress relaxation

Thomen (2000) developed the most comprehensive continuous hot-compression model for wood-based composites, which can predict the density profile formation during the entire pressing operation. The visco-elastic properties were modelled by five element Burger-Humphrey model.

1.6.9 Integrated Models:

Two essentially different approaches to model the hot pressing process of wood based composites can be found in the literature. The first one uses fundamental principles to describe the relevant physical or chemical processes. The second category of models employs statistical methods to link material and process variables to output parameters, such as mechanical properties of the final product. The first approach will be discussed here and second approach will be discussed in chapter six.

The first heat and mass transfer model based on fundamental physical principles that included vapour convection, heat conduction and convection, and phase change was developed by Humphrey (1982). The model predicted temperature, vapour pressure and moisture content development during hot pressing. A cylindrical coordinate system was employed to model a circular mat, so that cross-sectional as well as radial heat and mass transfer was accounted for. The internal environment at the corner of

the board was calculated by interpolating results obtained from inscribed and circumscribed cylinders of the rectangular shape of the board. The basis of this model was a modified finite difference approach. The model neglected the effect of press closing time and resin cure on the internal environment of the mat. Instead, instantaneous press closing was assumed, and variables were predicted only for the remaining part of the press schedule. The predicted data agreed well in trend with those observed experimentally for particleboard.

Haselein (1998) refined Humphrey's model and added a rheological component to account for mat compression and stress relaxation. An important limitation in Humphrey's model is that the shape of the modelled mat prevents the simulation of events occurring in the corners of a rectangular panel. Furthermore, differences between material properties in the production direction and that perpendicular to it are disregarded due to the cylindrical coordinate system. Another drawback of the model is the assumption that water vapour is the only gas in the mat. During the initial phase of pressing, air is clearly the prevailing gas component, before it is replaced by vapour later in the cycle.

Hata et.al (1990) described a two dimensional model to calculate the conductive heat flow in absolutely dry particle boards. Under such conditions, which do not occur in practice, vapour convection and moisture effects can be neglected. Hubert and Dai (1998) presented a one dimensional model for simulating hot pressing of OSB using an implicit finite element modelling approach. Mechanisms included were vapour convection, conductive and convective heat, heat transfer, phase change, adhesive cure and mat densification. The visco-elastic behaviour of the mat was neglected. Hubert and Dai compared model predictions of various parameters with measured data and reported that typical trends were predicted correctly, but that some magnitude discrepancies exist.

For MDF, a three-dimensional unsteady state model was presented (Carvalho and Costa 1998) describing the heat and mass transfer and predicting the spatial and time evolution of temperature, moisture content, steam pressure and relative humidity. The impact of press closing on the physical properties was neglected. Recently, the model developed by Humphrey (1982) for the hot-pressing of particleboard in a batch press

has been improved and extended to the continuous process (Thoemen 2000). However this model ignores the influence of resin cure. (Thoemen and Humphrey 2003) have further developed their model to predict advanced hot pressing technology such as steam injection and having a cooling zone in the continuous press.

Zombori (2001) developed a two dimensional heat and mass transfer model for Oriented Strand Board (OSB). The viscoelastic properties are measured by using modified Hook's law. The model was developed specifically for OSB. The mat formation in OSB is very different from MDF. The strands are oriented perpendicular to each other in OSB, due to which the void volume and physical properties are different from MDF.

Dai.et.al (2004) presented three dimensional model of wood composite. The coupled physical phenomenon is expressed in terms of mass conservation, momentum of gas flow, energy conservation, thermodynamics and resin curing kinetics.

1.6.10 Comparison of Main Models:

Table 1.2 compares the main models in the field of wood composite along with their merits and demerits.

SN	GUPTA , JORDAN & PANG (2006)	THOMEN & HUMPHREY (2000)	BALAZS .G.ZOMBORI (2001)	LUISA.CARVALHO & COSTA(1998)
1	MDF	MDF	Wood Composites(mainly OSB)	MDF
2	One Dimensional	Two Dimensional	Two Dimensional(with consideration of the thickness and width direction)	Three Dimensional
3	Resin curing considered	Not considered	Considered	Considered
4	Diffusion of bound water considered.	Not	Not	Not
5	Equation to calculate EMC refined can cover the whole range of pressing temperature	Old equation	Old equation	Old equation
6	Stepwise press closing considered	Stepwise press closing considered	Yes.	Not
7	Model can be applied for both Batch & Continuous press	Both	Only Batch press	Only Batch

SN	GUPTA , JORDAN & PANG (2006)	THOMEN & HUMPHREY (2000)	BALAZS .G.ZOMBORI (2001)	LUISA.CARVALHO & COSTA(1998)
8	Total heat through press platen & Resin Curing	Total heat through press platen	Press platen and exothermic reaction of resin curing	Press platen and exothermic reaction of resin curing
9	Model based on Thomen and Zombori model	Model based on earlier Humphrey model	Based on Stanish(1986) drying model but the physical properties are for OSB	Model based on the Stanish(1986) drying model but the physical properties are assessed for MDF in place of solid wood
10	Visco-elastic properties are measured by anology to Maxwell element	Visco-elastic properties are measured by anology to Humphrey and Burger model	Modified Hook's law and analogy to spring	By analogy to Maxwell, and Kelvin element
11	Time of simulation is fast	Slow	Slow	Slow
12	Graphical presentation higher	Avg	Avg	Avg
13	Software used in Programming Matlab	Software used in programming Visual C++	Differential- Algebraic system solver (DDASSL)	Stiff equation solver LSODES(Hindmarsh 1983)
14	New Hot pressing technology such as steam injection and cooling zone can be modelled	Yes	Not known	Not known

1. “Modelling and Optimisation of MDF Hot Pressing”, by Gupta, Jordan & Pang (2006).
2. “ Modelling and Simulation of the Hot Pressing Process”, by Thomen & Humphrey (2000).
3. “ Modelling the Physical Processes in Natural Fibre”, by Zombori (2001).
4. “Modelling the Transient Effects during Hot Pressing of Wood Based Composites”, by Luisa, Carvalho & Costa (1998).

Chapter- 2

Vertical Density Profile Model Development

Summary:

The vertical density profile (VDP) is one of the most important properties that determine MDF strength, stiffness and other physical properties. The vertical density profile formation is the result of many interacting process variables. During hot pressing, the internal conditions (temperature, moisture content) are continuously changing with time (in batch press) or with position (in continuous press). An unsteady, one-dimensional computer model based on fundamental analysis was developed in this work which can help to understand the relationship between processing parameters and density profile formation.

The transverse compression behaviour through the mat thickness is highly nonlinear due to the cellular structure of the fibre mat and non uniform mat formation, Dai and Steiner (1993). Additionally, the mat fibres show typical viscoelastic behaviour due to the interaction of time, temperature and moisture content change. The behaviour of the cellular structure is modelled with the modified Hooke's Law, which includes an additional nonlinearizing term. The model was solved using a numerical technique in which the mat is divided into a number of thin and plane layers. In each layer, the mat properties are assumed to be uniform through the layer thickness. The compressibility is the function of stress-strain, temperature and moisture content of the layer. From the theoretical model, the VDP was predicted for given operation conditions.

An empirical model was also developed on the basis of the experimental results. The results from both the theoretical and empirical models are compared and both the models are validated by comparing them with the experimental results.

2.1 Introduction:

During hot pressing of the MDF fibre mat, heat and pressure are applied simultaneously on both surfaces. Then the heat is transferred to the centre of the mat by conduction and convection. The moisture near the surface is vaporized and water vapour migrates towards the cooler zone in the centre. At the same time, a pressure of 5 MPa is applied by the hot platen to the loose fibre mat in order to achieve the target thickness. In commercial plants the platen pressure varies from 5-7 MPa. The maximum capacity of the pilot plant is 5MPa.With the interaction of temperature, pressure and moisture content change, the viscoelastic properties of the resin and fibres also change with time during the pressing. As a consequence, a density gradient develops in the MDF panel.

The VDP or density distribution through the panel thickness has long been identified as one of the important panel characteristics that correlate well with strength, stiffness and other physical properties of wood-based composite panels.

Harless et al. (1987) developed a theoretical model to predict the density profile of particleboard. In their model, heat conduction, gas transport, layer compaction and water phase changes were included. Their simulation terminates when the mat is compressed to the required thickness. However, changes in the density profile that might occur after press closure due to differential relaxation were ignored in the model.

Suo and Bowyer (1994) developed a separate model of the particleboard density profile in which the particleboard was considered as a system consisting of a number of thin and uniform layers. The compression properties such as stress, strain and density of these layers were determined as a function of the panel temperature and moisture content. The strain of each layer was calculated during consolidation, and the thickness change of each layer determined the density profile.

A finite-element method was used by Hubert and Dai (1997) in their model for simulation of the hot compression of wood-based composites. The model was one-dimensional and only final density profile predictions were reported, without reference to the time-dependent formation of the profile.

Wang et al. (2000) recommended a methodology to subdivide the density profile formation into two periods (consolidation and adjusting) and five stages in order to investigate the transient moisture and temperature effects. The principal drawing of the vertical density profile formation is shown in Figure 2.1.

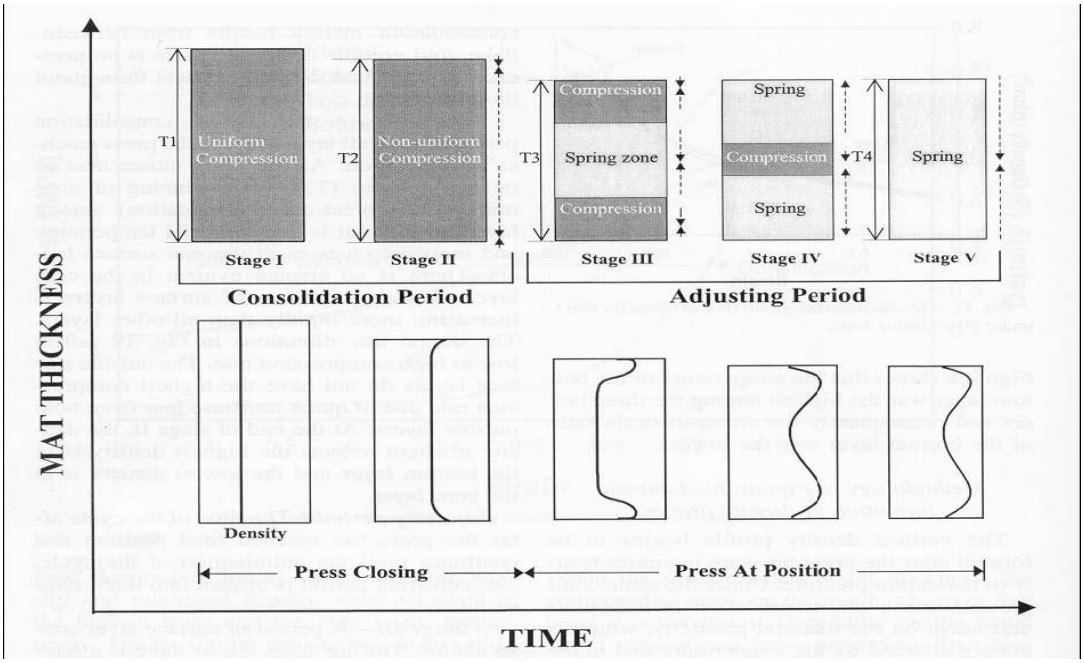

Figure 2.1: The five stages of vertical density profile formation during hot pressing. In the figure, T1 and T2 are the in-situ thickness of mat being pressed, T3 is the target thickness of panel and T4 is the actual thickness after venting (Wang, 2000a).

In Wang's analysis, the consolidation period starts from the press closing till the press reaching its final target position. The consolidation period contains two stages:

Stage I: It starts when the press begins to close and continues as long as the mat density is uniform. During this stage, the consolidation mainly results from the

decrease of void volume. There is no presence of a vertical density gradient throughout the mat with the maximum mat density reaching approximately 250 kg/m^3. Based on this assumption, the model was programmed so that no density gradient is formed until the mat density is increased to 250 kg/m^3. The displacement is uniformly distributed among all the layers and all layers have the same density.

StageII: This stage follows stage I and during this stage, non uniform consolidation occurs among all layers before the press reaches final position. However, the rapid density increase is observed only in the surface layers whereas the densities in the core layers remain relatively uniform. At the end of stage II , the density gradient reflects the highest density in the top and bottom layers, and the lowest density in other layers.

After the press has reached the final position, the press is in the adjusting period which continues until the completion of the press cycle. This period is divided into the three stages.

Stage III: As there is a temperature gradient in the mat, fibres in the surface layers continue to incur micro structural deformation under maximum pressure 5MPa and highest temperature. Generally, the vertical density profile develops from consolidation in stages II and III. However, if the press closing is very slow, then the vertical density profile mainly develops from consolidation in stage II.

Stage IV: With the press proceeding, the temperature and moisture content in the core region increase, therefore, the density of the core layers increases even at low compression stress.

Stage V: A period of spring back of the whole mat when the press opens to let steam escape from the mat. The spring back is not uniform through the mat thickness because of the variation in mat structure, temperature, moisture content, and density gradients in the mat. High spring back is expected in the core layer.

Thomen (2000) developed the most comprehensive model for continuous hot-compression of wood-based composites, which can predict the density profile formation during the entire pressing operation. The viscoelastic properties of the panel were modelled by Thomen (2000) using the five element model of Burger-Humphrey Ren (1991). Zombori (2001) calculated the viscoelastic properties by modified Hooke's law in each time step which determines the stress by multiplying the linear function of strain by a non-linear strain function to represent the nonlinear response of the cellular material to an induced strain.

The present model has overcome some of the limitations of previous models and reduces the computation time significantly. The equation to calculate the modulus of elasticity (MOE) is modified so as to reflect the effects of temperature, moisture content and density of the layer combining the equations of Carvalho et al. (2001) and Palka (1973).

2.2 Literature Review of Stress Calculation:

2.2.1 Non Linear Transverse Compression Behaviour of the Wood Fibres:

Cellular materials generally show a characteristic non-linear behaviour during transverse compression, resulting from the collapse of the cellular structure. Figure 2.2 shows a typical stress-strain curve for the cellular materials.

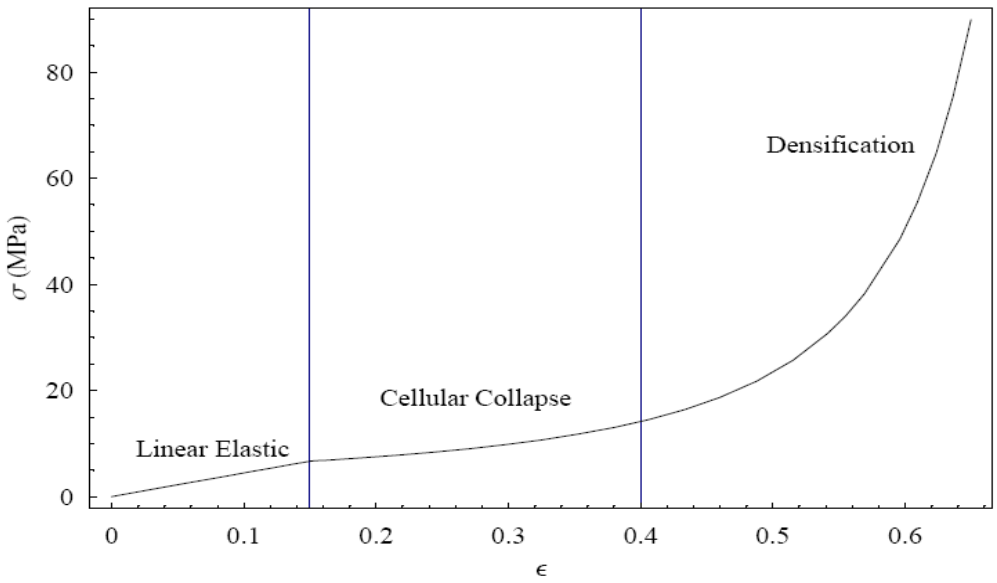

Figure 2.2: Characteristic stress-strain curve for cellular materials Wolcott (1989).

Three characteristic regions can be observed in both man-made and natural cellular materials: linear elastic, cellular collapse and densification. The material at the beginning of compression deforms in a linear elastic manner. Due to the cumulative collapse of the cell walls, the material continues to deform at a nearly constant stress level. Cellular collapse occurs either by elastic buckling, plastic yielding or brittle crushing, depending on the type of the cell wall material. Wolcott (1989) demonstrated that elastic buckling is a viable assumption as the form of collapse of the wall of wood cells. At the end of the collapse region the cell wall structure starts to consolidate. At this point most of the cells are collapsed and opposing cell walls are in close contact. The characteristic of the densification region is the rapid stress increase as the compression continues. These regions are present in all types of cellular structures, but the initiation and the length of the regions are a function of the cell geometry. The cell geometry is characterized by the relative density (ρ_r), which is defined as the ratio of the bulk density of the cellular material to the density of the cell wall material:

$$\rho_r = \frac{Bulk Density\ of\ Cellular\ Material}{Density\ of\ Cell\ Wall} \tag{2.1}$$

The modulus of elasticity of the cellular material is related to the modulus of elasticity of the cell wall (E_{cw}) and the cellular geometry represented by the relative density (ρ_r) as follows Gibson and Ashby (1997):

$$E = E_{cw}\rho_r^{\,3} \qquad (2.2)$$

The relative density is the ratio of density of cellular material to the density of cell wall. The value used is 0.31, the same as for most of the soft woods Zombori (2001).

In which E is the modulus of elasticity of the cellular material and E_{cw} is the modulus of elasticity of the cell wall. The above equation derived for solid wood is used to calculate the modulus of elasticity of the fibre mat in the model.

This equation states that the modulus of elasticity (E) of any wood species could be derived as the product of the constant cell wall modulus (variation of the cell wall modulus is negligible for different species) and the relative density (related to the specific gravity) of the species. Consequently, the modulus of the wood species is only a function of the cellular structure, as represented by the relative density.

The characteristic shape of the stress-strain curve can be described by a non-linear multiplier, $\psi(\varepsilon)$, called the nonlinear strain function, in the modified Hooke's Law as follows:

$$\sigma = E \cdot \varepsilon \cdot \psi(\varepsilon) \qquad (2.3)$$

Where σ is stress and ε is strain.

The influence of the geometry of the cellular structure on the consolidation behaviour of the material is accounted for by the non-linear strain function. It can be determined

experimentally (Meinecke and Clark 1973) or from the characteristic plastic strain observed in a stress-strain diagram (Rusch, 1969).

Maiti et al. (1984) derived a relationship between the nonlinear strain function and the applied strain based on the yield strain of the cell wall material, as follows:

$$\psi(\varepsilon) = 1; \qquad \varepsilon \le \varepsilon_y \tag{2.4}$$

$$\psi(\varepsilon) = \frac{\varepsilon_y}{\varepsilon}\left(\frac{1-\rho_r^{1/3}}{1-\rho_r(\varepsilon)^{1/3}}\right)^3; \qquad \varepsilon > \varepsilon_y \tag{2.5}$$

Where:

$\varepsilon_y =$ yield strain of the cell wall, $\varepsilon =$ applied strain, $\rho_r =$ relative density,

$\rho_r(\varepsilon) =$ relative density function.

The nonlinear strain is a function of applied strain and relative density as plotted in Figure 2.3 (Maiti et al., 1984).

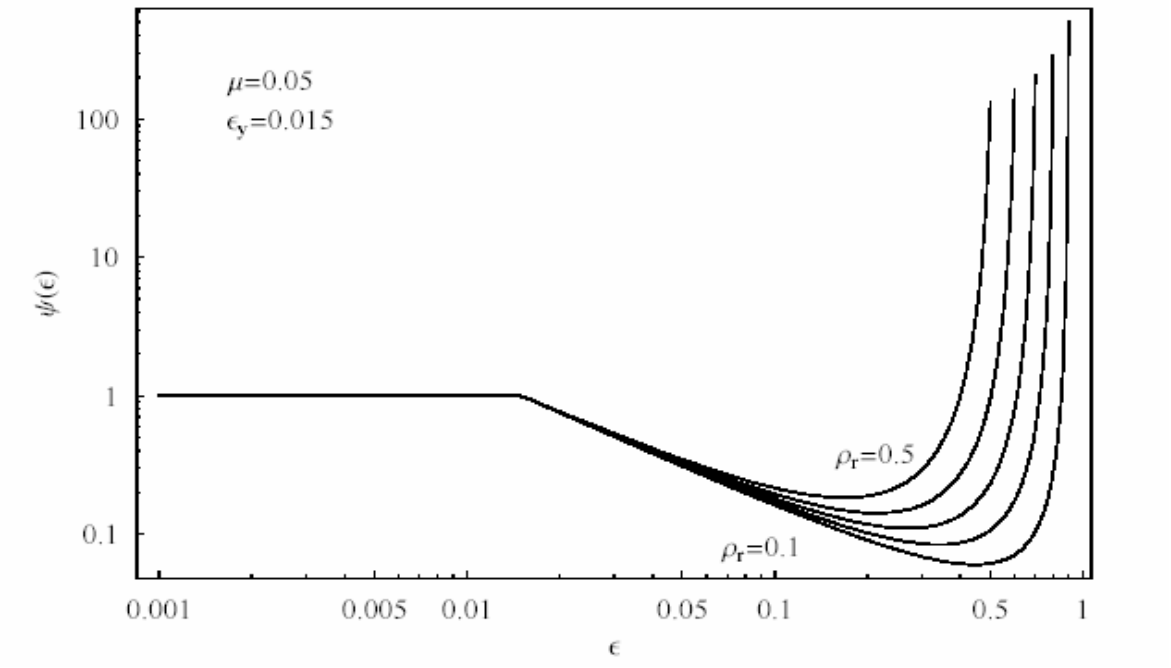

Figure 2.3: The nonlinear strain function $\psi(\varepsilon)$ as a function of strain, with relative density ρ_r as parameter Maiti et al. (1984).

The yield strain of the cell wall of wood was determined by Wolcott (1989) as 0.015.The nonlinear strain function has a value of unity when the strain is below the yield strain of the cell wall. In this case, the modified Hook's Law remains the ordinary form for describing the linear elastic behaviour of the cell wall under low levels of strain.

The relative density of the material increases during the transverse compression of the cellular structure. The relative density function, $\rho_r(\varepsilon)$), takes into consideration the dilation (also called barrelling) effect as shown in figure 2.4(Kasal 1989).

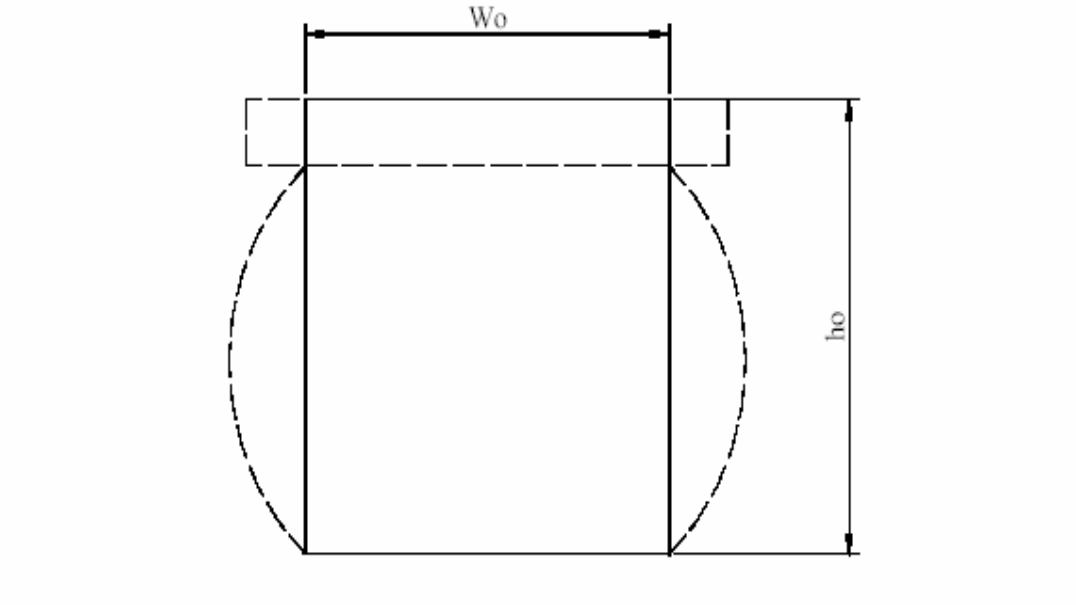

Figure 2.4: The "barrelling effect" of wood under transverse compression. W_o and h_o are the initial width and height of the specimen (Kasal 1989).

The modified equation given by Kasal (1989) to calculate relative density function is as follows:

$$\rho_r(\varepsilon) = \rho_r\left(1-(\varepsilon-\varepsilon_y)+\frac{2}{3}\mu(\varepsilon-\varepsilon_y)-\mu(\varepsilon-\varepsilon_y)^2\right)^{-1}, \qquad (2.6)$$

Where μ is the expansion ratio which is defined as the ratio of the lateral strain to compressive strain in the nonlinear stress-strain region. It was found experimentally that the expansion ratio is a function of specimen height (Wolcott, 1989). The expansion ratio

is larger for taller specimens, because the frictional restrictive effect of the loading surfaces is not as pronounced. The expansion ratio also affects the strain function as shown in Figure 2.5.

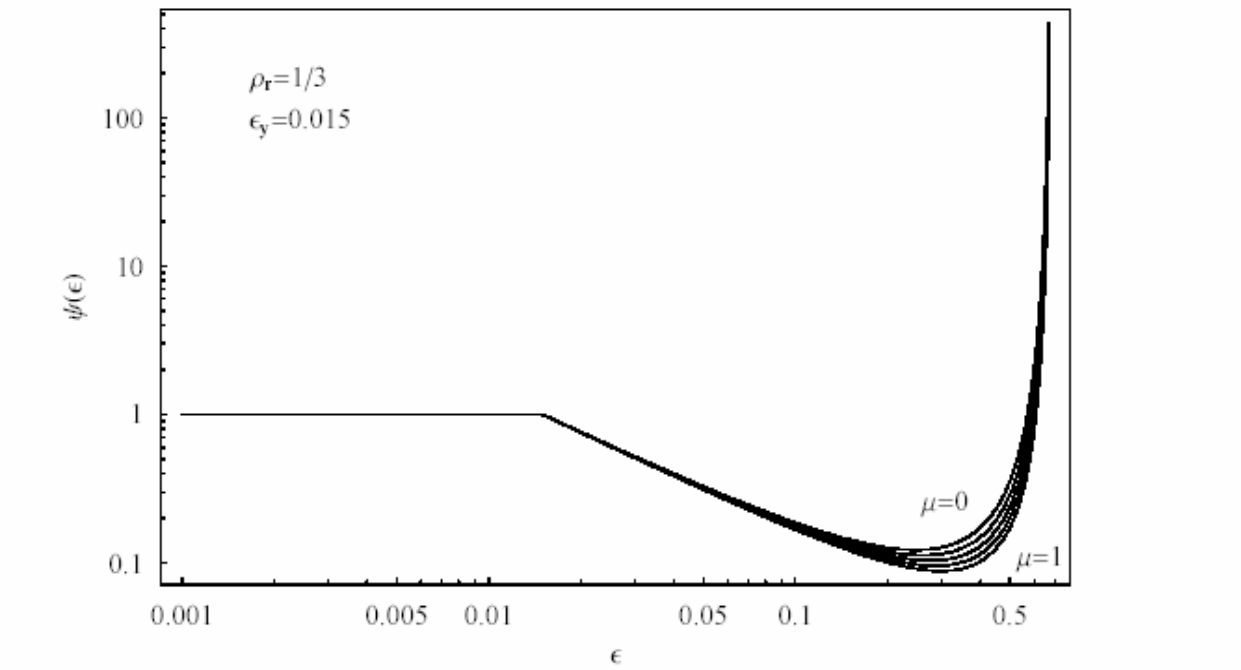

Figure 2.5: The nonlinear strains function $\psi(\varepsilon)$ as a function of expansion ratio μ.

2.2.2 Deriving the Stress Relaxation Curve:

In order to calculate the time-dependent response of the fibres to a loading history, either in the integral or the differential form, the creep or relaxation response of the material for a prolonged period is necessary. However, prolonged testing of the material is not feasible. Therefore, the time-temperature-moisture superposition technique was used by Wolcott (1989) to experimentally determine the relaxation curves for a long time period. The measured temperature and moisture shift factors were combined and a second-order equation was fitted to the surface, as proposed by Maksimov et al. (1971, 1974, 1975, 1976):

$$\log a(T,M) = \alpha + \beta_1.T + \beta_2.T^2 + \beta_3.M + \beta_4.M^2 \qquad (2.7)$$

Where:

$a(T,M)$ = temperature and moisture shift factor,

T = temperature (K),

M = moisture content (%) on dry basis, $\alpha = 8.9361$ $\beta_1 = 1.027 \times 10^{-1}$, $\beta_2 = 1.361 \times 10^{-4}$,

$\beta_3 = 1.1908$, $\beta_4 = 2.598 \times 10^{-2}$.

Figure 2.6 shows changes in the relaxation modulus with the time..

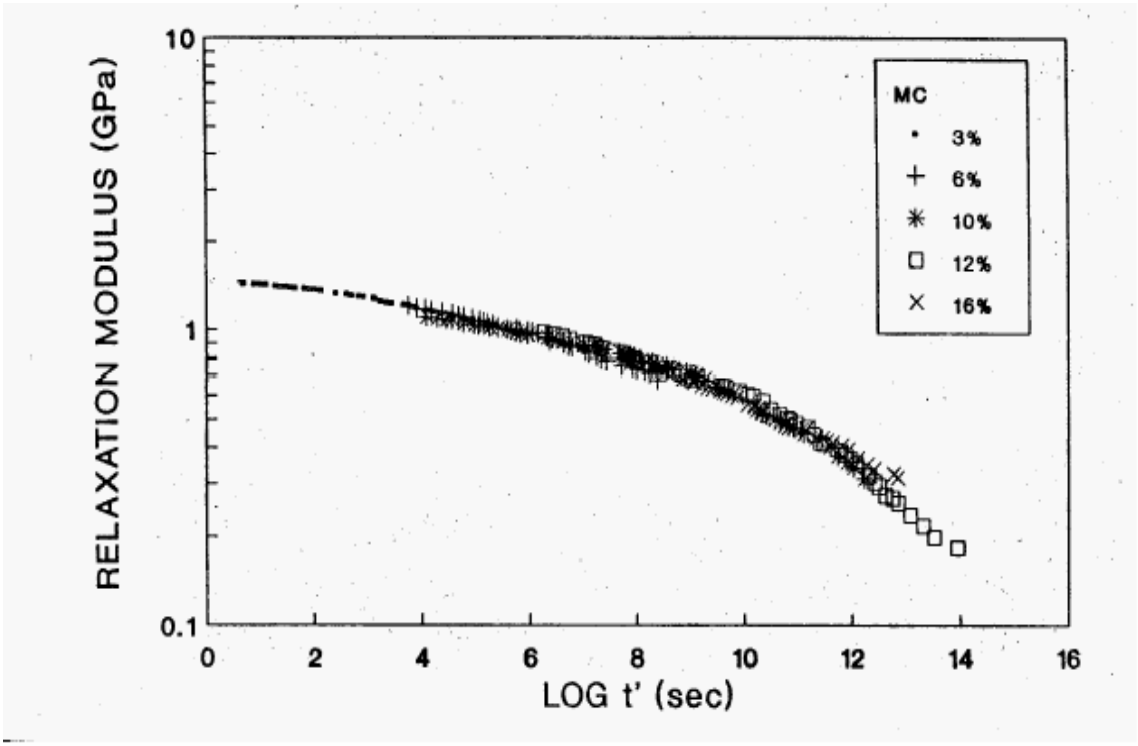

Figure 2.6: Relaxation modulus E (t') master curve plotted against reduced time (t'). The master curve is shifted to a reference temperature of 60 °C and a moisture content of 3% (Wolcott 1989).

2.2.3 Method of Reduced Variables:

The relaxation modulus "master curve" describes the long term response of the material at the reference temperature $(60^{\circ}C)$ and moisture content (3%). In order to derive viscoelastic properties at different temperature and moisture levels, the master curve has to be shifted on the time scale with the temperature and moisture shift factor. The new time scale is represented by the reduced time (t') which is given by the relation, Wolcott (1989):

$$t' = t / \alpha(T, M) \qquad (2.8)$$

In which, t' = reduced time (s), t = time (s), $a(T, M)$ = temperature and moisture content shift factor. The compressibility of the fibres is determined from an empirical equation based on experimental data, Zombori (2001).

2.3. Theoretical Model Development:

2.3.1. Determination of Stress- Strain:

In the press model developed in this work, the MDF board is symmetrically divided into a number of thin layers (Figure 2.7), each of which exhibits uniform properties everywhere. Viscoelastic and physical properties of each layer vary with the levels of stress and strain as well as moisture content and temperature in the layer. A denser layer is the result of more deformation or compression having occurred in that layer. The compressibility of a layer is in turn affected by the layer's viscoelastic and physical properties.

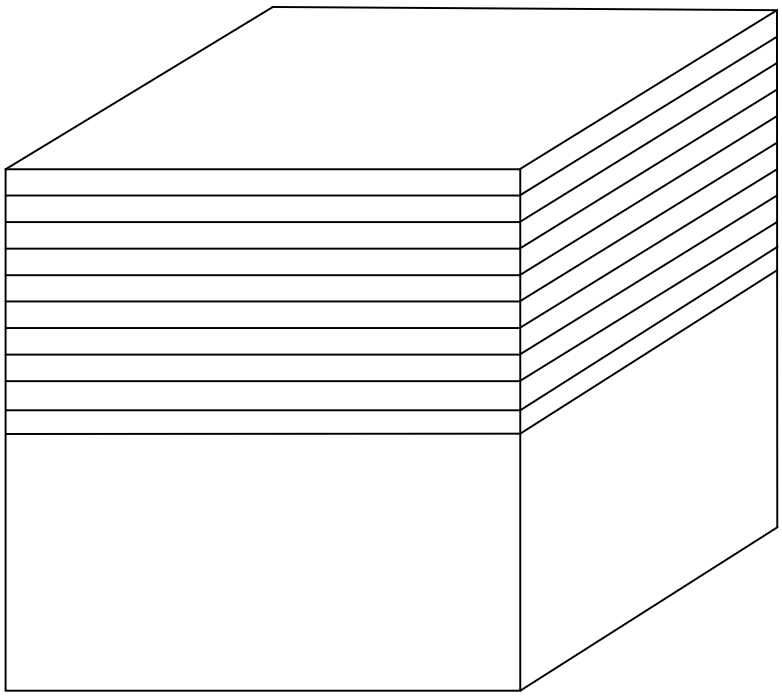

Figure 2.7: The mat is symmetrically divided into two halves and the upper one is divided into a number of layers for simulation.

The MDF panel is assumed to be symmetric about the plane of mid-thickness. Thus the density model equations are solved for only half the panel. At the start of the simulation, all layers are assumed to have the same mass of fibres and the same initial thickness.

The mat variables are calculated through a series of time steps during which the board is compressed to the target thickness and then held for a time at that thickness. For each time step, the relative compression in each layer is assumed to be inversely proportional to the MOE of that layer at the start of the time step. This follows the approach of Suo and Bowyer (1994). In the model of Suo and Bowyer, ε is used as strain but in the model equations ε was defined as the change in thickness.

The relationship between the strain distributed in different layers and their corresponding MOEs can be described as follows:

$$\varepsilon_{1(\Delta t)} : \varepsilon_{2(\Delta t)} : \ldots\ldots : \varepsilon_{i(\Delta t)} : \ldots\ldots : \varepsilon_{n(\Delta t)} = \frac{1}{E_{1(t-1)}} : \frac{1}{E_{2(t-1)}} : \ldots\ldots : \frac{1}{E_{i(t-1)}} : \ldots\ldots : \frac{1}{E_{n(t-1)}} \qquad (2.9)$$

By considering the symmetric nature of the panel, the total deformation of the panel over a time step Δt in the thickness direction is:

$$2\sum_{i=1}^{n} d_{i(\Delta t)} = D_{(\Delta t)} \qquad (2.10)$$

Where $d_{i(\Delta t)}$ is the displacement induced in layer *i* during time interval Δt, and $D_{(\Delta t)}$ is the total displacement in the mat in the same time interval, corresponding to the movement of the platen. $E_{i(t-1)}$ is the modulus of elasticity of layer *i* determined from the conditions of previous time step at time *t-1* ('old time'). The number of 2 in equation (2.10) is for the whole board as *n* is the number of layers in half the board.

Let

$$S = \sum_{i=1}^{n} \frac{1}{E_{i(t-1)}} \tag{2.11}$$

Then the displacement induced in each layer can be calculated as follows:

$$d_{1(\Delta t)} = \frac{\left(\frac{1}{E_{1(t-1)}}\right)}{S} \times D_{(\Delta t)} \tag{2.12}$$

The MOE of each layer can be related to the MOE of individual fibres (E_{fo}) by using the equation derived by Carvalho et al. (2001). This equation was derived from the experimental data of Wolcott et al. (1990) under various conditions of temperature and moisture content.

$$E_{i(t)} = E_{fo} \exp\left(-\frac{\beta_T}{T + T_0} + \frac{\beta_H}{MC - MC_0}\right) \tag{2.13}$$

In which,

β_T = -1820°,

$\beta_H = 0.0695$,

$T_0 = 447^0 C$,

$E_{fo} = 6.74 MPa$,

$MC_0 = 0.2925$

MC = moisture content of fibres

The effect of density on the layer's MOE is quantified by employing Palka's empirical equation developed for solid wood (Palka, 1973):

$$E_{i(t)} = E_{i(t-1)} \times \left(\frac{\rho_{i(t)}}{\rho_{i(t-1)}}\right)^p \tag{2.14}$$

In which $E_{i(t)}$ is the modulus of elasticity of layer *i* at new time *t*, $\rho_{i(t)}$ is the density of the layer and $\rho_{i(t-1)}$ is the density of the layer at the old time *t-1*. p is the modifications constant for which Palka gives a value of 1.25 for the solid wood. After initially trying other values of "p", to improve the agreement between model and experiment. The value of 1.25 is used in the model to predict the vertical density profile and other properties such as stress, strain and relaxation factor.

The strain at time *t* in the mat is defined as:

$$\varepsilon_{(t)} = \frac{M_{(t_0)} - M_{(t)}}{M_{(t_0)}} \tag{2.15}$$

Where

$M_{(t_0)}$ = initial mat thickness which is the thickness after pre-pressing of the mat,

$M_{(t)}$ = mat thickness at time *t*.

During the hot-compression, the movement of the hot platen is controlled. Therefore, the total strain of the mat is known. However, the stress relaxation in each layer needs to be determined to determine the strains in each layer. In doing so, the time dependent viscoelastic properties are needed. These can be described mathematically by the Maxwell relaxation equation.

Maxwell Body: A Maxwell body consists of a spring and a dashpot joined in series as shown in Figure 2.8. It is used to model the rheological behaviour of wood. A dashpot is an additional element attached to a spring, which is used to describe the time- dependent behaviour of the wood. A dashpot consist of a piston inside a container filled with a viscous fluid. The term dashpot is used for describing the force-displacement behaviour of this type of element. The governing differential equation of a single Maxwell body given by Zombori (2001) is used to calculate the stress relaxation in different layers.

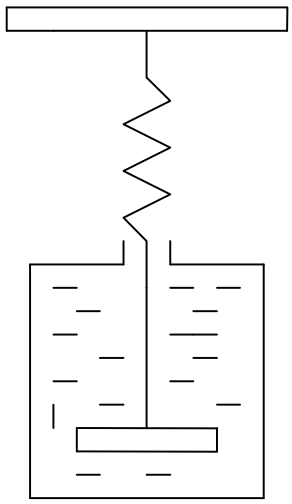

Figure 2.8: Maxwell body consist of a spring and dashpot.

From the Maxwell model, the stress change with time is a function of MOE and stress level:

$$\frac{d\sigma}{dt} = E\frac{d\varepsilon}{dt} - \frac{1}{\tau}\sigma \tag{2.16}$$

By applying this equation over a short time step (Δt), the stress change over this short time interval can be calculated by:

$$\Delta\sigma = E\Delta\varepsilon - \frac{1}{\tau}\sigma\,\Delta t \tag{2.17}$$

Therefore the iteration formula for a single Maxwell element is:

$$\sigma_{i(t)} = \sigma_{i(t-1)} + E_i(\varepsilon_{i(t)} - \varepsilon_{i(t-1)}) - \frac{\Delta t}{\tau_i}\sigma_{i(t-1)} \tag{2.18}$$

The effects of temperature and the moisture content on the relaxation of the element are taken into consideration through their influence on E_i and by including the moisture shift factor *a(T, MC)* as given in Equation (2.7). The relaxation time (τ) is reduced with the temperature and moisture shift factor as follows:

$$\sigma_{i(t)} = \sigma_{i(t-1)} + E_i(\varepsilon_{i(t)} - \varepsilon_{i(t-1)}) - \frac{\Delta t}{\tau_i a(T, MC)}\sigma_{i(t-1)} \qquad (2.19)$$

In the above equation, the first term on the right-hand side is the stress in the 'old time' step and the second term is the stress related to the elastic strain in the current time step, and the third term represents the stress relaxation as a function of time, temperature and moisture content. The temperature and moisture content were calculated at the mesh points. The Maxwell ladder representing the material response was positioned between the mesh points, and therefore, the average temperature and moisture contents at the two bounding mesh points were used to calculate the shift factor. The shift factor was calculated by Wolcott (1989).

2.3.2. Matlab Programming:

The program is written in the Matlab software to solve the above model for simulation of the MDF density profile. In the simulation, the MDF mat is symmetrically divided into two halves and, once the calculation for each layer is complete, graphs of output properties such as density, stress, and strain for the complete thickness are generated. All the variables are declared in the beginning of the m file. The user can change the value of variables in the beginning. The whole m file is divided into several blocks and every block has all the concerned variables. The simulation programming flow-chart are shown in Figure 2.9 and discussed as follows.

- All the variables related to density profile calculation are the layer properties, such as stress, strain, density, non linear strain function.
- All the variables related to heat and mass transfer calculation are the interface properties such as moisture content, temperature.
- There are two main loops, the outer one is the time loop and the inner one is the layer loop. Firstly all the changes across the layers are calculated and once this is completed, the changes in all layers are then calculated for next time step.

- There are two main sections: the first one is for the calculation of stress and strain and all the related variables such as density and stress relaxation. The second section is to calculate the updated temperature and moisture content with every time step. The second loop needs to call a heat and mass transfer model which will be discussed in Chapter 4.
- In the beginning of the stress- strain part, there is a conditional loop, to check the movement of the press platen.
- There is an iteration loop across the temperature and moisture content section, so as to converge the solution.
- In all the simulation graphs, “Number of Layers”, stands for “layer number” counting from one surface.

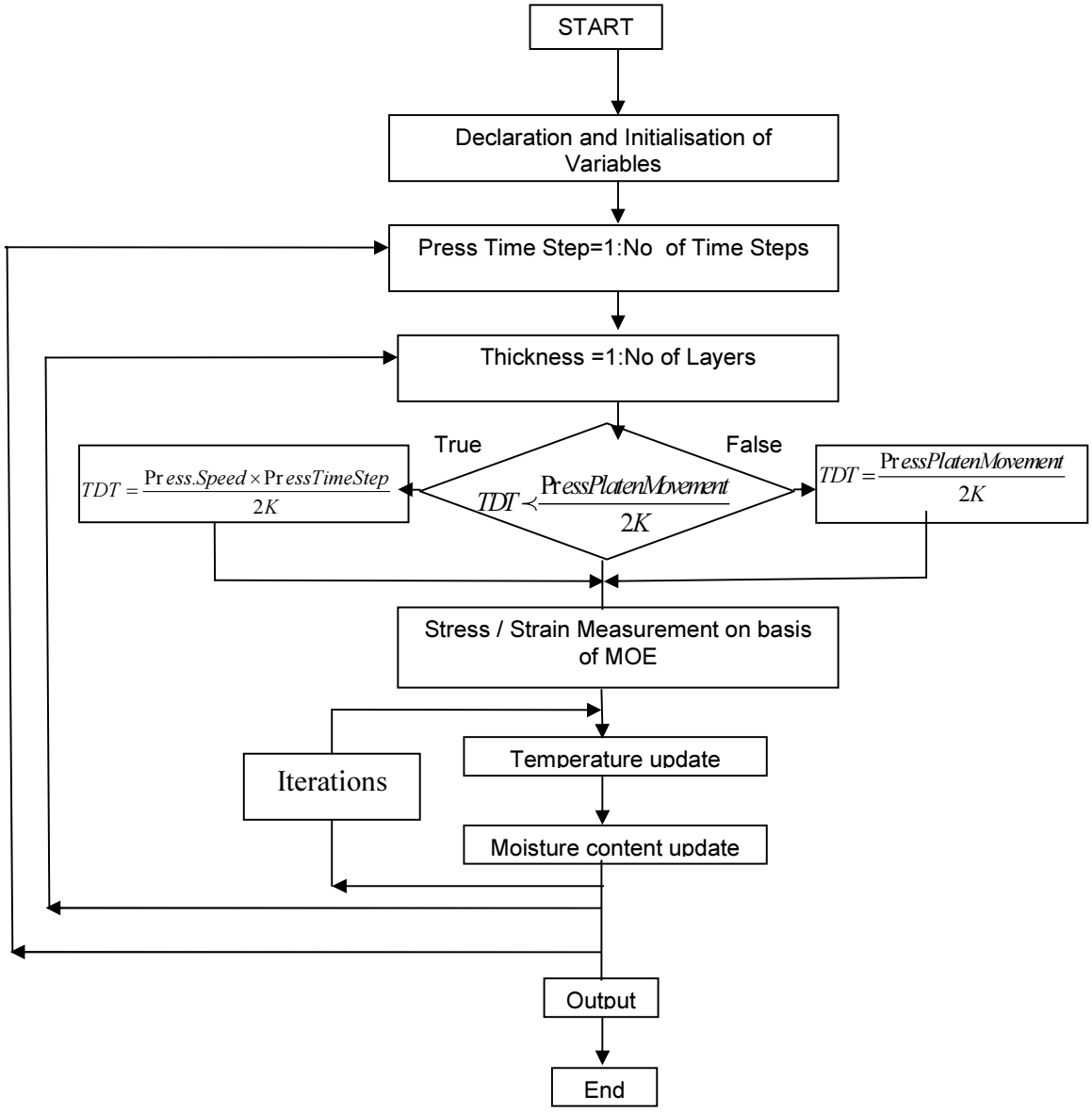

Figure 2.9: Flow Chart for the programming showing the over- all calculations

2.3.3. Stress and Strain Calculations:

The Figure 2.10 shows the steps followed for the calculation of stress and strain. As the pressing starts, the platen movement with time is known. This helps in calculating the over all mat strain. The displacement in each layer is inversely proportional to the modulus of elasticity of that layer. From the displacement, the density of each layer and other parameters can be calculated such as new strain, new stress and relative

density function. These steps are followed in the stress-strain block shown in Figure 2.9.

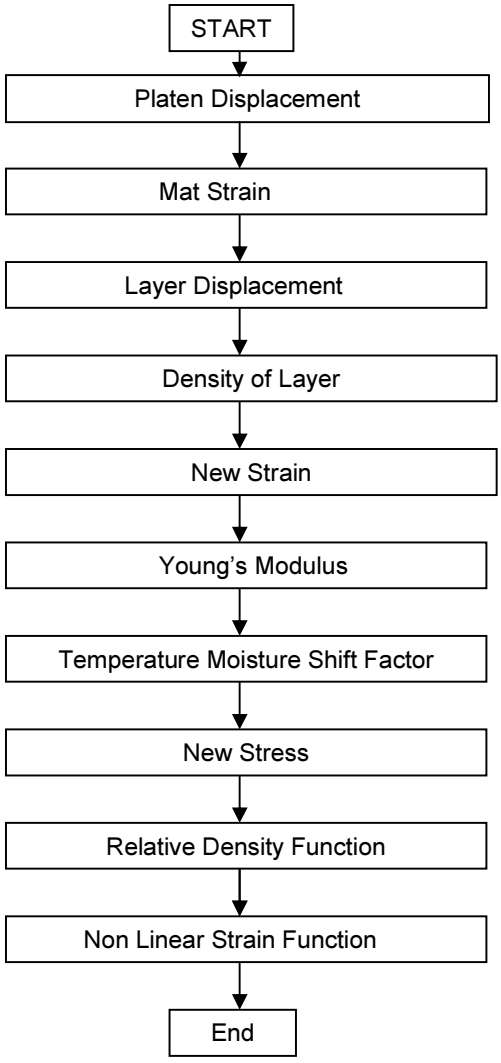

Figure 2.10: Procedures for stress and strain calculations.

2.3.4. Heat and Mass Transfer calculations:

In the beginning of the programme, there is a conditional loop, which will check, whether the equilibrium moisture content (EMC) is equal to the moisture content of the fibres. As it is known that in a small time the EMC value will be equal to the moisture content of the fibres, it is assumed for the modelling purpose that EMC will be reached instantaneously. The difference in these values will give the amount of evaporation or condensation of moisture content in the layers. The loop will iterate four times to converge the solution at each time step. All other transport variables such as binary diffusion, permeability, viscosity are calculated. The equations to calculate these variables are described in detail in the heat and mass transfer chapter. The total amount of vapour in a layer depends on net vapour flux and the vapour generated by curing of resin and loss or gain due to evaporation or condensation of moisture content as explained in the governing equations.

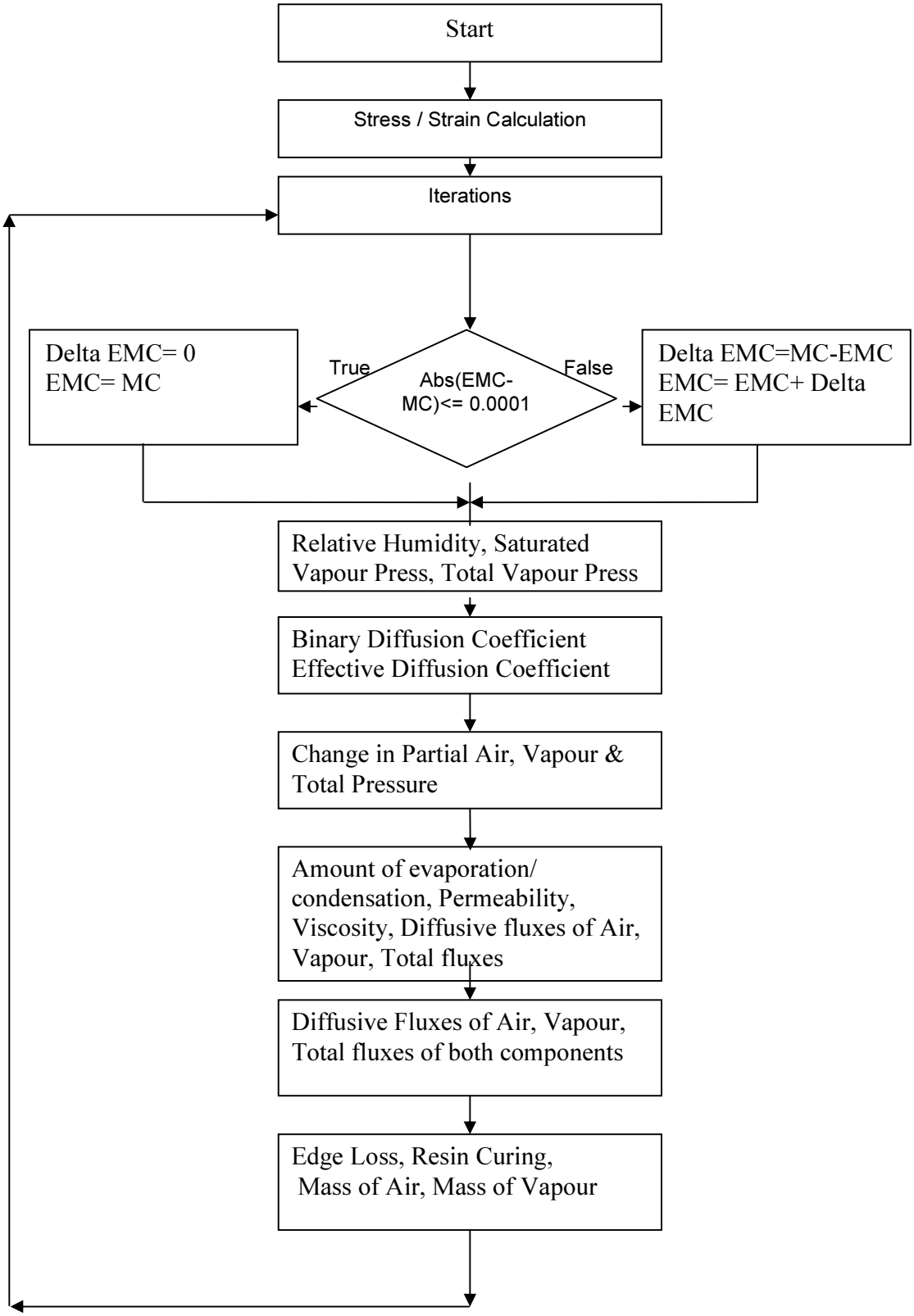

Figure 2.11: Procedures for heat and mass transfer calculation inside the iteration loop

2.3.5. Simulation Parameters and Simulation Results:

The parameters for a sample calculation are listed in Table 2.1 and the results plotted in Figures 2.12 -2.18. In the simulations, 50s of press time is shown to focus on the initial development of the density profile. In Figure 2.19, the sensitivity of the MOE modification constant was examined.

Table 2.1. Initial parameters for simulation

Target panel density	650 kg/m^3
Weight of fibre in one sample	1.11 kg
Moisture content	6.78 %
Resin content	9.5 %
Platen temperature	198°C
Pressing time	150 s
Press closing time	12 s
Average thickness	19 mm
Cycle used	Position
Value of p	1.25
Number of layers in half board	10
Initial mat thickness	38 mm

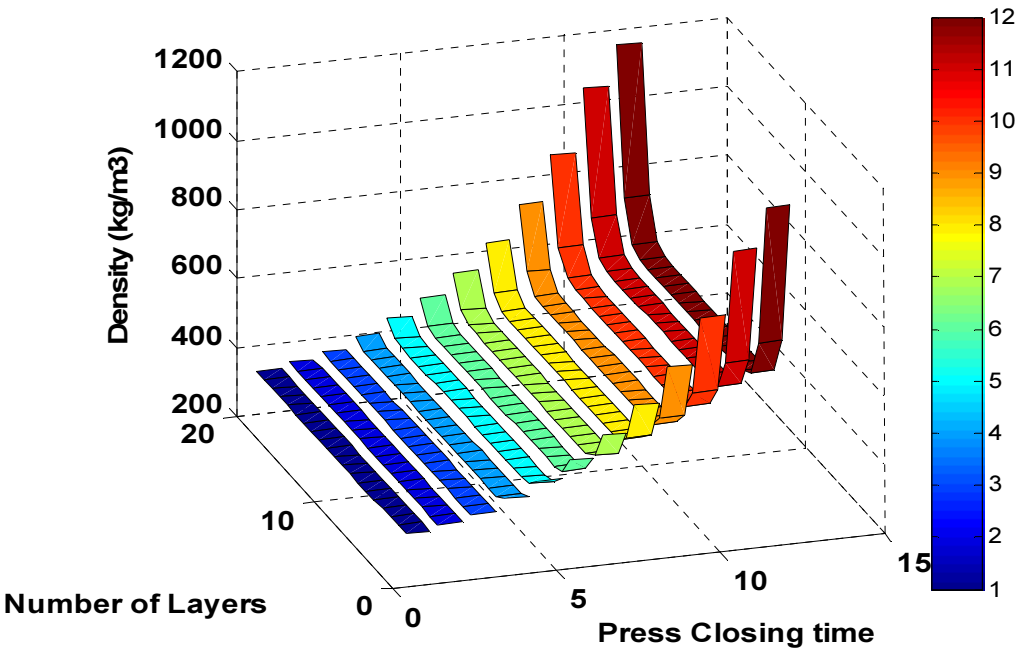

Figure 2.12: The development of density profile during press closing (time unit in sec).

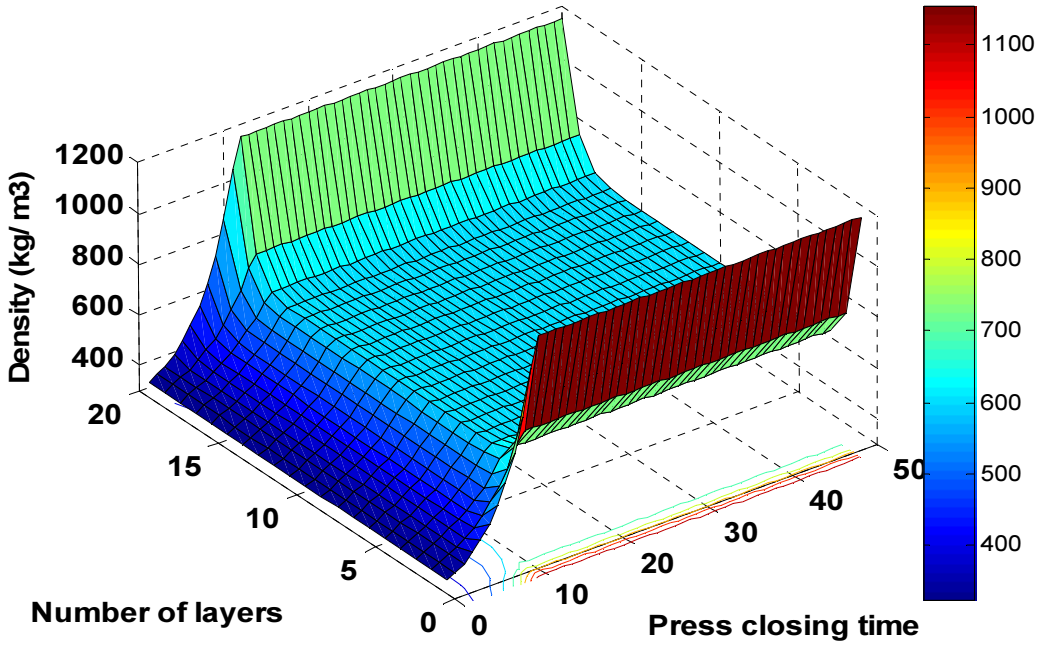

Figure 2.13: Simulated mat density of different layers as a function of pressing time

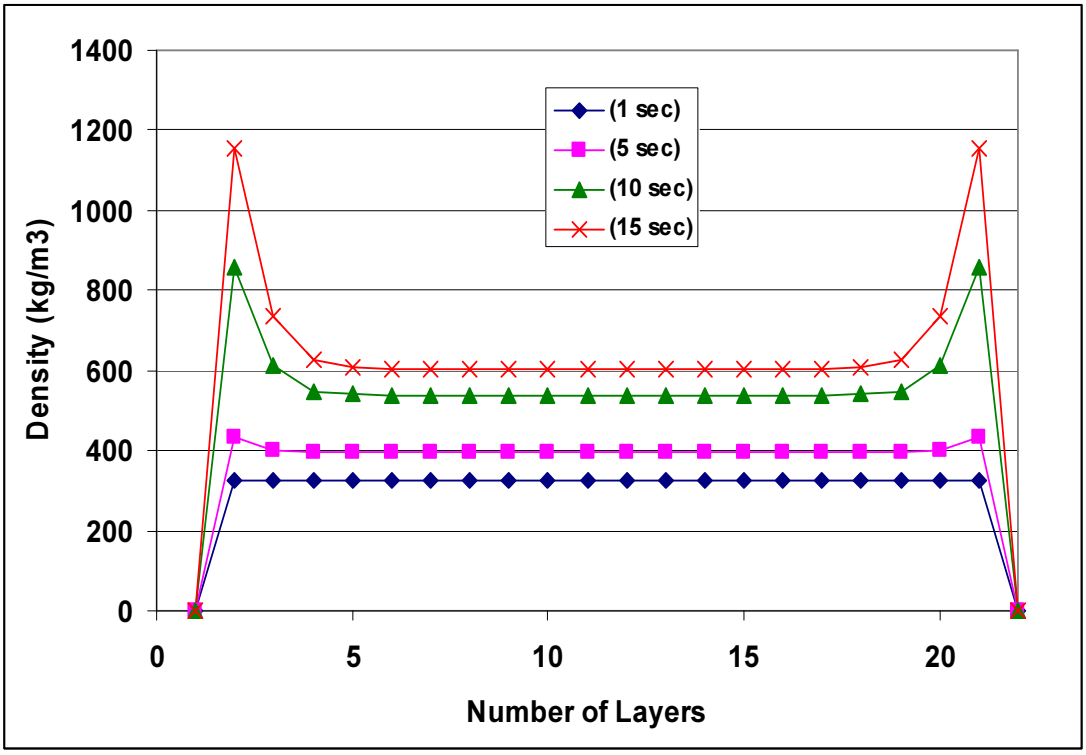

Figure 2.14: Development of density profile in the first 15 sec press cycle

The simulation is done for 150 seconds but the graphs are generated for only the initial 50 seconds, as most of the changes occur in the density profile are in the initial press closing time. (Press closing time is the time taken by the press platen to move from the initial stage, after pre-pressing, to the final thickness of the board). There is only slight density adjustment occur due to relaxation of fibres after this time.

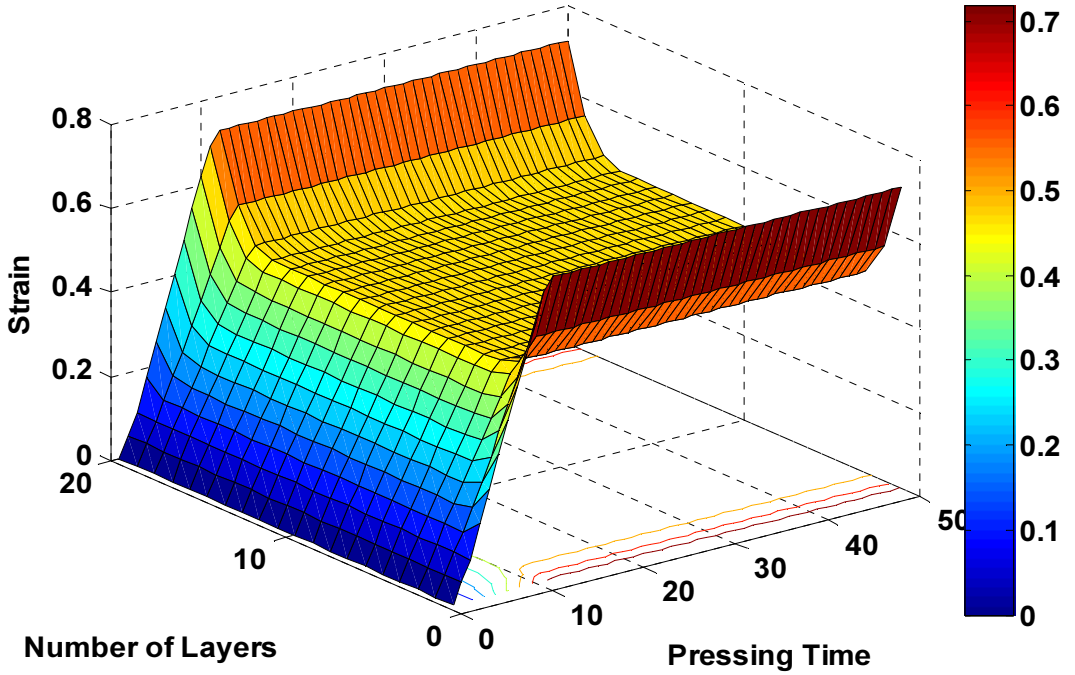

Figure 2.15: Strain development in different layers while pressing

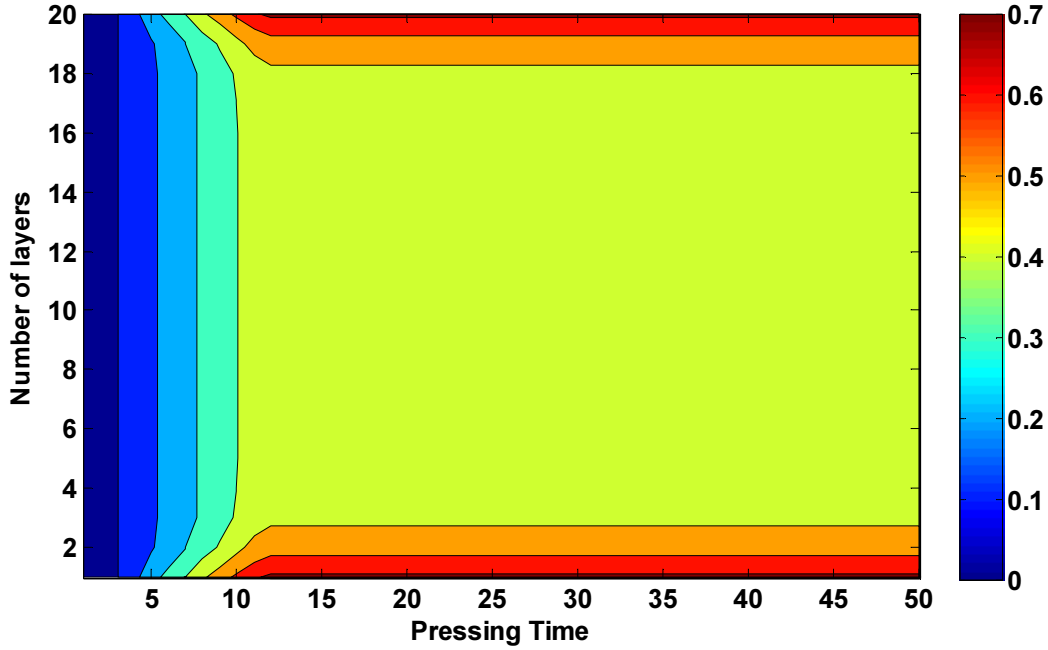

Figure 2.16: Contour figure of strain in different layers with time.

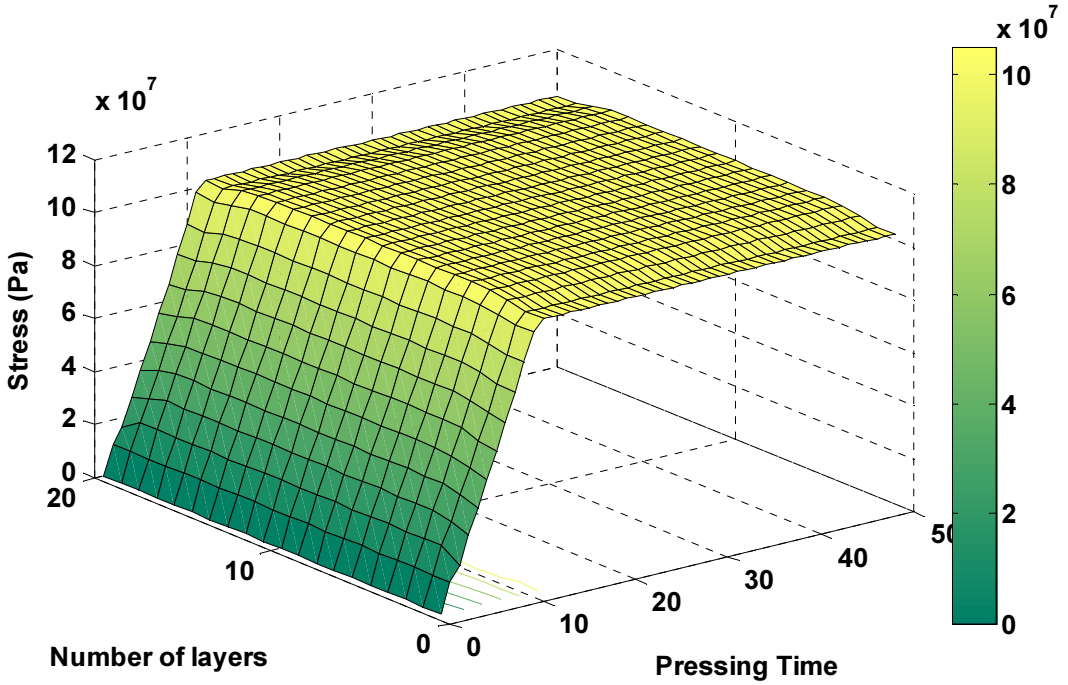

Figure 2.17: Stress development in different layers during pressing

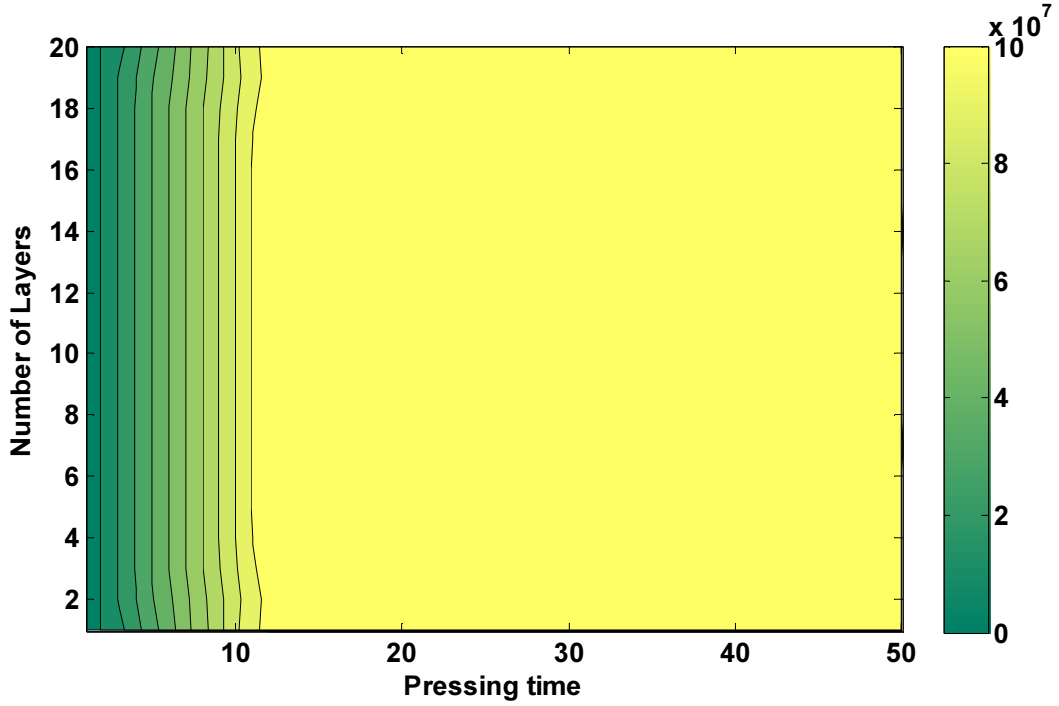

Figure 2.18: Contour figure showing stress in different layers with time.

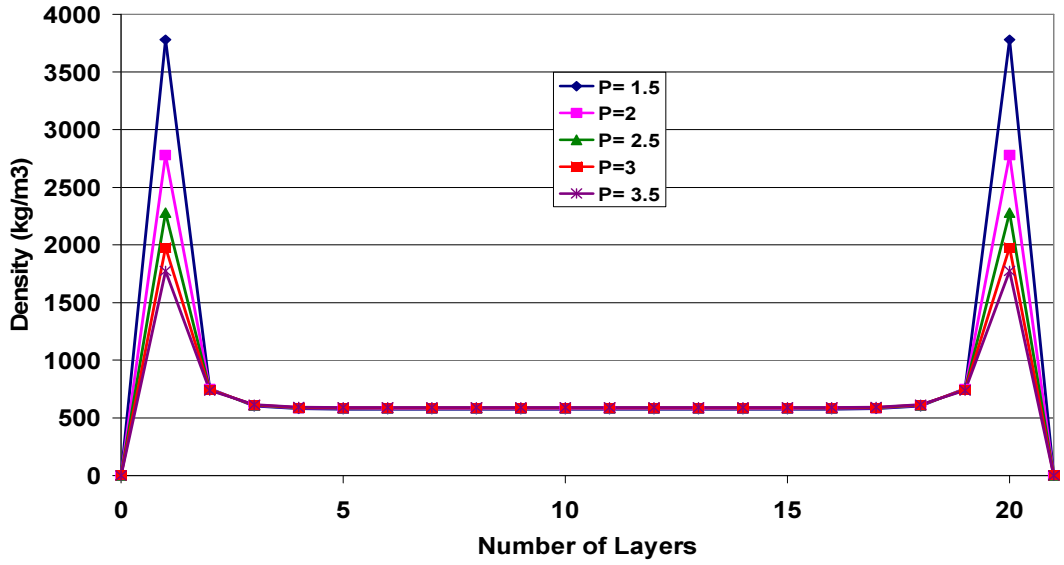

Figure 2.19: Effect of different values of MOE modification constant "P" on the predicted VDP.

2.3.6. Simulation Results for Gradual rise of Surface Temperature:

The earlier assumption that the surface layer reaches the platen temperature instantaneously is changed to the gradual rise of surface temperature in the press closing time and then the simulation results are compared.

As observed in the experimental work of Wang et al. (2000), there is a gradual rise of the surface layer temperature over the press closing time. For the modelling purpose, a similar trend can be obtained by assuming a linear rise of temperature with time until the platen reaches the final position. After that stage, the surface remains at the platen temperature for the rest of the press cycle.

Temperature Gradient (TG) = (Platen Temp – Initial Temp) / (Press Closing Time)

Surface Temperature = (TG x Time) + Initial Temperature.

Suppose the press closing time is 15 s and the platen temperature is 180˚C.Then the rise of surface layer temperature will follow the trend, as shown in Figure 2.20

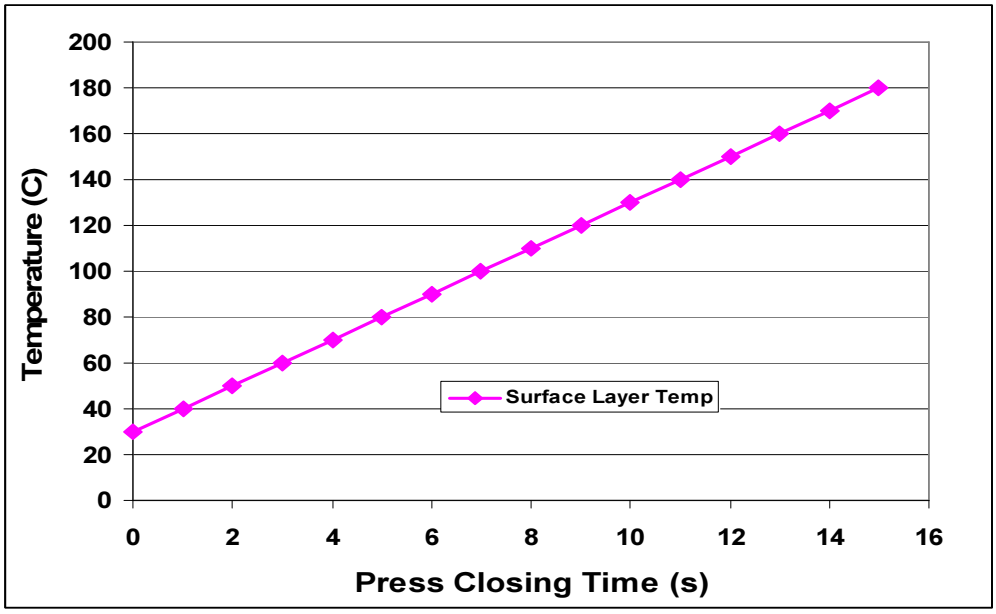

Figure 2.20: Showing the rise of surface temperature during the press closing time

Figure 2.21 shows the surface layer temperature for the complete press cycle.

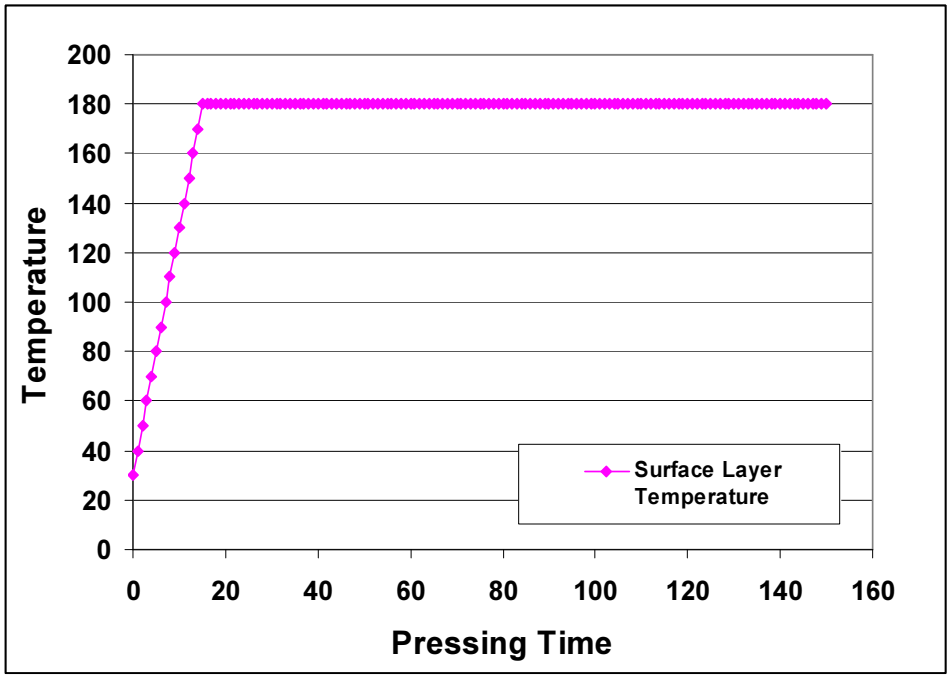

Figure 2.21: Showing the surface temperature in the complete pressing time.

To check the impact of press closing time on the density profile, three simulations were done at three different press closing times of 20, 25 and 30 seconds. The total pressing time was 60 seconds. The VDP obtained from the model is shown in the Figure 2.22.

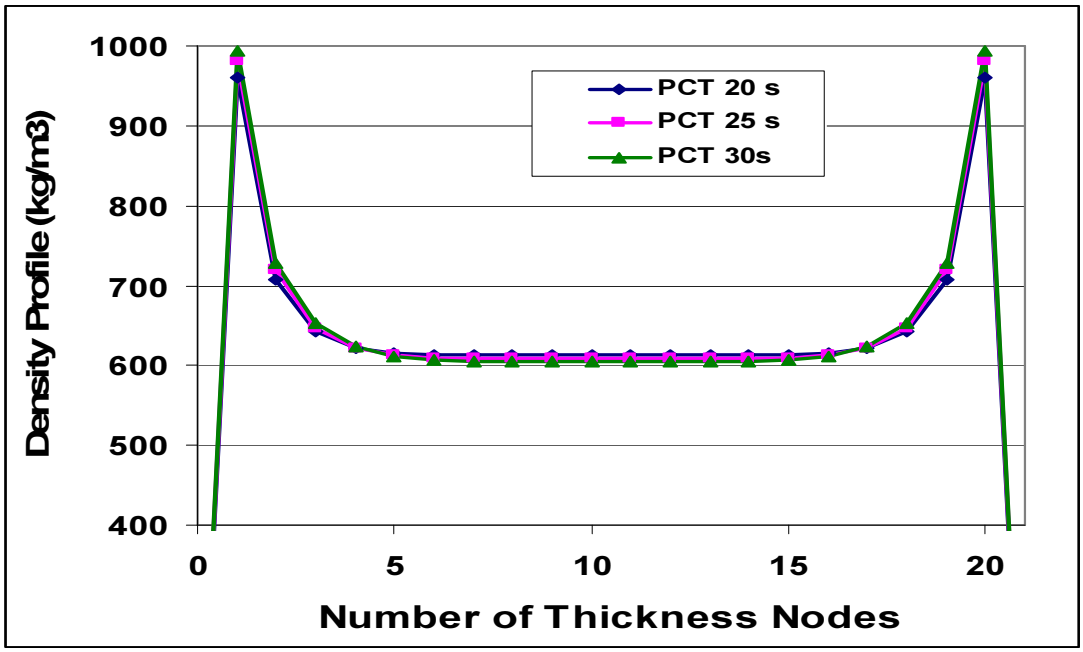

Figure 2.22: Showing the comparison of VDP at three different press closing times.

Table 2.2 Showing the peak and core densities at three different press closing time

Number of Thickness Nodes	Press Closing Time (20s)	Press Closing Time (25s)	Press Closing Time (30s)
Peak Density	960.96	980.54	993.64
Core Density	612.94	608.83	605.42

It is observed that with the increase of press closing time, the peak density increases and the core density decreases. The decrease in core density is very small.

For the same pressing parameters as given in table 2.1, the peak density is lower by 200 kg/m^3 and the core density increase by 15 kg/m^3. The results are closer to the experimental values than the results of simulations run using the earlier assumption. The reason for this difference lies in the fact that in the earlier case, due to the instantaneous

high temperature of surface layers, the modulus of elasticity reduced drastically, which results in high density of peak at the cost of core density. In the second assumption of gradual rise of surface temperature to the platen temperature, there is a more even distribution of temperature and so the pattern of density distribution is more close to the experimental results.

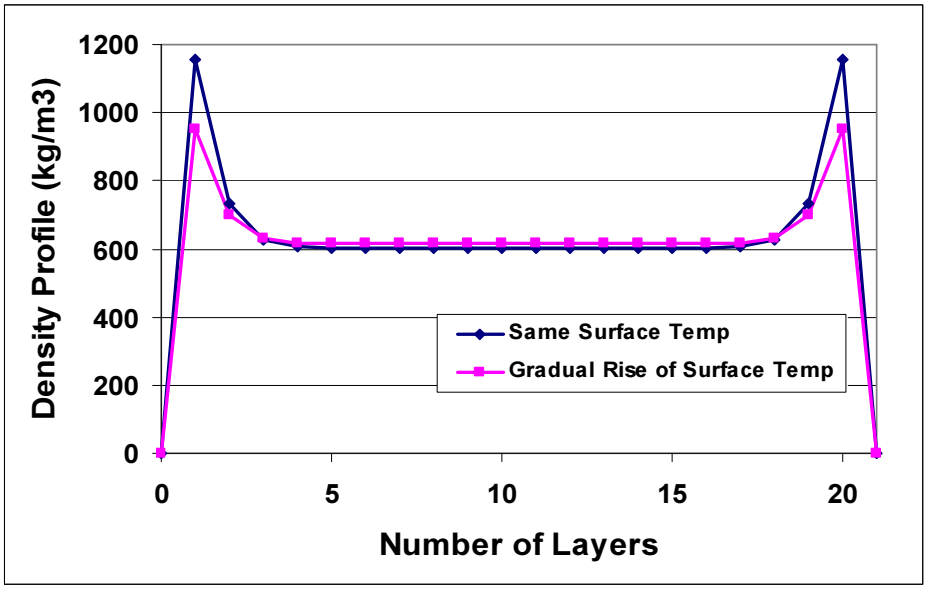

Figure 2.23: Comparison of density profile at two different surface temperature assumptions.

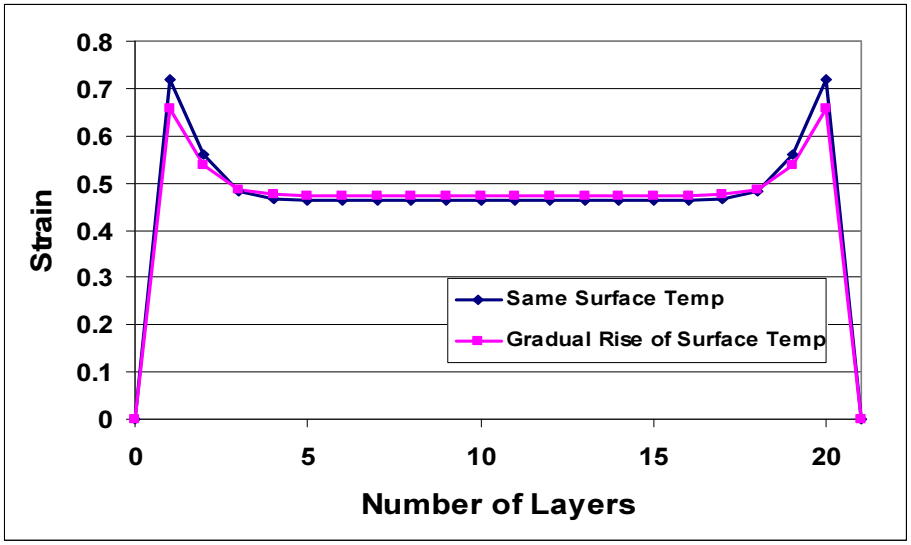

Figure 2.24: Showing the comparison of strain at two different assumption of surface temperature.

2.3.7. Simulation results for gradual rise of surface temperature with the constant time to reach surface layer the platen temperature:

Several simulations have been done with the changed assumption that surface layer reaches the platen temperature in a fixed time. In the first case, it is assumed that surface layer reaches the platen temperature in 12 seconds. The press closing time varies from 10 sec to 20 seconds. The simulation parameters are same as given in Table 2.1 The results are summarised in a Table 2.3.

Table 2.3 shows the peak and core densities at three different press closing time case one

Number of Thickness Nodes	Press Closing Time (10s)	Press Closing Time (15s)	Press Closing Time (20s)
Peak Density	810.17	991.73	1253.03
Core Density	610.96	585.47	561.95

It is observed that comparative increase in peak density and decrease in core density is higher than the earlier assumption.

In the second case, the time taken by surface layer to reach the platen temperature is 24 seconds. The results for the simulation are summarised in Table 2.4.

Table 2.4 Showing the peak and core densities at different press closing time case two

Number of Thickness Nodes	Press Closing Time (10s)	Press Closing Time (15s)	Press Closing Time (20s)
Peak Density	699.68	765.25	847.17
Core Density	631.48	616.43	600.89

As observed from Table 2.4, the difference in peak and core density in 10 second press closing time is less and the increase in peak density is also less.

2.3.8. Discussion:

Figures 2.12 to 2.14 show the sequence of development of the density profile during press closing. Initially all the layers have the same density but with the pressing proceeding, the density in the peak area increases much faster in comparison with the core region. The reason for this is that when the press-platen starts moving, the fibres near the surfaces are exposed to the immediate force and high temperature, and thus start compressing earlier than fibres in other parts of the mat. After a certain time, this compression zone moves towards the centre of the board and increases the core density. From the beginning of the programme, the press is assumed to have an iso-stress position. It means that all the layers will be under the same pressure in the thickness direction. Once the platen reaches its preset position for the target panel thickness, there is only minor adjustment in the density due to spring back action, but the overall density remains the same.

Figures 2.15 and 2.16 shows the development of strain in different layers. The mat after pre-press is considered as the beginning of press and at zero strain position. It is clear from the contour figure that all the layers have the same strain in the beginning but with the pressing time proceeding, strain near the surface increases much faster than the core layer. From Equation (2.9) it is known that the strain in different layers is inversely proportional to the modulus of elasticity of that layer. The value of MOE of layers near the surface is lower and the MOE in other layers is increasing towards the core region. The value of strain near the surface layer is between 0.6- 0.7 and the value in the core region lies between 0.4- 0.5.

Figures 2.17 and 2.18 shows the changes in stress in different layers with the pressing time. The calculations of stress are done as given in Equation (2.19) and follow the sequence as depicted through Figure 2.10. From Equation (2.19), the stress in the new time step consists of three components: stress in ‘old time’, strain change related stress

change and relaxation induced stress change. Due to the influence of all these three components, the stress near the surface is slightly lower than the core region and does not strictly follow the iso-stress position. But once the platen reaches to its final position corresponding to the target thickness the stress in all the layers is the same.

In Figure 2.19, all other conditions were kept constant and the value of the modification constant (p) was changed. The predicted peak density decreases significantly with increasing p while the core density only increases slightly with p. Based on these findings and practical VDP data, it is concluded that for MDF, the value lies somewhere in the range of 3 to 3.5

From the Figure 2.23, it is clear that changing the assumption, that surface temperature will immediately reach the platen temperature to that of the gradual increase during the press closing time, makes a significant difference in the prediction of peak and core density. For the same pressing parameters as given in table 2.1, the peak density is lower by 200 kg/m^3 and the core density has increased by 15 kg/m^3. The results are closer to the experimental values than the earlier assumption. The reason for this difference lies in the fact that in the earlier case, due to the instantaneous high temperature of surface layers, the modulus of elasticity reduced drastically, which resulted in high density of peak at the cost of core density. In the second assumption of gradual rise of surface temperature to the platen temperature, there is an even larger distribution of temperature and so the density of the board. Figure 2.24 shows the comparison of strain in both the boards.

2.4. Calculation of VDP based on An Empirical Model:

Mathematical modelling of the MDF density profile can predict the average density and density gradient through the panel thickness on given press conditions. This model consists of a number of mathematical formulae and needs mat physical properties and property correlations. For the purpose of practical operation and validation of the sophisticated mathematical model, an empirical model was also established based on experimental results and operation data. The empirical model offers simple correlations

to calculate target density profile from given operations conditions, mat initial thickness, target panel thickness and resin loading.

The advantage of this model is that it is easy for the people working in the industry. It did not require the knowledge of heat and mass transfer processes, viscoelastic properties and computer programming. It can be easily correlated from data collected by the production and quality department of MDF plant, during production of every thickness board. The production department record all the pressing parameters such as total amount of pressure applied, temperature of hot platen, total amount of pressing time and even press closing speed. In general the press cycle remains the same; it is only the duration of pressing time that differs in different thickness. The most important things, the quality department needs to know are peak and core density. On the basis of that, physical properties such as modulus of rupture (MOR), internal bonding (IB) and modulus of elasticity (MOE) can be correlated. The relationship of mean density with these physical properties is discussed in detail in Chapter six (Empirical Model).

2.4.1 Fitting Correlation for Empirical Model:

In order to validate the mathematical MDF density profile model and to develop an empirical model, experiments were performed in which 12 MDF boards of various thicknesses were made. The flat dimensions of the board were 50 cm length and 50 cm width. The amount of fibres in each board was the same (1.11 kg) but the thickness of the boards is different. The pressure cycle followed the same pattern as in commercial production. The starting pressure was one MPa but the pressure quickly reached 6 MPa which is needed to compress the fibre mat to achieve the required density profile. After the platens reached the final position corresponding to the target thickness, the pressure was reduced to 2 MPa. The temperature of the platen remained the same 198 ºC for all the twelve boards

Figure 2.25 shows the pressure cycle and Figure 2.26 shows the movement of the platen during the board making. The data for the pressure cycle and the platen position is

recorded for every ten seconds. The density data recorded for the twelve boards is shown in Table 2.5.

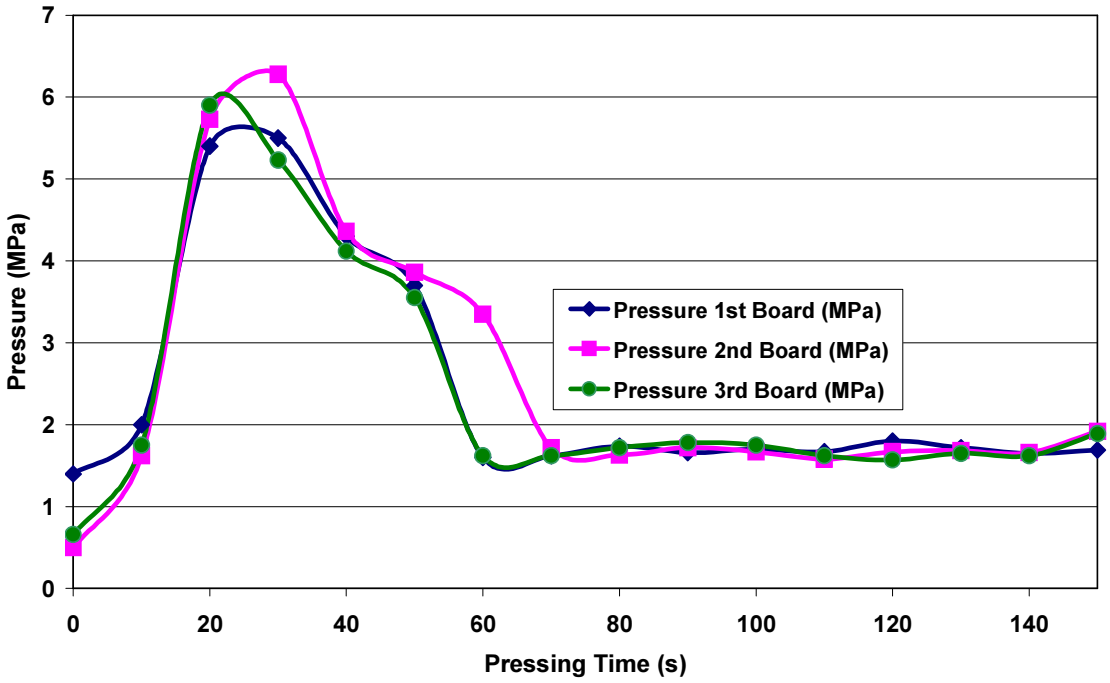

Figure 2.25: Change of platen pressure with time in the board making experiments.

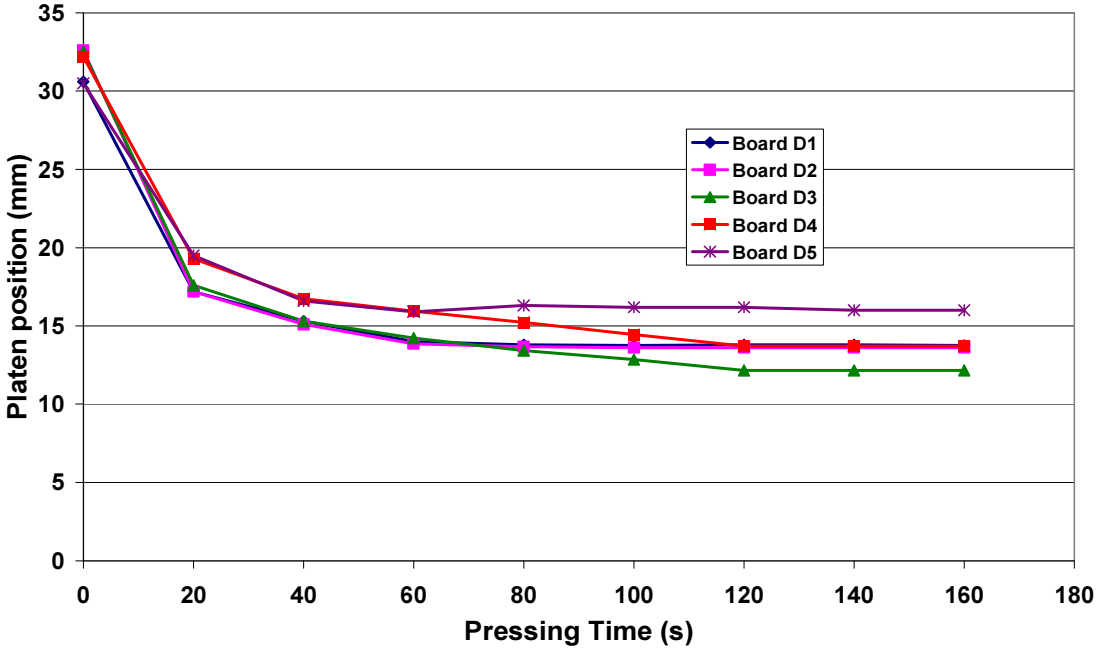

Figure 2.26: The change of platen position with time in the board making experiments.

From each of the MDF boards made, a sample of 50mm x 50mm was cut and placed in a density profile machine (ProScan) to obtain its vertical density profile (VDP) graph and typical examples are shown in Figure 2.27. The ProScan profiler works by measuring the amount of gamma radiation transmitted through the sample as emitted by a low energy radiation source, the working principle of ProScan is described in detail in Chapter three.

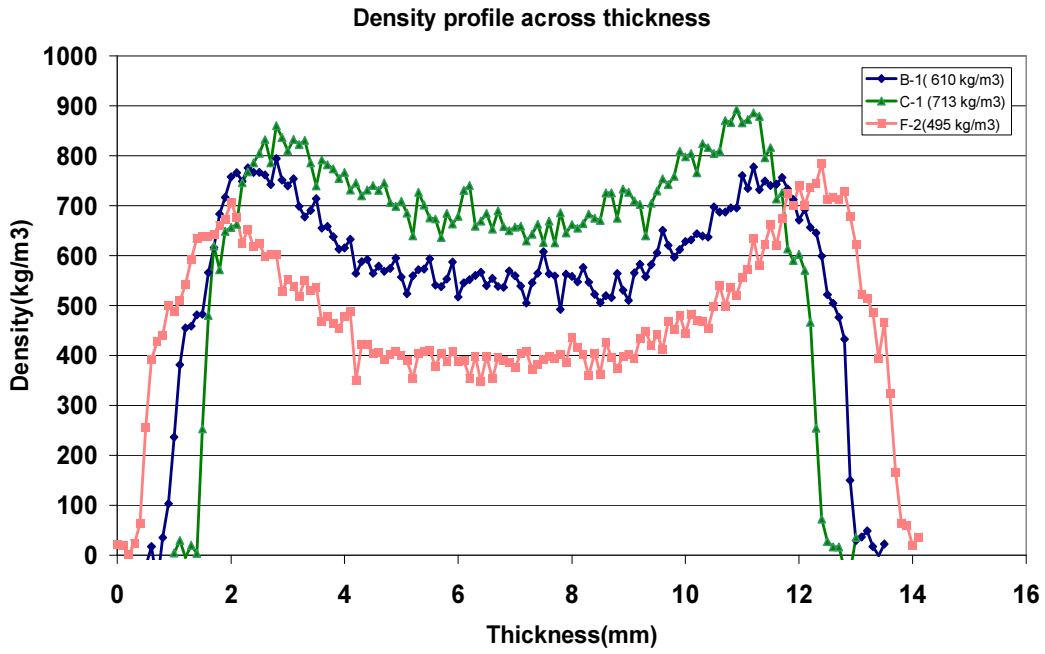

Figure 2.27: Typical density profiles across the thickness for three samples

Table 2.5. Experimental density data of 12 MDF boards

Mean density (kg/m^3)	Peak density (kg/m^3)	Core density (kg/m^3)	Difference between the peak and core density (kg/m^3)
485	706	398	308
516	821	418	403
524	792	419	373
526	792	423	369
545	805	445	360
547	817	420	397
565	854	452	402
587	794	552	242
600	876	563	313
616	817	530	287
717	915	694	221
718	853	666	187

Figures 2.28 and 2.29 plot the data of table 2.5. Figure 2.28 shows the relationship of peak and core density as a function of panel mean density. A linear relationship between the core density and the mean density shows a high correlation ($R^2 = 0.94$) whereas the correlation for a linear relationship between the peak density and the mean density is low ($R^2 = 0.57$). These two correlations have been used to predict the peak and core density for a given mean density.

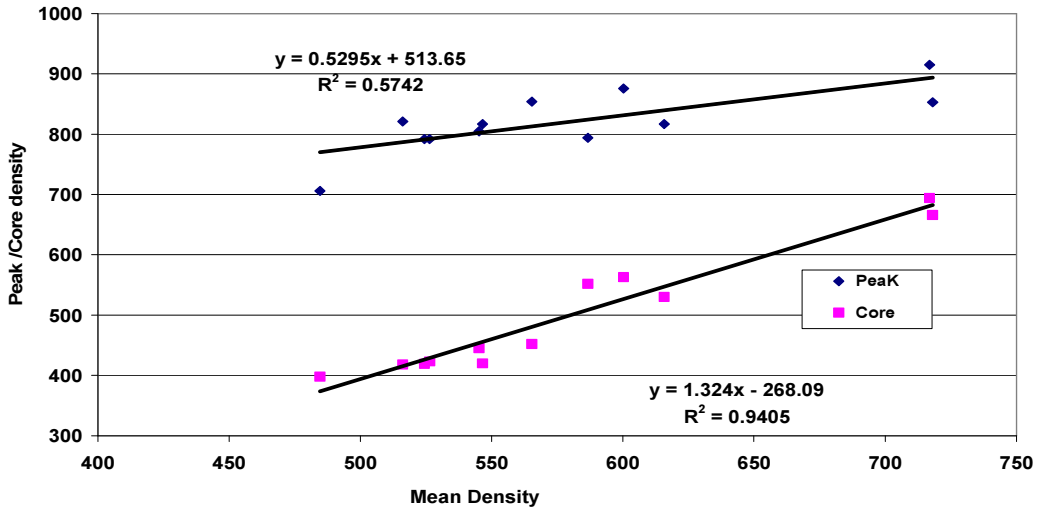

Figure 2.28: Fittings of the peak density and the core density as a function of with the panel mean density.

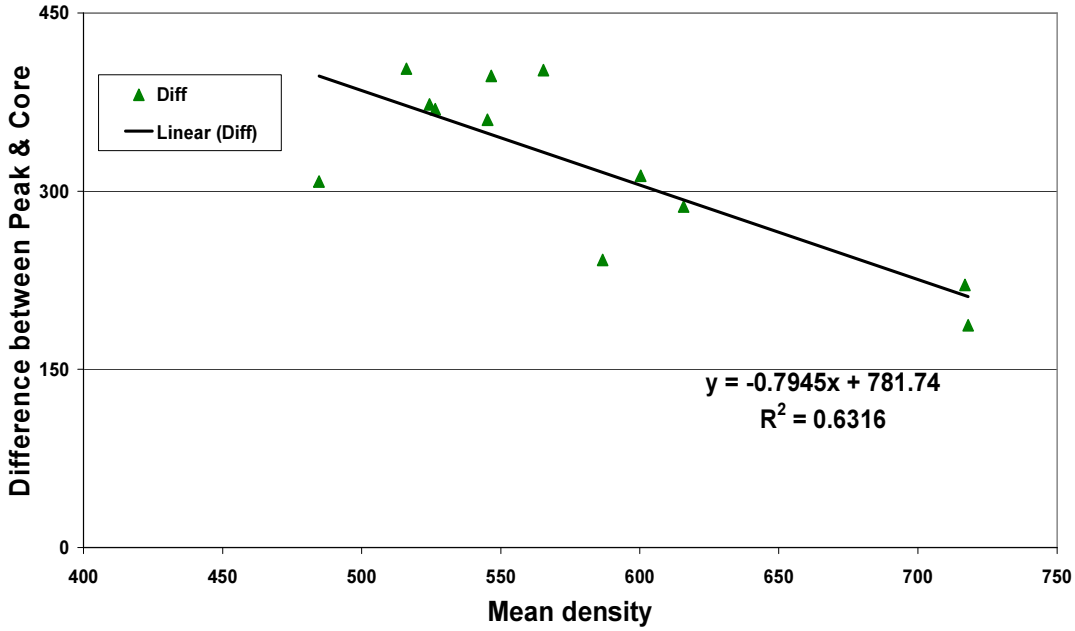

Figure 2.29: Fitting of difference between the peak and core densities as a function of panel mean density.

Figure 2.29 shows the relationship of the differences between the peak density and the core density as a function of the panel mean density. The difference between the peak and

core density tends to decrease with the increase of the mean density. A linear trend line was fitted between the mean density and the difference between peak and core density with reasonable correlation ($R^2 = 0.63$) as seen in Figure 2.29.

.

2.4.2. Results and Discussion:

To compare the results from both the mathematical model and the empirical model, eight simulations runs were performed in the mathematical model, using the same initial parameters as the experimental conditions. The peak and core density obtained from the mathematical model (Assumption: surface layer reaches platen temperature instantaneously) is then compared with the peak and core density predicted by the correlation derived from the empirical model and these are shown in Figures 2.30 and 2.31 together with the experimental data. From the Figure 2.30, it is observed that peak density from the mathematical model is higher than the experimental results. There will be a decrease in the difference by getting simulation results with the changed assumption of gradual rise of surface temperature, as discussed earlier in (Section 2.3.6). However, the core densities from both the models follow the same trend as that of the experimental data (Figure 2.31).

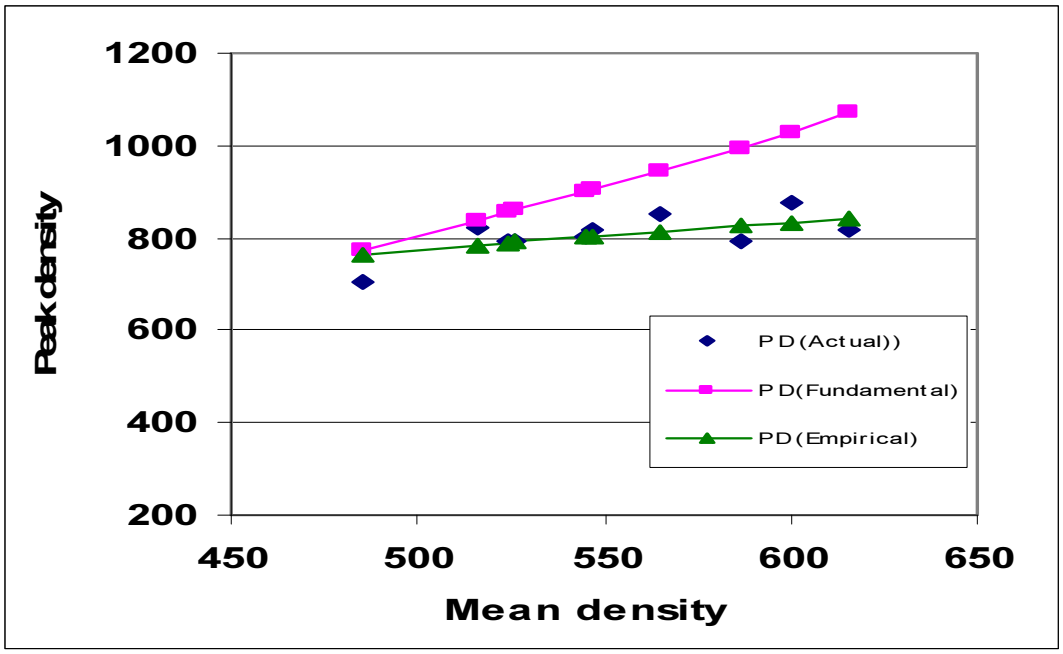

Figure 2.30: Change of peak density with mean density from the two models.

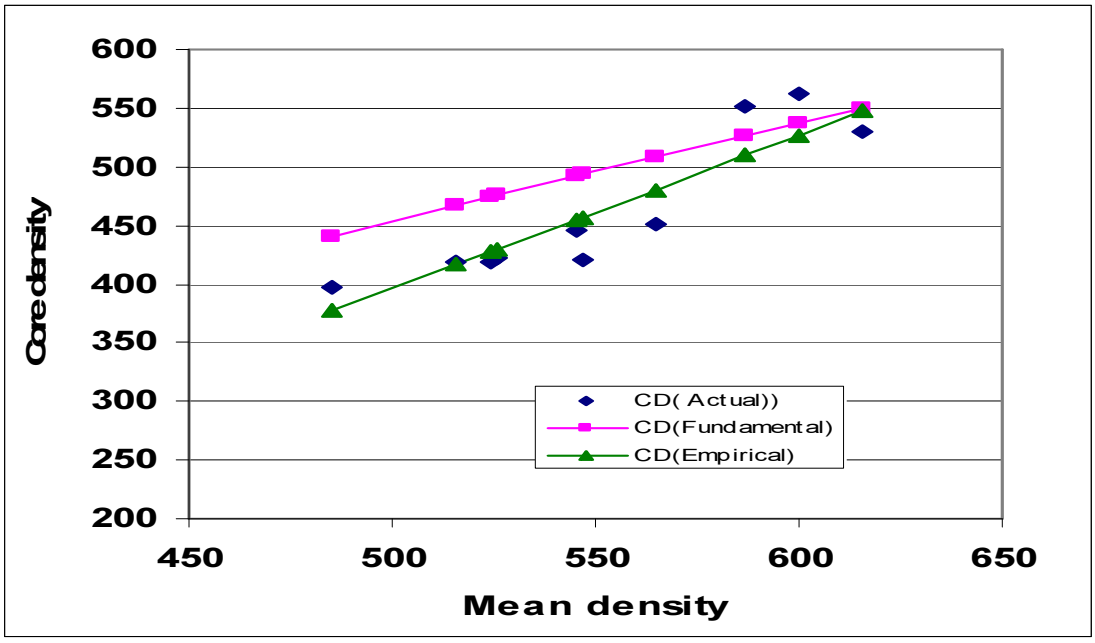

Figure 2.31: Comparison of core density from the two models

2.5 Conclusion of both Models:

Two different approaches have been tried to model the VDP of MDF board, each having its own merits and demerits. The fundamental, mathematical model has the capability to predict VDP for a wide variety of conditions. We can change several parameters such as platen temperature, initial moisture content of fibres, press closing speed and can observe the impact of these parameters on the final shape of VDP. The accuracy of the model can be improved by further fine-tuning the equations to calculate modulus of elasticity. The improvement may also be achieved by searching some other mechanical options, other than a Maxwell body to accurately simulate the viscoelastic properties of fibre mat under hot pressing. Thomen (2000) had tried a Burger-Humphrey model to predict the VDP but there were large differences between predicted and experimental results.

The Empirical approach is simple and straightforward thus can be applied in commercial operation for control and optimisation. The empirical model can predict peak and core density within the limits in which those relationships are derived, however, it needs

extensive experimental data and may induce large errors when being used beyond the condition range of the experiments.

More details are given in chapter six, about how the physical properties such as modulus of rupture, elasticity and internal bonding are related to the mean density.

Chapter- 3

Experimental Validation of Vertical Density Profile Model

Summary

The validation of the fundamental model among different pressing parameters is the focus of this chapter. In this chapter simulation results will be generated to predict the impact of different variables on the final density profile and the simulation results will then be compared with the experimental results. The ProScan profiler is used to measure the final density profile of the board. The model is validated for different platen temperature and different densities.

3.1 Introduction:

The density profile of MDF is not uniform; there is very high density near the surface and low density in the core region. All the physical properties such as modulus of rupture, modulus of elasticity and internal bonding are affected by the shape of the density profile. The bending strength increases when there is a large difference between peak and core density, but the internal bonding decreases. To manufacture high quality MDF board, there is a need to develop a better understanding of the whole process that takes place during hot pressing. Modelling of viscoelastic properties of fibres is one of the best options, as it will reduce the need for expensive experiments and we can observe all the parameters, which are otherwise difficult to see

3.2 Background:

Heebink et al (1972) found that moisture content, moisture distribution, press closing time and press platen temperature were the most important variables contributing to the vertical density formation, and other variables have only minor effects. They also

confirmed that an extremely rapid press closure time caused the highest density in the surface layer and a large density gradient. Strickler (1959) concluded that a high moisture gradient form in the case of high moisture content panels, and consequently the final density gradient, is more severe. He also found that rapid press closing results in high surface density and low core density. Andrews (1998) has clearly reinforced the previous findings that increasing moisture content enhances the vertical density gradient and that the peak density actually moves closer to the surface. Smith (1988) reported that the shape of the density profile is a function of the press closure rate, with a fast closing rate (30s) causing "U- shaped", and a slow closing rate (100s) causing "M-shaped", density profiles.

The above literature review indicates that production parameters affect the density distribution of the mat in the vertical direction. The following study exhibits the use of the modelling approach. The simulation gives good qualitative results and further refining of the equation to calculate viscoelastic properties of fibres will give more accurate quantitative results.

3.3 Materials and Methods:

3.3.1 Raw materials: The resinated fibres of *Pinus radiata* were supplied by Carter Holt Harvey Pine Panels, Rangiora. The moisture content of the fibres was 6.78% and resin content was 9.5 %, both based on the oven dry weight of fibres. The resin used was urea-formaldehyde. All the manufacturing of boards was done in two days before the expiring of the self life of the fibres.

3.3.2 MDF making: Fourteen MDF boards were made in the pilot press of Chemical and Process Engineering Department from the same batch of resinated fibre. The dimensions of board made were 300 mm x 300 mm. The target board thicknesses were 19mm and 24 mm. The target density was 600 and 650 kg/m^3 respectively A thermocouple wire and a transducer were inserted in the middle of the board after pre-pressing to get the core temperature and core gas pressure. The core temperature, core gas

pressure, platen pressure and position were recorded at 10 second intervals. The platen temperature was maintained at 160ºC and 198ºC.

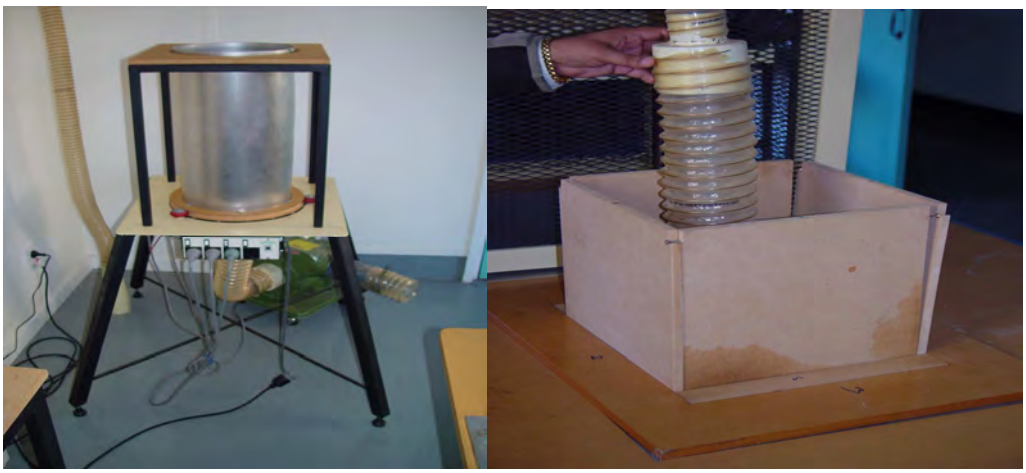

Figure 3.1: Rotatory bin for mixing of fibres and formation box to prepare fibre mat

3.3.3 MDF Press Cycle: The press cycle used for making these boards was similar to the cycle followed in batch pressing of commercial boards. The total pressing time was 350 seconds. A constant pressure control press cycle was used. In this case a force was applied to the platen by the hydraulic cylinder, which causes the platen to move to a position, where the force developed by the resistance of the material was equal to that developed by the hydraulic system at the current operating pressure. Two rectangular iron gauge bars of 19 mm and 24 mm thick were placed beside the mat to stop the press from compressing the board beyond the target thickness.

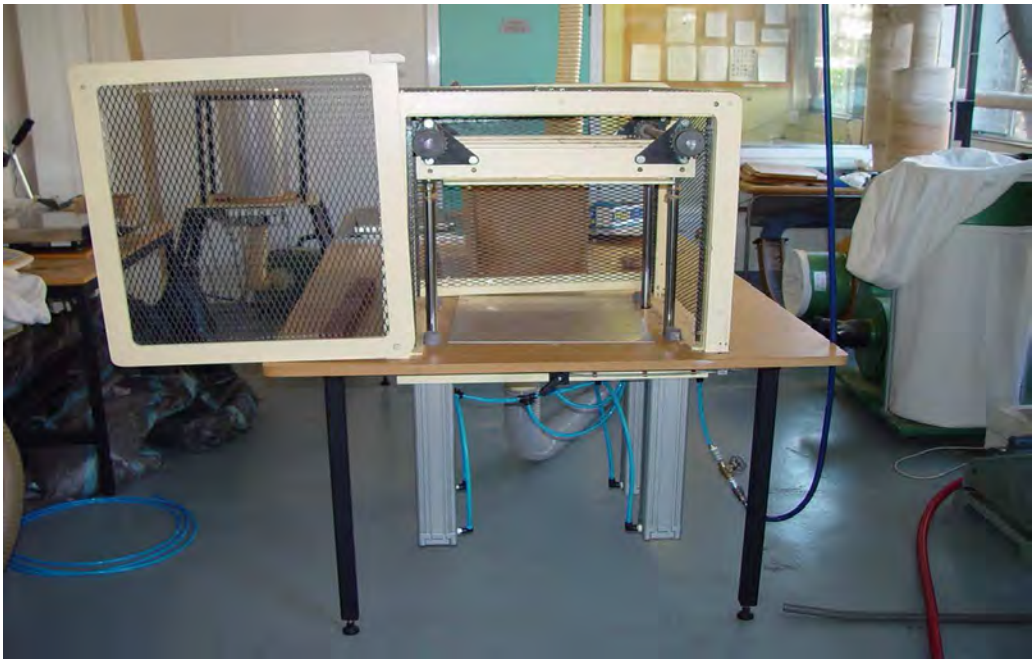

Figure 3.2: Prepress for compressing the mat

Figure 3.3: Pilot press for making board in the laboratory

3.3.4 MDF Testing: The boards were tested for their physical properties. A sample of 50mm x 50mm was cut and placed in a density profile machine (ProScan) to obtain its vertical density profile (VDP) graph. The ProScan profiler works by measuring the amount of gamma radiation transmitted through the sample as emitted by a low energy radiation source. After the VDP test, both surfaces of the sample were sanded to remove the precure layers of the board. The samples were then tested for internal bonding, modulus of rupture (MOR) and modulus of elasticity (MOE). All tests were conducted according to the procedure specified in AS/NZS 4266.5 (2004).

3.3.5 Measurement of the Final Density Profile:

The final vertical density profile was measured by ProScan Profiler, Model Number-9501 in the Forestry Department, University of Canterbury. The instrument is shown in Figure 3.4.

Figure 3.4: ProScan density profiler

Principles of Operation: A radiation detector is used to measure the amount of gamma radiation transmitted through the sample from a low energy radiation source as the sample travels through the beam. The higher the density of the sample in the path of the radiation, the lower is the amount of radiation transmitted. The radiation detected is confined to a narrow beam by slits in front of the source and detector and the radiation path is precisely aligned to be parallel to the sample faces, giving a high resolution profile.

Samples, nominally 50 mm square are mounted on the guide channel and the clamp is securely fastened to ensure the faces are parallel to the radiation beam. The samples are moved through the radiation beam on a stepper motor driven carriage, with linear steps of 0.015mm. This enables the sample to be driven between the source and detector in a precisely controlled fashion. As the sample is stepped through the radiation beam, the density is measured at the required points and a graph of the density plotted on the computer screen. Once the entire thickness of the sample is scanned the overall profile is sharpened, then displayed and stored together with summary information.

3.4 Results:

3.4.1 Case One: Effect of different densities on density profile:

Boards of two different average densities 600 kg/m^3 and 650 kg/m^3 were made and the other pressing conditions remained the same. The pressing parameters are given in Table 3.1. Press closing time means the time taken for the movement of press platen from the initial to the final thickness. After that the platen remains at that position for the rest of the time.

Table 3.1 Pressing parameters for two different densities but similar other conditions

Density	600,650 kg/m^3
Moisture content	6.78 %
Resin content	9.5 %
Platen temperature	160 ºC
Pressing time	390 s
Average thickness	19 mm
Cycle used	Pressure Cycle
Press closing time	45 s
Number of measurement points in half layer	10

Figure 3.5 shows the VDP of both the boards measured using the ProScan profiler. The pattern from both the boards follows the same shape because of the same pressing parameters. In ProScan results, all the density points are shown but for comparison with the model results, selected points are drawn. Each one mm of thickness in the 19mm board is divided into ten points by the ProScan profiler. The density value of every 10th point from ProScan result is compared with the Model. The purpose is to reduce the excessive number of ProScan points.

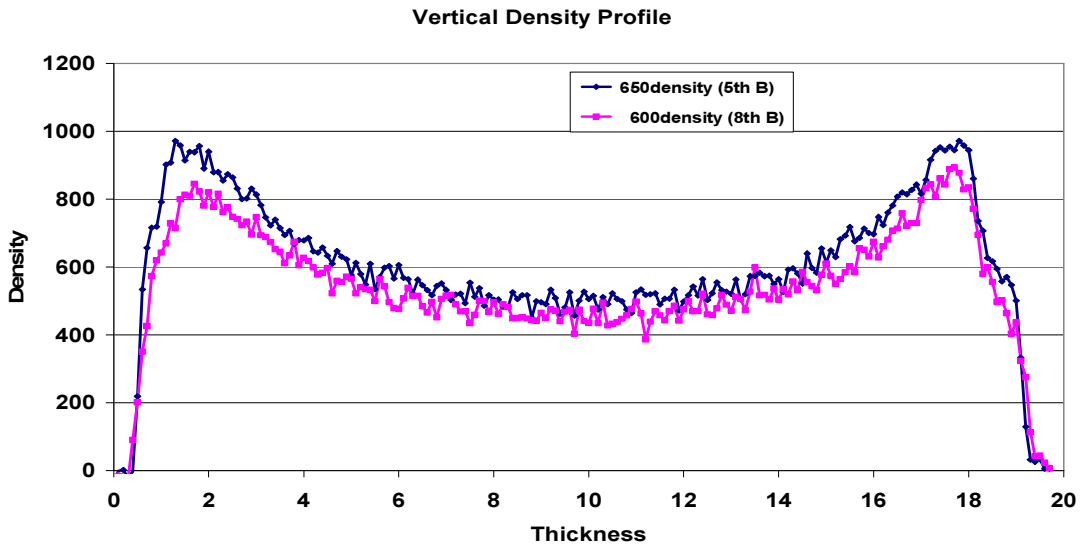

Figure 3.5: Density profile across boards of two different densities with similar pressing conditions. Experimental results from ProScan profiler.

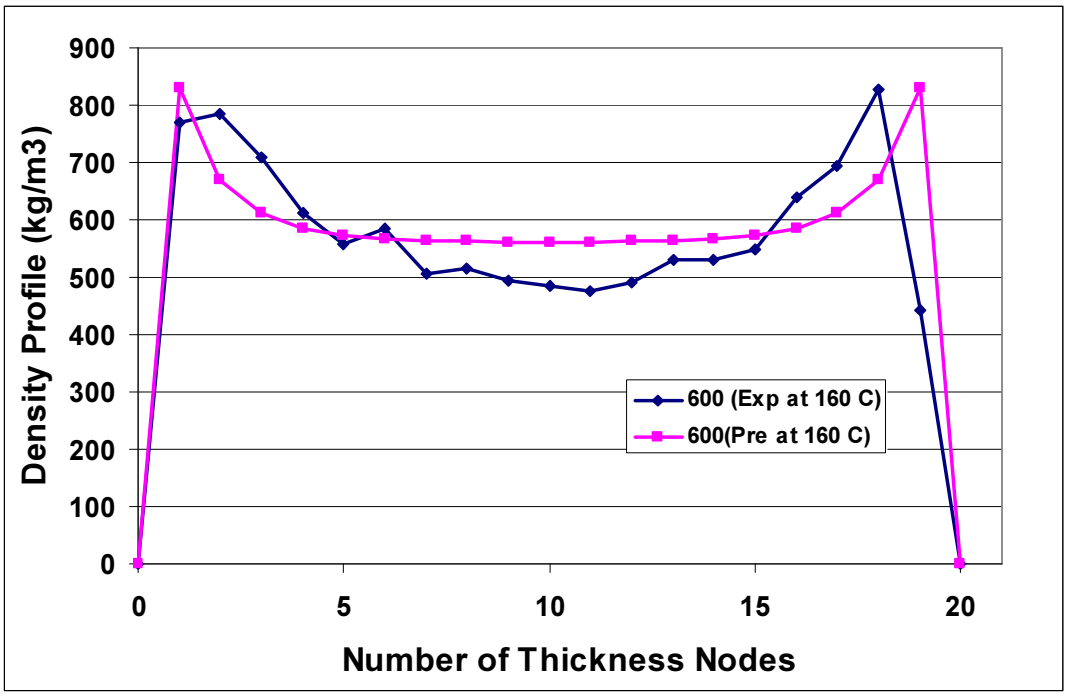

Figure 3.6: Comparison of predicted and experimental value of VDP for 600 kg/m^3 mean densities

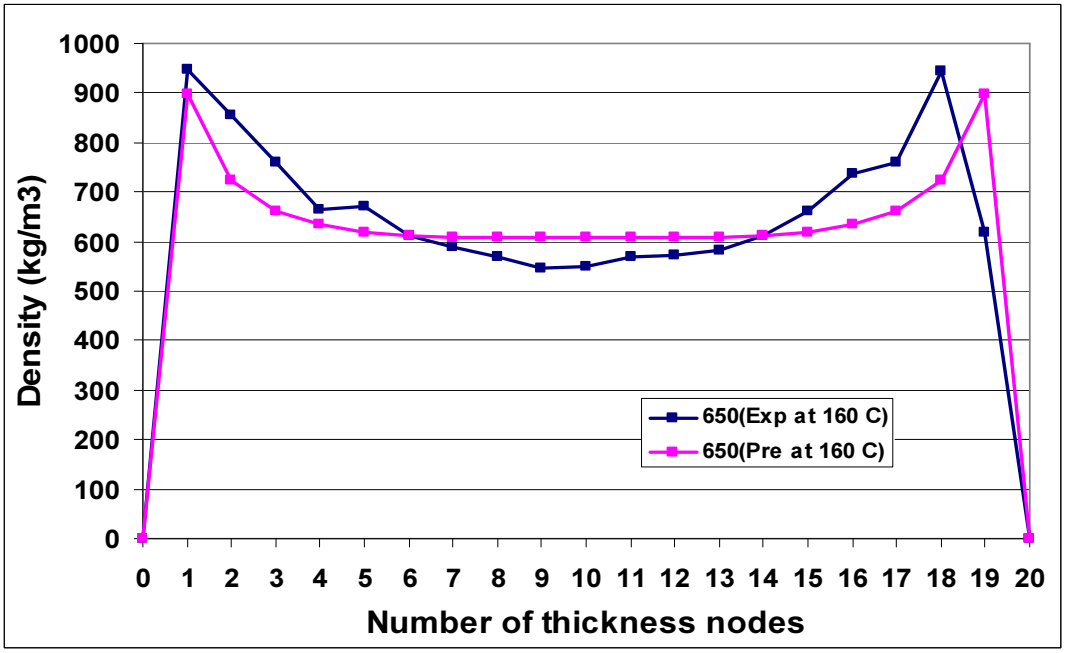

Figure 3.7: Comparison of predicted and experimental VDP for boards with mean density 650 kg m^{-3}

Figure 3.6 shows the comparison of VDP from both experiment and model for 600 kg/m^3 board, the peak density is nearly same as that of experimental value but the core density is higher. Figure 3.7 shows the comparison for 650 kg/m^3 density board. The peak density from the model is slightly lower than from the experiment.

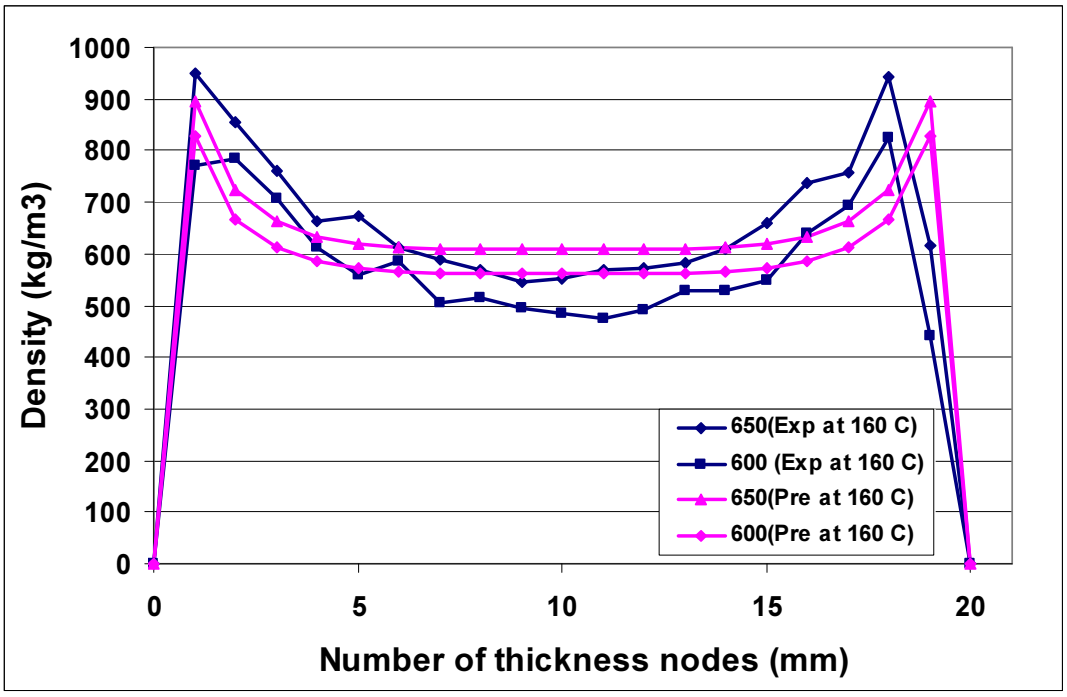

Figure 3.8: Comparison of VDP for the two boards from model and experiment

Figure 3.5 to 3.8 shows the comparison of predicted and experimental results. Figure 3.8 shows both the densities in one figure.

3.4.2 Case Two: Effect of different platen temperature on density profile

Two boards of same density of 600 kg/m^3 but with different platen temperature 160ºC and 198ºC were made. Pressing conditions are listed in Table 3.2.

Table 3.2 Pressing parameters for 600 kg/m^3 density but two different platen temperature

Density	600 kg/m3
Moisture content	6.78 %
Resin content	9.5 %
Platen temperature	160ºC & 198ºC
Pressing time	390 s
Average thickness	19 mm
Cycle used	Pressure Cycle

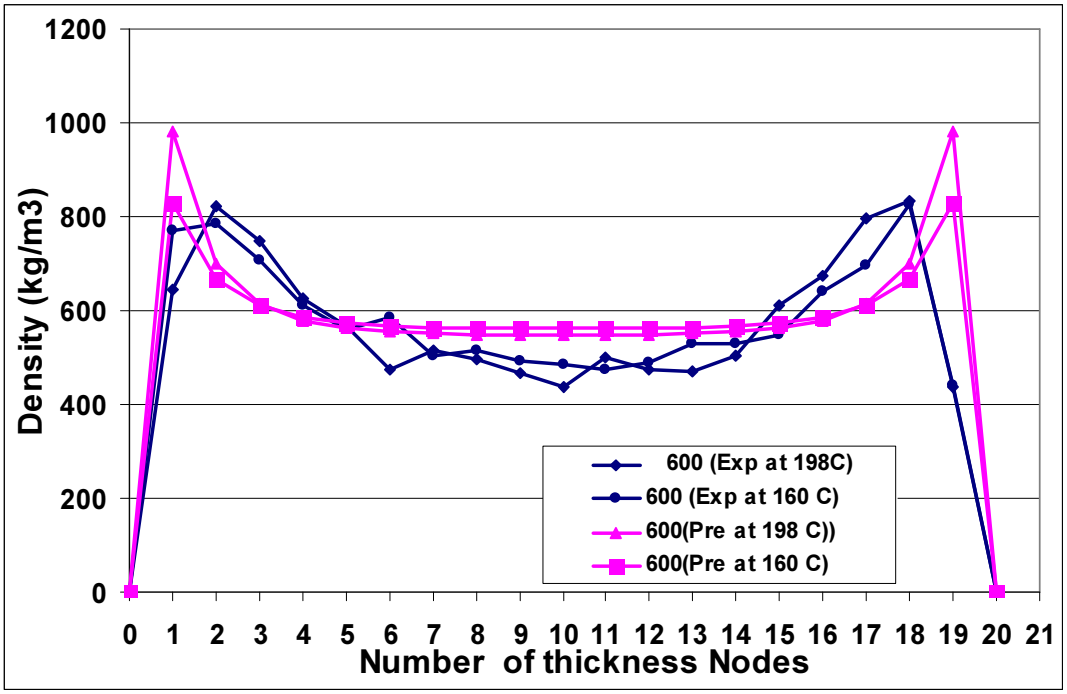

Figure 3.9: Comparison of VDP at two different temperatures

Figure 3.9 shows the comparison of predicted and experimental results for the similar pressing conditions but with different platen temperature. It is observed that with increasing platen temperature, the peak density increases and the core density decreases.

3.4.3 Case Three: Effect of different platen temperature on density profile

Two boards of same density of 650 kg/m^3 but with different platen temperature 160ºC and 198ºC are made, the pressing conditions is given in table 3.3.

Table3.3Pressing parameters for 650 kg/m3 density att two different platen temperatures

Density	650 kg/m3
Moisture content	6.78 %
Resin content	9.5 %
Platen temperature	160ºC & 198 ºC
Pressing time	390 s
Average thickness	19 mm
Cycle used	Pressure cycle

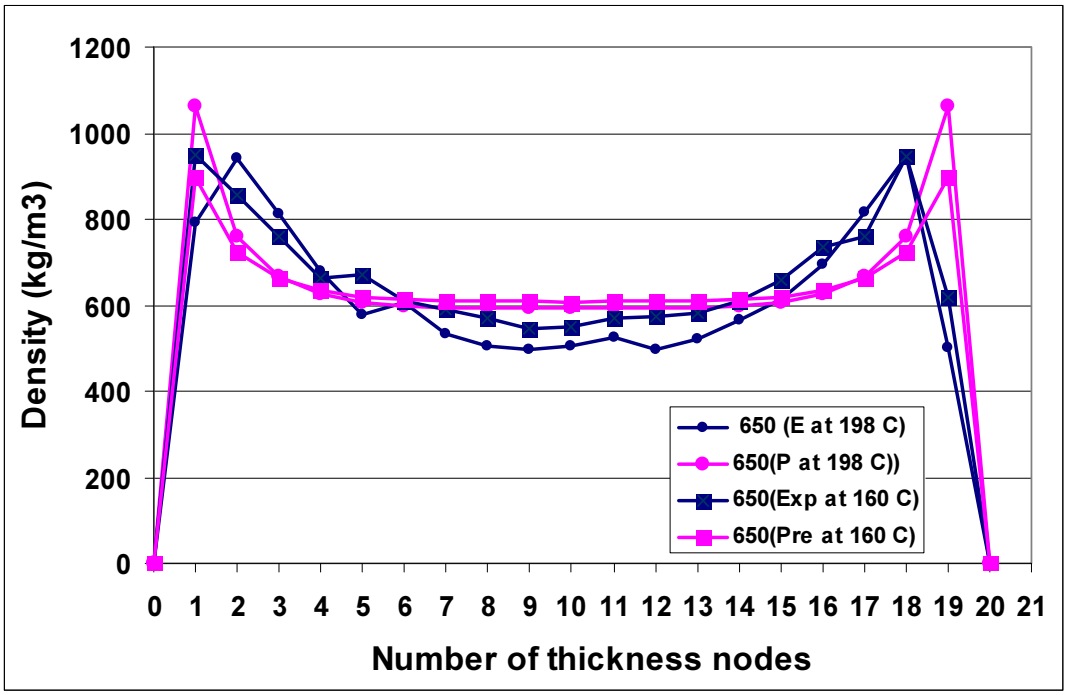

Figure 3.10: Comparison of VDP at two different temperatures

Figure 3.10 shows the comparison of predicted and experimental results for average density of 650 kg/m^3, and similar pressing conditions but with different platen

temperature. As in the previous case study, it was observed that with increasing platen temperature, the peak density increases slightly and the core density decreases.

3.5 Discussion of Validation of VDP results:

To describe the validation results in a better way, the mat is divided symmetrically into two parts, upper and lower half. The upper half is further divided into 10 layers (L1-L10). The surface layer is (L1) and central core layer is (L10).

Figures 3.5 to 3.8 show the comparison of density profile from the model and the experiments for two different density boards. In both these boards, the weight of the fibre is different, while the other pressing parameters are the same. It is observed in Figure 3.6 that predicted peak density (L1) and core density (L10) are slightly higher in comparison to the experimental results, but the other layers have lower density than obtained in the experimental results. With the increase in mean density by 50 kg/m^3, the predicted peak density decreases and the core density increases. The predicted surface layer (L1- L4) has lower density and the (L7 –L10) has higher density.

As explained earlier in chapter two, we know the displacement of the platen with time. This displacement is distributed in different layers in inverse ratio of modulus of elasticity (MOE) of that layer to the sum of modulus of elasticity of all the layers in the previous time step. The value of MOE depends upon temperature, moisture content, density and Palka constant (p) as given in equations 2.13 and 2.14. Due to the high temperature and low moisture content of the surface layer, the value of MOE is very low. This resulted in high density of the surface (L1) layer and low density of the subsequent layers as the mass of the fibre is conserved.

The value of Palka constant (p) also plays a significant part in the distribution of density in different layers. I did several simulations to check the impact of (p) on the density profile. As seen in figure 2.19, with the increase in the value of (p), the peak density decreases and core density increases across the thickness. For the present validation work the value of “p” is 1.25.

Figure 3.9 shows the impact of platen temperature on the density profile. In general the peak density increases and core density decreases with the increase of platen temperature. There is a distinct increase in predicted peak density by 150 kg/m^3 in comparison to the experimental result, where the increase is only by 10 kg/m^3. There is a large decline (50 kg/m^3) in core density in the experimental results in comparison to only a slight decline (13 kg/m^3) in the predicted results.

The increase in platen temperature resulted in higher peak density. The increase in platen temperature increases the plasticity of the surface layer, which causes more compression of the fibres and an increase in peak density. The high platen temperature increases the surface temperature and as a result lowers the value of the MOE. As the density distribution is inversely proportional to MOE, the surface density increases. The total amount of fibres is the same, final thickness is the same, average density is the same, so if the peak density increases, then the density in the core must decrease.

The reason for the decrease in core density is that the final thickness of both the boards with different platen temperature is the same. The total amount of platen movement is the same. Due to the high temperature there is more displacement in the surface layer and less in the core layers. This will result in a lower core density. In other words, due to less compression in the core region the density of the core is less.

Figure 3.10 shows the density distribution at higher density boards. The results follow the same trend as discussed in the earlier case of Figure 3.9.

Earlier, other researchers have used different analogues to simulate the viscoelastic properties of wood mat. Thomen (2000) used the Burger-Humphrey model to predict the VDP of wood composite. In the validation experiments in his thesis, he found that the predicted peak density was lower by about 200 kg/m^3 and core density was higher by 200 kg/m^3 in comparison to the experimental results. Zombori (2001) used modified Hooke's law in time. He calculated the stress of different layers, assuming a linear behaviour and

then multiplied it with a nonlinear strain function to represent the nonlinear response of a cellular material to an induced strain. In Zombori (2001) validation work, the predicted peak density was higher by 200 kg/m^3 and core density was slightly lower by about 20 kg/m^3 in comparison to the experimental results.

The probable reasons for the difference in predicted peak and core density in the present model are some simplifying assumptions. It is assumed in the present model, that the surface layer of the mat reaches the platen temperature gradually in the press closing time. If the press closing time is too small, then this assumption may not give accurate results. Secondly, it is assumed that all the moisture from the surface evaporates and brings the moisture content of the outer layer to zero percent. This may not be completely true; the outer surface may have a 1-2 % moisture content. There is no experimental data to show how the moisture content of the surface falls.

3.6 Conclusions:

The model predicted the general effects of production variables on the density profile formation qualitatively. The probable reasons for the differences in density profile from model and experimental work are first the mats for experimental boards were formed manually, which may result in non-uniform distribution of fibres. Secondly, the MOE was calculated from a modified equation which was initially derived for solid wood, so it gives higher values for initial conditions of fibre mat, when its density is much lower then wood.

The simulation results give the general trend for the MDF VDP. The model predicted the general effects of production variables on the density profile formation qualitatively. For quantitative prediction, more reliable data on modulus of elasticity (MOE) and stress relaxation modulus of the fibres needs to be determined experimentally.

Chapter- 4

Modelling the Heat and Mass Transfer during Hot Pressing of MDF

Summary

This chapter discusses the development of a one-dimensional mathematical model to describe the heat and mass transfer during the hot-compression of MDF composite panels. Five primary variables were considered during the model development: air content, water vapour content, bound water content, and temperature within the mat, and the extent of the cure of the adhesive system, characterized by the cure index. Different heat and mass transfer processes were identified for the transport of the heat and of the moisture phases. The heat was transported by conduction and convection due to a temperature gradient, and the exothermic energy released by the curing of the urea formaldehyde resin, while the water phases were transported by bulk flow and diffusion due to total pressure and concentration gradients. The resulting differential-algebraic equation system was solved by the finite difference method. The mathematical model predicted temperature, moisture content, partial vapour pressures and extent of adhesive cure within the mat structure under a typical hot-compression process. The model results allow a better understanding of the interacting mechanisms involved in a complex production process. The model can also assist to optimize the hot-pressing parameters for improved quality of MDF panel products, while reducing pressing time.

4.1 Introduction:

In the hot pressing of MDF panel, moisture content and temperature profile within the panel affect the mechanical and rheological properties of the mat thus also influence the density profile. The temperature profile is a result of heat transfer from the press surfaces, heat release of adhesive curing and the moisture phase change (water evaporation or condensation). The moisture content profile is caused by moisture phase change and moisture transfer within the panel during pressing.

Due to the interaction between the heat and mass transfer, the modelling of the temperature and moisture content profiles is highly non-linear and complicated. In this work, the heat release from the adhesive curing is modelled using empirical correlations and the heat and moisture mass transfer are modelled based on fundamental physical principles that include vapour convection, heat conduction and convection, and phase change, as initially proposed by Humphrey (1982). The heat and mass transfer model predicted temperature vapour pressure and moisture content development during the hot pressing. In Humphrey's model, a cylindrical coordinate system was employed to model a circular mat, so that axial as well as radial heat and mass transfer was accounted for. The model was solved using a finite difference method. The predicted data agreed well in trend with those observed experimentally for particleboard.

Hata et al. (1990) described a two-dimensional model to calculate the conductive heat flow in absolutely dry particle boards. Under such conditions, which do not occur in practice, vapour convection and moisture effects can be neglected. Hubert and Dai (1998) presented a one dimensional model for simulating hot pressing of oriented strand board (OSB) using an implicit finite element modelling approach. Mechanisms included are vapour convection, conductive and convective heat, heat transfer, phase change, adhesive cure and mat densification. The visco-elastic behaviour of the mat is neglected. Hubert and Dai (1998) compared model predictions of various parameters with measured data and reported that typical trends are predicted correctly, but that some magnitude discrepancies exist.

For MDF, a three-dimensional unsteady state model was presented by Carvalho and Costa (1998) describing the heat and mass transfer and predicting the spatial and time evolution of temperature, moisture content, steam pressure and relative humidity. Recently, the model developed by Humphrey (1982) for the hot-pressing of particleboard in a batch press has been improved and extended to the continuous process by Thomen (2000). However this model ignores the influence of resin cure. The present heat and mass transfer model is briefly described in Gupta.et.al (2007, 2006a, 2006b).

4.2 Model Development and Assumptions:

The heat and mass transfer model published by Thomen (2000) was adopted in this thesis as the basis for further model development. The resin curing and the heat released from resin curing are included in the heat transfer part of model. The equations used to calculate relative humidity and equilibrium moisture content are modified from earlier models. The bound water diffusion, which was neglected, is included in this model. The model is developed specifically for MDF and for batch and continuous pressing.

Several assumptions have been adopted to solve the problem imposed by the coupled heat and moisture transfer mechanisms during the hot-compression. These assumptions are:

1. The model is one dimensional, with changes normal to the platens considered.
2. Solid and gaseous phases are considered, and these two phases are always in local thermodynamic equilibrium.
3. The gas phase located in the voids is composed of an air-water vapour mixture, and the components follow the Ideal Gas Law.
4. Water can be present as bound water in the cell wall or as water vapour in the voids. The free water component is ignored due to the low initial mat moisture content of 8-12% typical for wood composite manufacture.
5. The heat supply of the process comes from the hot press platens and from the heat of reaction of the resin curing.
6. The physical and transport properties are functions of temperature, moisture content, density, porosity and steam pressure. Therefore they may vary with respect to space and time.
7. The heat is transported by conduction due to temperature gradient and by convection due to the vapour flow.
8. The vapour is transferred by bulk flow according to Darcy's Law and its diffusion in the air following Fick's Law. The driving force of the bulk flow process is the total pressure differential, while the driving force of diffusion is the concentration

difference which can be converted to partial pressure differential.

9. The migration of the bound water occurs by molecular diffusion due to a gradient in moisture content of the bound water molecules across the thickness.
10. The loss of gas through the edges is not considered in the simulation.

4.3 Heat Transfer:

In the modelling of heat transfer within the MDF mat, some thermal properties of the mat and the moisture will be needed and will be discussed first. These thermal properties include thermal conductivity and specific heat. Then the governing equation for the heat transfer will be developed based on energy conservation analysis.

4.3.1 Thermal Conductivity:

Von Haas (1998) measured the thermal conductivity of the MDF at zero moisture content and 30°C in the mat thickness direction through the mat, and gave a correlation as a function of mat density:

$$k_t^{0,30} = 4.86.10^{-8}\rho^2 + 4.63.10^{-5}\rho + 4.38.10^{-2} \qquad (4.1)$$

In which ρ is the mat density in kg m^{-3}.

$k_t^{0,30}$ denotes the thermal conductivity (W m^{-1} K^{-1}) at 0% moisture content and 30°C.

In order to reflect the effect of moisture content and temperature on the thermal conductivity, Haselein (1998) evaluated data presented by Shao (1989) and Kuhlmann (1962) and derived a correction term as follows:

$$\Delta k_t = 4.9\times10^{-3} MC + (1.1\times10^{-4} + 4.3\times10^{-5} MC)(T - T_{\exp}) \qquad (4.2)$$

Where MC is the mat moisture content (%) on dry basis and T is the mat temperature (°C). $T_{\exp}$ is the average experimental temperature used when measuring the thermal conductivity.

Therefore the full expression for the mat thermal conductivity is given as:

$$k_t = k_t^{0,30} + \Delta k_t \qquad (4.3)$$

An estimation of the effect of heat flux direction relative to the MDF panel on the thermal conductivity has been reported by Humphrey and Bolton (1989a). They suggested a separate correlation to calculate the thermal conductivity parallel to the mat plane:

$$k_{t,x-y} = 1.5 k_t . \qquad (4.4)$$

4.3.2 Specific Heat:

Haselein (1998) derived the following equation for the specific heat of the particleboard:

$$c = \frac{1131 + 4.19T + 4190MC}{1 + MC} \qquad (4.5)$$

In which c is the specific heat of the wood particleboard panel at current moisture content (J kg^{-1} $°C^{-1}$), T is the temperature (°C) and MC is the moisture content (%) on dry basis

4.3.3 Heat Conservation Equation:

In a general form, the energy balance on a differential volume element may be written as:

(Input)- (Output) + (Sources) = (Accumulation) (4.6)

The input and output terms account for energy flow through the faces of the volume element. These include the conductive heat flux (q) and the convective heat flux of the sensible heat (q_{sens}) carried by the moisture and the air. The sources term accounts both for the release or consumption of latent heat due to phase change, as well as for the

change of internal energy due to differences in specific heat (c) of the bound water and the water vapour.

Four components; dry wood, bound water, water vapour and dry air are considered in establishing the energy balance equation, which are represented by subscripts *w, b, v and a*, respectively.

The dimensionless mass content $u_i = m_i / m_w$ is defined as the local mass ratio of components *i* to the dry wood.

The mass content of dry wood, u_w, is defined as 1, the dimensionless mass content of bound water, u_b is the moisture content of wood on a dry weight basis.

The heat conservation equation for three-dimensional heat flow may be written in a form that follows the formulation of Nasrallah and Perre (1998) for convective drying of porous media.

(Conductive heat flow)- (Sensible heat flow in vapour) – (Phase change) = (Accumulation)

$$-\nabla.q - \nabla.\sum_{i=v,a}(c_i j_i T) - H_v^a m_{ev} = \rho_w \frac{\partial}{\partial t}\sum_{i=w,b,v,a}(c_i u_i T) \qquad (4.7)$$

Where H_v^a is defined by $H_v^a = H_v + (c_b - c_v)T$ (4.8)

The accumulation term on the right hand side describes energy storage in an infinitesimally small control region, while c_i denotes the specific heat of component *i,* ρ_w is the density of the dry wood and *T* is the local temperature.

The first term in the left hand side ($-\nabla q$) denotes the conductive heat flow. The second term on the left hand side, $-\nabla.\sum_{i=v,a}(c_i j_i T)$, expresses the sensible heat transport

associated with the mass flow (j_i) of the vapour or the air. The third term, $-H_v^a m_{ev}$, describes the energy source term due to the phase change. In the above equation, H_v denotes the latent heat of vaporisation of the bound water (J kg^{-1}) and m_{ev} is the evaporation rate in kg m^{-3} s^{-1}. The expression of $(c_b - c_v)T$ accounts for the difference in specific heat between bound water and water vapour.

As the mass of the moisture vapour and the air within the mat is very small compared to the mass of the wood and the bound water, the transfer of sensible heat associated with the gas flow, as well as heat consumed or released when increasing or decreasing the temperature of the gas may be neglected. A simplified form of the above equation may be written:

$$-\nabla.q - H_v m_{ev} + H_r m_r = c_u \rho_u \frac{\partial T}{\partial t} \qquad (4.9)$$

c_u : the specific heat of wood at current moisture content

ρ_u : the density of the mat at current moisture content.

The above equation includes conductive heat transfer as well as that share of convective heat transfer that comes from phase change. Convective heat transfer resulting from the transport of sensible heat is neglected.

4.4 Mass Transfer:

In the modelling of mass transfer within the MDF mat, some physical properties of the mat and the air will be needed and will be discussed first. These properties include viscosity of the air and vapour, vapour diffusion coefficient in the air, equilibrium moisture content and the humidity relationships. Then the governing equation for the mass transfer will be developed based on mass conservation analysis.

4.4.1 Viscosity:

For ideal gases, the viscosity (η) is independent of pressure and this applies to water vapour and air as a good approximation for pressure levels that can occur within a wood-furnish mat during pressing. The relationship of viscosity of gases with temperature is given by the Sutherland equation:

$$\eta = \frac{aT_{abs}^{1.5}}{T_{abs} + b} \tag{4.10}$$

Where T_{abs} is the temperature in *K*, and *a* and *b* are constants to be determined by fitting the equation to the experimental data. Humphrey and Bolton (1989a) derived the following equation for the viscosity of water vapour:

$$\eta_v = \frac{1.12 \times 10^{-1} (T + 273.15)^{1.5}}{T + 3211.0} \tag{4.11}$$

Thomen (2000) derived an equation for the air by fitting the experimental data of Munson *et al.* (1990). From this fitting, the air viscosity (η_a) is related to temperature by the following equation:

$$\eta_a = \frac{1.37 \times 10^{-6} (T + 273.15)^{1.5}}{T + 358.9} \tag{4.12}$$

The viscosity of a gas mixture also depends on its composition.

4.4.2 Molecular Diffusion Coefficient:

The empirical correlations most frequently found in the literature for gaseous diffusion suggest that the diffusion coefficient is inversely proportional to the total gas pressure and directly proportional to $T^{1.75}$ (Fuller *et al.,* 1966). From this relationship, the diffusion coefficient (*D*) at temperature *T* and pressure *P* can be calculated as:

$$D = D_1\left(\frac{P_1}{P}\right)\left(\frac{T}{T_1}\right)^{1.75} : \qquad (4.13)$$

Where D_1 is any known diffusion coefficient measured at temperature T_1 and pressure P_1. To derive such an expression for the binary diffusion coefficient (D_{va}) of the vapour-air pair, the experimental data reported by Cussler (1984) were substituted into Eq.(4.14):

$$D_{va} = 2.60\times10^{-5}\left(\frac{101325}{P}\right)\left(\frac{T_{abs}}{298.2}\right)^{1.75} \qquad (4.14)$$

Where:

D_{va} is the binary diffusion coefficient of the vapour-air gas pair ($m^2\ s^{-1}$).

P is the total gas pressure (Pa).

T_{abs} is the temperature (K).

4.4.3 Obstruction Factor for Molecular Diffusion:

The above diffusion coefficient is for the binary gas system, but in the MDF fibre mat, the gases diffuse within a porous medium. Therefore, an obstruction factor is introduced to reflect the resistance of the porous medium to the diffusive flux. The obstruction factor is a material property that depends upon the pore structure of the medium and is independent of the gas properties.

An equation derived from the experimental data measured at the Ordinariat fur Holztechnologie (University of Hamburg, Germany) to relate the dimensionless obstruction factor of the MDF mat to the mat density is given below:

$$k_d = 0.334e^{0.00508\rho}. \qquad (4.15)$$

4.4.4 Relationship between MC Change and Moisture Phase Change:

The principle of mass conservation requires that the mass change of the bound water is equal to the mass of the evaporated or absorbed water. The relationship between the evaporation rate m_{ev} and change in moisture content ΔMC during a small time step Δt is described by the equation

$$m_{ev} = -\rho_w \frac{\Delta MC}{\Delta t} \tag{4.16}$$

Where ρ_w is the density of the dry mat. The moisture content is the mass ratio of the bound water (m_b) to the dry wood (m_w) and is defined as

$$MC = u_b = \frac{m_b}{m_w} \tag{4.17}$$

The unit of the moisture content may be % or kg kg^{-1}.

4.4.5 Relative Humidity:

The relative humidity (RH or ψ) is defined as the ratio of the moisture vapour mass in the inert gas at a given condition to the moisture vapour mass when the gas is at saturation at the same temperature. Quantitatively, the relative humidity is equal to the ratio of the vapour partial pressure (p_v) to the saturated vapour pressure (p_{sat}), at a given temperature:

$$\psi = \frac{p_v}{p_{sat}} \tag{4.18}$$

The relative humidity can be defined in % or as a dimensionless variable.

The saturated vapour partial pressure (p_{sat}) at temperature T can be calculated by using fitted correlations from experimental data. Using Yaw's suggestions (Kayihan, 1983), the saturated vapour partial pressure can be estimated by:

$$p_{sat} = \frac{1.0133 \times 10^5}{760} \times 10^{f(T)} \tag{4.19}$$

in which $f(T)$ is a function of temperature which has a form as follows:

$$f(T) = 16.3737 - \frac{2818}{T} - 1.6908 \log_{10}(T) - 5.7546 \times 10^{-3} T + 4.007 \times 10^{-6} T^2 \tag{4.20}$$

4.4.6 Equilibrium Moisture Content:

Equilibrium Moisture content (EMC) is defined as the moisture content at which the material neither gains nor loses moisture at given conditions (temperature and relative humidity). EMC is a function of relative humidity and temperature.

For temperature above 150°C, the equation of Day and Nelson (1965) gives more stable results which have the following form:

$$EMC = \left[\frac{1}{A} . In(1 - \psi) \right]^{\frac{1}{B}} \tag{4.21}$$

The coefficients in equation (4.23) can be fitted from experimental data for low temperature (USDA, 1999; Ball *et al*., 2001) and for high temperatures (Resch *et al.*, 1988; Strickler, 1968). The following fitted coefficients are for average EMC of desorption and adsorption (Pang, 1997):

$$A = -0.34 \times 10^{-16} T^{5.98} \tag{4.22}$$

$$B = 348 T^{-0.946} \tag{4.23}$$

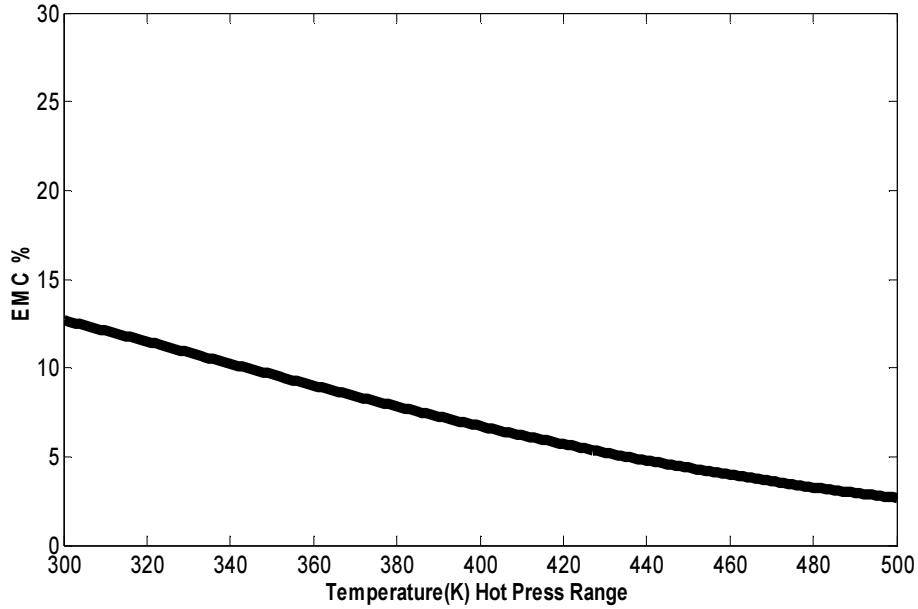

Figure 4.1: Change of EMC with temperature at RH= 0.75

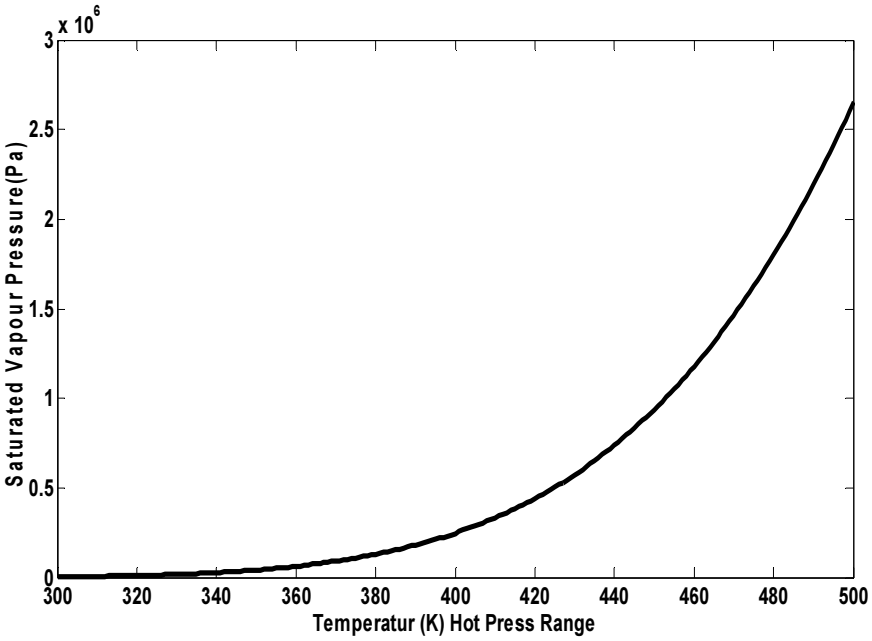

Figure 4.2: Change of saturated vapour pressure with temperature in hot press range

4.4.7 Equations Governing Mass Transfer:

Darcy's Law describes that the flux of a viscous fluid (which can be a liquid or a gas) in a porous medium is directly proportional to the pressure difference in the flow direction. The gas in the porous mat is regarded as a two-component mixture of air and water vapour. A convective (or viscous) flux j^c of the gas mixture develops in response to a total pressure gradient. The flux can be calculated by applying Darcy's Law. There is also diffusive flux (j^d) of each of the gas components due to concentration gradients of each component. The diffusion rate can be calculated by Fick's first law. The total flux j^i is the sum of both convective and diffusive fluxes.

$$j_i = j_i^d + j_i^c \qquad i = v \text{ or } a \tag{4.24}$$

The diffusive and convective fluxes, respectively, can be calculated from:

$$j_i^d = -D_{eff} \frac{M_i}{RT_{abs}} \nabla p_i \qquad i = v, a \tag{4.25}$$

$$j_i^c = -\frac{k_p M_i}{\eta R T_{abs}} p_i \nabla p \qquad i = v, a \tag{4.26}$$

Where

v, a Subscripts to denote vapour or air;

$j_i^{d,c}$ Diffusive or convective flux, respectively, of component *i* (kg m^{-2} s^{-1});

D_{eff} Effective diffusion coefficient (m^2 s^{-1});

M_i Molecular mass of component *i* (kg mol-1);

p_i Partial pressure of component *i* (Pa);

p Total gas pressure (Pa);

R Gas constant (J mol^{-1} K^{-1});

T_{abs} Absolute temperature (K);

k_p Permeability coefficient (m^2);

η Dynamic viscosity of the gas mixture (Pa s).

The effective diffusion coefficient, D_{eff}, is dependent on the binary diffusion coefficient, D_{va}, of the vapour-air gas pair and on the dimensionless obstruction factor, k_d,which is a property of the porous material (Krischer, 1963):

$$D_{eff} = \frac{D_{va}}{k_d} \tag{4.27}$$

4.4.8 Derivation of Modified Mass Conservation Equation:

The equation given by Thomen (2000) for the calculation of mass conservation has neglected the water vapour evolved from resin curing of urea-formaldehyde. The equation has been modified here to include that term. The equation derivation is given below:

In general form, the mass balance is established based on a small volume element which has a volume of $V = \Delta x \Delta y \Delta z$. The mass balance is considered as follows:

(Input)- (Output) + (Sources) = (Accumulation) (4.28)

or

$$(\Delta y \Delta z \Delta t . j_x\big|_x \; - \Delta y \Delta z \Delta t . j_x\big|_{x+\Delta x} \ldots - \ldots) + V . \Delta t . m_{ev} + V . \Delta t . m_r = m\big|_{t+\Delta t} - m\big|_t \tag{4.29}$$

Where the expression within the brackets contains the fluxes j in the direction of all three coordinates. The variables t, m_{ev}, m_r and m denote time, evaporation rate, water from resin curing and mass of vapour respectively. Dividing by V and Δt and writing

the equation in a one-dimensional form, we get the one-dimensional moisture mass conservation equation as follows:

$$-\frac{\partial j}{\partial x} + m_{ev} + m_r = \frac{1}{V}\frac{\partial m}{\partial t} \tag{4.30}$$

It is assumed that all the water produced by the curing of resin is in vapour form. In the above equation, m_r is the rate of water vapour produced during adhesive curing (kg m^{-3} s^{-1}) and m_{ev} is the evaporation rate of the bound water (kg m^{-3} s^{-1}).

If the gas within the porous material is assumed to be an ideal mixture of perfect gases, then the Ideal Gas Law can be used to relate the vapour mass m within the void volume of the material (V_{eff}) to the prevailing partial vapour pressure (p) and the absolute temperature (T_{abs}):

$$p.V_{eff} = \frac{m}{M} R.T_{abs}$$

In which, M is the molecular mass of the vapour and R is the gas constant. Substituting m into the previous equations yields:

$$-\frac{\partial j}{\partial x} + m_{ev} + m_r = \frac{M}{R}\frac{1}{V}\frac{\partial}{\partial t}\left(\frac{p.V_{eff}}{T_{abs}}\right) \tag{4.31}$$

Applying the relationship of the void fraction of the porous material, where $\phi = \frac{V_{eff}}{V}$, the above equation may be written as:

$$-\frac{\partial j}{\partial x} + m_{ev} + m_r = \frac{M}{R}\frac{\partial}{\partial t}\left(\frac{p\phi}{T_{abs}}\right) \tag{4.32}$$

Differentiation with respect to t on the right hand side yields:

$$-\frac{\partial j}{\partial x}+m_{ev}+m_r=\frac{M}{R}\left[\frac{1}{T_{abs}}\frac{\partial(p\phi)}{\partial t}-\frac{p\phi}{T_{abs}^2}\frac{\partial T_{abs}}{\partial t}\right]=\frac{M}{RT_{abs}}\left[p\frac{\partial\phi}{\partial t}+\phi\frac{\partial p}{\partial t}-\frac{p\phi}{T_{abs}}\frac{\partial T_{abs}}{\partial t}\right] \tag{4.33}$$

Multiplying by R and T_{abs}, and dividing both sides by M give:

$$-\frac{RT_{abs}}{M}\frac{\partial j}{\partial x}+\frac{RT_{abs}}{M}m_{ev}+\frac{RT_{abs}}{M}m_r=p\frac{\partial\phi}{\partial t}+\phi\frac{\partial p}{\partial t}-\frac{p\phi}{T_{abs}}\frac{\partial T_{abs}}{\partial t} \tag{4.34}$$

After rearranging the terms, the equation may be written in its final form:

$$-\frac{RT_{abs}}{M}\frac{\partial j}{\partial x}-p\frac{\partial\phi}{\partial t}+\frac{p\phi}{T_{abs}}\frac{\partial T_{abs}}{\partial t}+\frac{RT_{abs}}{M}m_{ev}+\frac{RT_{abs}}{M}m_r=\phi\frac{\partial p}{\partial t} \tag{4.35}$$

The mass conservation equation for the dry air has the same form, except that the terms m_{ev} and m_r can be ignored as no air is generated or consumed within the volume element.

4.4.9. Moisture Content Profile:

In solving the model, the initial mat moisture content is assumed to be uniform throughout the thickness. When the hot platen touches the surface of the mat, the water from the surface starts to evaporate. Due to the low humidity and high temperature at the mat surfaces, it is assumed that the surface layer soon reaches to zero moisture content level after hot pressing starts. This causes a steep moisture content gradient between the surface and the core layer and thus the bound water movement by transverse diffusion. At the start of hot pressing, moisture vapour starts moving inward and condensing where the temperature is below the boiling point.

After a short period of time, from the start of the hot pressing, the moisture evaporation and condensation may not be significant and in this case the moisture content profile can be modelled by Fick's second law as proposed by Siau (1984):

$$\frac{\partial MC_f}{\partial t} = \frac{\partial}{\partial x}\left(D_m \frac{\partial MC_f}{\partial x} \right) \qquad (4.36)$$

Where,

D_m: Transverse diffusion coefficient for moisture movement ($cm^2\ s^{-1}$);

MC_f: Bound water moisture content (%)

t: Elapsed time (s),

x: Distance from the top surface of the board (cm).

The diffusion coefficient, D_m, may be obtained by the following formula Siau(1984):

$$D_m = \frac{0.07}{(1-a^2)(1-a)} \exp\left(-\frac{9200 - 70MC_f}{RT} \right) \qquad (4.37)$$

Where,

R: Universal gas constant (1.987 cal/mol K)

T: Temperature (K);

a^2: Porosity of wood $a^2 = 1 - G(0.667 + 0.01MC)$

G: Density of the mat in ($g\ cm^{-3}$).

If the average value of D_m can be determined then Equation (4.39) becomes:

$$\frac{\partial MC_f}{\partial t} = \bar{D}_m \frac{\partial^2 MC_f}{\partial x^2} \qquad (4.38)$$

Where $\bar{D}_m$ is the mean of the diffusion coefficient.

The above equation can be modified to include the loss or gain of bound water moisture content due to evaporation or condensation. The equation below gives all the changes in the bound water.

$$\frac{\partial MC_f}{\partial t} = D_m \frac{\partial^2 MC_f}{\partial x^2} \pm \frac{\partial MC_{ev/cond}}{\partial t} \tag{4.39}$$

4.4.10 Cure Properties of Adhesive:

In the wood composite industry, two main types of resin are used and these are urea formaldehyde (UF) and phenol formaldehyde (PF). The curing reaction of both of these resins is included in the present model. Carvalho (1999) obtained the kinetic model for the UF resin polycondensation reaction by using Raman spectroscopy. He concluded that the evolution of the bands attributed to methylene groups follows first order kinetics. Although the cross linking is mainly obtained by the formation of methylene bridges, other reactions, such as the formation of cyclic structures are also involved. However, as a good approximation, Carvalho *et al.* (2003) considers the kinetics of the formation of methylene bridges [B] representative of the polycondensation kinetics. So the rate of the polycondensation reaction of UF resin (in s^{-1}) can be calculated by:

$$(-r) = \frac{1}{A_o}\frac{d[B]}{dt} = \frac{1}{2}k\exp(-kt) \tag{4.40}$$

$(-r)$: Reaction rate for resin polycondensation (s^{-1});

A_0: Initial concentration of methylol groups (mol kg^{-1});

k: Rate constant calculated using the Arrhenius equation with $k_0 = 71.597 s^{-1}$ and E_{act} = 33 (kJ mol^{-1});

t: Time (s).

The water production by the polycondensation reaction was calculated, keeping in mind that for each methylene bridge formed a water molecule is released. We can calculate the water production in kilograms of water per kilogram of resin per second using the following the expression:

$$\left(-r'\right)=\frac{d\left[-H_2O\right]}{dt}=\frac{1}{2}A_0 k\exp\left(-kt\right)MM_w \qquad (4.41)$$

MM_w : Water molecular weight (kg mol^{-1});

ΔH_r ; Resin polycondensation enthalpy (J kg^{-1});

Using data obtained in a quantitative (Carbon 13) $^{13}C-NMR$ analysis Carvalho *et al.* (2003) obtained:

$A_0 = 7.9$ (mol kg^{-1})

To calculate the heat released by the resin cure reaction, the polycondensation enthalpy $\left(\Delta H_r\right)$ for UF resin is needed. For the UF resin Yin (1994) obtained a value of 84.13 (J kg^{-1}) using DSC for the resin with 1.5% (w/w) of hardener $\left(NH_4Cl\right)$, which is the typical hardener content used in MDF production.

$\Delta H_r = 84.13$ J kg^{-1}

The temperature dependence of the viscous component for the wood-resin model was estimated by Carvalho *et al.,* (2001) using an Arrhenius-type equation:

$$\mu=\mu_\infty \exp\left(\frac{\Delta E_\mu}{RT}\right) \qquad (4.42)$$

In which $\mu_\infty = 1\times10^8$ (Pa s) and $\Delta E_\mu = 3241$ (J mol^{-1}).

A computer programme is developed in Matlab (software) to simulate the resin curing behaviour of UF resin on the basis of the above equations. Figure 4.3 shows that the rate of resin polycondensation changes with time if the temperature is increasing one degree with every time step.

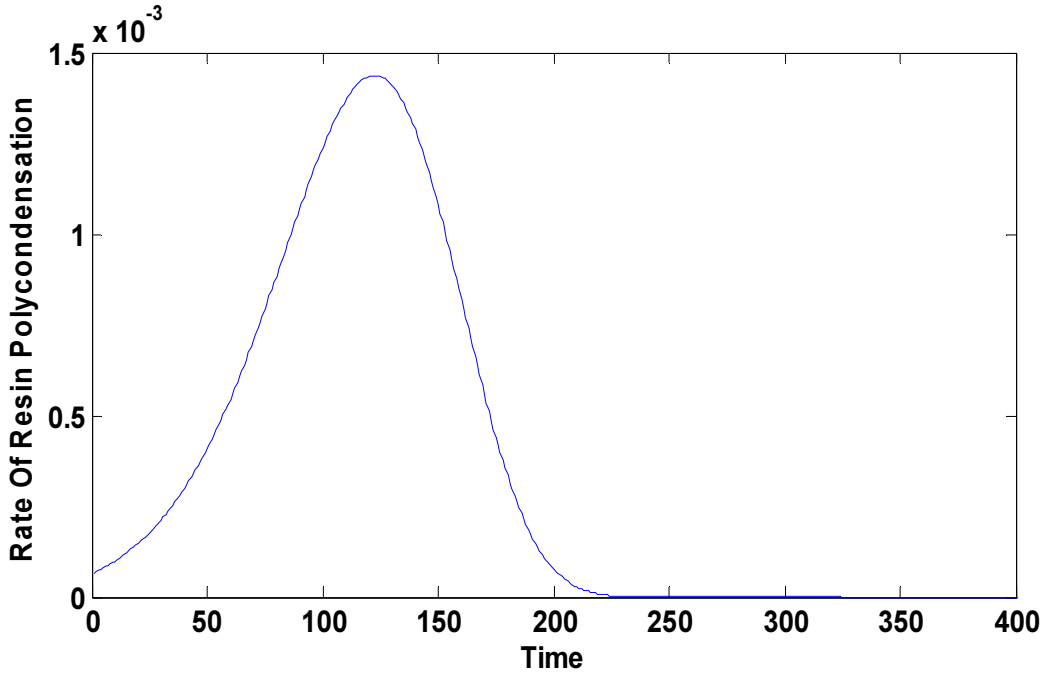

Figure 4.3: Change of reaction rate of resin polycondensation with time

Figure 4.4 shows the changes in the rate of resin polycondensation with temperature,

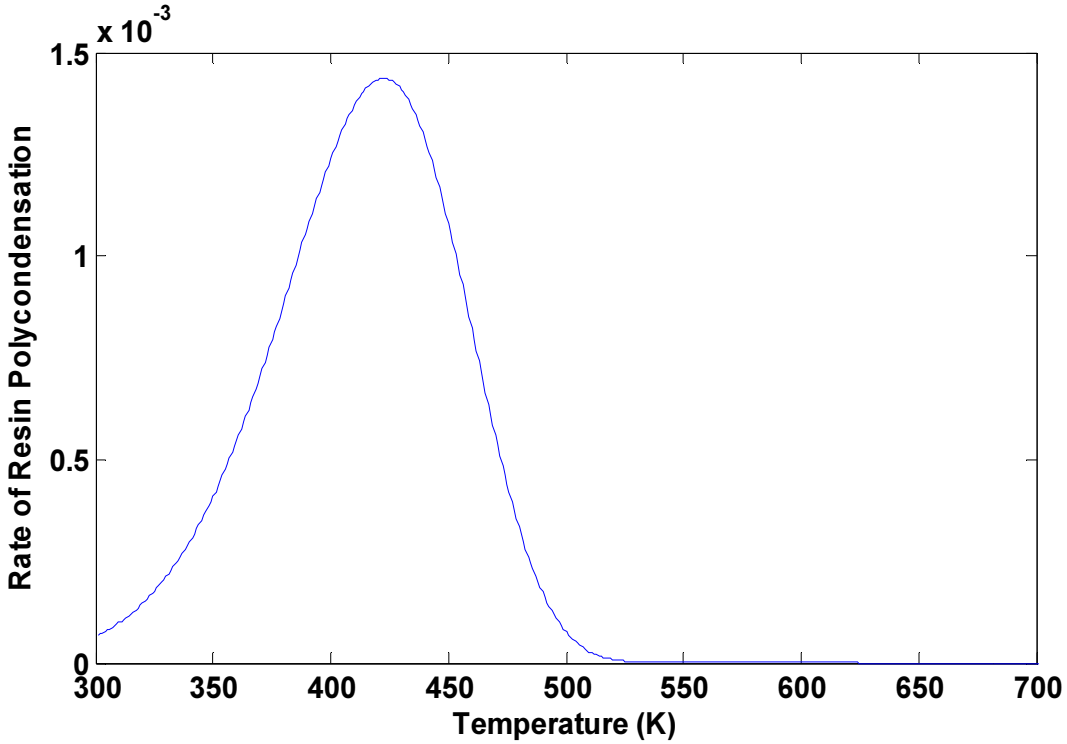

Figure 4.4: Change of reaction rate with temperature

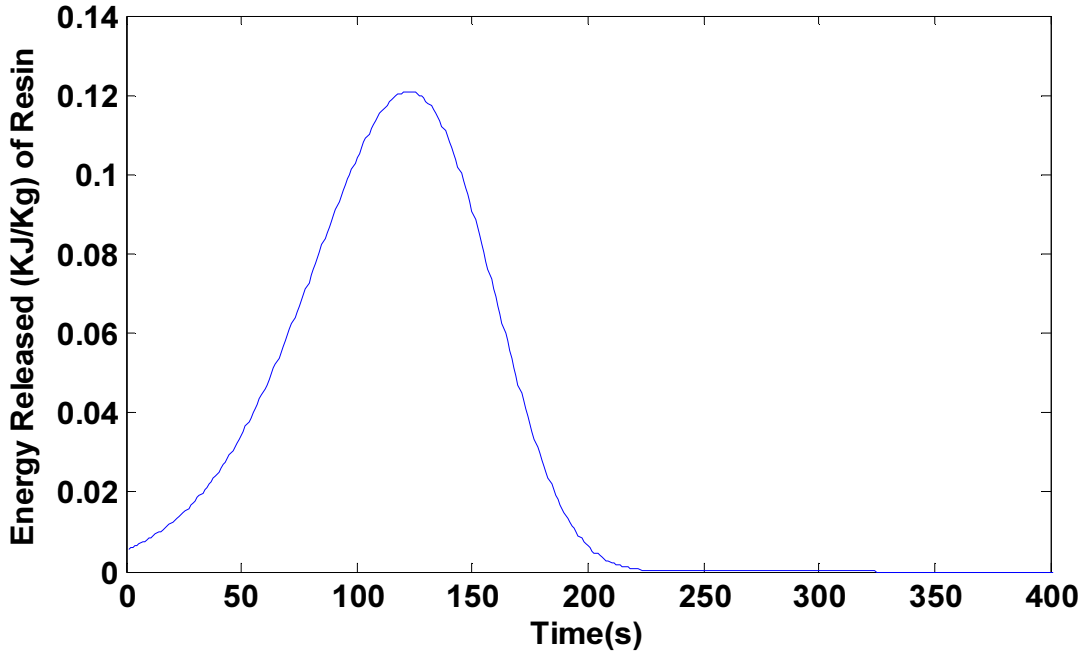

Figure 4.5: Rate of exothermic energy released with time at constant temperature

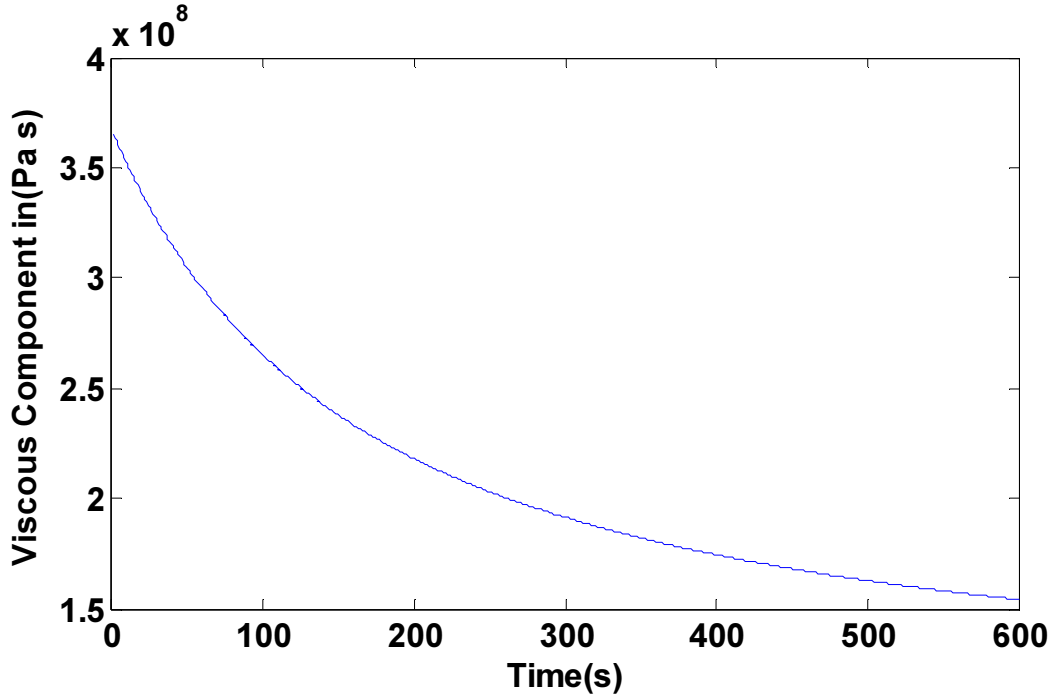

Figure 4.6: Change of viscous component with time

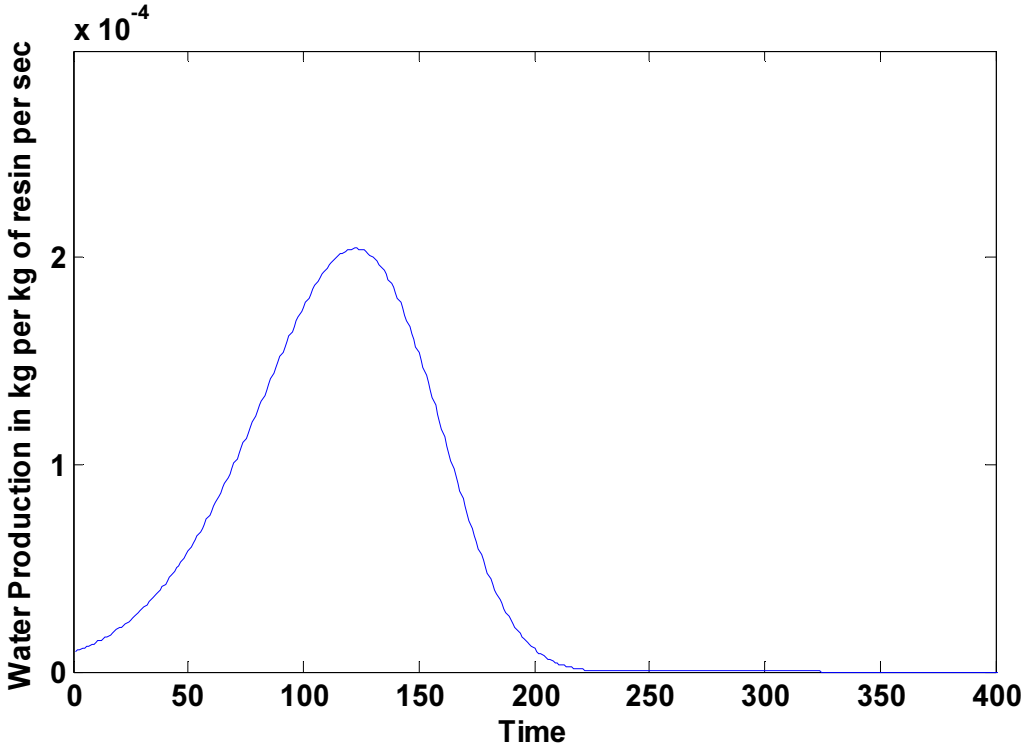

Figure 4.7: Release of water in kg per kg of resin per second

The cure kinetics equation of the Phenol Formaldehyde resin (PF) is given by Scott (1989), and Kiran and Iyer (1994):

$$\frac{\partial F}{\partial t} = Ae^{-(\frac{E}{RT})}.(1-F)^n \qquad (4.43)$$

Where F is the extent of reaction (Cure Index).

The parameters used in Equation (4.43) for the PF resin were determined empirically by Ahmad (2000) using the same procedure and technique as described by Sernek *et al.* (2000) and the values for these parameter are as follows:

Reaction constant, $A = 0.25$ (s^{-1});

Universal gas constant, R = 8.31696 (J mol^{-1} k^{-1});

Activation energy, E = 12423.0 (J mol^{-1});

Order of reaction, $n = 0.587$.

4.4.11 Vapour Loss from the Edges:

In commercial MDF production, there is a significant loss of moisture through the edges of the panel. In small laboratory manufacture of boards, the edge loss is more important because of the increased ratio of edge surface to panel area. An edge loss equation given by Zombori (2001) was dimensionally incorrect, so we modified his equation to the present form. Equation (4.44) gives the loss of air through the edges and Equation (4.45) gives the loss of vapour through the edges. As the model is one dimensional across thickness, so most of the simulation is done without considering the edge loss. The coefficients such as external bulk flow coefficient and external diffusion.coefficient were adjusted to compare the one dimensional model results with the core pressure from the experiments. The difference in values from the model and experiment were too high and it was concluded that a 2-D model will be needed to predict the vapour loss from the edge. The present simulation results are without considering vapour losses from the edges.

$$j_a^{edg} = -\rho_a \frac{\kappa}{\eta_g}(P_{Amb} - P) - M_a(\frac{1}{RT})D^j(p_a - p^B{}_a) \tag{4.44}$$

$$j_v^{edg} = -\rho_v \frac{\kappa}{\eta_g}(P_{Amb} - P) - M_v(\frac{1}{RT})D^j(p_v - p^B{}_v) \tag{4.45}$$

The above equation will give the loss of air and vapour from edges

where

j^{edg} is the mass flux (kg/m^2/s)

η_a viscosity of air (kg/m^2/s)

ρ_a density of air (kg/m^3)

κ external bulk flow coefficeint (m)

P_{amb} total pressure of air (Pa)

P total gas pressure inside the board(Pa).

M_a molecular weight of air (kg/mol)

D^j external diffusion coefficient at the edge (m/s)

p_{amb} partial air pressure in the atmosphere (Pa)

p_a partial air pressure inside the board. (Pa)

The above equation will give the edge loss in (kg/m^2/s). As all the calculation in the model is in (kg/sec), the gas leakage is the same from the both the edges and it is given by multiplying the equation (4.45) by the edge surface area

4.4.12 Governing Equations:

Calculation of various transport phenomena in one-dimensional heat and mass flow involves the solution of mass and energy conservation equations. The governing equations describe the physical phenomena involved in a conventional hot-compression process.

Conservation of mass of vapour equation:

$$\frac{\partial m}{\partial t} = (-\nabla . j + m_{ev} + m_r) \times V \qquad (4.46)$$

Conservation of energy equation used to calculate temperature:

(4.47)

$$\frac{\partial T}{\partial t} = \frac{(-\nabla.q - H_v m_{ev} + H_r m_r)}{c_u \rho_u}$$

Where the conduction heat flux is given by Fourier's law. $q = -k_t \nabla T$

Conservation of moisture content of fibres equation:

$$\frac{\partial MC_f}{\partial t} = D_m \frac{\partial^2 MC_f}{\partial x^2} \pm \frac{\partial MC_{ev/cond}}{\partial t} \quad (4.48)$$

Where

c_u Specific heat of wood at current moisture content (J kg^{-1} K^{-1})

ρ_u Density of wood at current moisture content. (kg m^{-3})

k_t Thermal conductivity (W m^{-1} K^{-1})

H_v Latent heat of sorption from vapour to the bound water state per unit mass (J kg^{-1})

m_{ev} Evaporation rate (kg m^{-3} s^{-1})

V Volume of mat layer (m^{-3})

∇T Temperature gradient in the flux direction (K)

Remaining terms are given in the nomenclature list. Details of the equation are given in different sections. A negative sign indicates loss and a positive sign indicates gain.

4.4.13 Air in the Mat:

The gas mixture within the wood-furnish mat consists mainly of air and water vapour. Initially air is the dominant component in the mixture. As the pressing process proceeds, vapour is generated and replaces most or all of the air within the mat. The only data reported in the literature that describe the variation of the gas composition over time were published by Denisov *et al.* (1975). The authors inserted a small tube of 900 mm in length into the core layer of a mat during industrial particleboard pressing to sample the

gas mixture during different stages of the pressing cycle, which were termed as phases I-IV. The gas composition was analyzed by using a chromatography method. Results of the gas analysis, summarized for these phases, are presented in Table (4.1).

Table 4.1: Composition of the gas mixture sampled from the core layer of a particle mat during consolidation in an industrial batch press (Denisov et al., 1975)

Phase	Time of sampling (min)	Volumetric proportion of water vapour (%)	Volumetric proportion of air and other gases (%)
I, II	0- 3.0	0	100
III	3.0- 3.5	71.1	28.9
IV	4.5- 10	99.5	0.5

Although vapour is generated in the outer mat layers in the early stage of the hot-press, no vapour was detected by Denisov *et al.* (1975) in the core layer during the first three minutes. The onset of phase three was defined as the time when the core reaches a temperature of 100°C. The volumetric proportion of the vapour in the analysed gas, averaged over the first 30 seconds of phase III , was 71.1%. The actual proportion of the vapour in the mat must be higher during this period, as some of the vapour was reported to condense at locations where the temperature is below the boiling point (100°C). Finally, almost all air in the mat was displaced by vapour (phase IV). In addition to the vapour and air, a small proportion (0.5%) of other gaseous organic substances was found to exist in the mat.

4.5. Initial and Boundary Conditions:

4.5.1 Initial conditions:

In order to solve the proposed heat and mass transfer model using a numerical method, the panel was divided into two symmetrical halves in thickness, as described in Chapter (two). Initially each layer has a constant thickness over horizontal (y-z) plane and it is assumed that the conditions and all of the properties are uniform across this plane before

the hot-pressing starts. The pressing pressure is zero at the onset of press closure. Mathematically these initial conditions are expressed as:

$$T\big|_{x,t=0} = T_0;$$

$$MC\big|_{x,t=0} = MC_0;$$

$$\rho\big|_{x,t=0} = \rho_0;$$

$$p\big|_{x,t=0} = p_{amb};$$

$$p_v\big|_{x,t=0} = f(T_0, M_0);$$

$$d\big|_{x,t=0} = d_0.$$

$$\sigma_{press}\big|_{x,t=0} = 0;$$

4.5.2 Boundary conditions

Three types of spatial boundaries are considered in solving the heat and mass transfer model and these boundary conditions are: the top surface of the MDF mat which is in contact with the hot platen; the interface between the MDF mat and ambient air, and the the symmetry planes of the mat. The mat is always regarded as symmetrical across its length, width plane, and along the thickness. It is assumed here that the rectangular mat is symmetrical in all directions. The boundary conditions are presented here for a batch press.

4.6. Numerical Solution:

The program is coded in the Matlab software. Due to the complexity of the problem, a modular programming style was chosen. The modular approach ensures the flexibility necessary for incorporation of changes and expansions in the future. The model has been solved for one-dimensional simulation along the mat thickness and thus the mat is symmetrically divided into two halves as discussed in Chapter two for the MDF density profile modelling. From the simulation program, graphs for the complete thickness are generated from the symmetrical assumption. The programme is divided into separate *m* files and they were called into the main programme during execution.

Input data to specify a model run and material property data are read directly from a *m*-file. Input specifications include raw material and surrounding conditions, pressing conditions, model definitions and output organization. The input data can be changed in the *m*-file before starting a model run. The flow diagram is given in Chapter two (Figure 2.11) , explaining the steps followed in the programme.

4.7. Results of a Simulation Run:

4.7.1 Simulation Run for Standard Conditions:

The proposed model on the heat and mass transfer has been solved using the finite difference numerical technique to predict profiles of temperature, moisture content, vapour pressure, and extent of the adhesive curing with time. Several simulations were completed under different pressing conditions to test the robustness of the program.

The basic capabilities of the model will be demonstrated on a MDF mat hot-compression simulation for one type of mat and press schedule specification. The next chapter will compare the model predictions with experimental data among a wide range of pressing schedules. The simulated mat was positioned in the "virtual hot press" (computer model) to further analyze the temperature, moisture and internal gas pressure distribution in the thickness direction of the panel. For the simulation run, the platen temperature, the initial moisture content and temperature of the mat, resin content and the press schedule were specified. These parameters, together with other simulation input parameters, are given in Table 4.1. In the discussion section, the results of the simulation are analyzed.

The time dependent changes such as temperature, moisture content, total gas pressure, and adhesive kinetics (cure index) are considered. Several three-dimensional graphs of the basic variables were created at certain stages of the hot-compression simulation to demonstrate the changes taking place in the internal environment of the mat.

Table 4.2. Hot compression parameters used in the simulation.

SN	Contents	Value	Units
1	Wt of fibre(Kg)	1.11	kg
2	Initial Moisture Content	6.78	%
3	Initial Temperature	27	ºC
3	Resin content on solid basis(Phenol formaldehyde)	9.5	%
4	Dimension of Mat		
	Length-	0.3	m
	Width-	0.3	m
	Initial Thickness-	0.038	m
	Final Thickness	0.019	m
7	Platen Temperature	198.2	ºC
8	Duration of pressure applied:	400	s
	Delata time step	0.5	
9	Control Mode	Position	
10	Target density of board	650	kg/m^3
11	Batch / Continuous press	Batch	Batch
12	Time steps	800	s
13	Number of layers in half board	10	

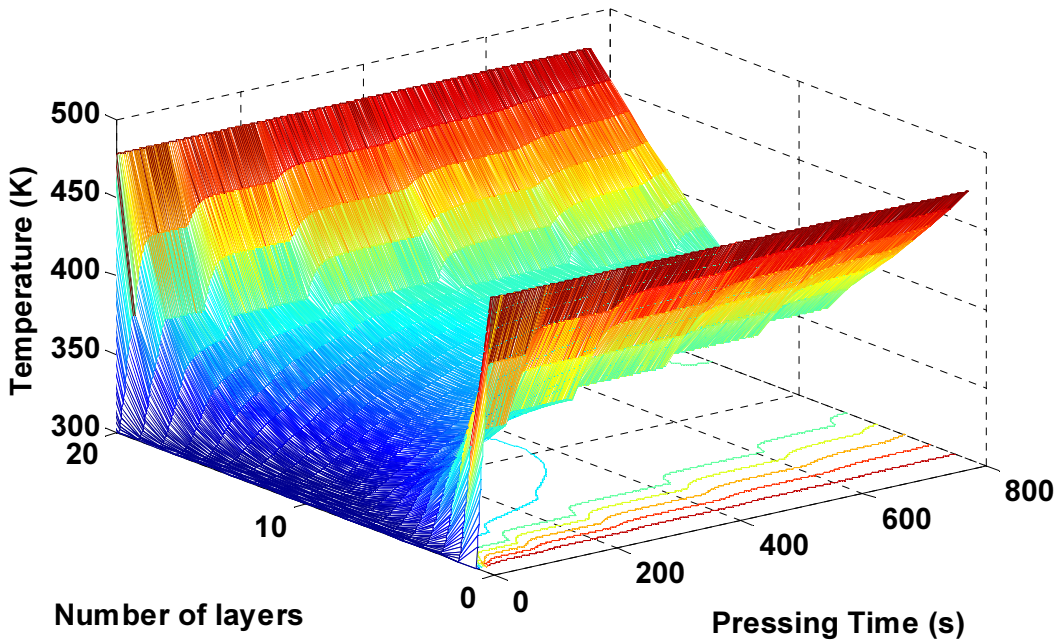

Figure 4.8 Change of temperature across thickness 3D graph for complete thickness.

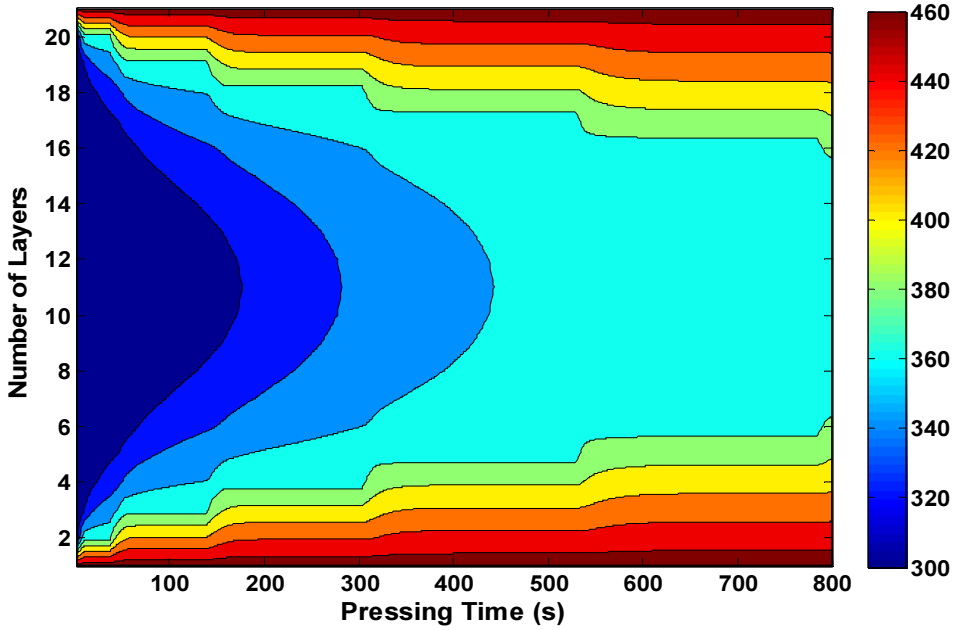

Figure 4.9 Change of temperature across thickness contour plot.

Figure.4.8 and 4.9 shows the development of temperature across the mat thickness. Each mesh line represents one layer. The top surface layer reaches the platen temperature soon after entering the press. The core temperature increases slowly as shown in figure 4.9.

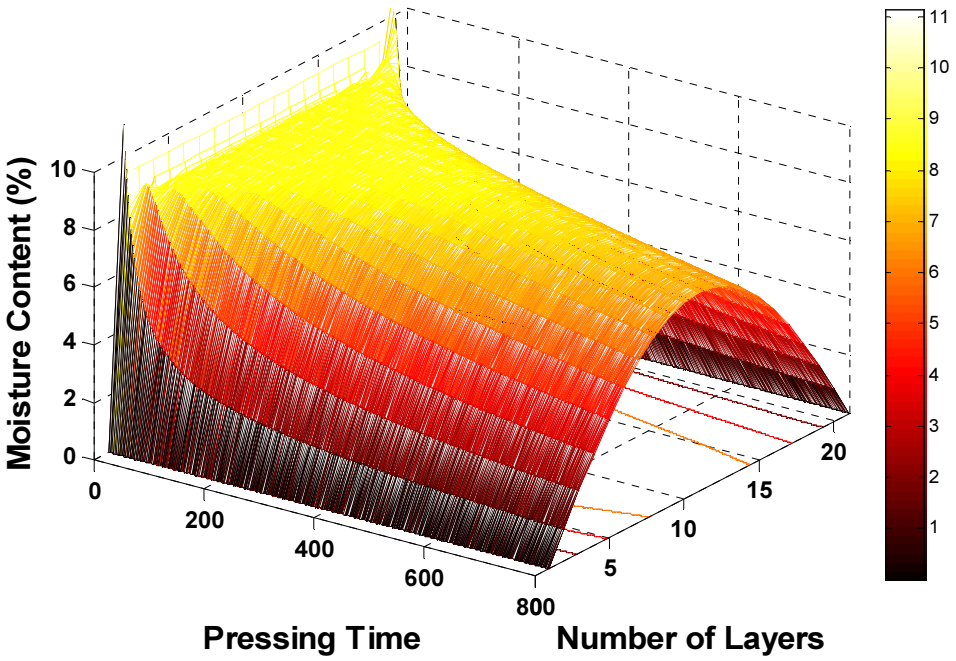

Figure 4.10: Change of moisture content across thickness

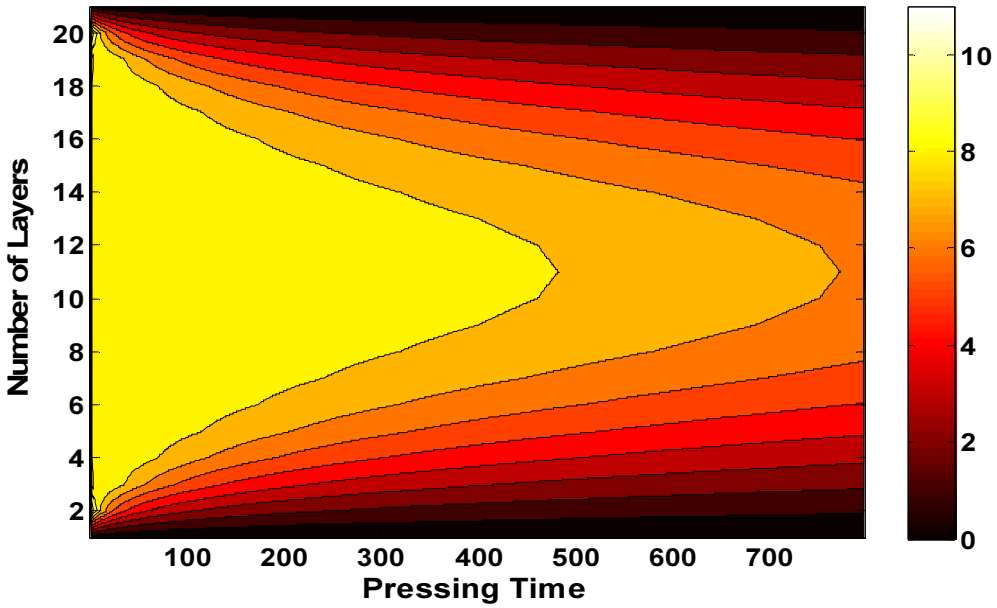

Figure 4.11 Contour plots of moisture content (% dry basis) changes across thickness

Figures 4.10 and 4.11 represent the development of the moisture content profile across thickness. The moisture content at the surface soon reaches zero, as the hot platen touches the surface. The highest moisture content is always at the centre, in the core region.

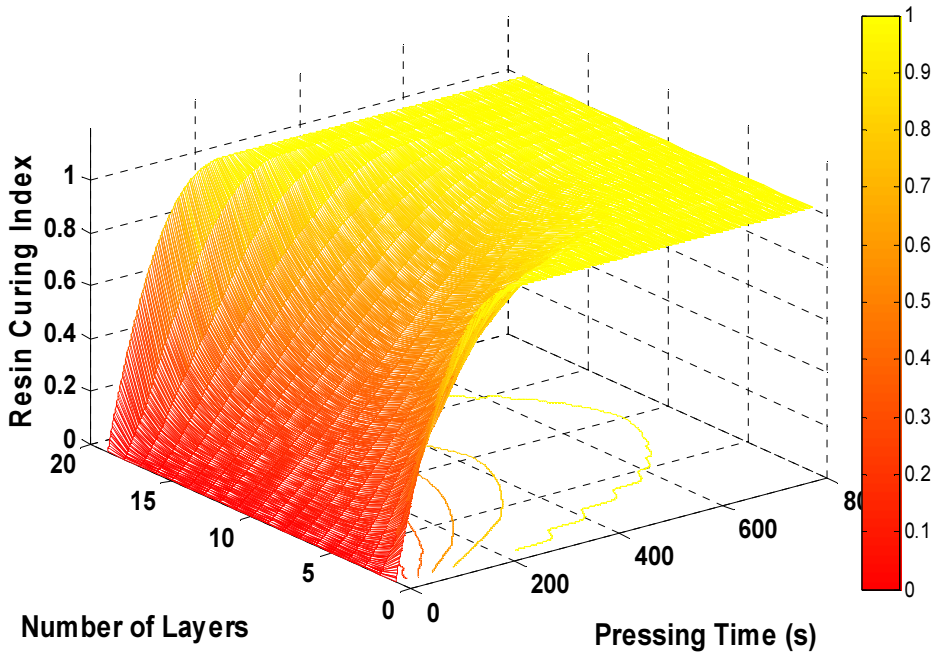

Figure 4.12 Extent of resin cure in different layers while pressing

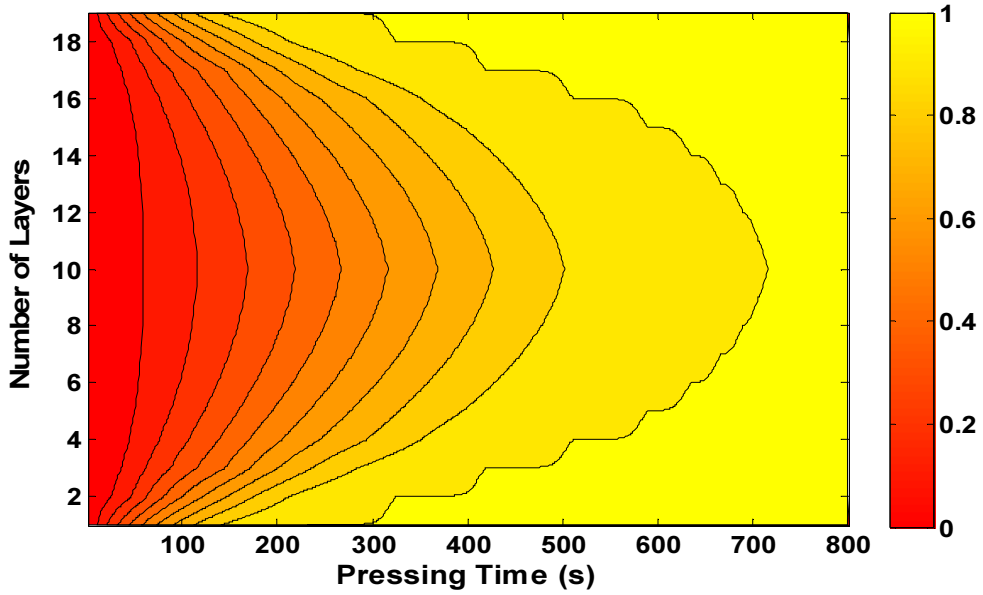

Figure 4.13 Contour plot of resin curing index across thickness with time

Figures 4.12 and 4.13 show the curing of resin across the thickness. The resin at the surface cures much faster due to high temperature and it takes much longer for the resin in the core region.

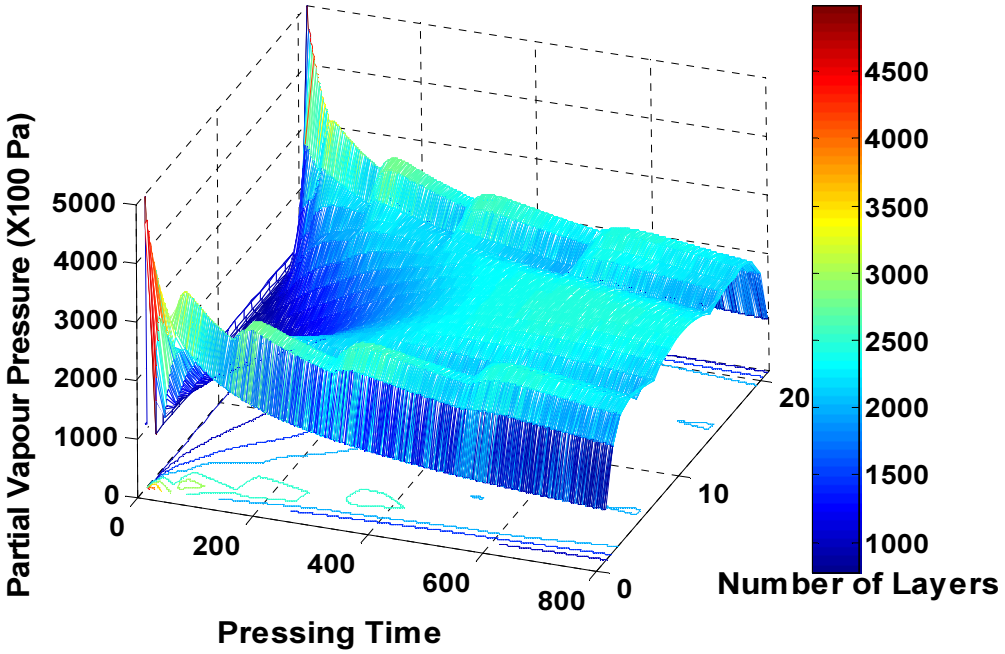

Figure 4.14: Partial vapour pressures across thickness

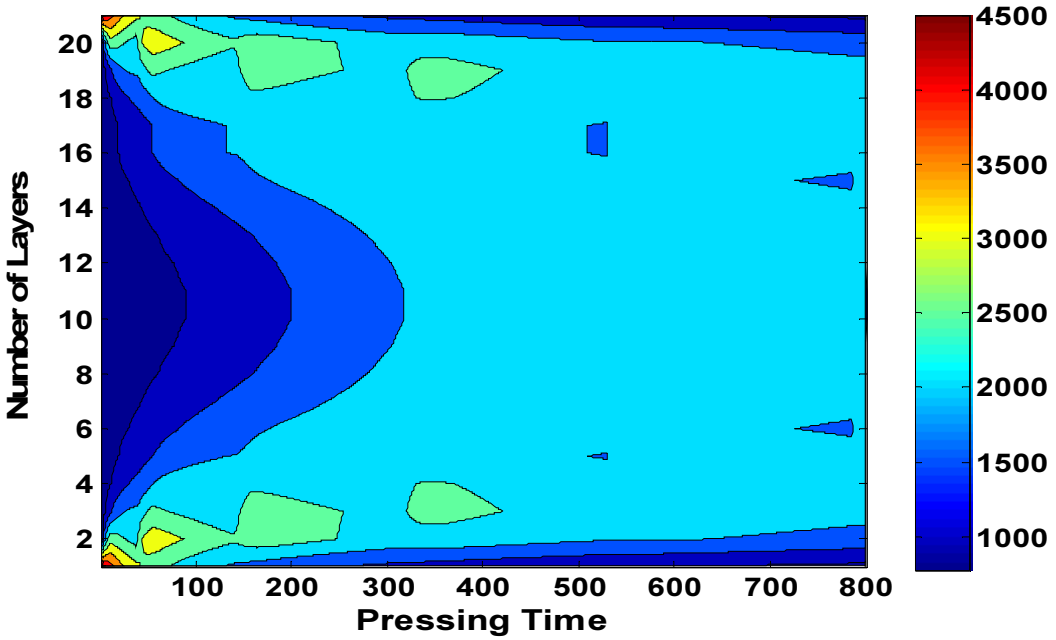

Figure 4.15: Contour plot of changes in partial vapour pressure across thickness

4.7.2 Discussion for Standard Conditions:

At the beginning of the hot pressing (0 s), the temperature of the mat is a uniform 27^{o}C and the temperature of the hot platen 198ºC. The moisture content is 6.78 % in the mat. The total pressure inside the board is in equilibrium with the atmospheric pressure at the beginning of the hot pressing. Relative humidity is 57% within the mat. The cure index is zero every where in the beginning.

During the press closing period which is (25 s), the platen moves from the initial position (38mm) to the final thickness (19mm). The top and bottom surface of the mat reaches the platen temperature instantly (Figure 4.8). The temperature in the core area is still near the room temperature in the first (50 s). This large temperature gradient in the vertical direction initiates conduction heat transfer from the hot platens to the cooler core area. The resin near the surface starts curing due to high temperature (Figure 4.12). All the moisture content from the surface evaporates as the platen touches the surface of mat (Figure 4.10), due to which the moisture content of the fibres becomes zero at the surface. It causes a large moisture content gradient between surface and core and results in the bound water diffusion.

As it is evident from the experimental work of Denisov et.al (1975), that water vapour plays a very important role in the hot pressing of wood composite. All the air is replaced by water vapour soon after the beginning of hot pressing. In the beginning as the hot platens touches the surface of the mat, all the moisture evaporates and increases the total pressure of the surface zone (Figure 4.14 and 4.15). The figure shows the total gas pressure without any edge losses. The core pressure still remains at a lower value. The hot vapour can not escape through the impermeable metal plate but will move by bulk flow and diffusion towards the centre, due to the total and partial vapour pressure gradients in the vertical direction. The early stage of the hot pressing is characterized by having large vertical movement of heat and moisture content.

As the pressing time approaches the middle of the press cycle (400s), the temperature near the surface layers approaches the platen temperature and the temperature in the core

region approaches the boiling point of water. The moisture content near the surface zero and the water vapour that is evaporated from the surface condenses in the core region, resulting in increasing the moisture content of the centre. In this stage the resin curing is accelerated due to high temperature of all the layers and curing index of all the layers lies within 0.5 to 0.8. If the value reaches near to 0.9, the resin is almost cured.

The last (400 s) of the press cycle are less dynamic. At the end of the press cycle, the layers at the surface have almost reached the platen temperature (Figure 4.8 and 4.9). The main source of heat flow at this stage is conduction. The heat flow by convection slows down as there is no vapour pressure gradient between peak and core layers. The moisture content near the surface layers is very low but the core regions still have higher moisture content (Figure 4.10, 4.11). The curing index in all the layers reaches a value near to 0.9, which signifies that the resin is almost cured in all the layers (Figure 4.12, 4.13).

An inventory check was carried out on the sum total of moisture in the fibre and in the vapour state for the whole board. This total was almost constant throughout the transient simulation, showing that the moisture lost by the fibre was accounted for by the increase of moisture in the vapour. In figure 4.10, the moisture content of the layer does not show the small peak before dropping which was seen in the simulation results of Humphrey.et *al.* (1989). In their model, the bound water diffusion due to moisture content gradient was neglected. This effect is included in the present model and has the effect of decreasing the peak moisture content levels predicted by Humphrey et al.

Detailed Analysis: The simulation result of the hot MDF pressing provides a lot of information. The most common way to present information is the Time Analysis and is followed by Zombori (2001) and Thomen (2000) for describing their model results. Time Analysis means to display the dependent variables (temperature, moisture content, resin curing and partial vapour pressure) as a function of time, using space as the parameter. The whole press cycle is divided into three periods and later each period is described in detail. Each number represents the layer (with finite thickness). In the figures below zero

represents the surface layer, 5th number represents the middle layer (25% from the surface) and 10th layer represents the central core layer.

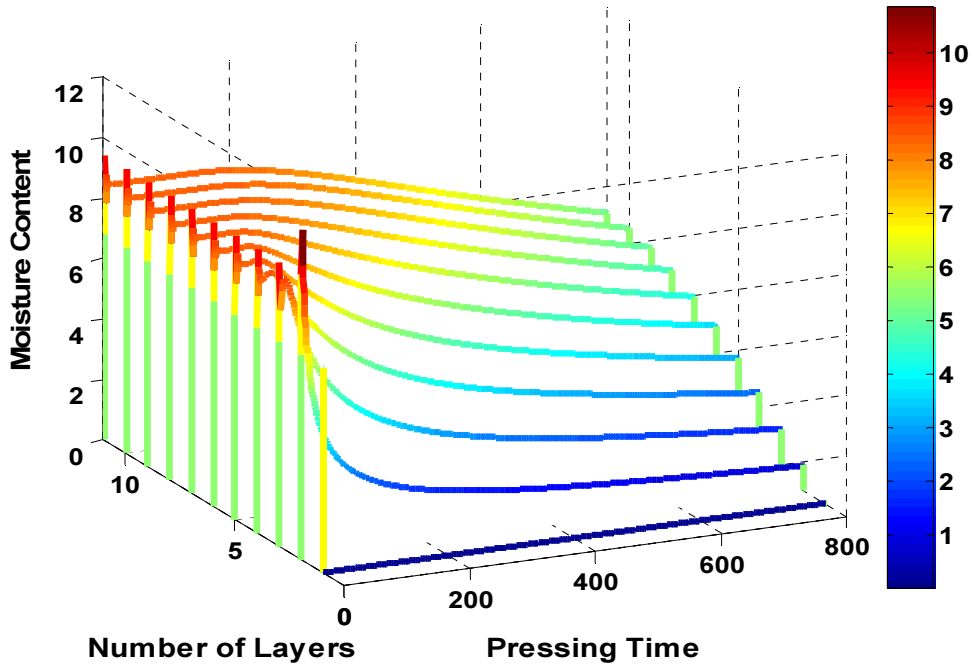

Figure 4.16 Change of moisture content (% dry basis) with time in half board

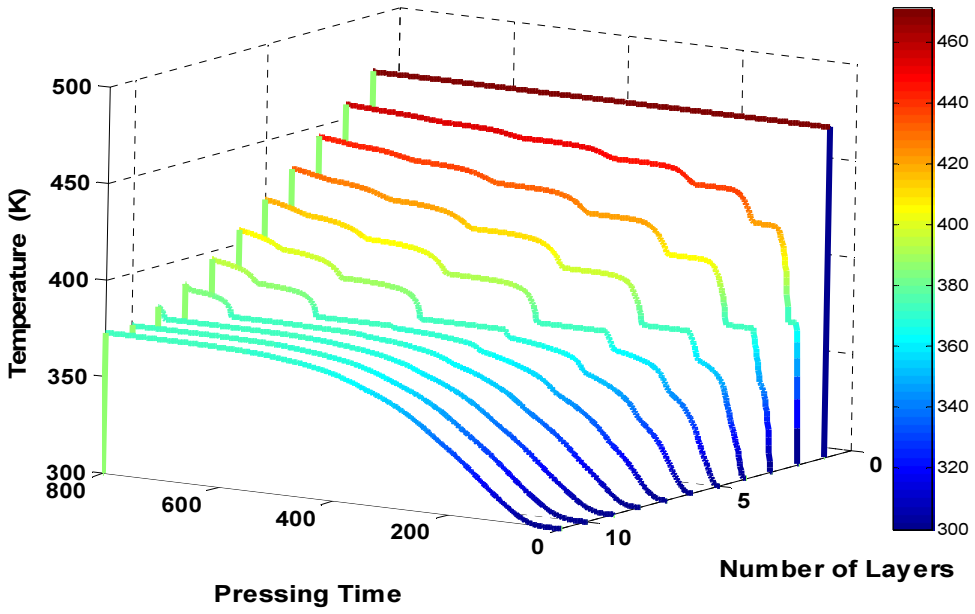

Figure 4.17: Change of temperature with time in half board

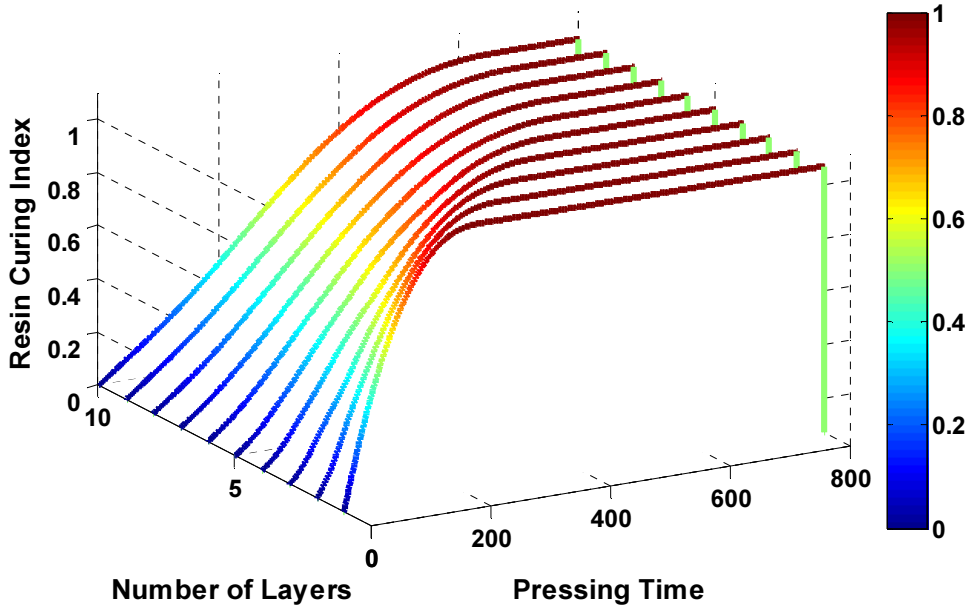

Figure 4.18: Resin curing index in different layers with time

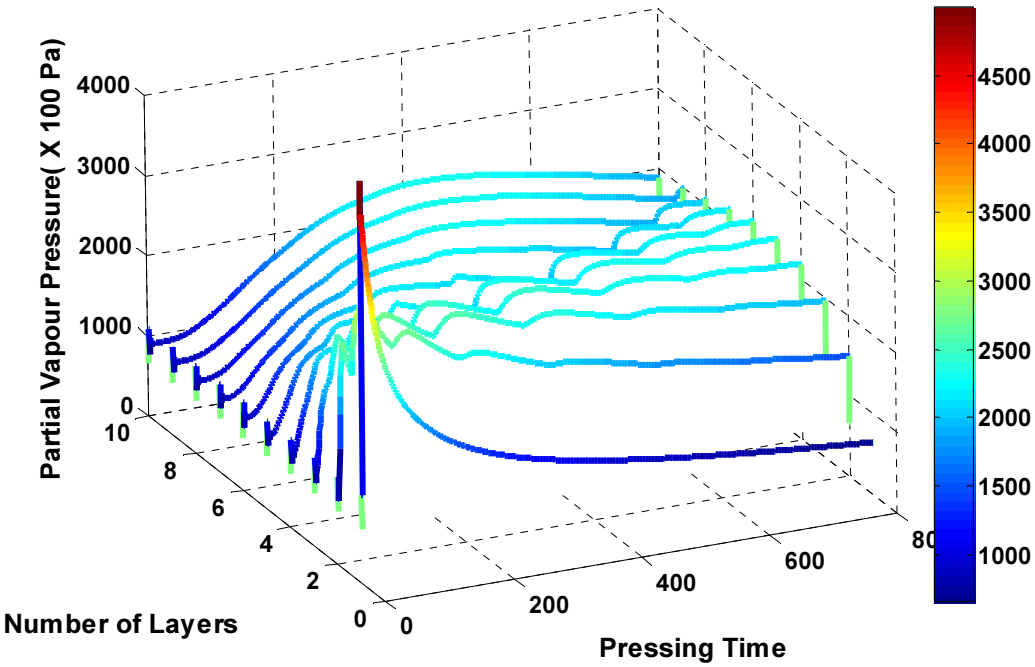

Figure 4.19 Change of vapour pressure with time in half board

The *first period* is the time taken by the press platen to move from the initial stage to the final thickness (19mm), in the present simulation it is (25 s). The top-most surface instantaneously reaches the platen temperature. The temperature in the core is still around room temperature. This period is marked by the presence of high temperature and moisture content gradient between the peak and core layers. As the mat is compressed towards the final thickness, all the air that is filled between the spaces leaves the mat, due to which the value of thermal conductivity increases and heat transfer by conduction becomes more important with time. Humphrey (1989) hypothesized that any change in temperature will affect the equilibrium moisture content of wood and therefore, the partial vapour pressure. As the temperature increases, there is more evaporation of water which in turn raises the value of partial vapour pressure and lowers the value of EMC. Due to the high value of partial vapour pressure and total pressure in the surface layers, it drives the hot vapour towards the core region by bulk flow and diffusion. Humphrey and Bolton (1989a) have pointed out that any change in temperature will affect the equilibrium moisture content and vapour is therefore generated as soon as the temperature of the wood particles increases.

The *second period is* initiated after press closing till the middle of the press cycle, in this case until (400s). All the heat and mass transfer described in the previous sections are still going on in this phase. The heat transfer through conduction increases as all the air space trapped between the fibres is eliminated which enhances the thermal conductivity of the mat. Due to the high temperature, a large amount of water vapour is generated at every location of the mat. At the end of this period, the majority of the gas is water vapour. Due to compacting of the mat, the permeability and diffusivity of the mat decreases. It slows down the flow of water vapour from the surface to the core region. The moisture content of the surface layers have been already depleted to a much lower level. The value of resin curing index in the surface layers has reached to more than 0.9, which signifies that, a lot of curing has already taken place. The complex relationship of resin curing on the heat and mass transfer is still not well understood. Due to the low percentage of weight of resin compared to total mass of fibres, the impact is usually neglected. The core pressure becomes high due to the high amount of vapour that is generated due to evaporation from

the fibres and the water vapour that is transferred from the surface to the core region. It is assumed in this model that EMC is reached instantaneously. Due to heat transfer by conduction and convection, the temperature of the fibre changes. It changes the value of EMC of the fibres. To bring the internal conditions to the equilibrium, the fibres lose moisture content in the form of evaporation of water vapour or gain moisture content due to condensation of moisture from the air. The changes in the temperature also raise the saturated vapour pressure and, indirectly, the relative humidity of the air. It is assumed in this model that no free water exists in any condition inside the mat. The temperature of the core at this stage reaches near to the boiling point of water. From the validation experiments, it was found that the core temperature reaches 104ºC before becoming stagnant. The reason for this behaviour is that at this stage of pressing, the mat is in very compact form, most of the air voids are eliminated due to crushing of fibre walls. The permeability and diffusivity of the mat also decreases. The curing of resin also reduces the permeability of the board. The water vapour which had collected in the core region due to evaporation of moisture content from the fibres and from the transfer from the surface raises the saturated vapour pressure, which indirectly increases the boiling point of the core region. The core temperature stays near the boiling point for some time, as all the energy that is being transferred from the hot platen to the core region and the exothermic energy released by the curing of resin is consumed in the form of latent heat to convert all the moisture content of fibres into vapour form.

The *third period* starts from middle of the press cycle to the end of the cycle. Most of the processes which were described earlier are still going on. The temperature difference between the surface and core has reduced. The core temperature has reached near to the boiling point of water and will stay there for some time, before it starts increasing again. The resin curing index has reached the value of more than 0.9 in most parts of the board, as seen in Figures 4.12 and 4.13. The high curing index is represented by the yellow colour. The partial vapour pressure has increased in the core region. In a commercial batch press, the press platen is moved slightly upwards near the end of the press cycle, for giving easy passage to gas from the edges. This is the safe way to protect the thicker boards from the problem of delamination. It is always a problem in the commercial plants

to determine the optimum time required for pressing of the boards. If the boards are not kept inside the press for sufficient time, then the resin in the core will not be completely cured and the board will have lower internal bonding strength. From the model, it can be determined, how long it takes for the resin curing index to reach the value above 0.9, when it will be the optimum time for particular thickness.

Another way of analysing data is to describe the changes that take place in various layers. As described earlier, *(d = 0)* zero represents the surface layer, 5^{th} number represents the middle layer (25% from the surface) and 10^{th} layer represents the central core layer.

Surface Layer *(d=0)* behaviour:

The surface layer represents the interface between the hot platen and beginning of the second layer. The main source of heat transfer is by means of thermal conduction from the hot pressing platen into the layer. The temperature of the layer instantaneously reaches the platen temperature as shown in Figure 4.8 and 4.9. Due to high temperature, the moisture content of the layer evaporates and reduces the moisture content of the surface to zero percent as seen in Figure 4.10 and 4.11. The dark black colour in the contour Figure 4.11 represents the value of moisture content near to zero. Due to the high moisture content gradient between the surface and core layers, bound water starts diffusing from the core to the surface. Increasing the temperature also plasticizes the wood fibres and is the main reason for having high peak density on the surface of the board. The resin curing index has increased to 0.4. Due to the fast increase of temperature in the first stage of the pressing, the temperature curve flattens out and slowly approaches the platen temperature as seen in Figure 4.17. The moisture content stays at a low level until the end of the simulation.

Intermediate layer *(d=5)* behaviour:

As seen in Figure 4.14 and 4.15. The partial vapour pressure is high on the surface layers and much lower in the core layer, but as pressing progresses, the high pressure zone starts moving towards the core. This zone of water vapour is mainly responsible for increasing the temperature of the inner parts of the mat. All the changes in this layer occur in a slow

process. This layer lies between two extreme situations. On the outer surface, the temperature is very high, near to 198ºC, and moisture content is near to zero and on the other side of this layer is the core zone; the temperature is low at around 30ºC and the moisture content is near to the initial value.

The temperature of this layer reaches the boiling point of water in the middle of the press cycle and then stays there for the rest of the pressing time. The moisture content is about 6% in the middle of the press cycle and in the end it is about 5 %, so there is not a huge reduction of moisture in this layer. In the beginning the partial vapour pressure of this layer is 0.018 MPa. It starts increasing till the middle of the press cycle and reaches 0.226 MPa. After that it starts decreasing and is 2.19 MPa at the end of the press cycle. The resin in this layer gradually solidified, in the middle of the cycle the value of the index was 0.86 and in the end of the cycle it becomes one, which means resin is completely cured in this layer.

Core layer *(d=10)* behaviour:

The temperature in the core layer increases very slowly. In the middle of the press cycle, it reaches to the value of 82ºC and before the end of cycle to 100ºC. The increase in vapour pressure starts much earlier than the increase observed in total pressure from the experimental results. Similar behaviour was also observed by the Thomen (2000), with his wood composite model.

Rauch (1984) has stated that the onset of the total gas pressure rise should coincide with the moment, when the core temperature reaches the boiling temperature of water. Thomen (2000) has explained this behaviour in the small scale boards. In the small mat, where gas can escape easily from the edges, vapour pressure hardly exceeds atmospheric pressure, which is the main reason that the boiling point in the small scale mat lies near to 100ºC. For industrial boards the boiling temperature is slightly higher due to increase in the vapour pressure inside the boards. The resin curing index has reached the value of 0.75 in the middle of the press cycle and 1.0 before the completion of the cycle. Once the resin is cured in the middle of the board, it is the best time to remove the board from the press.

4.7.3 Simulation Runs for Steam Injection Pressing:

The simulation is done to predict the temperature and moisture content, for the steam injection pressing, or pre-heated mat. The advantage of steam injection pressing is that it increases the heat transfer through convection of vapours without creating the risk of blowing of the board from the edges, due to high vapour pressure. It reduces the total time required to press the board, and increases the total production of the plant.

The steam injected from the top and bottom surfaces, increases the temperature of the layer to 100º C and moisture content to 15% due to condensation of steam near the surface. The surface constitutes nearly 30% of the mat, the remaining 70 % of the mat remains at room temperature 27º C and moisture content remains at 8 %, as shown in figure 4.16.

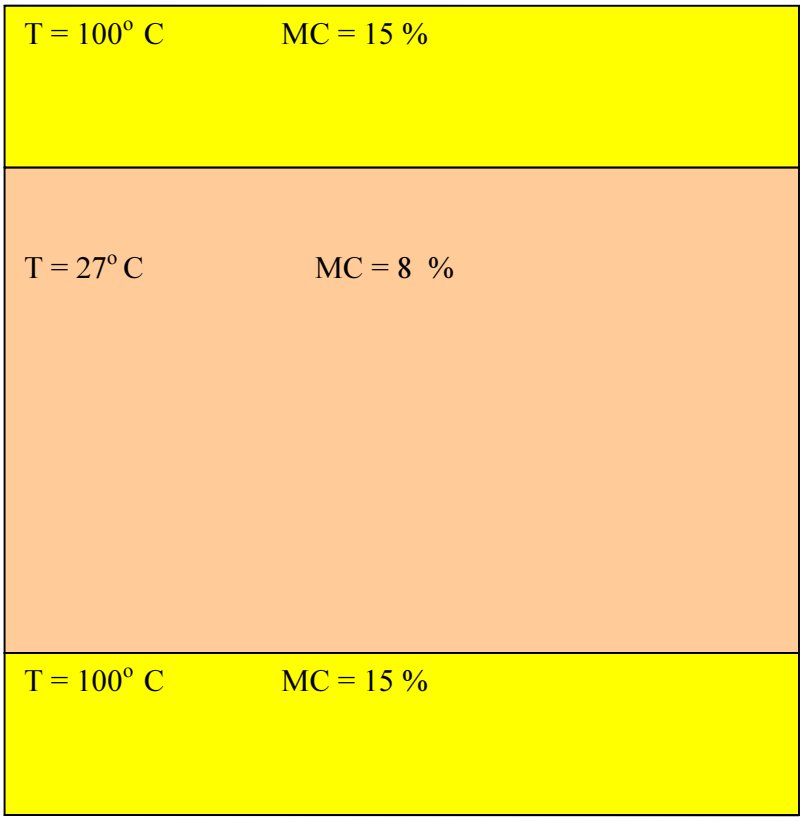

Figure 4.20: Initial temperature and moisture distribution in different layers in steam injection pressing.

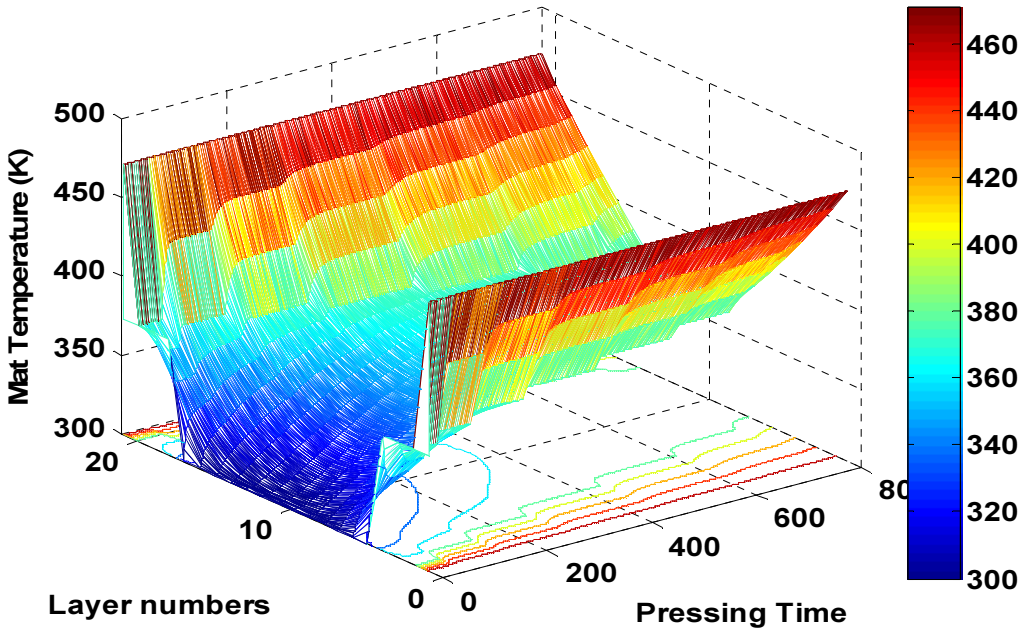

Figure 4.21: Change of temperature across thickness (Pre-heated mat with steam injection pressing)

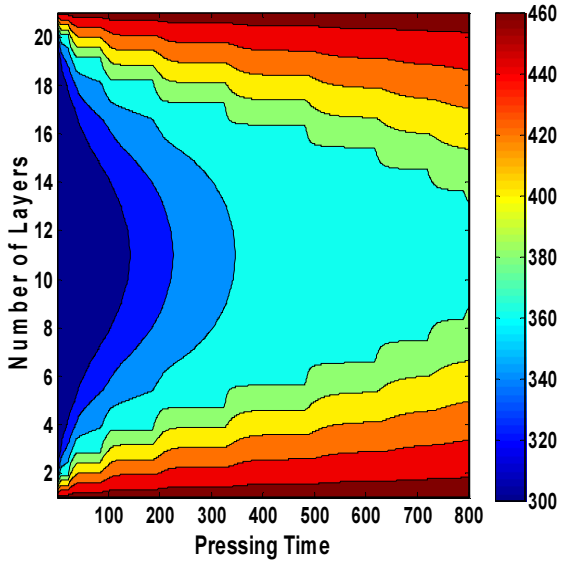

Figure 4.22 Temperature profile across thickness in standard pressing conditions

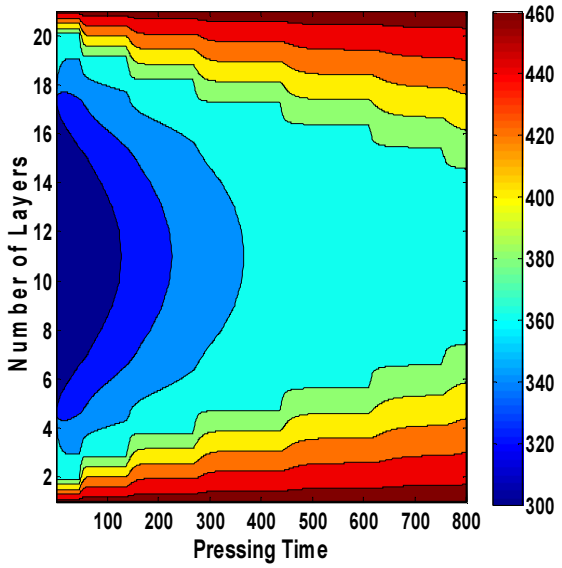

Figure 4.23 Temperature profile across thickness in steam injection pressing

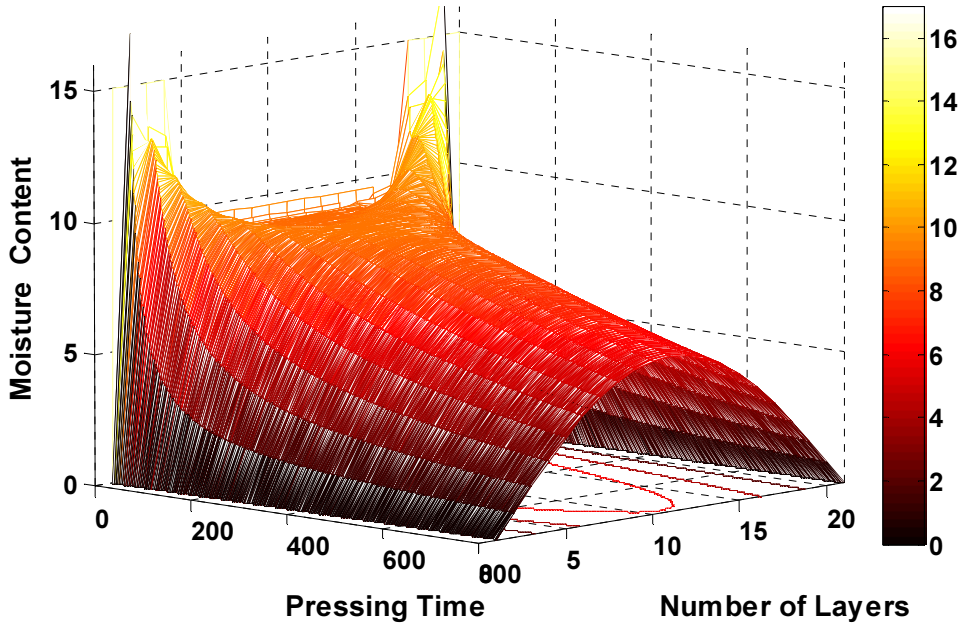

Figure 4.24 Change of moisture content with time (Pre-heated mat)

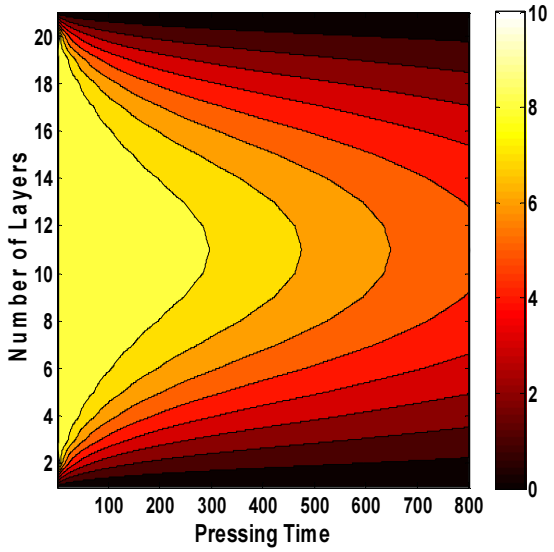

Figure 4.25 MC profile across thickness in standard pressing conditions

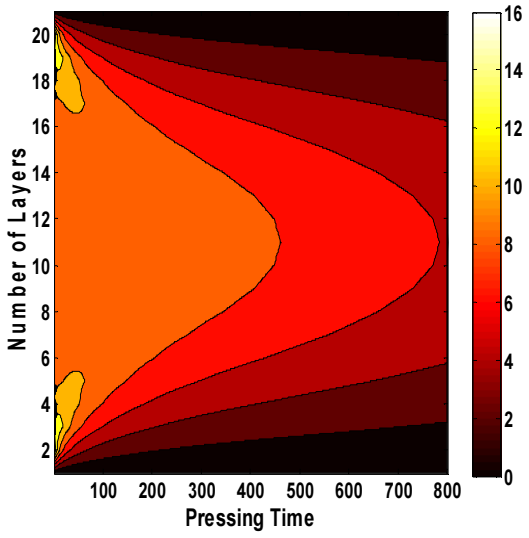

Figure 4.26 MC profile across thickness in steam injection pressing

Figure 4.21 shows the development of temperature across thickness in the steam injection pressing board. The surface layer reaches the platen temperature in a very short time and

the rest of the heat from the hot platen is transferred in the core region to increase the core temperature. Figures 4.22 and 4.23 show the comparison of temperature distribution in the standard pressing and the steam injection pressing. The increase in core temperature in the steam injection pressing is higher in comparison to the standard pressing. The reason for the accelerated rate of heat transfer is that not much energy is consumed to bring the temperature of the surface layer near to platen temperature and secondly the increase of moisture content increases the heat transfer by means of vapour convection.

Figure 4.24 shows the distribution of moisture content across the board during pressing. The surface layer has higher moisture content in comparison to the rest of the board. Later on the difference between the layers decreases. The moisture content in the core region is comparatively lower in the steam injected board than the standard board. Even though the average moisture content of both the boards is the same, the pattern of distribution is different. Figure 4.25 and 4.26 shows the comparison of moisture distribution in across the thickness in both types of pressing.

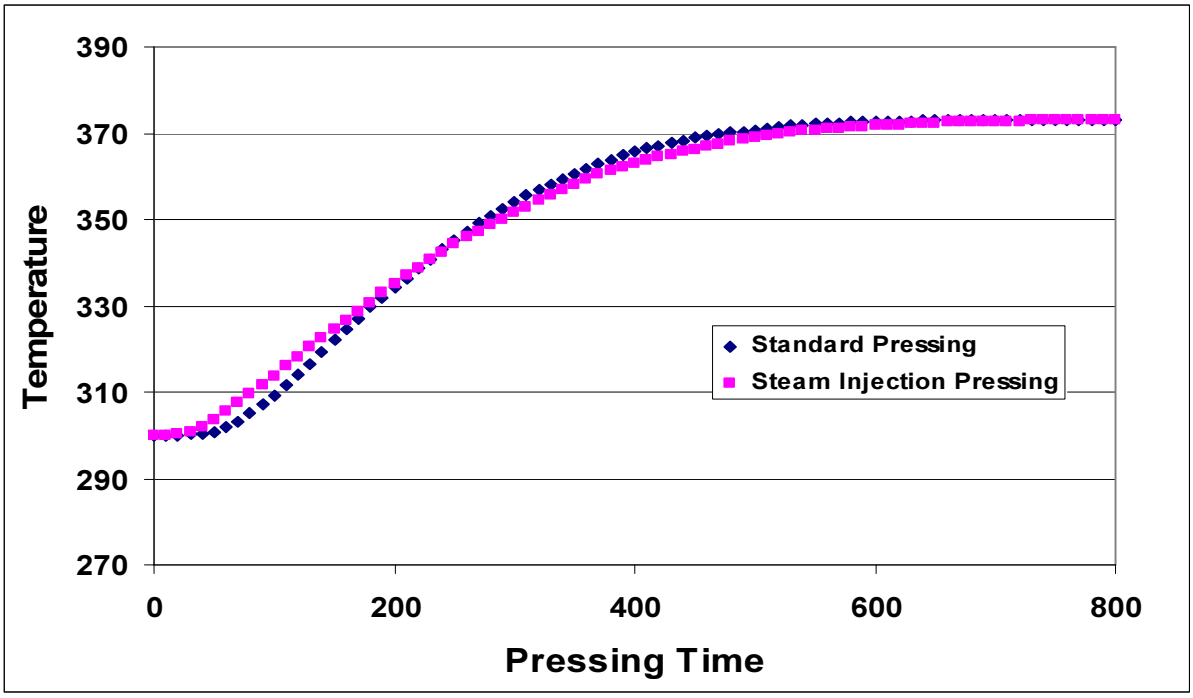

Figure 4.27 Comparison of core temperature from both standard pressing and steam injection pressing.

As shown in Figure 4.27, the core temperature with steam injection is higher than the standard simulation run in the beginning but later on decreases and again becomes the same as that of standard simulation run. The prediction of core temperature in steam injection pressing is only slightly higher than the standard run.

Thomen (2001) gave several reasons for the reduction of pressing time in steam injection pressing. First, the surface layers have a temperature of 100ºC before entering the press, so all the energy supplied by the hot platen is utilised in increasing the temperature of the core. Second, the high moisture content on the surface and low moisture content in the core promotes convective heat transfer. Third, the thermal conductivity in the surface layers is increased due to the high moisture content level.

4.7.4 Simulation Run for Cooling Zone in Continuous Press:

A new hot pressing technology, having a cooling zone in the last section of the continuous press has been introduced by Metso Panel board. The present model is able to simulate the new pressing technology and will increase the understanding of the internal changes going go on by pressing with this technology. The cooling zone covers from one-third to one-fourth of the total press length. The platen temperature is reduced from 198ºC to 80 °C in the last part (30%) of the pressing time; the other simulation parameters remain the same.

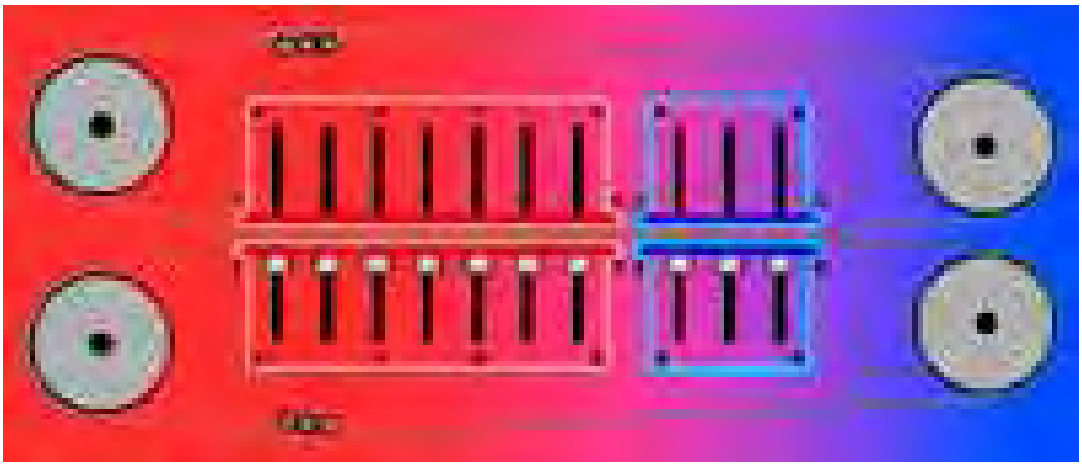

Figure 4.28: Two different zones in continuous press with different temperatures (Courtesy: MetsoPanel board USA)

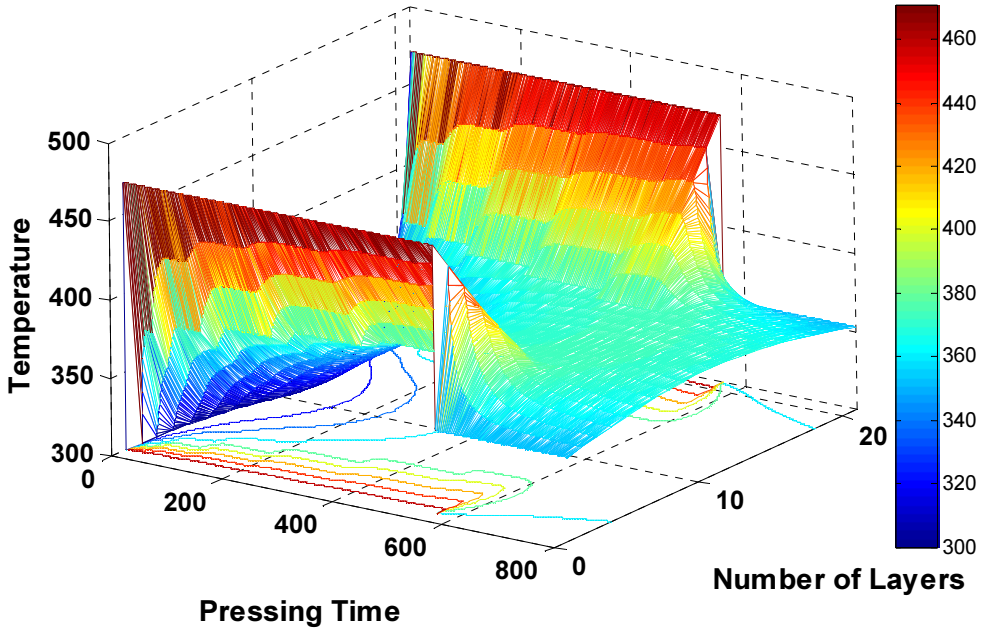

Figure 4.29 Change of temperature with time with the application of a cooling zone

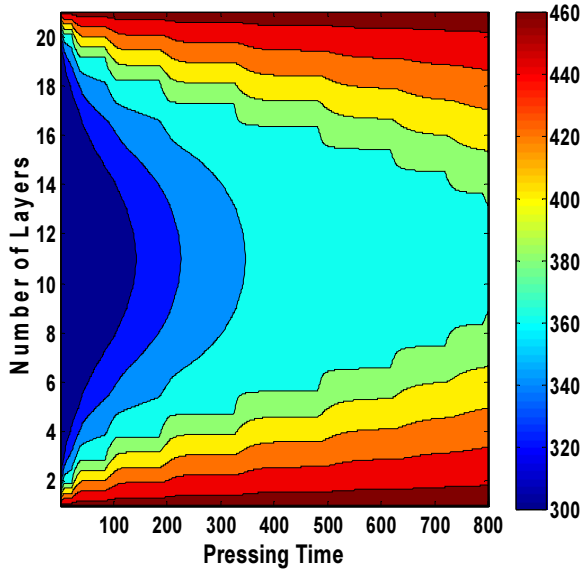

Figure 4.30 Temperature profile across thickness in standard pressing conditions

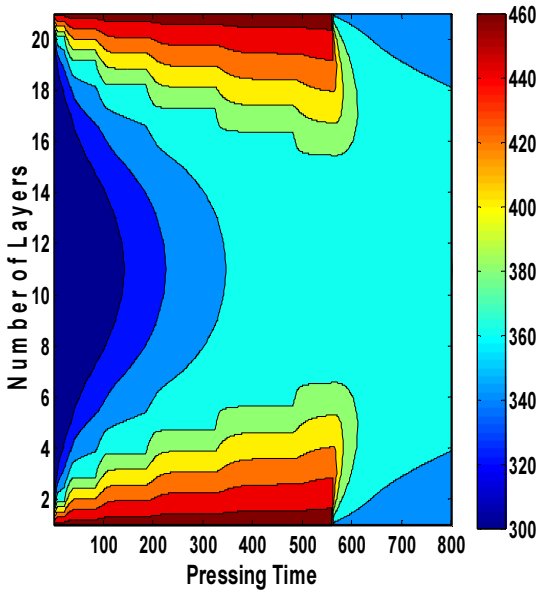

Figure 4.31 Temperature profile across thickness in cooling zone pressing conditions

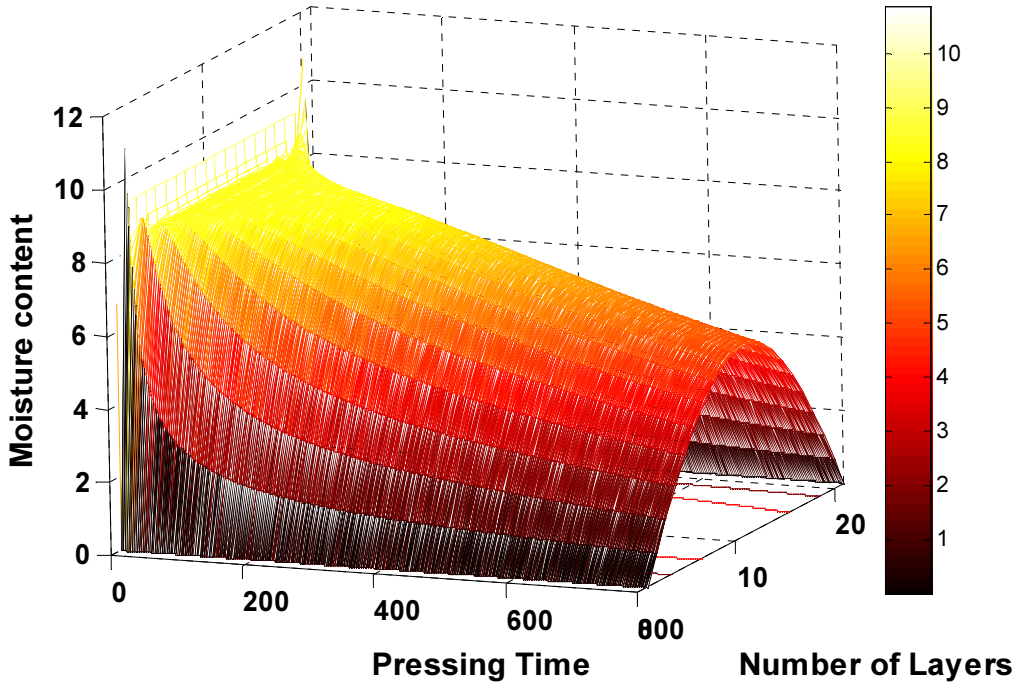

Figure 4.32 Change of moisture content with the time in cooling zone

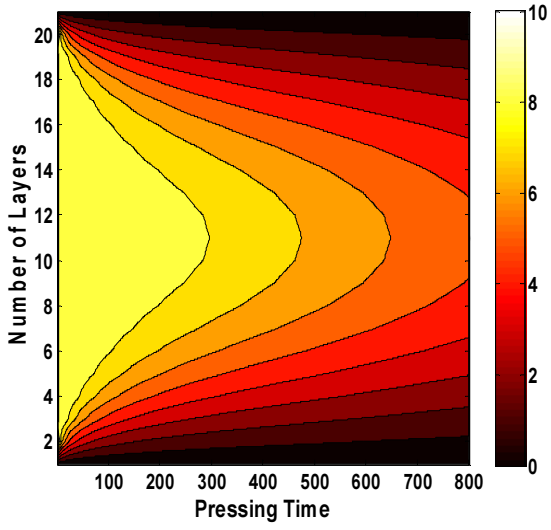

Figure 4.33 MC profile across thickness in standard pressing conditions (contour plot)

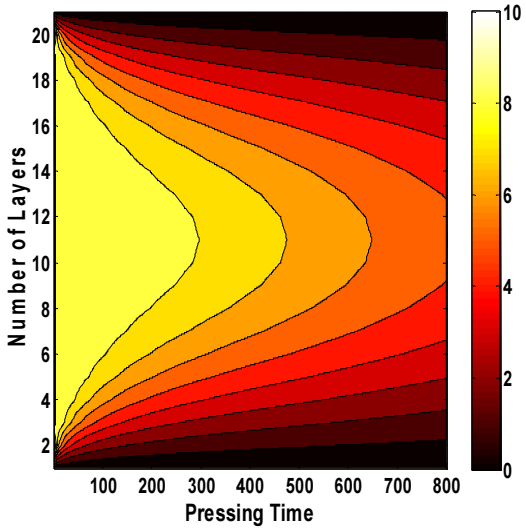

Figure 4.34 MC profile across thickness in cooling zone pressing (contour plot).

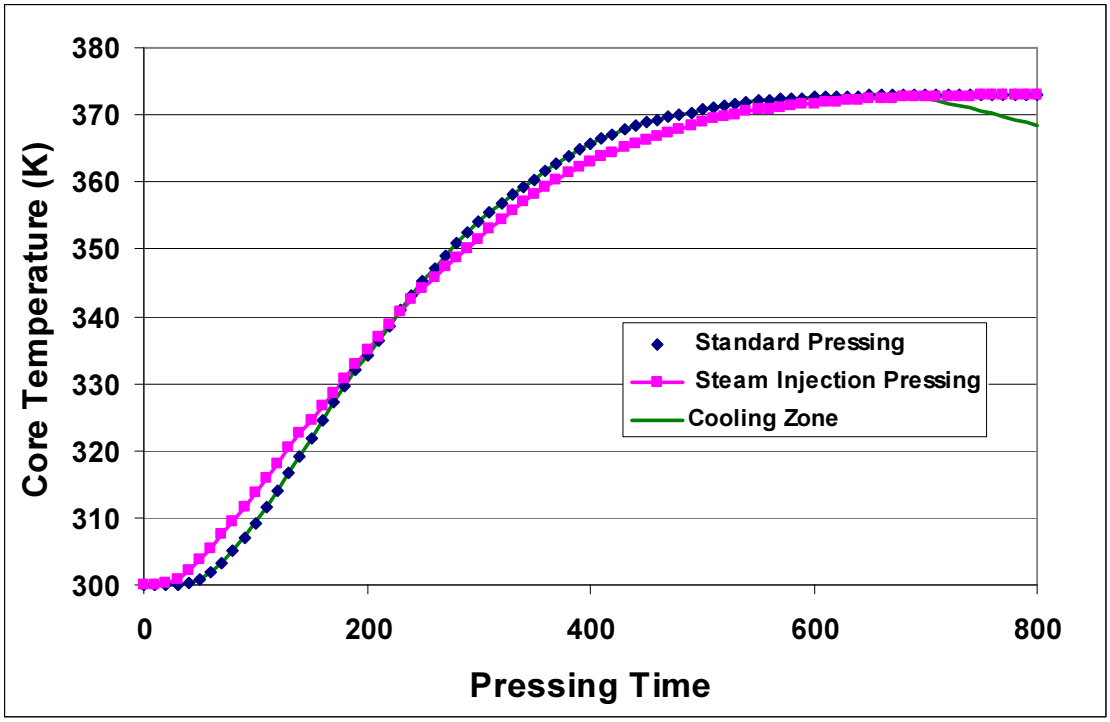

Figure 4.35 Comparison of core temperature from standard, steam injection pressing and cooling zone pressing.

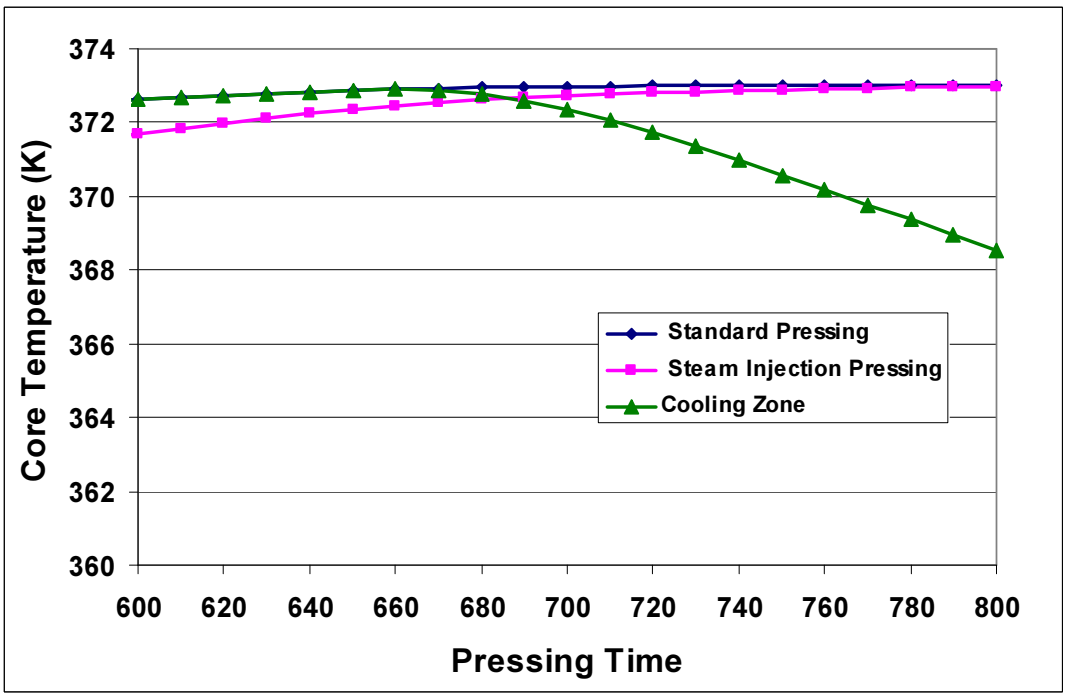

Figure 4.36 Comparison of core temperature from standard, steam injection pressing and cooling zone pressing in last section of pressing (600-800 sec)

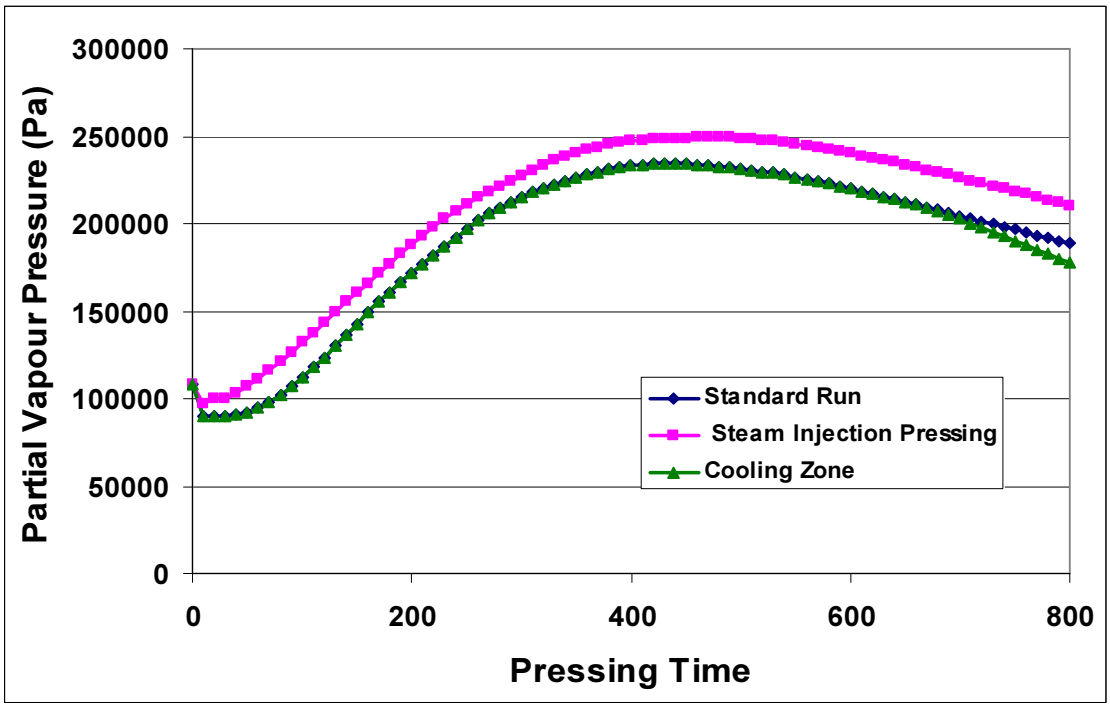

Figure 4.37 Comparison of core pressure from standard, steam injection pressing and cooling zone pressing.

Bluthardt et al. (2001), have reported the following benefits achieved by Metso Panel Board when using the cooling zone in the continuous press.

- The gas pressure in the board at the press outlet is reduced as the cooling temperature decreases.

- The initial moisture content of the fibre mat can be increased. This accelerates the heat transfer into the fibre mat during hot pressing and increases the out of press moisture content of the finished boards.

- The production capacity can be increased by 10 to 20%.

- The internal bonding will increase by 5-10 % and there will be a lower risk of blisters and delamination.

- Energy savings of around 10% are achieved, when the thermal energy taken out by cooling is recovered in the production process.

4.7.5. Discussion about New Pressing Technology:

Figure 4.28 shows the temperature in a continuous press with cooling zone. The first frame has a temperature of 198ºC and covers 70 % of the press length; the second frame covers 30 % of the press length and has a temperature of 80ºC. The continuous press is divided into two sections which are, as far as possible, thermally unlinked, but at the same time form one mechanical unit that keeps the pressure continuously on the product. The heat is provided by means of heated oil inside the platens. The heat is transferred through a rolling system (roller chain) and the steel belt into the product that has to be pressed. It is important to note that the complete press length (press platen = heated zone + cooled zone) does not become longer than a standard continuous press system.

Figure 4.29 shows the results of a simulation run. The surface layers have a temperature near the platen temperature. The core region, shown by the blue colour, has a temperature near the boiling point of water. In the second half due to the presence of the cooling zone, the temperature of the outer layer falls. The main source of heat transfer is by the conduction in the last stage of pressing. The temperature in the core also starts falling, due to compaction of the mat and evaporation of the available water. The only source of heat transfer is by means of conduction. Figures 4.30 and 4.31 shows the 2-D contour plot of temperature distribution in the standard and cooling zone simulation run. As seen from the standard simulation run, once the board has reached the final thickness stage, the only purpose of heat supply is to cure the resin inside. The resin on the surface layers reaches the curing stage in the beginning of the press cycle. Having a high temperature beyond that stage is not adding value but is a waste of energy. The purpose of the cooling zone is to reduce the waste. In the contour plot it is seen that most of the part in the cooling zone area is sky blue, showing a temperature near the boiling point of water.

Figure 4.32 shows the moisture content distribution across thickness with time. Figure 4.33 and 4.34 is shows the contour plots of both standard conditions and having cooling zone. It was found that there is not any significant difference in moisture content distribution between the two types of pressing. The moisture content is slightly less in the cooling zone in the later stage of pressing. It gives scope to increase the initial moisture content of the fibres to increase the rate of heat transfer without the risk of blowing or delamination of the boards.

Figure 4.35 shows the comparison of core temperature from all the three pressing technologies. The curve can be divided into three stages for easy description. The *first stage* is from (0- 100 sec). In this initial stage the core temperature in the steam injection pressing is the highest, followed by the temperature in the cooling zone and the standard conditions. The core temperature from the standard conditions and the cooling zone overlaps in most parts of the press cycle. It is only in the last section that the core temperature is higher than the cooling zone. The reason for having a higher temperature in the steam injection case is due to steam saturation in the outer surfaces of the board. The surface temperature rises to 100ºC and moisture content to 15 % as seen in the Figure 4.20. The heat transfer by the vapour front from the surface to the core region increases and also less heat is needed for the surface and the remaining heat can easily transfer to the core region. The *second stage* is from (100-600 sec). In this stage the core temperature from all the three pressing technologies overlap each other and have very minute differences between them. The *third stage* is from (600-800 sec). In this stage the core temperature from the standard run is the highest, having reached the boiling point of water and become stagnant there. The reason for becoming stagnant at that point is the latent heat consumed in the evaporation of water into vapour form. The core temperature from the steam injection also catches up with the standard conditions. The core temperature of the cooling zone starts decreasing due to lowering of platen temperature to 80ºC in the outer zone of pressing. Even though the surface temperature in the cooling zone is reduced quickly, the core temperature decreases much more slowly. Thus the core can maintain relatively hot even the platen is much cooler.

Figure 4.37 shows the comparison of core pressure from all the three pressing technologies. It is assumed in this model that the equilibrium moisture content (EMC) is reached instantaneously in the layer. When the heat is transferred from the platen to the mat, it changes the value of the EMC, relative humidity and saturated vapour pressure. From this, we get the partial vapour pressure without edge losses. The figure 4.27 shows the comparison of core pressure without edge loss. The value of core total pressure lies between 1 Bar to 2.5 Bar, similar results for partial vapour pressure are shown by Humphrey (2005). The reason for getting similar values is, first the comparative losses from the core region are much less than the surface layers. Second in the continuous press there are only two sides available for the edge losses, so the results are more comparable with the continuous press.

To describe Figure 4.37 in a better way, the whole curve is divided into three stages. *First stage* (0- 150 sec). The core pressure from the steam injection is highest, followed by the cooling zone and the standard conditions. The core pressure from the standard conditions and cooling zone overlaps in most part of the press cycle until the platen temperature is same for both (i.e 600 sec). The reason for having higher core pressure in the steam injection pressing is the high amount of moisture content in the surface layers (15 %), comparative to other conditions having moisture content of (10 %). A comparatively large amount of vapour is available to transfer heat and after the initial stage of pressing, it moves towards the core region and increases the core pressure. The *Second stage* is from (150- 600 sec). The core pressure from the steam injection pressing is still higher, after reaching peak it starts decreasing; the pressure from press with cooling zone and the standard simulation also follow the trend. The *Third stage* is from (600 – 800 sec). The core pressure from the steam injection is still higher than the other conditions. The core pressure in the cooling zone start decreasing slightly in comparison to standard and steam injection conditions.

Humphrey (2005) through his experimental work on resin has shown that the strength of the internal bond lies between 0-4 MPa. From the present model, we can get the resin

curing index which lies between 0-1. The resin is completely cured when the index reaches the value of one. The strength of the internal bond will be 4 MPa at that stage. We can derive a simple relationship on basis of these results to analyse the data more accurately.

$$Bond\ Strength\ (MPa) = Resin\ Curing\ Index \times 4$$

We can get the value of vapour pressure from the model and can examine the percentage of moisture content creates more risk of delaimnation. Delamination is a common experience in the commercial plants. If there are no bursting sounds near the end of the press cycle, the boards are of good quality. But if there are some bursting sounds than the whole lot of boards are of no use. They are down graded and normally thrown in the furnace to heat the boiler. It is a huge waste of raw material, man-power and energy. Another problem is that by the time the production people realise about the delamination, the second lot of twelve mats is already loaded in the batch press and the fibre in the continuous line is also wasted. One of the main objectives of this modelling work is to develop better understanding of the inter-relationship between various inputs, and the impact they have on the final product quality.

The reason for this behaviour is that in the initial stages, there were enough gaps in the mat so that gas can easily leak from the edges. But as the pressing progresses, the internal bonds start forming through the mat. The core region is the last section to get the higher temperature and so the bonds are formed in the last. After crossing half of the pressing time, the amount of vapour formation increases, which increases the vapour pressure. The prediction of vapour pressure is more important than the pressure by air. By experimental work of Denisov (1975), it was proved that all the air is replaced by the vapour in the later stages of the pressing.

If the vapour pressure exceeds the value of internal bonding in the last stage of pressing, then the board will delaminate. The risk is greater when the vapour pressure exceeds the value of 2.5 Bar and the value of curing index in the core region is below 0.6. Further

desirable improvements in the programming and the various mathematical equations derived to predict the physical properties of wood composite, rather than wood, includes factors such as modulus of elasticity, temperature moisture shift factor, Palka constant and mean diffusion coefficient for bound water diffusion. The present model will increase the accuracy to predict the risk factor and to manipulate the initial moisture conditions, platen temperature to avoid defects.

From figure 4.37, it is clear that the core pressure in the steam injection pressing is higher than other two pressing conditions. Cooling zone is having the lowest core pressure.

4.8. Conclusions:

The present simulation results show the capability of the model to simulate not only the standard pressing technology but also the new technology such as steam injection and having a cooling zone in the continuous press. There are few previous models capable of predicting new pressing technology. The model is efficient to predict changes in temperature, moisture content, resin curing and to some extend the partial vapour pressure inside the board.

The simulation results were generated to analyse the claims made by Bluthardt et al. (2001), about the advantages provided by the cooling zone in the continuous press. It was proved by the results that the gas pressure inside the board is lower than the standard conditions and gives allowances to the production people to increase the initial moisture content of the fibres to increase the heat transfer. There will be less risk of blowing and delamination. But the claim that internal bond will increase by 5-10 % is not predicted by the model and more experimental work is needed to prove this point. Another claim that cooling zone will increase the production is also not verified. To increase production, the total pressing time is to be reduced. But cooling zone is not contributing in any way to reduce the time.

Thomen.et al. (2005) have shown from their wood composite model that in steam injection pressing, the total time required to press the board is reduced. The present model has shown that in the steam injection pressing, the temperature of the core is slightly higher than the standard conditions but later on becomes same as that of standard conditions.

Both the new pressing technologies have distinct advantages as mentioned in the discussion section. A new continuous MDF press incorporates both steam injection pressing and a cooling zone. This reduces the length of the continuous press and the total pressing time. There is a great improvement in production and quality of the boards according to Thomen et al. (2005).

The new MDF plants such as, Donghwa Pvt. Ltd plant in Malaysia is using both steam injection pressing and cooling zone in a continuous press None of the plants in New Zealand is using these latest technologies. The computer model will help in educating them and to remove the hidden fear of risk involved in it.

The model has helped to develop better understanding of the causes of delamination and blowing of the boards. Further refining of the programming and mathematical equations will increase the accuracy of prediction. This computer model will become a useful tool in the hands of wood technologists, process engineers and wood composite manufacturers. This computer model will help in increasing the understanding of the process, optimise the present conditions, and to develop new methods, which can save energy and increase the quality of boards.

Chapter-5
Experimental Results and Validation of the Heat and Mass Transfer Model

Summary

Experiments were conducted to validate the model results. Fourteen small size MDF panels were made using the pilot-scale press. During the hot pressing, all the press cycle parameters such as platen position, platen pressure, core temperature and core pressure were recorded after every ten seconds. The first part of this chapter analyses, how the operation parameters (platen temperature, pressure) and material properties (fibre moisture content) influence the core temperature, gas pressure and density of the board. The results obtained are then analysed to develop better understanding of MDF manufacturing. In the second part, the experimental results are compared with the model simulations and thus the accuracy of the model prediction is analysed

5.1 Introduction:

The present chapter examines the capability of the model to predict the internal mat environment among different pressing operations. Three production parameters, the initial mat moisture content, the platen temperature, and the final panel density were investigated.

The internal temperature of the mat can be measured by inserting thermocouples to the core of the MDF mat before pressing. The total core pressure of the gas phase within the mat has been measured by pressure probes. However, the moisture content of the mat during the pressing cannot be measured using the non-destructive method, thus the model validation was performed only using the experimental results of core temperature and pressure.

5.2 Materials and Methods

The detailed description of material and methods is covered in section 3.3. The boards were tested for their density profile. A sample of 50mm x 50mm was cut and placed in a density profile machine (ProScan) to obtain its vertical density profile (VDP) graph. The details of ProScan are given in Chapter three.

5.3 Analysis of Experimental Results:

Fourteen MDF boards were made within a span of two days before the shelf life of the resin expired. The average moisture content of the fibres was 6.78 % and the resin content was 9.5 % on the oven dry basis by weight. The boards were made with different combinations of platen temperature, thickness, moisture content and density. The readings of all the parameters were recorded every ten seconds. The objective of this research was not only to develop better understanding by means of computer model but also to increase the understanding by experimental means and to optimize the hot pressing of MDF manufacturing. Pressure and temperature probes were used. Silicon oil was used to fill the space between probe and instrument to avoid the loss of vapour in the connecting path. The pressure due to the hydrostatic head in the silicon column was 0.04 MPa that needs to be subtracted from the measured value. The pressure transducer measured gauge total pressure (pressure above the total pressure of the environment at the ambient temperature). The overall analysis is divided into six major groups and then the results are interpreted in the following sections. See Table 5.1 for an overview of the range of experimental conditions.

Table 5.1 Summarising Experimental Design:

Number of Boards	14		
Platen temperature (C)	160	198	
Thickness (mm)	19	24	
Moisture content (%)	6.78	16.78	
Densities (kg/m3)	650	700	826
Pressing time (s)	350		
Dimension of board	30 cm length	30 cm width	

Figure 5.1: A pair of thermocouple wires and a pressure transducer is inserted in the middle of the board.

5.3.1 Effect of density on core pressure, temperature and density profile

In order to investigate the effect of board density, three 19mm thick boards with densities of 650, 700 and 826 kg/m^3 were made whereas the other operation conditions and the fibre properties remained the same for all of the three boards as given in Table 5.2. The experimental results are shown in Figures 5.2 to 5.4.

Table 5.2: Pressing parameters for three different densities

Board density	650,700, 826 kg/m^3
Fire moisture content	6.78 %
Resin content	9.5 %
Platen temperature	198 ºC
Pressing time	390 s
Board thickness	19 mm
Press cycle used	Position control

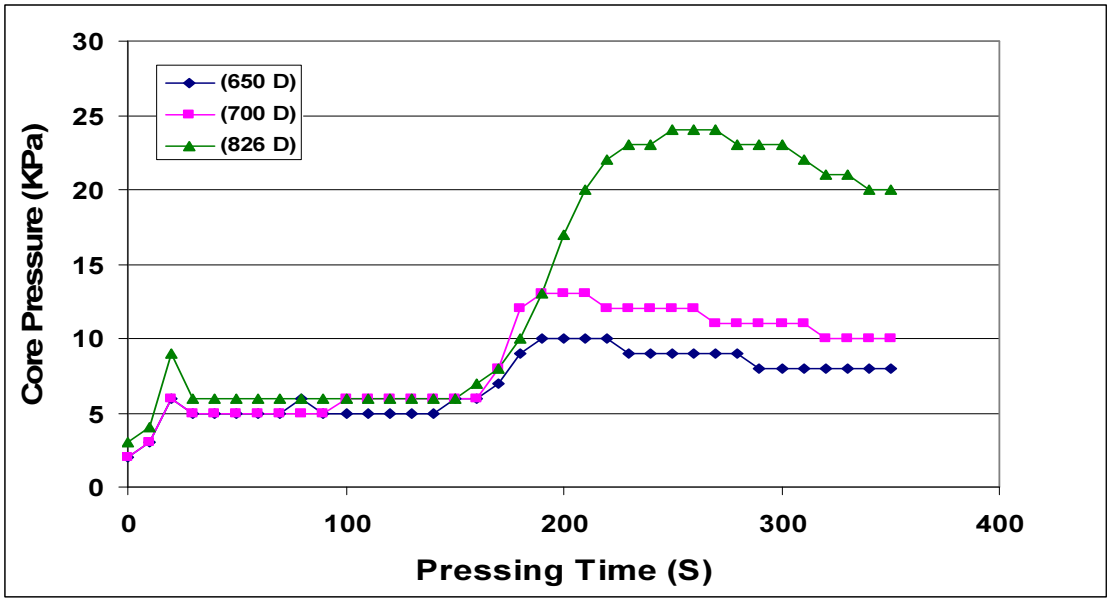

Figure 5.2: Core pressure in three different density boards

Figure 5.2 shows the core pressure profile during the hot pressing of the three different density boards. It was observed that initially the core pressure rises due to compression of the mat. As the air entrapped in the mat tries to escape, the pressure drops and remains constant for some time. At this stage most of the pressure is due to slow evaporation of water as most of the air has escaped from the edges in the beginning. After about 150 seconds from start of the press, the core pressure starts rising again but at a fast rate due to rapid increase in partial pressure of water vapour. The peak pressure corresponds to the temperature in the core approaching the boiling point of the water.

At the peak pressure and afterwards, the core pressure is higher in the high density board and lower in low density board. This can be explained by two factors. One factor is the higher total amount of water in the higher density board which will produce more vapour at the same temperature. The second factor is that the higher density board has lower gas permeability As the board is pressed, the permeability of the board keeps on decreasing. In high density boards, the permeability is low, so less vapour escapes from the board edges in comparison to the low density boards. This results in high core pressure in high density board and low core pressure in the low density board. The core pressure indirectly raises the boiling point of water by 4ºC. The core pressure in the small scale lab board is

lower than the actual board in a commercial plant. The reason for this is that the flat dimensions of the lab made MDF board are much smaller than those in the commercial panels (normally 1.2m wide and 2.4 m long) and thus the air-vapour goes a shorter distance to escape from edges.

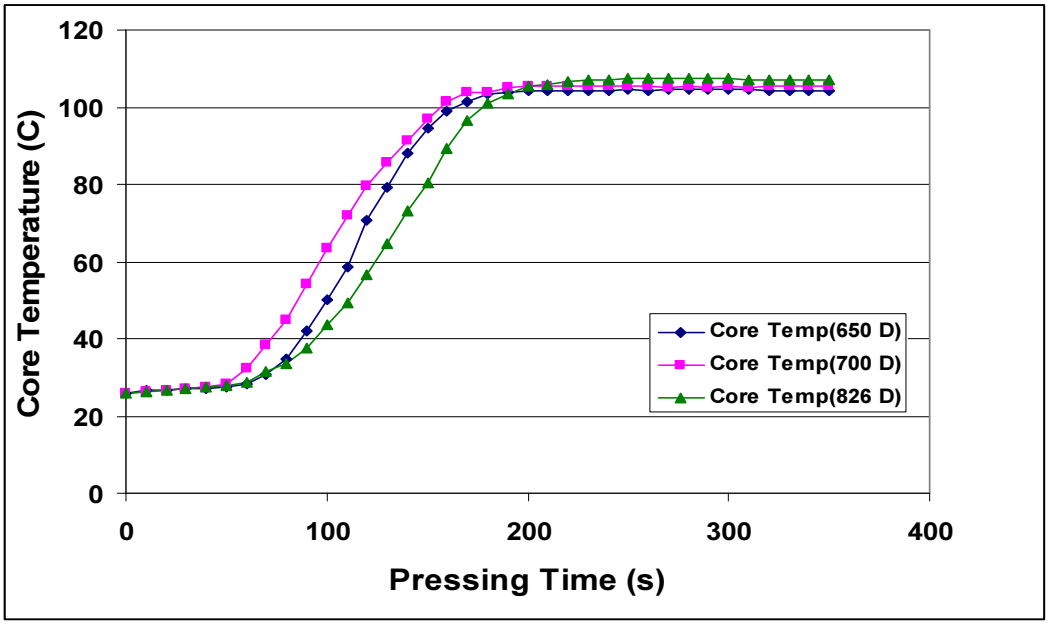

Figure 5.3: Core temperatures in three different density boards

The core temperatures measured for the three different density boards are shown in Figure 5.3. As depicted in the figure, the core temperature remains unchanged for the first 40 seconds. After that the core temperature starts increasing gradually and after reaching 104ºC it remains steady until the completion of the press. The first reason for having constant temperature over 100°C is that the core pressure becomes higher than atmospheric pressure, which raises the boiling point of water. Secondly, after the temperature reaches the boiling point of the water, all the energy is used in the change of phase from bound water to the vapour state. The increase in core temperature is slower in high density board in comparison to the low density board, as more energy is needed to raise the temperature of thicker mat layer and wood fibre in comparison to the thinner boards.

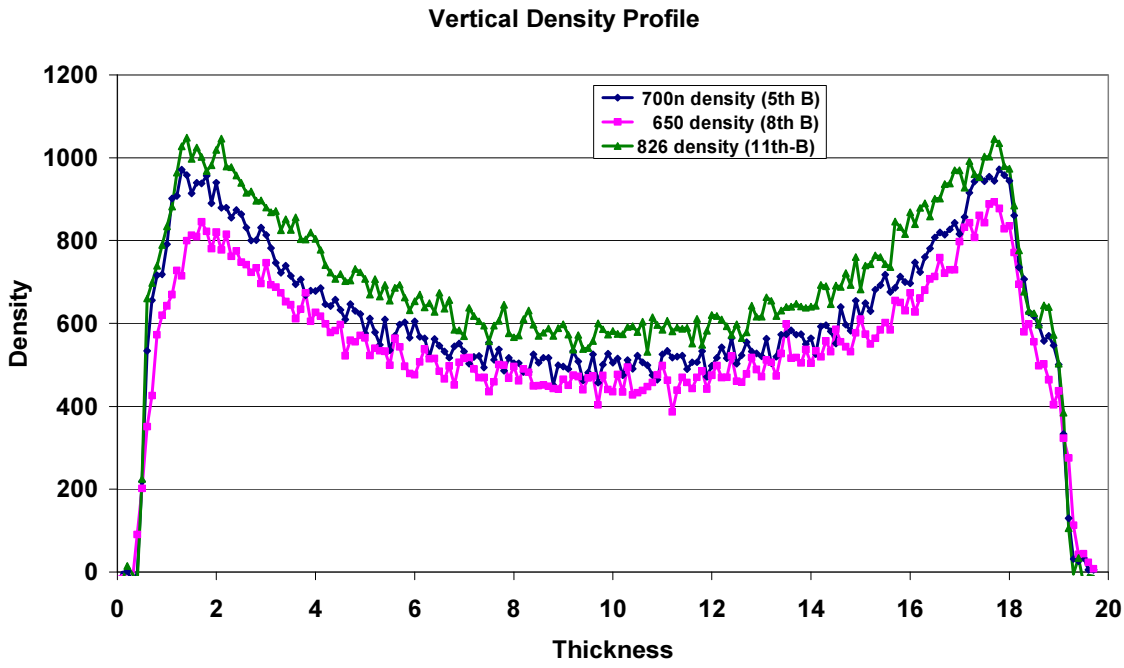

Figure 5.4: Density profile across three densities with similar conditions

Figure 5.4 shows the development of density profile in three representative boards. The higher density board has higher peak and core density than the lower density boards. However, with the press-cycle and other pressing conditions remaining the same, the pattern of the density profile is the same for the different density boards.

5.3.2 Effect of platen temperature on core pressure, temperature and VDP

Two 19 mm thick boards of same density of 650 kg/m^3 were made using platen temperatures of 160ºC and 198^{o}C, respectively, to investigate the effects of pressing temperature. The details of the operation conditions and the fibre properties are given in Table 5.3 and the experimental results are shown in Figure 5.5 for core temperature, in Figure 5.6 for core pressure and in Figure 5.7 for density profile.

Table 5.3: Pressing parameters for same density but different platen temperatures:

Density	650 kg/m^3
Moisture content	6.78 %
Resin content	9.5 %
Platen temperature	160 ^oC & 198 ^oC
Pressing time	390 s
Average thickness	19 mm
Cycle used	Position

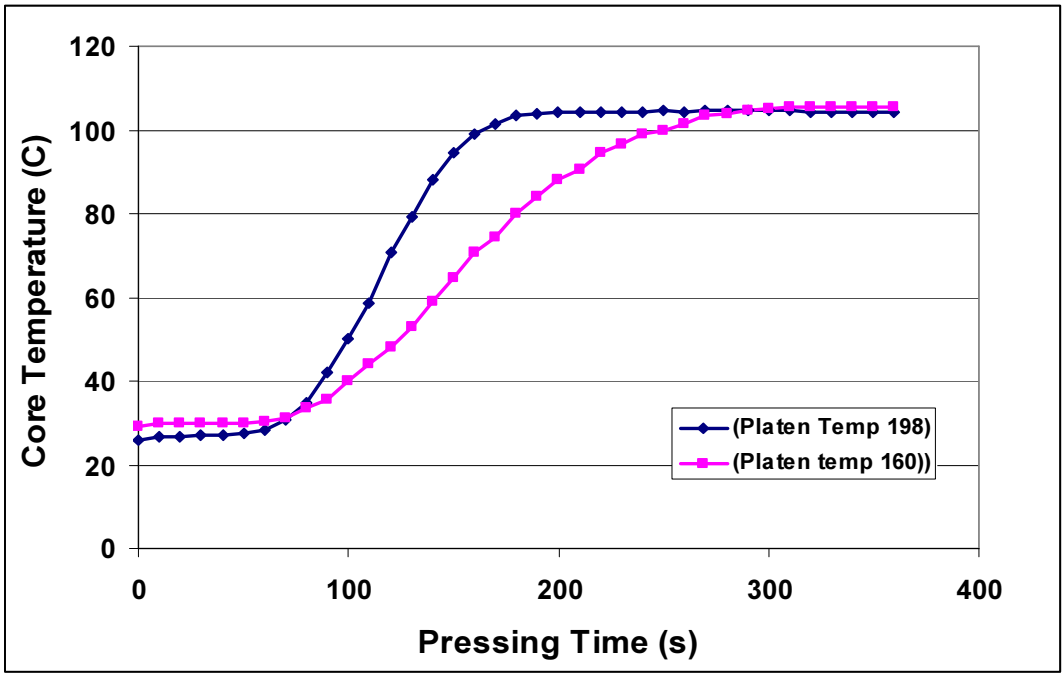

Figure 5.5: Profile of core temperature with two different platen temperatures

As observed in Figure 5.5, the core temperature rises much faster when the platen temperature is higher and becomes almost constant at 104ºC in the final stage of the hot pressing. The reason for fast rising of core temperature is the larger amount of heat flow through conduction and convection of vapours in the core region. The higher temperature gradient between surface and core layers accelerates the heat transfer towards the core.

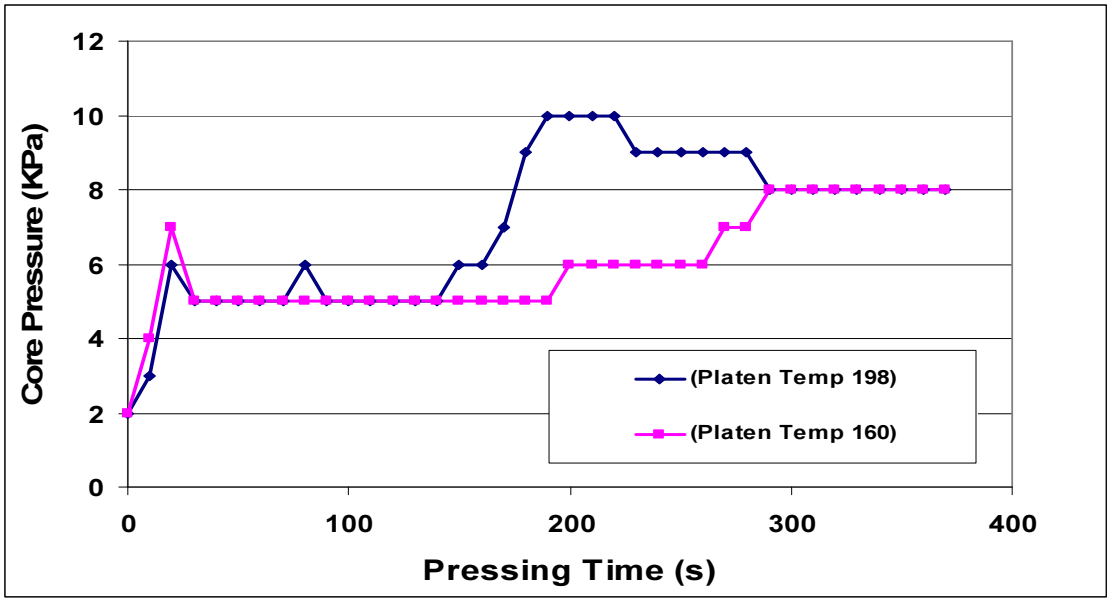

Figure 5.6: Profile of core pressure with two different platen temperatures

As seen in Figure 5.6, after about 180 seconds from the start of the hot pressing, the core pressure with the platen temperature of 198°C, the core temperature starts rising while at the same time the core temperature in the board with lower platen temperature 160°C still remains at 5 KPa. Although the core pressure with the lower platen temperature increases to 6 KPa after about 200 seconds this is much lower then the core pressure measured in the board with the high platen temperature. The reason is that high platen temperature causes fast increase in core temperature and it soon reaches the boiling point of water. This is one of the main reasons for increase in core pressure sooner in the high platen temperature board.

The core pressure with the higher platen temperature reaches the peak value earlier due to fast increase of core temperature to the boiling point of water and after that start coming down, where as in the second case with lower platen temperature. Core pressure takes more time to reach to the peak value.

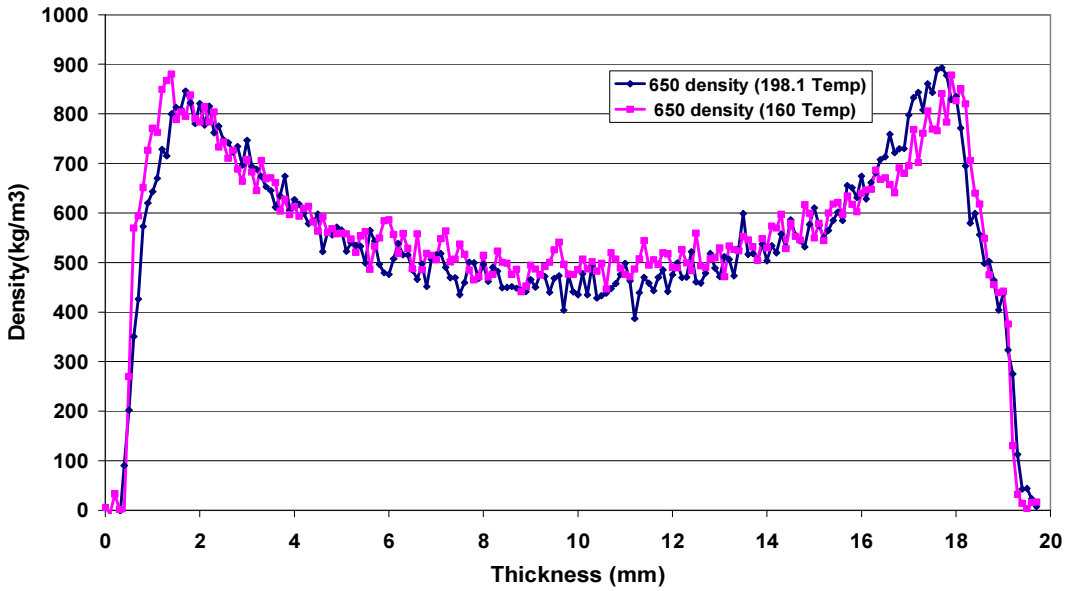

Figure 5.7: Density profile at two different platen temperature but same other conditions

As seen in Figure 5.7, the impact of platen temperature on the peak density is not distinct but is noticeable in the core region. The core density decreases with increasing platen temperature. From the density profile model simulation discussed in Chapter 3, it was found that with the increase in platen temperature peak density increases and core density decreases slightly. The probable reasons is that increasing temperature increases the plasticity of the top layers, due to which there is greater compression in peak layers and less in the core.

5.3.3 Effect of platen temperature in higher density board

Two boards of same density of 700 kg/m^3 but with different platen temperature 160ºC and 198ºC. In the case the density is increased by 50 kg/m^3 and the result are analysed.

Table: 5.4 Initial parameters for same density but different platen temperatures;

Density	700 kg/m3
Moisture content	6.78 %
Resin content	9.5 %
Platen temperature	160 ^{o}C & 198 ^{o}C
Pressing time	390 s
Average thickness	19 mm
Cycle used	Position

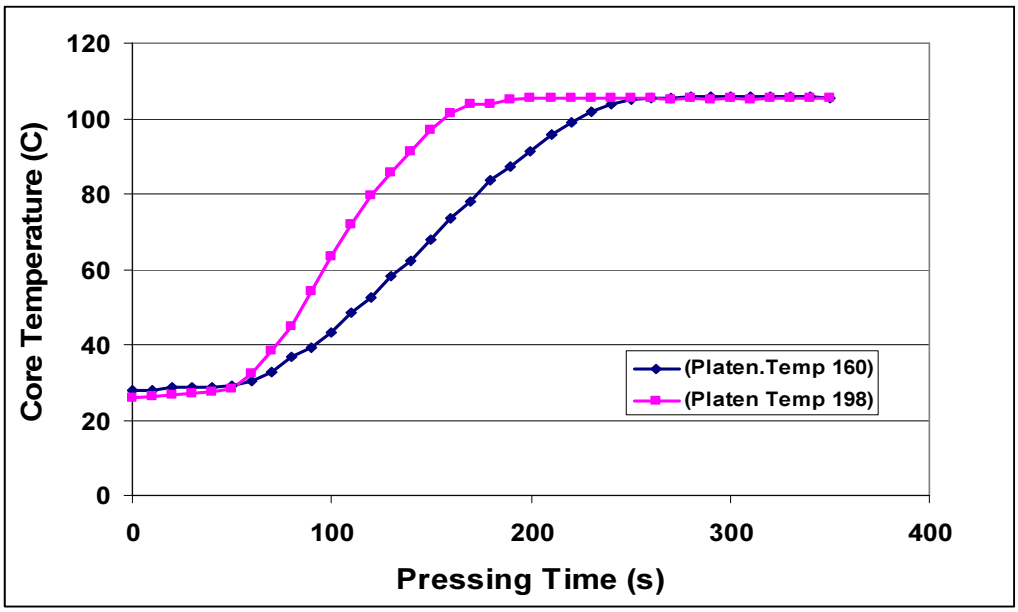

Figure 5.8: Change in Core temperature with two different platen temperatures

As seen in Figure 5.8, the core temperature rises faster with the increase in platen temperature; the reason is the high amount of heat flow due to conduction and convection of water vapour towards the core region.

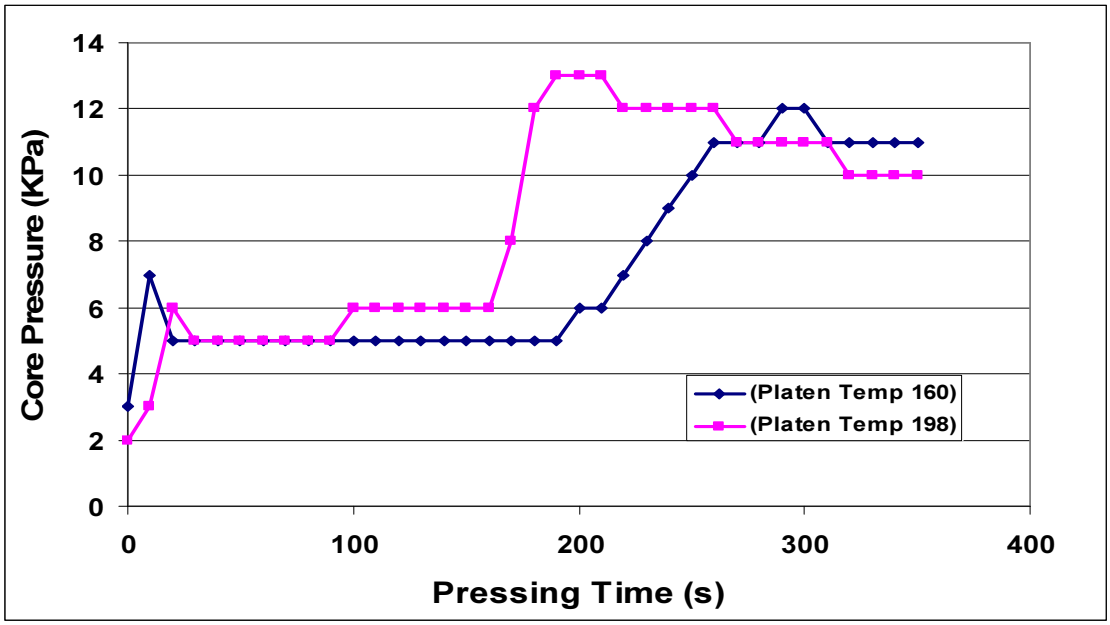

Figure 5.9: Change in core pressure with two different platen temperatures

Figure 5.9 shows that the core pressure raises much faster in the board made with higher platen temperature, the reason is that the core temperature reaches to boiling point quicker and causes the evaporation of water. The reason for this particular behaviour is explained in the above section.

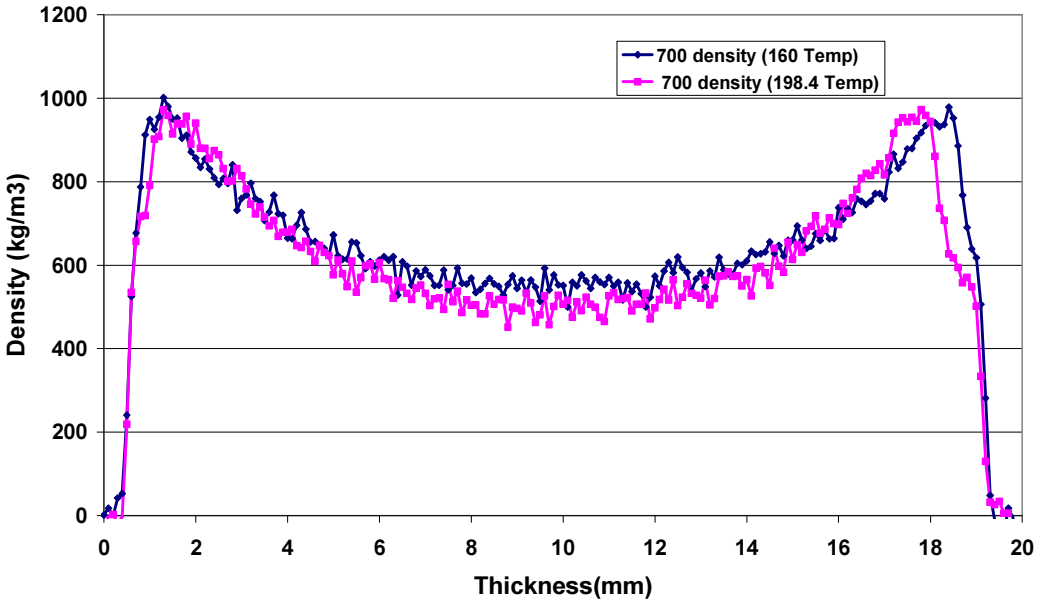

Figure 5.10: Effect of platen temp on vertical density profile.

Figure 5.10, shows the impact of platen temperature on the density profile. There is no clear impact on the peak density but the core density decreases with the increase of platen temperature.

5.3.4 Effect of moisture content on core pressure and core temperature

Two 19 mm thick MDF boards of a density of 650 kg/m^3 were made with mat initial moisture contents of 6.78 % and 16.78 %, respectively. The higher moisture content mat was created by adding about 10 % of water by weight to the fibers during the mat formation. The main purpose was to experimentally investigate the effect of the mat initial moisture content on core temperature and gas pressure. The operation conditions and mat properties in these two runs are given in Table 5.5 and the results are shown in Figures 5.11 and 5.12.

Table: 5.5 Pressing parameters for same density but different moisture content boards:

Density	650 kg/m^3
Moisture content	6.78 % & 16.78 %
Resin content	9.5 %
Platen temperature	198 ˚C
Pressing time	380 s
Average thickness	19 mm
Cycle used	Position

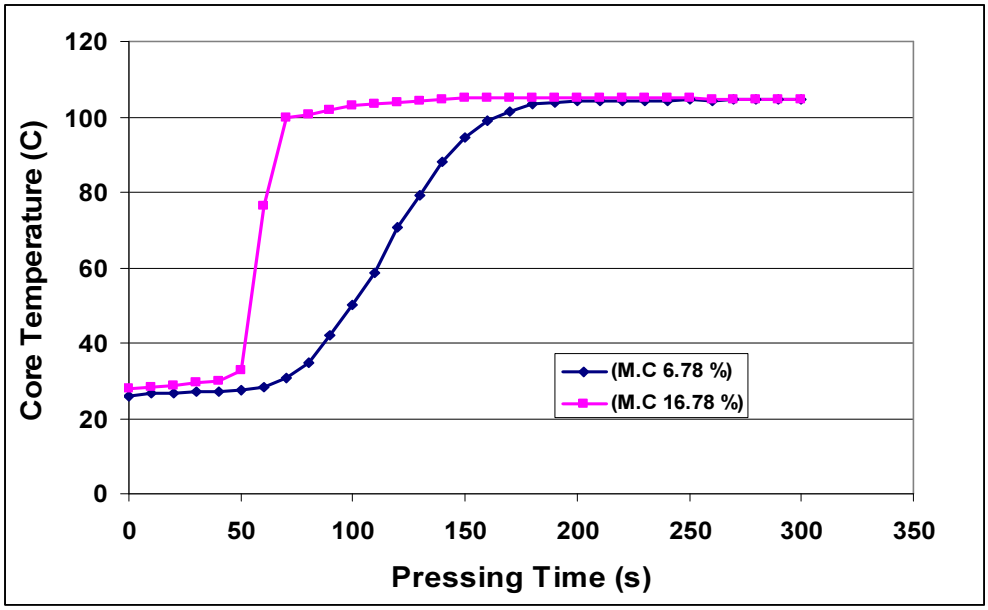

Figure 5.11: Profile of core temperature in MDF boards with two different initial moisture contents

As observed in the Figure 5.11, the core temperature in the higher moisture content board rises very fast after about 50 seconds from the start of the hot pressing, and in the final stage of the pressing the core temperatures with the two initial moisture contents becomes stable at 104ºC. There are two factors which may contribute to the faster increase in the core temperature with the high initial moisture content. With higher initial mat moisture content, the heat conductivity of the mat is higher thus the heat conduction within the mat is faster. More importantly, with higher mat initial moisture content, more vapour evaporation occurs near the surface and more vapour condensation in the core. The latter can be confirmed from the core pressure measurement. The main reason is the higher amount of heat transfer by convection.

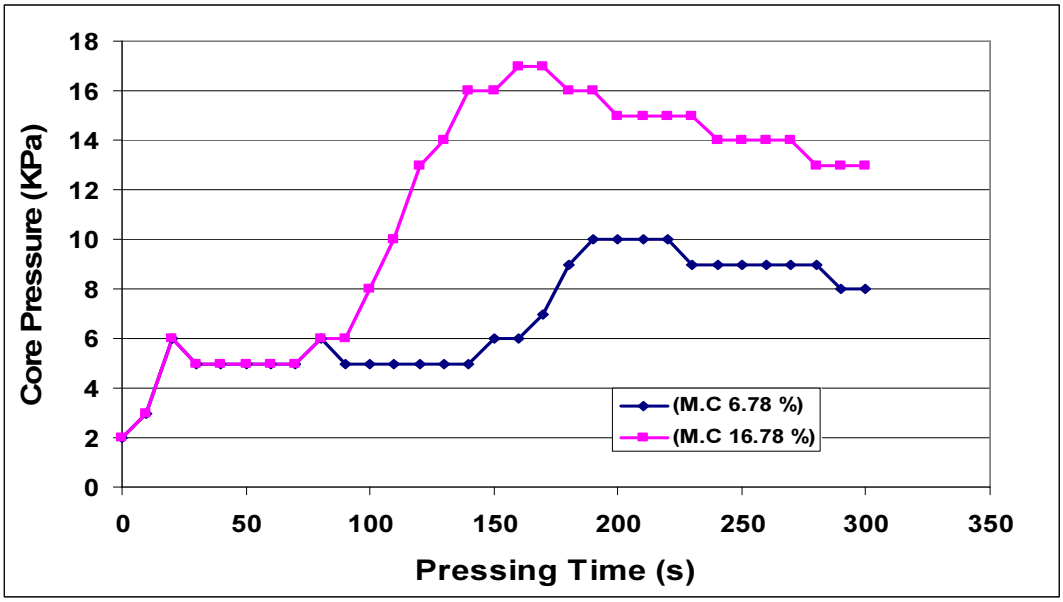

Figure 5.12: Profile of core pressure in boards with two different moisture contents.

As seen in the Figure 5.12, the core pressure rises very fast, with the addition of moisture. The high amount of moisture content creates high vapour pressure in the centre which induces a risk of delamination of the board. The mechanism of board delamination is complicated but wherever the stress caused by the high gas pressure within the board exceeds the internal bonding, small cracks may be generated and spread, inducing board delamination after the hot pressing. Then the gas will start leaving the boards from the edges.

5.3.5 Analysis of core pressure and temperature in Delaminated board

Table 5.6 Initial pressing parameters for delaminated board:

Density	1356.56 kg/m3
Moisture content	6.78 %
Resin content	9.5 %
Platen temperature	160 ^{o}C
Pressing time	360 s
Average thickness	11.5 mm
Cycle used	Position

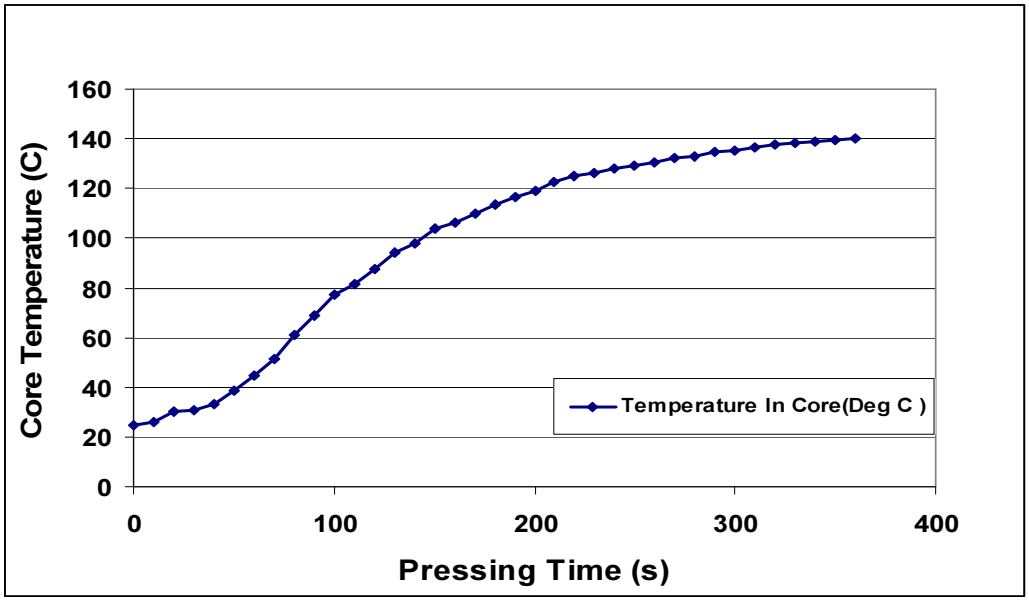

Figure 5.13: Change in core temperature with time in delamination board.

Figure 5.13 shows the development of core temperature in the delaminated board. As this is a high density board, the core temperature keeps on rising with the pressing time, indicating that the core pressure kept increasing.

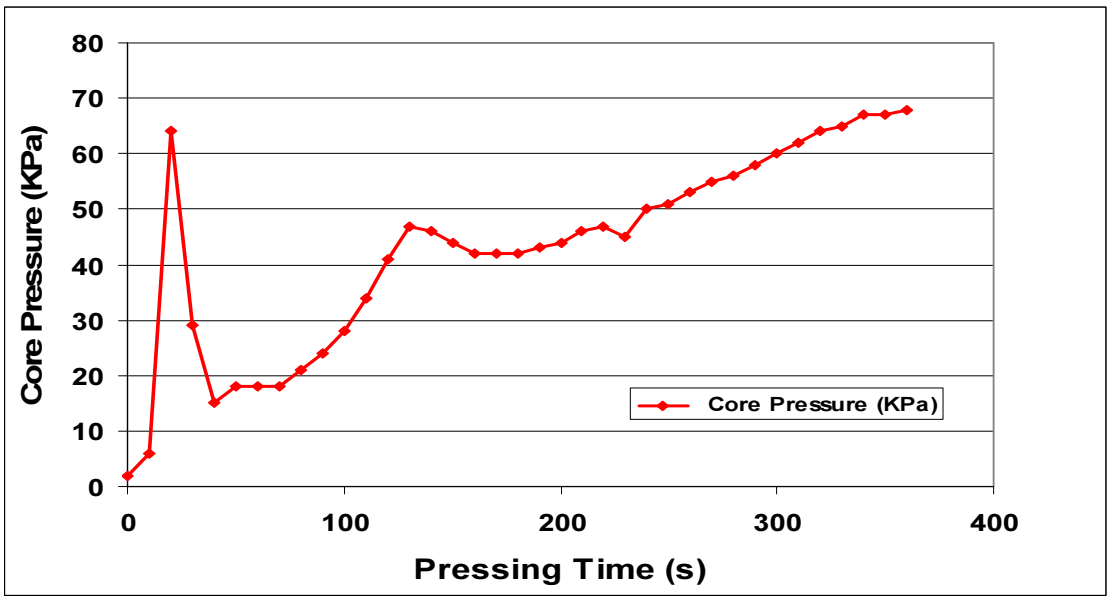

Figure 5.14: Change in core pressure with time in delaminated board.

Figure 5.14 shows the development of core pressure in the delaminated boards. In comparison to other normal boards, when the maximum pressure was 20 KPa. In this example, the core pressure had reached the highest value of 60 KPa. The high internal gas pressure causes the blowing of the board.

5.3.6 Analysis of internal changes in different thickness board:

Two boards of same density of 650 but with different thickness

Table 5.7: Pressing parameters for same density but different thickness boards:

Density	650 kg/m3
Moisture content	6.78 %
Resin content	9.5 %
Platen temperature	198ºC
Pressing time	390 s
Average thickness	19 mm & 24 mm
Cycle used	Position

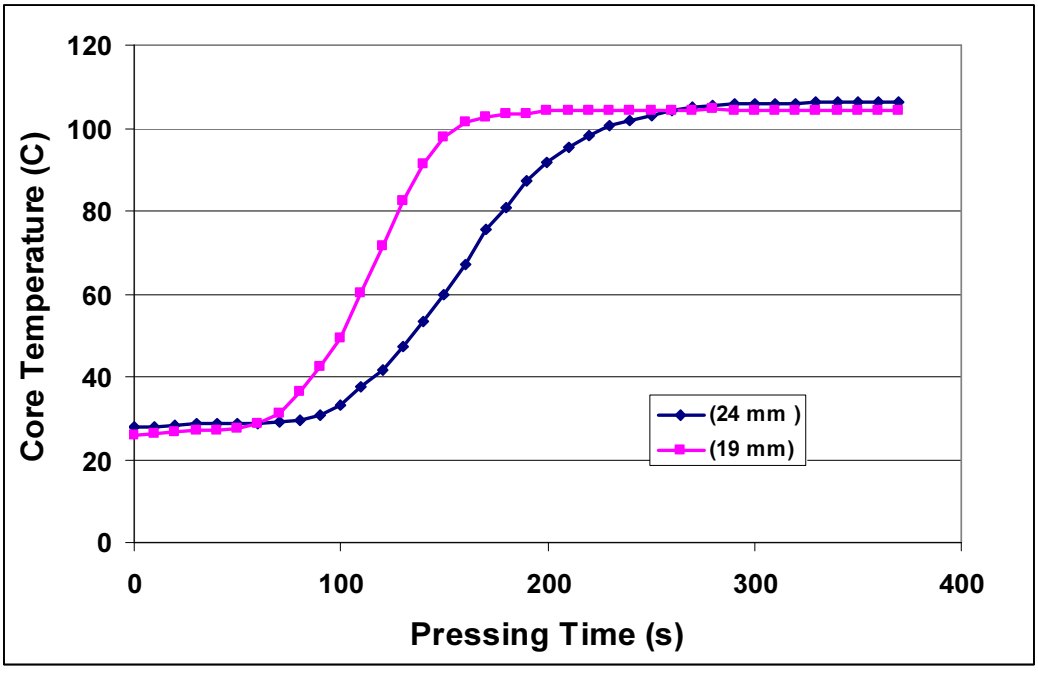

Figure 5.15: Change of core temperature with time for boards of two thicknesses.

Figure 5.15, shows the development of core temperature. If all other conditions remain the same, then temperature rise is faster in the low thickness board.

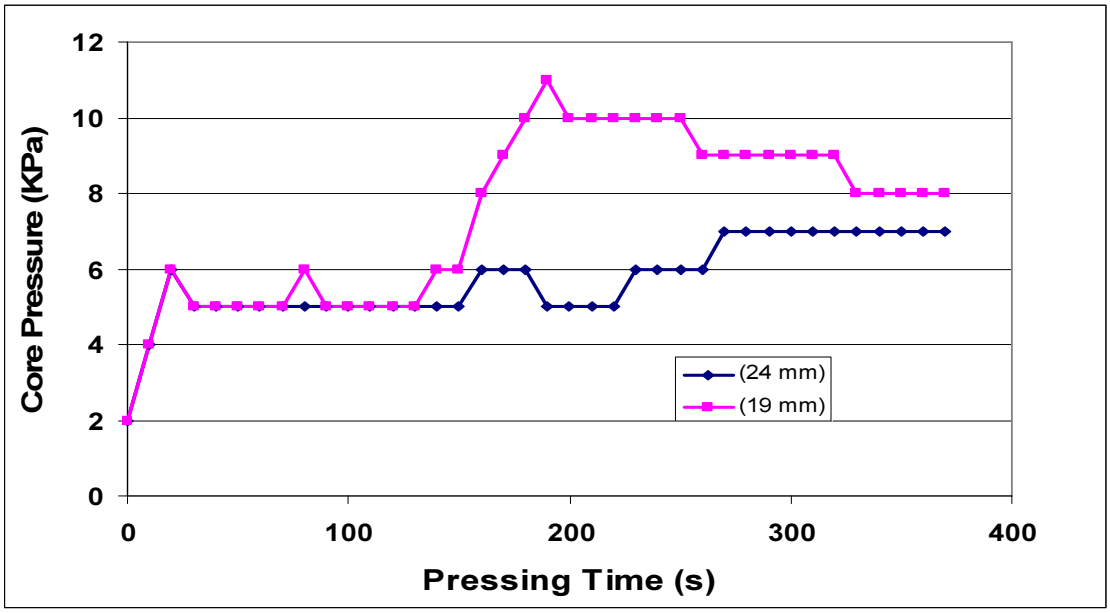

Figure 5.16: Change of core pressure with time for boards of two thicknesses.

As shown in Figure 5.16, the core pressure rises much faster in low thickness board.

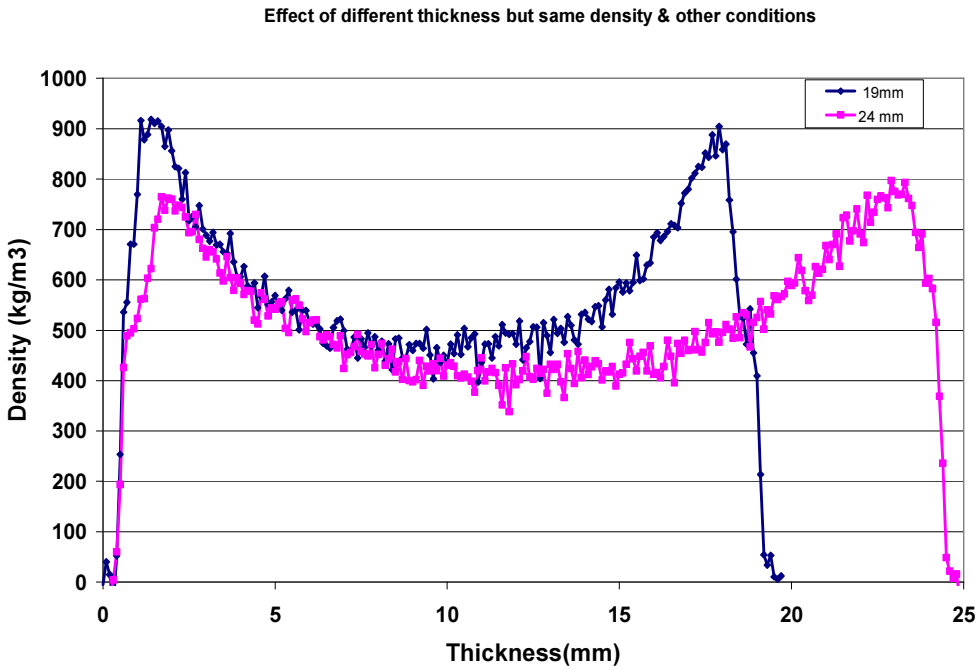

Figure 5.17: Effect of same density but different thickness on vertical density profile.

As shown in Figure 5.17, the peak density is higher in low thickness board, than the high thickness board.

5.4 Comparison of the Experimental and Model Predicted Results:

As the model is one dimensional, only core temperature can be validated. We had tried to validate the core pressure by comparing it with the partial vapour pressure without the edge loss.

5.4.1: Comparison of Core Temperature at Higher Platen Temperature:

A board of target density 700 kg/m3 was made in the pilot plant. The core temperature and core pressure is recorded after every ten seconds. The recorded core temperature is compared with the model results. The platen temperature in this case was 198˚C

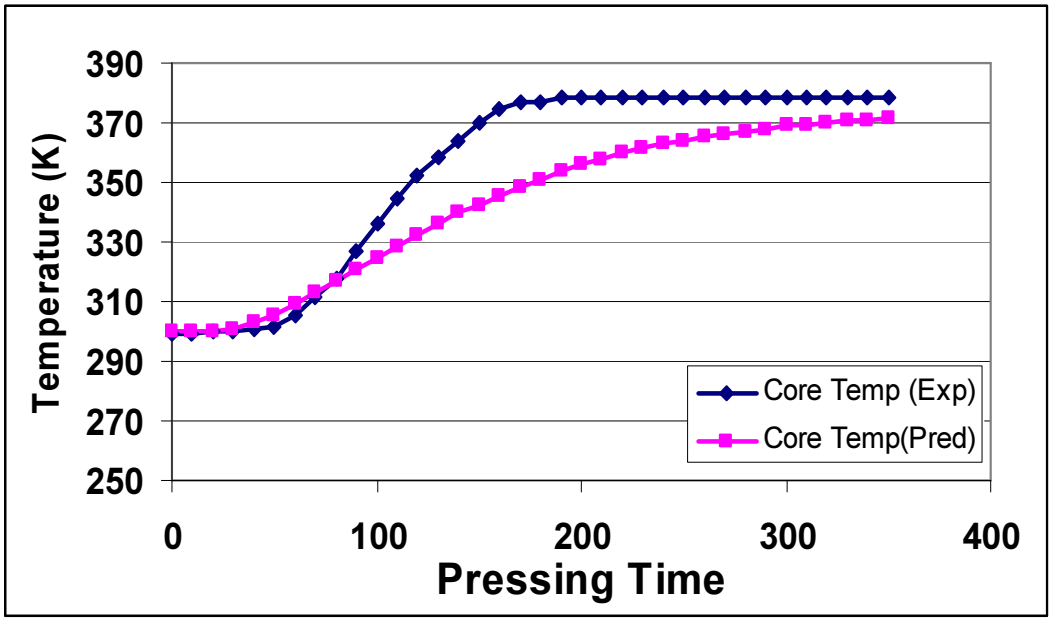

Figure 5.18: Comparison of core temperature from model and experiment

As seen in Figure 5.18, the core temperature from both experiment and model agree in the beginning, but as the press time increases, the rise in experimental value is much faster and stays at the higher value. There are four components, which play major role in the heat transfer. They are conduction, convection, exothermic reaction of resin and change of phase. If any one component is calculating less heat transfer, than the core temperature through model will be lower. The second probable reason for higher experimental temperature is that the thermocouple wire which was inserted in the middle of the board, might had moved upward towards the hot platen, during the course of press closing.

5.4.2: Comparison of Core Temperature at Lower Platen Temperature:

The board of target density 700 kg/m^3 is made in the pilot plant. In this case the platen temperature is decreased to 160ºC. The core temperature of the model is compared with the experimental results.

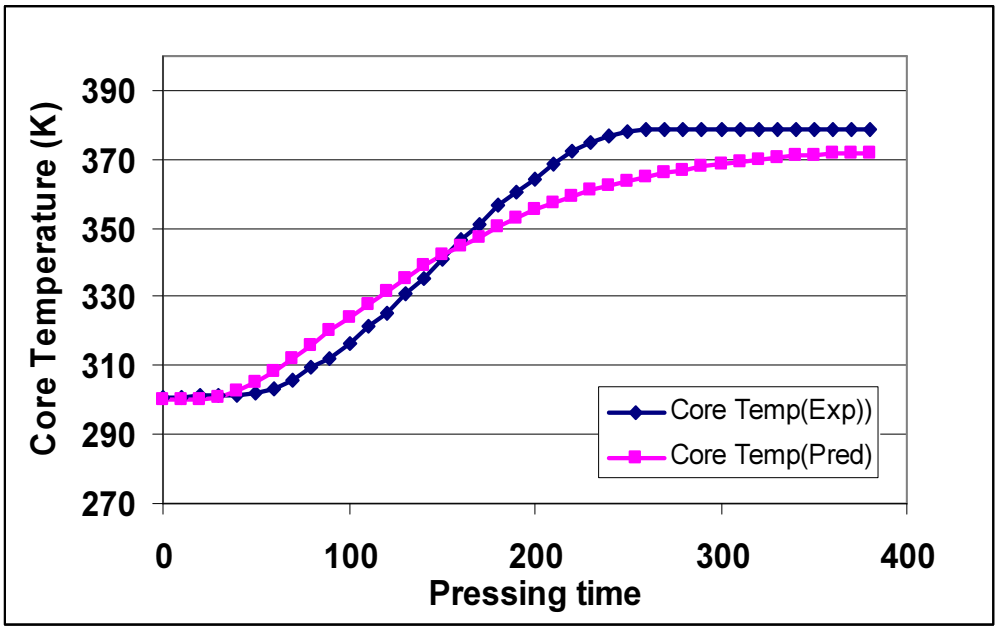

Figure 5.19: Comparison of core temperature from model and experiment

In most part of its course the core temperature from the model agreed well with the experimental value. It shows that model is capable of predicting core temperature of the experimental boards. The value of predicted core temperature from the model is slightly

lower than the experimental results. One of the probable reasons is that in the present model the heat transfer due to water vapour and air is neglected

5.4.3: Comparison of Core Temperature of 650 kg/m^3 density board:

The board of target density 650 kg/m^3 is made in the pilot plant. The platen temperature is kept at 198ºC. The comparison of core temperature from both the model and experiment is shown in Figure 5.20.

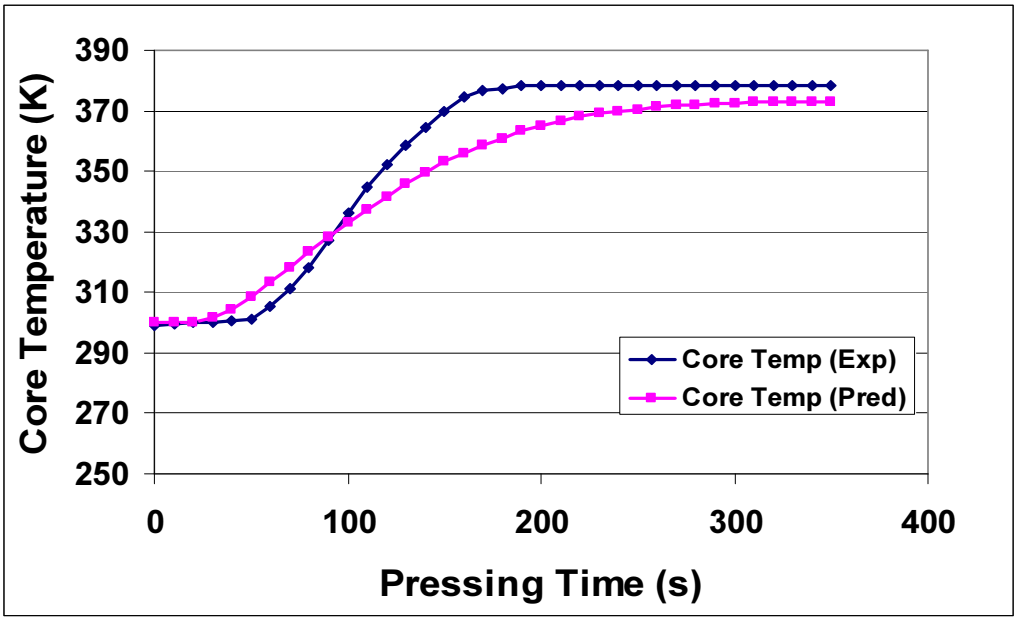

Figure 5.20: Comparison of core temperature for 650 kg/m^3 density board.

The core temperature from the experiment shows no increase until 30 seconds and after that there is a gradual rise mainly due to heat transfer due to conduction and convection of the vapour phase. Once the temperature reaches 100º C, the rise in core temperature stops, as all the heat transferred from the platen is consumed by the change in the phase from water to vapour. The core temperature from the model is initially higher than the experimental one but later on decreases from the experimental one.

5.4.4: Comparison of Core Pressure for 650 kg/m^3 density board:

The core pressure from 650 kg/m^3 board is compared with the partial vapour pressure from the model without the edge loss. As per Denisov et al (1975) experiments all the air is replaced by the water vapour in the early stages of the pressing.

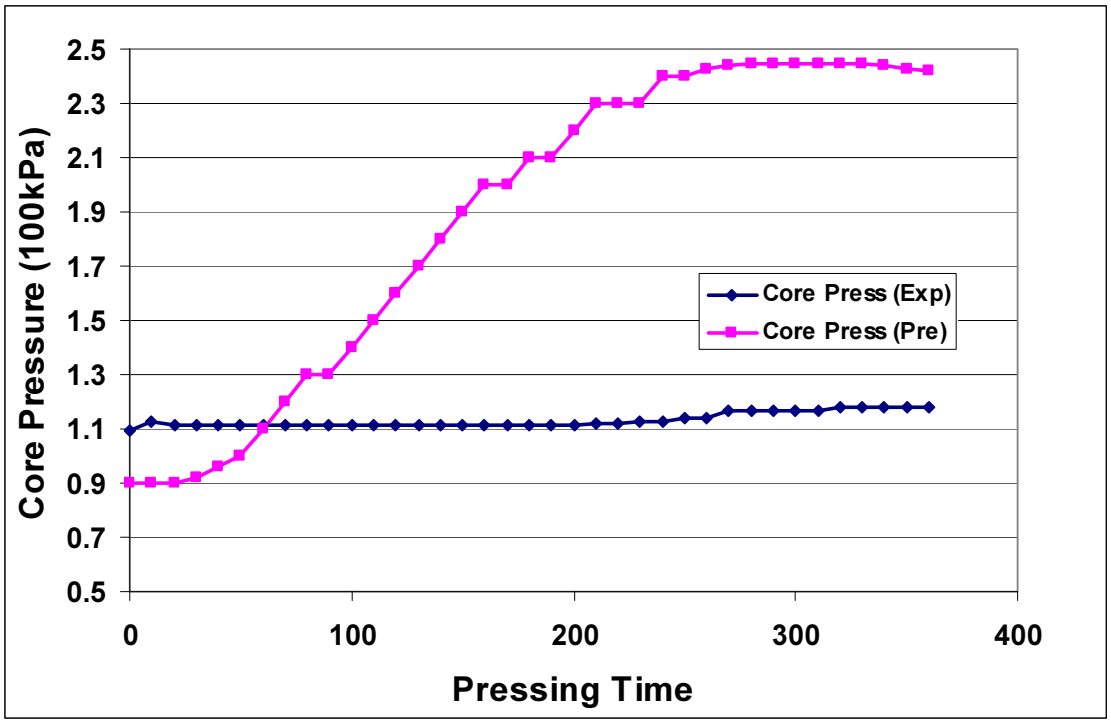

Figure 5.21: Comparison of core pressure from experiment to partial vapour pressure from the model without having the edge loss

The Figure 5.21 shows, in the beginning the vapour pressure is lower then the experiments, as at this point of time, the pressure is only by one component water vapour. As the pressing progresses, the vapour pressure increases much faster than total pressure. The reason is that, as no edge loss is considered, so the line is showing the pressure generated by the water vapour without having the edge loss. The difference between the two results lies between 0.11 to 0.06 MPa. From this figure, we can assume that the amount of edge loss from the core region lies between the above ranges. In the beginning the difference is more, due to presence of large number of voids around the core. But later on them reduces and also the resin around the surface starts solidifying.

5.5 Discussion:

The most important factor affecting the heat and mass transfer process is the initial moisture content of the mat. The thermal conductivity of the board increases together with the rate of conduction heat transfer. The initial moisture content raises the pressure gradient, which results in an accelerated rate of convection heat transfer by vapour flow. The core temperature of the MDF boards shows typical behaviour, it stabilizes at the boiling point due to latent heat required to vaporize the water and after that it starts increasing again. The board cannot be kept inside the hot press beyond certain limit, as there is a risk of charring of outer surface of the board. Figure 5.11 and Figure 5.12 show the impact of moisture content on the core temperature and core pressure

The most important impact of the initial mat moisture content is on the total time required to press the board. The higher the initial mat moisture content, the longer the pressing time needed to prevent panel delamination. The excess moisture has to be removed from the mat by releasing the platen for a short time which will increase the total pressing time. Some moisture content in the range of 8-10 % is needed for convective heat flow and hence to reduce the pressing time. Delamination will occur, even if the adhesive is properly cured in the centre, when the internal pressure is larger than the strength of the internal bond of the panel. Therefore, the initial mat moisture content is typically kept low (~10 %) and allowed to vary only within a limited range during industrial production. The initially uniformly distributed moisture migrates within the mat structure due to temperature effects, consequently large moisture gradients are building up during the press cycle.

As seen in Figure 5.3, it comparatively takes more time to increase the core temperature in the higher density board than the low density boards, as more amount of fibres need to be heated and due to low thermal conductivity of the wood fibres. If the press cycle and other pressing conditions remain the same, then the pattern of density profile formation is the same in all the three different densities, as shown in Figure 5.4.

Platen temperature is an extremely important pressing parameter and has to be carefully controlled in order to ensure adequate curing temperature for the resin at the core of the board without causing degradation at the surface. There is a close relationship among press time, panel thickness, and platen temperature. Boards of two different densities were made using two different platen temperatures of 160ºC and 198ºC. It was observed that increasing the platen temperature raises the core temperature faster due to increase in heat flow from the platen to the core. Increasing the platen temperature increases the temperature gradient and accelerates the heat flow by conduction. Due to high temperature of the surface, all the moisture content on the surface evaporates. Water vapour cannot leave from the impermeable steel plate, so it starts migrating towards the core region, which indirectly helps in further increasing the core temperature. The increasing of platen temperature reduces the total time needed for the pressing of the board, but over exposure also creates the risk of charring of the outer surface of the board. In commercial plant, usually the platen temperature is kept at 180º C.

In Figures 5.13 and 5.14 the temperature and core pressure development in the delaminated board is shown. The density of the board is very high, near to 1350 kg/m^3. In normal condition, the core temperature becomes constant near the boiling point of water but in this case the core temperature had shot to 140ºC and the core pressure had reached to 0.6 bar. The internal gas pressure was very high. Even though at this time most of the internal bonds have formed, the force created by the internal gas pressure was more than the internal bonding and suddenly the gas leaves from the surface of the board with a bang sound. This problem is quite common in the commercial plants, when boards of thickness more than 18mm are made. The thicker the boards, the more severe are this problem. The reason is that to increase the core temperature, more moisture content is needed, which will accelerate the heat transfer by vapour convection. But it also increases the core gas pressure. In the latter stage of the pressing, bonds were already formed around the edges and leave no space for the leakage of vapour. The stage will come when the force generated by gas pressure exceeds the internal bond and in most of the cases gas leaves from the edges. The problem of delamination is more severe in batch pressing than

in the continuous press. In the continuous press, during manufacturing the gap between the roller is adjusted to give way for the excess of gas.

A delicate balance of moisture content with the thickness is to be maintained. If we reduce the moisture content then resin will not be solidified in the core and will lower the internal bonding property. The surface of the board will also be rough after sanding. The rough surface degrades the quality of the board, as it is not suitable for polishing and painting.

The cure of the adhesive is not uniform, because the heating of the mat is not uniform throughout the thickness. The adhesive at the mat surface is cured first and the cure of the adhesive at the core of the mat takes a longer period of time. The press time has to ensure that the centre of the mat reaches adequate temperature for a prolonged time period. The higher the platen temperature, or the thinner the panel, the faster the board core reaches the necessary resin curing temperature, therefore shortening the required pressing time. However, there is an upper limit on the platen temperature to prevent the thermal degradation of the panel surface. Therefore, the control of the core temperature in practice is achieved by the increase of the pressing time. The press closing time is easy to change in an industrial environment. It mainly affects the vertical density profile formation. The density profile model described in chapter two gives more insight of its formation by changing some parameters.

The core temperature from the model is compared with the experimental results. The results from the model adequately predict the major trends in the core temperature. In the first case, the core temperature is higher than predicted. Another reason for higher temperature of experimental value is that the thermocouple wire may have moved slightly upward in the course of pressing. In the second and third validation case, the predicted core temperature is higher in the beginning but later becomes lower than the experimental value.

5.6 Conclusions:

In the first section of this chapter different experimental results were analysed. It helps in improving the understanding of changes that occur in core temperature, core pressure and density profile, by changing platen temperature, density, moisture content and thickness. In the second part of this chapter, experimental results are compared with the model predictions.

The core temperature from the model shows qualitative agreement with the experimental results. For further improvement in quantitative agreement, some of the equations that are derived for wood and particle board need to be refined. The model needs to be further developed into two dimensional for predicting the core pressure to measure the edge losses. The results can be further improved by a better estimation of the model parameters and by including the convective transport of heat through air and vapour.

Chapter- 6

Empirical Model to Predict Mechanical Properties of MDF Panels from the Mean Density

6.1 Introduction:

The pressing operation in composite wood is one of the most important and complicated operations in wood composites manufacture (Bolton and Humphrey, 1988; Kamke and Casey, 1988; Wang, 1992; Winistorfer, 1992). Complicated interactions of dynamic conditions occur during pressing, including heat transfer, moisture movement, development of gas pressure, wood stress relaxation, wood consolidation, resin curing and bonding between fibres, and eventual development of a non-uniform consolidation-induced density distribution through the panel thickness.

The advantage of MDF over other wood composites is the ease to manipulate the density profile for different uses. Wang.et.al (2004) stated that high density surface is needed for lamination, gluing, painting and grain printing. The homogeneous core of MDF is needed for embossing, molding, and general machining.

Although the effects of the density profile on the board properties have often been pointed out qualitatively, the real phenomena of density profile formation, and its specific effect on the board performance remain ambiguous. The presence of this vertical density gradient has been reported to result in higher bending strength, but lower internal bond and interlaminar shear strengths (Kelly, 1977).

The positive correlation between density of the surface layer and bending strength was confirmed by Kollmann (1957). However, Suchsland (1967) mentioned that such a shelling effect of the surface layers does not necessarily require higher surface densities.

Factors such as particle geometry and ratio of peak and core density could also lead to a shelling effect, even if the core and surface densities are similar.

Xu and Winstorfer (1995) reported an effect of the cross-sectional density profile on the dimensional stability of panels. It was suggested that a pronounced cross-sectional density profile with high densities close to the surfaces leads to improved dimensional stability since the time-dependent process of water absorption is retarded by the more highly densified surface layers

The layer in which the fracture during an internal bond strength test occurs has been reported to not coincide with the layer of lowest density, which usually is the central layer of the panel (Xu and Winistorfer, 1995; Schulte and Fruhwald, 1996). Preliminary simulation results of bond strength development reported by Humphrey (1991) supported this finding. These observations demonstrate again that the density cannot be the only criterion to assess the mechanical properties of the panel.

The present chapter investigates the relationships between the mean density, vertical density profile, and the physical and mechanical properties of MDF. The quantitative understanding of the above correlations is fundamental and vital for the attempts in simulating the density profile for the boards with desired properties for specific end uses. The empirical relationships help in understanding the dependence of physical properties on mean density. The regression equations obtained in the experimental work are used in an empirical model, which aims to correlate the density and mechanical properties of a panel for the particular fibre moisture content, resin content and press cycle used in obtaining the experimental data. The effect of mean density on physical properties is briefly described in Gupta.et.al (2005, 2006c)

6.2 Materials and Methods:

6.2.1 Raw materials and board manufacturing:

The moisture content of the fibres was 10.5 % and the resin content was 10.5%, both being based on the oven dry weight of fibres. The resin used was Urea-Formaldehyde. Once the fibres were received, the tests were performed in the same day to manufacture 12 MDF boards on a pilot press in the Department of Chemical and Process Engineering, University of Canterbury.

The dimensions of the boards made were 300 mm x 300 mm with the target board thickness being from 10 mm to 13.5 mm. All of the boards had the same amount of fibres and thus different thickness of the board had different density. This arrangement will also help to study the rate of increase of peak and core density for similar pressing conditions. During making the board, a thermocouple wire was inserted in the mid-thickness of the board after pre-pressing to measure the core temperature. The core temperature, platen pressure and position were recorded at 10 second intervals. The platen temperature was maintained at 180°C.

6.2.2 MDF Press Cycle:

The total pressing time was 150 seconds in order for the core temperature to maintain above 100°C for the few seconds needed for the resin to cure. Figure.6.1 shows the platen pressure through the press cycle, while Figure 6.2 shows the movement of platen position with time for a selection of the boards.

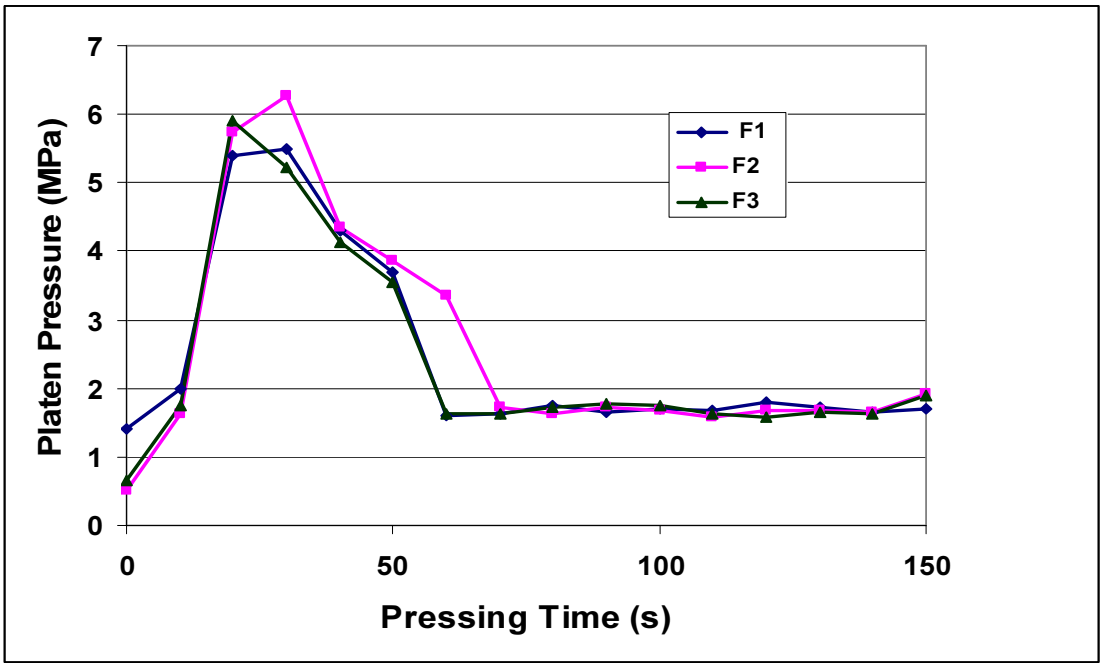

Figure. 6.1 Change of platen pressure with time for three boards

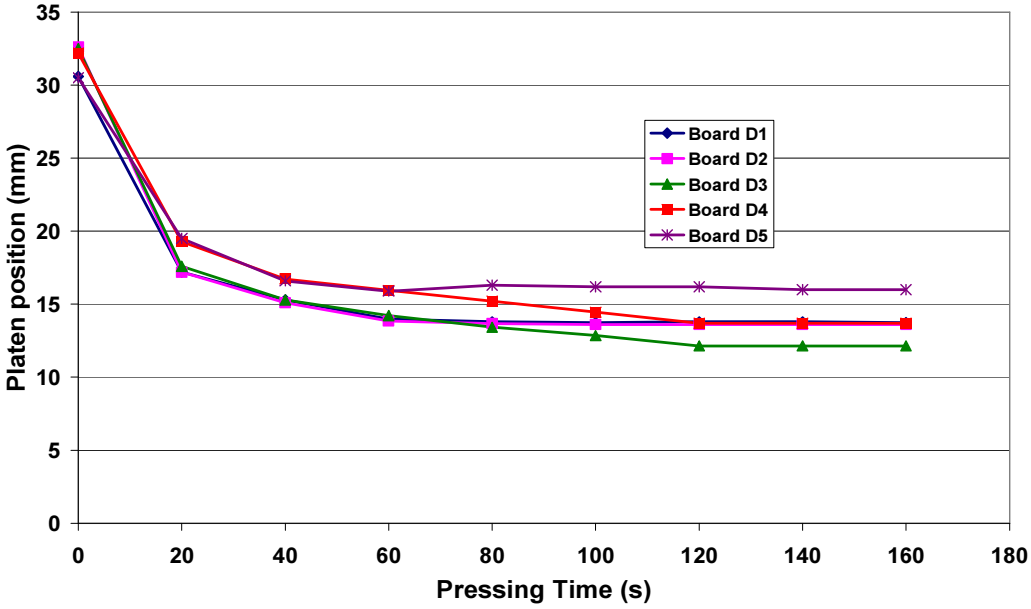

Figure. 6.2 Change of platen position with time for five boards

6.2.3 MDF Testing:

The boards were tested for their physical properties. From each board made, a square of 50mm x 50mm was cut and placed in a density profile X-ray scanning machine (ProScan)

to obtain its vertical density profile (VDP) graph. After the VDP test, both surfaces of the sample were sanded to remove the precure layers of the board. The samples were then tested for internal bonding, modulus of rupture (MOR) and modulus of elasticity (MOE). All tests were conducted according to the procedure specified in AS/NZS 4266.5 (2004). The details of the experiment and measured results are given in Table 6.1.

Table 6.1: Experimental data for empirical model:

					Density, ρ			
Sample ID	Thickness mm	Mean Density kg.m^{-3}	Break from top mm	IB MPa	Peak ρ kg.m^{-3}	Core ρ kg.m^{-3}	MOR MPa	MOE MPa
D-1	11.75	600	5.87	0.58441	876	563	28.06	2072.16
D-2	11.20	616	5.60	0.50749	817	530	29.14	2313.95
D-3	9.97	718	4.98	0.95351	853	666	34.56	2506.12
D-4	11.95	587	3.19	0.42739	794	552	20.15	1871.33
D-5	13.65	516	6.50	0.27120	821	418	19.48	1679.28
E-1	13.11	547	6.55	0.24035	817	420	21.08	1593.93
E-2	13.37	524	6.68	0.25205	792	419	20.74	1949.51
E-3	13.13	565	6.56	0.31738	854	452	23.99	2057.46
E-4	10.90	717	5.20	0.65604	915	694	35.77	2694.71
F-1	13.31	545	3.99	0.25037	805	445	14.98	1760.09
F-2	13.31	485	6.65	0.23891	706	398	20.66	1696.00
F-3	13.60	526	6.80	0.32841	792	423	20.07	2024.24

6.3 Experimental Measurements:

For clarity, the data for only three boards are plotted in Figures. 6.3-6.4, but the regression equations between mechanical properties and the mean density used the data for all twelve boards.

6.3.1 Temperature: The core temperature response is shown in Figure.6.3 for three boards (F-1,F-2, and F-3). A thermocouple wire is placed inside the core. The readings were recorded after every ten seconds.

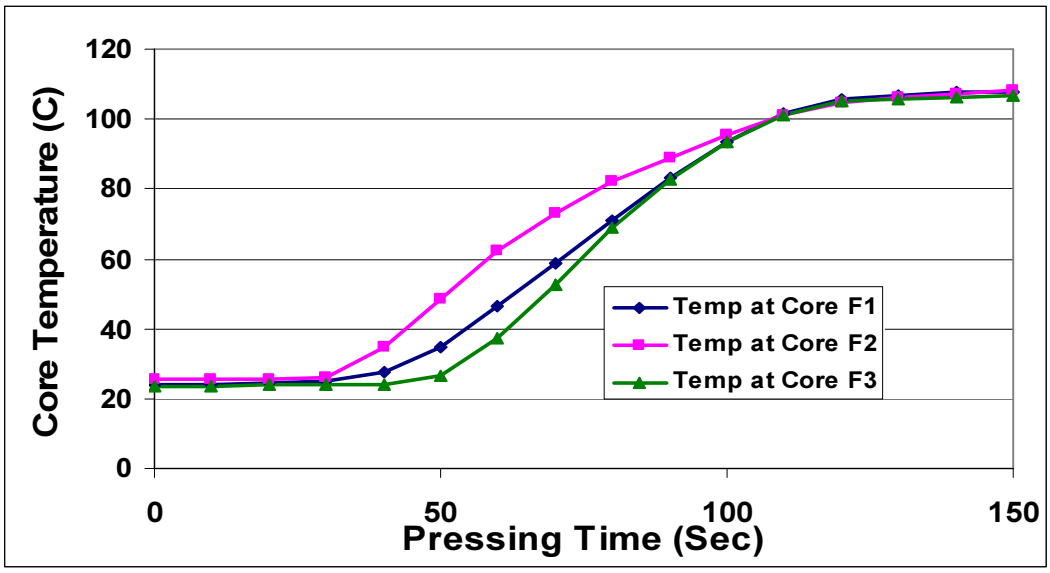

Figure.6. 3 Development of temperature at the mid-plane of the board

6.3.2 Density Profile: Figure. 6.4 show the VDP for three representative boards. These results were used to obtain equations to quantify the relationship of peak and core densities as a function of mean density. It was observed that with the increase in mean density, peak and core densities also increase almost linearly, but the effect on core density is substantially greater.

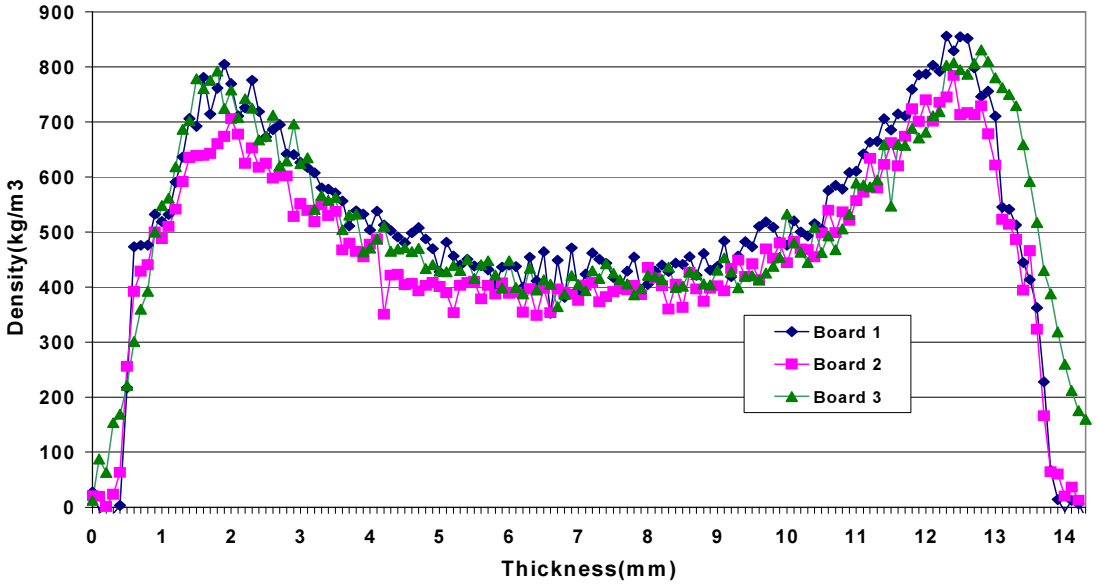

Figure.6. 4 Density profile across the thickness for three samples (F-1,F-2,F-3) from Proscan profiler

6.3.3 Internal Bond (IB) strength: One sample of $50mm \times 50mm$ was cut from the middle of each board. Approximately 0.5 mm of precure surface was sanded off by a small belt sander. The boards were then tested according to AS/NZS 4266.5 (2004). IB strength is calculated from:

$$IB = \frac{F_{\max}}{ab}, \qquad (6.1)$$

Where

$F_{\max}$ = breaking load in newtons;

a, b = Length and width of the test piece, in mm.

6.3.4 Modulus of Rupture: The MOR is one of the main parameters in measuring the bending strength of the board. The universal wood testing machine is used for conducting tests. A load moves with a constant speed towards the centre of a rectangular sample as shown schematically in Figure 6.5. The maximum load before breaking is used to calculate MOR. The bending strength (MOR) is calculated using the formula

$$R = 3WL / 2bt^2, \qquad (6.2)$$

Where

R = Modulus of Rupture (MPa);

W = Ultimate failing load in newtons with loading rate of 5 mm/min;

L = span between centre of supports in mm,

b =mean width of test piece in mm,

t = mean thickness of test piece in mm.

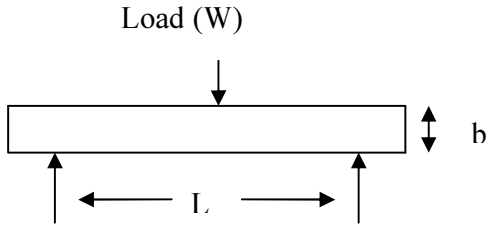

Figure 6.5: Schematic diagram of apparatus for MOR measurement

6.3.5 Modulus of Elasticity: Bending stiffness (MOE) is measured in MPa and is calculated from:

$$MOE = \frac{L^3}{4bt^3}\frac{\Delta W}{\Delta S}, \qquad (6.3)$$

Where

$\Delta W =$ Increment in load, in newtons, on the straight line portion of the load /deflection curve.

$\Delta S =$ Increment in deflection, in mm, resulting from increment in load ΔW .

6.4 Empirical Model

In commercial plant, a large amount of statistical data is available. The best way to use that data is by deriving correlations among different parameters. The objectives of the present study were to develop an empirical model to investigate the relationships between the mean density, vertical density profile, and the physical and mechanical properties of MDF. The quantitative understanding of the above correlations is fundamental and vital for the attempts in simulating the density profile for the boards with desired properties for specific end uses. It gives the degree of association of mean density with the physical properties. The regression equations obtained in the experimental work form an empirical model, which aims to predict the mechanical properties of the panel for the specific values of fibre moisture content, resin content and press cycle used in obtaining the

experimental data. The empirical model correlates the physical properties for a given press cycle, moisture content and resin content. The results are good for the given set of conditions for which the regression equations are derived, but cannot predict the effects of parameters which were not varied in obtaining the data to which the equations were fitted. Matlab software is used to run the programme.

6.4.1 Regression Equations:

From the experimental results, the following regression correlations have been obtained to relate various board properties.

1. Board peak density (PD) as a function of board mean density (MD):

$$PD = 0.529MD + 513.65 \quad R^2 = 0.5742 \tag{6.4}$$

2. Board core density (CD) as a function of board mean density:

$$CD = 1.324MD - 268.09 \qquad R^2 = 0.9405 \tag{6.5}$$

3. Board Internal Bonding(IB) as a function of board mean density:

$$IB = (3.601\times10^{-6}\,MD^2) - (1.672\times10^{-3}\,MD) + (1.622\times10^{-1})$$

$$R^2 = 0.8523 \tag{6.6}$$

4. Board Internal Bonding(IB) as a function of core density(CD)

$$IB = 2.886\times10^{-7}CD^{2.274} \qquad R^2 = 0.8949 \tag{6.7}$$

5. Board Modulus of Rupture (MOR) as a function of board mean density

$$MOR = 0.0771MD - 20.596 \quad R^2 = 0.7999 \tag{6.8}$$

6. Board Modulus of Elasticity(MOE) as a function of board mean density

$$MOE = 4.0701MD - 337.91 \qquad R^2 = 0.7926 \tag{6.9}$$

7. Variation of Core Temperature(CT) with time (t)

$$CT = -0.0071t^2 + 2.1515t - 53.214 \qquad R^2 = 0.9885 \tag{6.10}$$

Core temperature is below 30ºC until 30 sec and 104ºC after 120 sec. Equation (6.10) predicts core temperature between these time limits.

6.5 Results and Discussion:

6.5.1 Correlation of Peak Density with Mean Density: As observed from Figure 6.6, there is good relationship of peak density with the mean density for a given press cycle. It was found that in the beginning of the pressing, the increase in peak density was fast and once it reaches to about 800 kg/m^3, the increment becomes slow. The main reason for the initial increase is that all the air that is trapped between the loose fibres, leaves the mat due to large pressure. In the second stage, the cell wall of the fibres start crushing, this stage comes when the density lies between 500-600 kg/m^3. It takes a large amount of pressure to increase the density beyond this point. This is one of the reasons, that the increase in peak density is fast in the beginning but becomes slower later on. The correlation between the peak density and the mean density is lower than with the core density. As discussed in the literature review and in chapter two, the press closing speed has a significant impact in the formation of the density profile and in the value of the peak density. The variable x in the equations on the figures stands for the independent variable in each case. Due to high temperature and low moisture content of the surface layers, the plasticity of the fibres increases. The modulus of elasticity of the surface layer decreases and causes higher density. In the beginning the core temperature is still at room temperature and

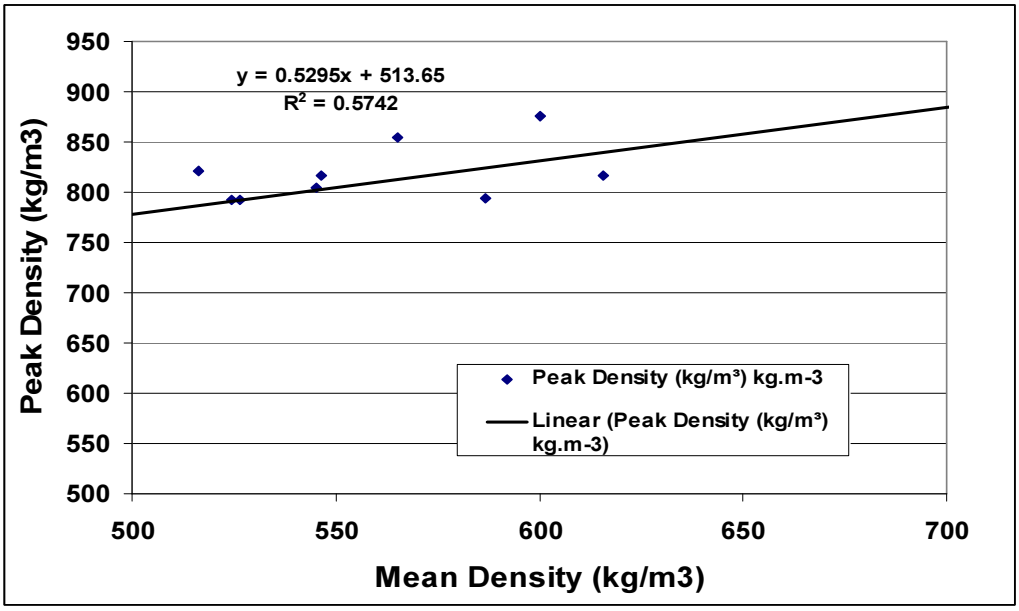

Figure.6.6. Change of Peak density with mean density

And not much changes in the moisture content from the initial conditions. The value of modulus of elasticity is high and causes less compression. As given in Figure 6.2, the press platen reaches to its final thickness in the initial 50-60 seconds. There is only very little rise in core temperature at this time, as seen in Figure 6.4. Most of the density profile formation takes place in the initial 60 seconds and later on minor adjustments due to spring back action and stress relaxation. Wang et.*al* (2004) has concluded that the reason for minor adjustment in the density profile is that mat is in an unsteady state during hot-pressing. Internal mat temperature, moisture content distribution, vapour pressure, layer density, and the compaction stress are all related to the pressing process.

6.5.2 Correlation of Core Density with Mean Density: The correlation of core density with the mean density is much higher with a R^2 value of 94 %. As seen in Figure 6.7, the core density keeps on increasing in a straight line for the given press cycle, moisture content and resin amount. From this relationship, if the press cycle is the same then we can predict the core density for the given mean density.

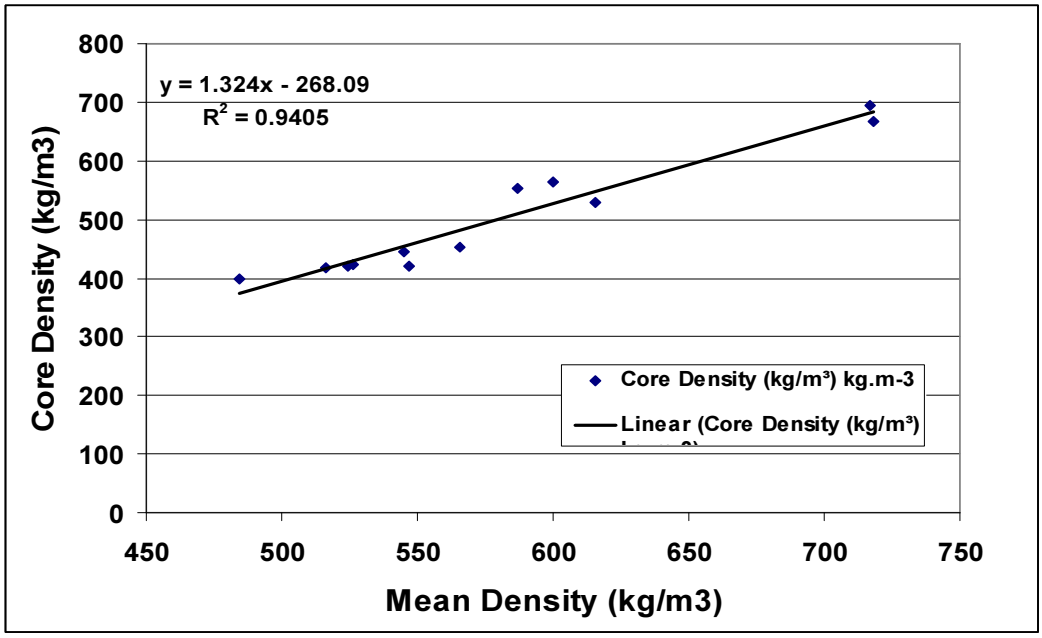

Figure 6.7. Change of Core density with mean density

6.5.3 Variation of Internal Bonding with Core Density: It was observed that internal bonding is much better related to core density then the mean density. This is because the breaking point depends on the lowest density of the board. Figure. 6.8 and 6.9 show that the IB strength increases with both the mean and core densities, with a marginally better correlation with the core density than with the mean density.

The internal bond is one of the main parameters to characterise the quality of MDF boards. It is an indicator of bonding of resin with fibres. The main cause of lower IB is either low percentage of resin content in the boards or incomplete curing of resin. The process of resin curing is given in chapter four, in the standard simulation run. For the complete curing of resin the value of resin curing index should be above 0.9. If it is below this value, then the bond strength is weaker.

The reason for higher correlation with the core density is that the weakest point in the board is in the core zone. Lower core density signifies lower IB. The relationship of mean density with the IB is not that simple. Generally, if the mean density is low then core density will also be low, which will result in low IB. But a lot of the density distribution pattern depends upon the press closing strategy. Sometimes, it happens in commercial

boards that even though the mean density is higher, most of the increase is in the peak density and the value of core density has not increased that proportionately, which causes lower IB with higher mean density. During the Internal Bonding test, it was observed that the weakest point is not always the centre in the core density region. The break occurred at 27% and 30% of the depth from the top of the board for samples D4 and F1 respectively. See the data in Table 6.1.

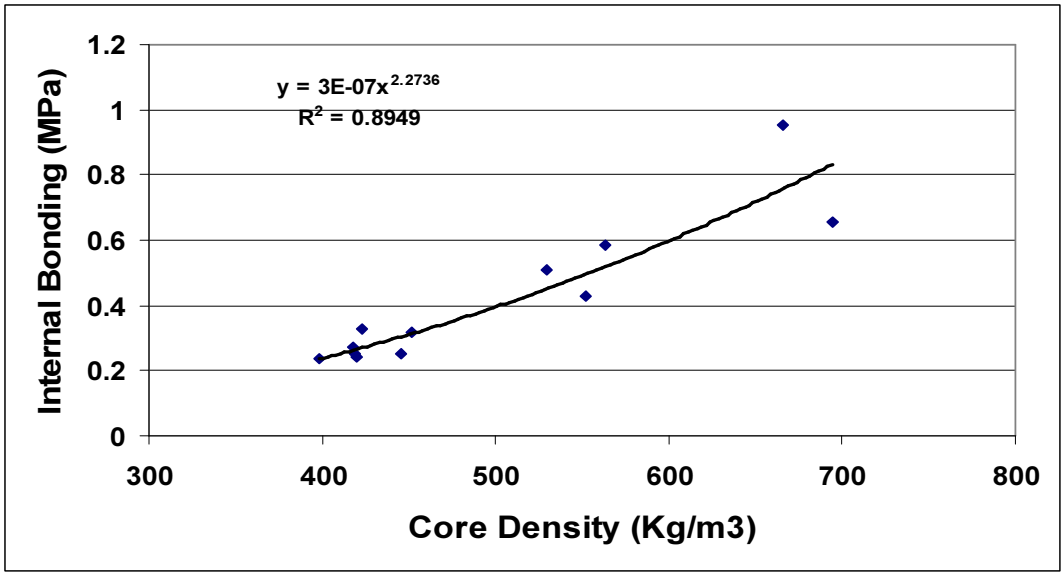

Figure. 6.8 Change of Internal bonding with core density

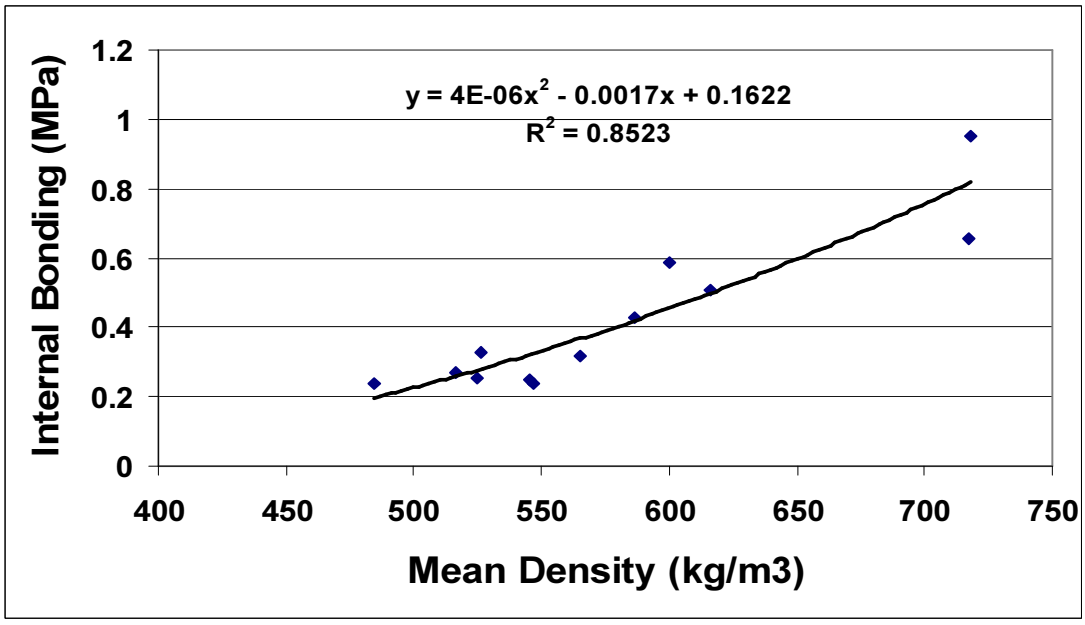

Figure .6.9. Change of Internal bonding with mean density

6.5.4 Modulus of Rupture as a Function of Mean density: The modulus of rupture was found to increase linearly with mean density as shown in Figure.6.10. As we increase the mean density, the fibre percentage in the same volume increases, which directly increases the strength of the board. Commercial boards, which usually have a mean density above 700 kg/m^3 should have MOR more than 45 MPa.

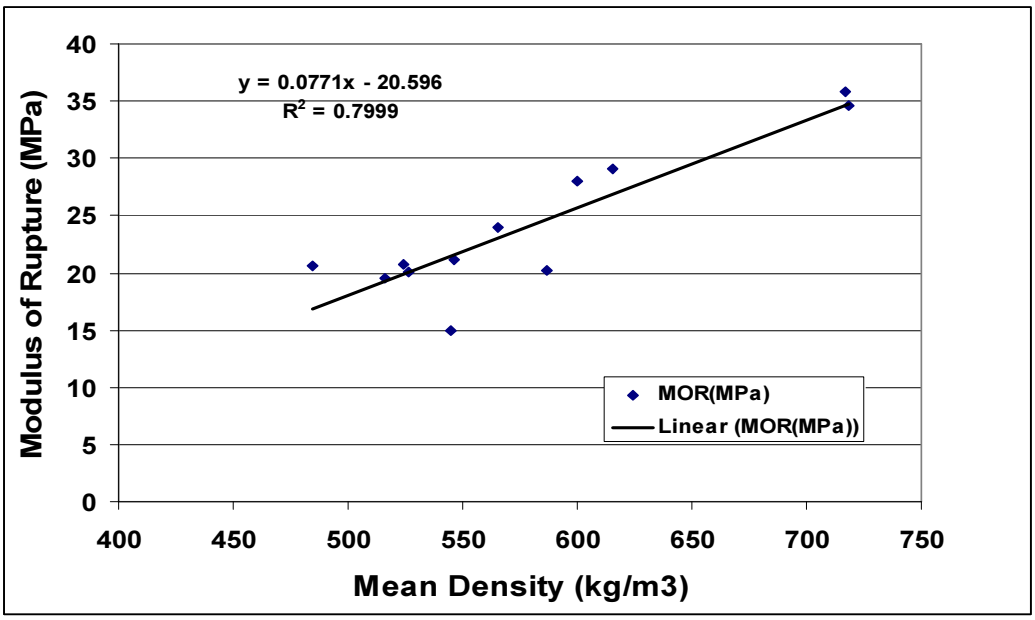

Figure 6.10 Change of MOR with mean density by experiment

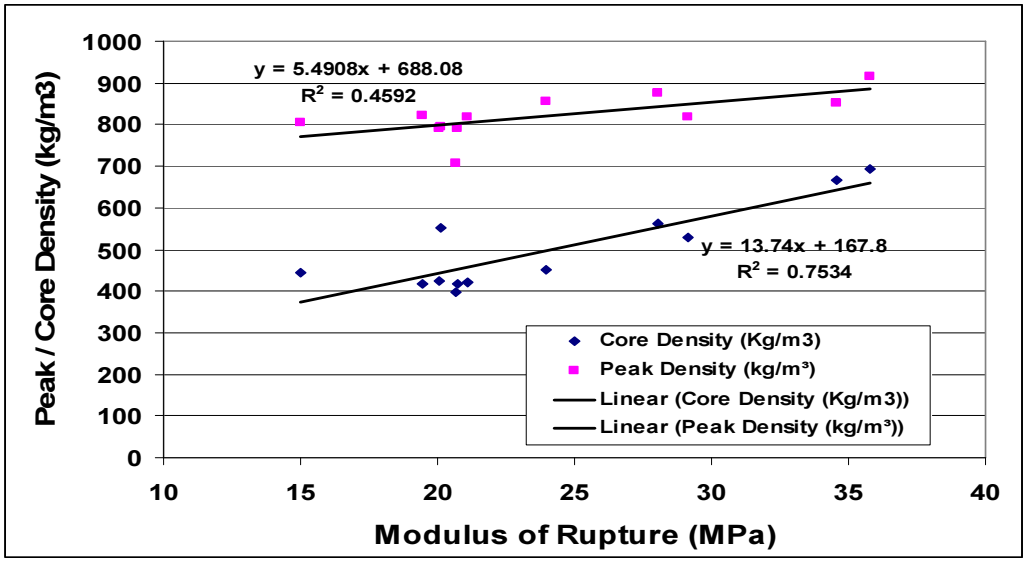

Figure 6.11 Change of MOR with peak and core density by experiment

The MOR is having better correlation with the core density (75 %) than with the peak density (45 %) as given in Figure 6.11. This means that boards with higher peak density may not have higher load bearing capacity. Core density is much better indicator of higher loading capacity. In simple terms, MOR means how much load a particular board can take before breaking. The value of MOR changes with the thickness as can be seen from equation (6.2). High value of MOR is needed, when the board is used for shelf, roof, table top and for similar other requirements.

6.5.5 Modulus of Elasticity as a Function of Mean density: The MOE also increases linearly with the mean density, with a similar correlation to that for the MOR (see Fig 6.12 and 6.13). MOE is having better correlation with mean and core density than the peak density for the given press cycle. Better correlation can be developed by doing experiments with different press closing strategies. MOE gives the bending strength of the MDF board. Even though the correlation of MOR and MOE is less with the peak density, it still plays important role in the commercial plants. If we change the press closing strategy and have different speed at different steps, there will be significant changes in the peak density in comparison to the core density. This behaviour can easily be explained by the theoretical density profile model, described in chapter two. When we increase the speed of pressing, the displacement of platen per second increases. This displacement is distributed in different layers in the inverse ratio of modulus of elasticity of the layers. As it is the beginning of the pressing, the temperature of the surface layer is very high and moisture content is low in comparison to all other layers. This will lower the MOE of the surface layer and resulted in high density. In slow closing speed, there will be more even distribution of temperature and moisture content and more even distribution of peak density in the surface layers. The high density will not be localised in the surface layer only.

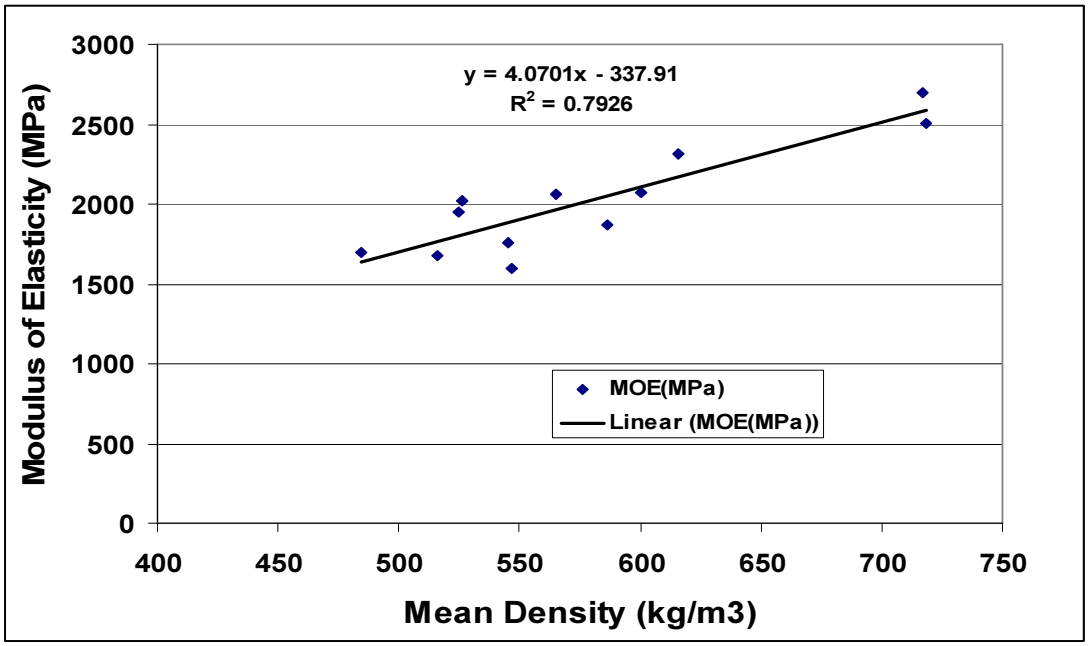

Figure. 6.12 Change of MOE with mean density

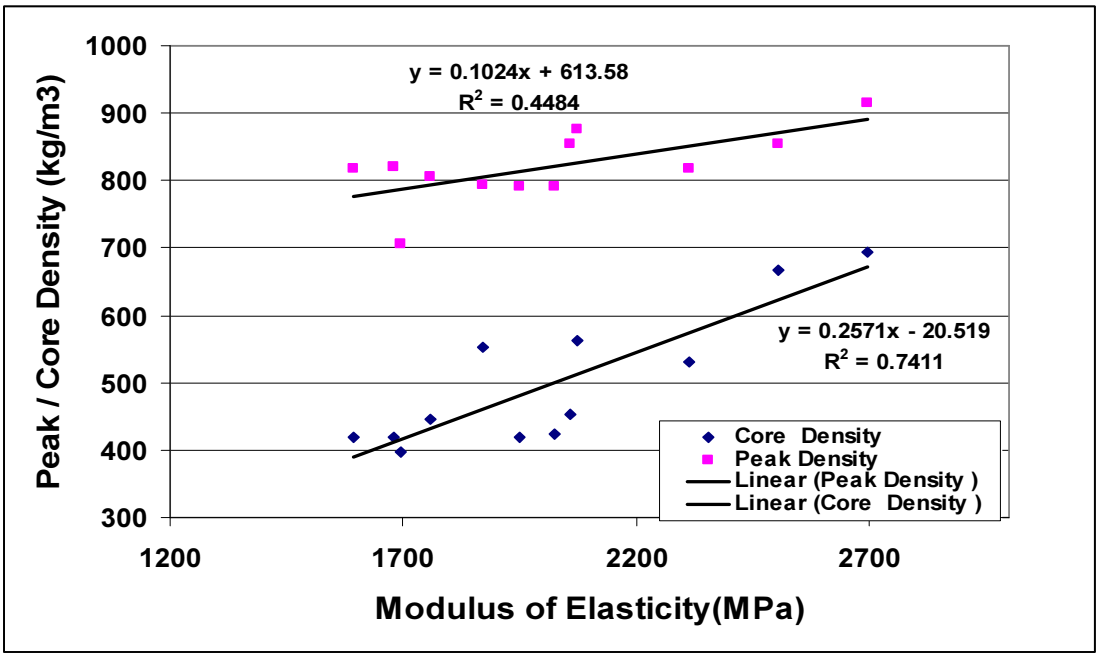

Figure. 6.13 Change of MOE with peak and core density

6.5.6 Core Temperature with time: The core temperature response is shown in Figure. 6.14 for three boards. It was observed that for the initial 30 seconds there was virtually no increase in temperature. After that the temperature rises quite rapidly until,

after it reaches 100 °C, the rate of increase dramatically slows .The rapid rise in temperature from about 30 seconds to 110 seconds is believed to be largely due to the movement of evaporated moisture from the region near the platens to the core. Once the temperature exceeds 100 °C, the heat transfer becomes limited to that from conduction through the mat. The reason for this behaviour is that wood fibre is a bad conductor of heat and it takes some time for heat to transfer from platen to the core. After that the temperature rises quite rapidly until, it reaches 100°C. The main source of heat supply is conduction and convection. Once the core temperature reaches to 100ºC, the temperature becomes constant, as most of the heat supplied by the platen is consumed in the change of phase from water to vapour.

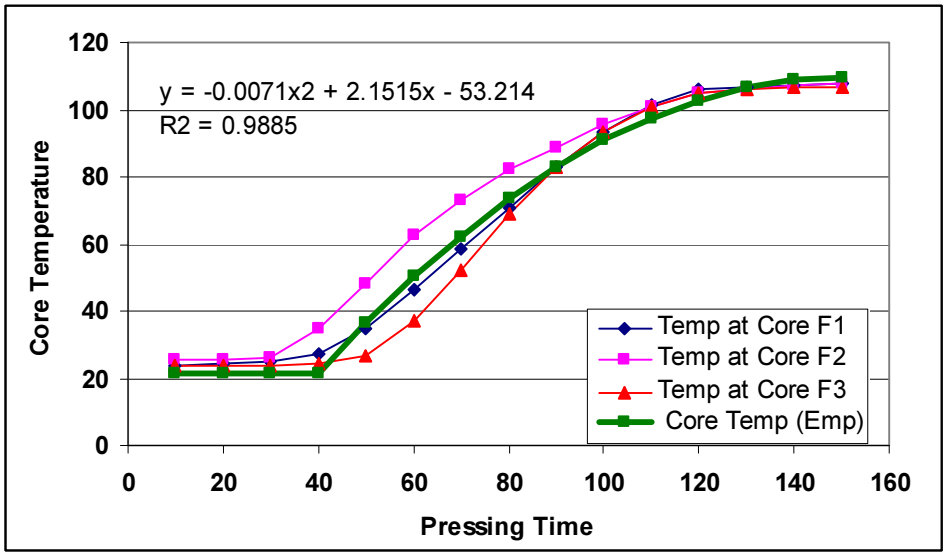

Figure 6.14 Change of core temperature with time

6.8 Conclusions:

Empirical modelling is good from the commercial point of view. MDF plants have required data from everyday production. On that basis they can develop correlation. It will be useful for them to predict the physical properties. The empirical model predicts the physical properties for a given press cycle, moisture content and resin content. The results are good for the given set of conditions in which the regression equations are derived but become less accurate beyond that condition

The model gives good results for thickness ranging from 10 to 13.5 mm and density ranging from 485 kg/m^3 to 718 kg/m^3. There is a higher correlation of internal bonding with the core density ($R^2 = 0.89$) than there is for the mean density ($R^2 = 0.85$) .Both the MOR (bending strength) and the MOE (bending stiffness) increase linearly with an increase in the mean density with a similar correlation coefficient ($R^2 = 0.80$) .

The prediction capability of empirical model can be increased by developing similar correlation for different press closing strategy, different range of moisture content and resin content. Different pressing conditions have different impact on physical properties. If we increase the resin content from 10 to 12 %, it will not have any significant impact on MOR, MOE. The only thing that will have impact is internal bonding which will increase with it. More experiments need to be performed to increase the accuracy and predictability of the empirical model.

Chapter 7

Final Conclusions and Recommendations

7.1 Final Conclusions

The first objective of this project was to investigate the process of hot pressing of MDF board, both experimentally and theoretically, to better understand the internal processes inside the board. In this work a mathematical model has been developed based on the fundamental engineering principles such as heat and mass transfer and viscoelastic properties using a mechanical analogue such as Maxwell elements. The model is able to predict stress, strain, vertical density profile, temperature, moisture content and the extent of resin cure in different layers at different time of hot pressing. The second objective was to implement the model into a simulation programme by using (Matlab) software. The model is capable of predicting the standard hot pressing conditions and also the advance technologies such as steam injection pressing and cooling zone in the continuous press.

In the heat and mass transfer part of model, the relationship among the fibre moisture content, vapour partial pressure and temperature is needed but the previous correlations for such a relationship have been used for solid wood with limitations only applicable to temperatures below 150ºC, Hailwood and Horrobin model (1946). One of the important features added in this model is that an equilibrium moisture content (EMC) equation given by Pang (1997), for solid wood was modified to be applicable for the MDF fibres. In addition, this EMC equation can cover the complete range of hot pressing temperature from 160ºC to 200ºC. The changes in fibre moisture content due to bound water diffusion are considered. The resin curing reactions due to phenol formaldehyde or urea formaldehyde are also incorporated into the model with the energy and water released

during the curing reaction being included in the energy balance. The validation of the heat and mass transfer model shows qualitative agreement between experimental and predicted results. For more accurate prediction of core temperature and core pressure further refining of equations to calculate permeability, effective diffusion, and impact of resin curing on physical properties are needed. The model needs to be converted into two dimensional.

The earlier concept of ratio of modulus of elasticity of the layer to the sum of modulus of elasticity of all the layers in the previous time step, given by Suo and Bowyer (1994) is refined with the latest findings. The equation given by Carvalho et al. (2001) is used to measure the MOE of different layers of the mat. The governing differential equation given by Zombori (2001) is used to measure stress, nonlinear strain function and relaxation of fibres. The model gives good agreement of peak and core density at lower platen temperature at 160ºC but with the increase of platen temperature, the rise in peak density is much too fast. The reason for this differences lies in the simplified assumption that surface layer reaches the platen temperature immediately. It was observed that by changing this assumption to that of gradual rise of surface layer temperature in the press closing time had lowered the peak density by 200 kg/m^3.

The second part of the project was the development of an empirical model to correlate physical properties from the MDF board mean density. The empirical model is simple and straightforward, and thus can be applied in commercial operation for control and optimization. The empirical model can correlate peak, core density, modulus of rupture, elasticity and internal bonding within the limits in which those relationships are derived. However, it needs extensive experimental data and may result in large errors when being used beyond the condition range of the experiments.

The integrated pressing model including the heat and mass transfer model and the mechanical model will become a very valuable tool in the hands of the wood composite industry, after further refining. The inter-relationship between the initial inputs such as moisture content of fibres, platen temperature, press closing speed on the core

temperature, core pressure and density profile can be better understood without the need for expensive experimentation. The new pressing technologies can be easily evaluated by changing the boundary conditions of the model, as has been shown by predicting the internal changes during steam injection pressing and the cooling zone in a continuous press.

The model can be used to visualize some of the parameters, which are otherwise difficult to observe through experimentation. It can become an important tool to train the people working in the quality and production departments of a wood composite factory, so they can better understand the happenings inside the board and manipulate the initial parameters to achieve the desirable density profile for the particular use. The simulation results help in understanding the interrelationship of moisture content with the heat transfer, mass transfer and the risk it creates of delamination. The results help in understanding that how the resin is cured across thickness and the internal bonding strength will decrease, if the resin is not fully cured.

7.2 Recommendations:

The present model is one dimensional; with further changes it can be converted into two and three dimensional. To run the present model, user needs the knowledge of Matlab, but with further programming a graphical user interface (GUI) can easily be developed, and then the user only needs to enter the initial parameters and graphs of results will be generated. By the use of an interface, Matlab (software) has the facility to record the data directly from the sensors such as thermocouple and transducer. This will help in visualizing the model prediction results and experimental results alongside each other. This will reduce the analyzing time and help in rectifying the initial inputs such as initial moisture content and platen temperature parameter immediately.

The equations to calculate viscoelastic properties need further refining. Palka (1973) gave the empirical equation to relate density with modulus of elasticity for softwood; it needs to be refined for the composite wood. The earlier assumption that surface layer

reaches the platen temperature immediately, is modified to the gradual rise of surface layer temperature during the press closing time. It requires further improvement. Secondly, the assumption that the moisture content in the surface layer falls to zero immediately, needs to be changed, to increase the accuracy in the predictions.

The impact of resin curing on the physical properties, heat and mass transfer is still unknown. The curing of resin on the surface will slow down the movement of vapour towards the core. The present equation to calculate modulus of elasticity neglects the impact of hardening of resin. There is a need to add some adjusting factor related to resin curing index with time.

The relationship between the resin curing index and internal bond strength is needed to predict accurately the risk of delamination. The model results are to be converted into simple form, so that people from wood industries and process engineering can understand and utilize the knowledge of this field.

Normally one percent wax is added in the fibres, to reduce the water swelling property of the board. The impact of wax on physical properties needs to be added in the model. The empirical relationship can be developed by testing physical properties for different percentage of wax.

In the present work, firstly we developed the theoretical model to predict the heat transfer, mass transfer and viscoelastic properties. Secondly the empirical model was developed to correlate physical properties such as MOR, MOE and IB. There is a need to integrate both the models to get all the needed information for making the MDF boards. This can be achieved by conducting more physical tests on boards with different press cycle, resin content and moisture content. From that we can get empirical relationships of physical properties with peak, core and mean density of the boards. From the theoretical model, we can already predict peak and core density and integrate empirical equations to predict physical properties.

The objective of the future model should be to increase the accuracy in prediction but also to reduce the time of computation. The time of computation at present is nearly 20 hrs in a personnel computer with Pentium four processor and one GB RAM. This can be achieved by high speed processor and higher value of RAM in a computer and further refining in the programming.

Due to fast reduction in forest resources in many countries, use of wood chips is becoming uneconomical. There is an increasing trend of using agriculture residues such as rice, wheat and sugarcane straw for making of boards. The physical properties of these agriculture residues are different from the wood fibre. The present model, after further modification in permeability, diffusivity, specific heat and void fraction can be used to predict the internal changes not only in straw board, but also in particleboard and oriented strand board.

References

AS/NZS 4266.5 (2004). *Reconstituted wood based panels-Methods of test, Method-5: Modulus of Elasticity in bending and bending strength.*

AS/NZS 4266.6 (2004). *Reconstituted wood based panels-Methods of test, Method-6: Tensile strength perpendicular to the plane of the panel (Internal bond strength).*

Ahmad, M., (2000). Cure characteristics of phenol formaldehyde resin. Unpublished Report. Dept. of Wood Science and Forest Products, VPI & SU, Blackburg, Virginia.

Andrews, C. K., (1998). The influence of furnish moisture content and press closure rate on the formation of the vertical density profile in oriented strand board: Relating the vertical density profile to bending properties, dimensional stability and bond performance. MS. Thesis University of Tennessee, Knoxwille, TN, USA.

Avramidis, S, and **P. Lau**., (1992). Thermal coefficients of wood particles by a transient heat-flow method. *Holzforschung*. **46(5):** 449- 453.

Ball, R. D., I.G. Simpson, and **S.Pang.**, (2001). Measurement, modelling and prediction of equilibrium moisture content in Pinus radiata heartwood and sapwood. *Holz als Roh- und Werkstoff* **59**: 457-462.

Bluthardt, G., Beck . P, and **U. Kaiser**., (2001). Technical and technological advantages of product cooling in the continuous Kusters press. *Proceedings 3rd European Wood-Based Panel Symposium*.

Bodig, J, and **B.A. Jayne.,** (1982). Mechanics of wood and wood composites. Van Nostrand Reinhold Company, New York. 712 pp.

Bolton, A.J, and **P.E. Humphrey**., (1988)**.** The hot pressing of dry-formed wood-based composites. Part I. A review of the literature, identifying the primary physical processes and the nature of their interaction. *Holzforschung* **42**:403-406.

Bowen, M.E., (1970). Heat transfer in particleboard during pressing. PhD Thesis, Colorado state Univ., U.S.A.

Carvalho, L. H, and **C. Costa.**, (1998). Modelling and simulation of the hot pressing process in the production of medium density fibreboard (MDF). *Chem. Eng. Comm.* **170:**1-21.

Carvalho, L.M., M.R.N. Costa, and **C.A. Costa.,** (2001). Modeling rheology in the hot-pressing of MDF: comparison of mechanical models. *Wood Fibre Sci* **33**: 395-411.

Carvalho, L.M.H., M.R.N. Costa, and **C.A. Costa.,** (2001). A global model for the hot-pressing of MDF. *Wood Sci Technology* **37**: 241-258.

Carvalho, L.M.H., (1999). Estudo da Operacao de Prensagem do Aglomerado de Fibras de Media Densidade(MDF): Prensa Descontinua de Pratos Quentes. Dissertation, University of porto, Portugal.

Cussler, E.L., (1984). Diffusion. Mass transfer in fluid systems. Cambridge Univ. Press. 525 pp.

Dai, C, and **C. Yu.,** (2004). Heat and Mass transfer in wood composite panels during hot-pressing: Part one. A physical-mathematical model. *Wood and Fibre Science*. **36 (34)**: 585-597.

Dai, C.,C. Yu, and **X.Zhou**.,(2005). Heat and Mass Transfer in wood composite panels during hot pressing Part two. Modelling void formation and mat permeability. *Wood and Fibre Science*. **37 (2)**: 242-257.

Dai, C.,(2001). Viscoelastic behaviour of wood composite mats during consolidation. *Wood and Fibre Science*. **33 (3)**: 353-363.

Dai,C, and **P.R.Steiner**.,(1993). Compression behaviour of randomly-formed wood flake mats. *Wood and Fibre Science*. **25 (4)**: 349-358.

Day, D.L, and **G.L. Nelson.**, (1965). Desorption isotherms for wheat. Trans. Amer. Soc. *Agri. Eng* **8**: 293-297.

Denisov, O.B., P.P. Anisov, and **P.E.Zuban**., (1975). Untersuchung der Permeabilitat von Spanvliesen. *Holztechnologie.* **16(1)**: 10-14.

Denisov, O.B, and **M.S. Sosnin.,** (1967). Besonderheiten der Veranderung von Temperatur und Dampfdruck in grobformatigen Holzspanplatten wahrend der Pressung. *Derev Prom*. **16(8):** 11 (in Russian).

Denisov,O.B., P.P. Anisov, and **P.E. Zuban**., (1975**).** Untersuchung der Permeabilitat von Spanvliesen. *Holztechnologie*. **16(1):** 10-14.

Engelhart,F., (1979 Untersuchungen uber die Wasserdampfsorption durch Buchenholzim Temperatubereich von 100oC bis 170oC. *Holz als Roh-und Werkstoff* **37**: 99-112.

Fuller, E.N., J.C. Giddings, and **P.D. Schettler.,** (1966)**.** A new method for prediction of binary gas-phase diffusion coefficient. *Jour. of Industrial and engineering Chemistry* **58(5)**: 19-27.

Gefahrt, J., (1977). Zur Spanevorwarmung mit Hochfrequenzenergie-Modell zur Berech nung des Temperaturverlaufes in Vliesmitte bei der Heibpressung. *Holz als Rohund Werkstoff.* **35**: 183-188.

Gibson,L.J, and **M.F.Ashby**., (1997). Cellular Solids: Structure and Properties .Cambridge University Press, Cambridge, UK.

Gupta, A., P.J. Jordan, and **S.Pang.,** (2007). Modelling of the development of the vertical density profile of MDF during hot pressing. Electronic Journal: *Chemical Product and Process Modelling,* BePress. Vol **(2)** Art (1).

Gupta, A., P.J. Jordan, and **S.Pang**., (2006a). Modelling of vertical density profile of MDF in hot pressing. Proc. of CHEMECA 2006 Symp**.** Auckland, N.Z.

Gupta, A., P.J. Jordan, S.Pang, and **K.M.Chapman.,** (2006b). Modelling of hot pressing of MDF. Proc. of 10th European Panel Product Symp. Llandudno, U.K. 265-277**.**

Gupta, A., P.J. Jordan, and **S.Pang.,** (2006c). Development of an Empirical Model for MDF Hot press and Comparison with a Fundamental Model. 8th Pacific Rim Bio-based Composites Symp. KL, Malaysia. 379-389.

Gupta, A., P.J. Jordan, S.Pang, and **K.M.Chapman.,** (2005). Dependence of mechanical properties of MDF panels on the panel density. Proc. of the 2005 joint conference of SCENZ / FEANZ. Symp. Christchurch, N.Z., 6-13.

Hailwood, A.J, and **S. Horrobin**., (1946). Absorption of water by polymers: analysis in terms of a simple model. *Trans. Farady Soc*. **42B**: 84-92

Harless, T.E.G., F. G. Wagner, P.H. Short, R. D. Seale, P.H. Mitchell, and **D. S. Ladd.**, (1987). A model to predict the density profile of particleboard. *Wood Fibre Sci.* **19(1):** 81-92**.**

Haselein, C.R., (1998). Numerical simulation of pressing wood-fibre composites. Ph.D. Thesis, Oregon State univ., U.S.A. 244 pp.

Hata.T., Kawai .S, and **H Sasaki**., (1990). Computer simulation of temperature behaviour in particle mat during hot pressing and steam injection pressing: *Wood Science Technology*: **24**:65-78.

Heebink, B. G., W. F. Lehmann, and **F. V. Hefty**., (1972). Reducing particleboard pressing time: Exploratory study. USDA. Forest Service Research Paper FPL. 180. For. Prod. Lab., Madison, Wisconsin

Hood,J.P., F.A. Kamke and **J.Fuller.,(2005).** Permeability of oriented strand board mats. *For. Prod.J.* **55(12):**194-199**.**

Hubert, P, and **C. Dai**.., (1998). An object-oriented finite element processing model for oriented strand board wood composites. Proc. of the 13th Int. Conf. on Composite Materials, Paris, France.

Hubert, P, and **C. Dai**., (1997). Process modelling for wood-based composites. Part 2. A modular approach to modelling mat consolidation during hot-pressing. Proceedings Forest Products Society Structural Panels Technical Interest Group 51st Annual Meeting, Vancouver, British Columbia, Canada.

Humphrey, P.E., (1991). Pressing issues in panel manufacture: internal behaviour during pressing and its impact on time minimization, properties and profit. *Proc. of the 25th Particleboard and Composite Materials Symp.,* **25:**99-108.

Humphrey, P.E, and **A.J. Bolton**., (1989a). The hot pressing of dry-formed wood based composites. Part II . A simulation model for heat and moisture transfer. *Holzforschung*. **43(3)**: 199- 206.

Humphrey, P.E., (1982). Physical aspects of wood particleboard manufacture. PhD Thesis, Univ. of Wales, U.K.

Kamke, F.A, and **L.J. Casey**., (1988a). Gas pressure and temperature in the mat during flake board's manufacture. *Forest Prod. J*. **38** (3):41-43.

Kamke, F.A, and **L.J. Casey**., (1988b)**.** Fundamentals of flake board manufacture: internal mat conditions. *Forest Prod. J*. **38 (6)**: 38-44.

Kasal, B., (1989). Behavior of wood under transverse compression. MS Thesis, V.P.I & S.U., Blacksburg, VA,USA.

Kavvouras, P.K., (1977). Fundamental process variables in particleboard manufacture. PhD. Thesis, Univ. of Wales, U.K. 156 pp.

Kayihan, F, and **J.A. Johnson**., (1983). Heat and moisture movement in wood composite materials during the pressing operation-a simplified model. *Numerical Methods in heat Transfer* **2**: 511-531.

Kelly,M.W., (1977). *Critical literature review of relationships between processing parameters and physical properties of particleboard,* pp 4-15. Madison: USDA Forest Service.

Kelsey, K. E, and **L.N. Clarke.,** (1956). The heat of sorption of water by wood. *Australian Jour. of Applied. Sci*. **7(2):** 160-175.

Kiran, E, and **R. Iyer**., (1994). Cure behaviour of paper-phenolic composite systems: kinetic modelling. *J. Applied Polymer Science* **51**: 353-364.

Kollmann, F., (1957). Uber den Einflub von Feuchtigkeitsunterschieden im Spangut vor dem Verpressen auf die Eigenschaften von Holzspanplatten. *Holz als Roh-und Werkstoff* **15 (1)**: 35-44.

Kollmann, F., (1959). *Uber die Sorption von Holz und ihre exakte Bestimmung. Holz als Werkstoff* **19(3)**: 73-80.

Krischer,O., (1963). Die wissenschaftlichen Grundlagen der Trocknungstechnik. 2nd ed. Springer- Verlag, Berlin. 491 pp.

Kuhlmann, G., (1962). Untersuchungen der thermischen Eigenschaften von Holz und Spanplatten in Abhangigkeit von Feuchtigkeit und Temperatur im hygroskopischen Bereich. *Holz als Roh-und Werkstoff* **20**: 259-270.

Kunesh, R.H., (1961). The inelastic behaviour of wood: A new concept for improved panel forming processes. *Forest Prod. J.* **11(9)**: 395-406.

Lang, E.M., and **M.P.Wolcott.,**(1996). A model for viscoelastic consolidation of wood strands mats: Part two: Static stress-strain behaviour of the mat. *Wood and Fibre Science.* **28(3):**369-379.

Maiti, S. K., L.J.Gibson, and **M.F.Ashby.,** (1984). Deformation and energy absorption diagrams for cellular solids. *Acta Metall*. **32(11):**1963-1975.

Maksimov,R.D, V.P.Mocahlov, and **Y.S.Urzhumstev**., (1971). Time-moisture superposition. *Mekhanika Polimerov* 5780-786.

Maksimov,R.D, E.A.Sokolov, and **V.P.Mochalov**., (1974). Effect of temperature and moisture on the creep of polymeric materials. Part I .One-dimensional extension under stationary temperature-moisture conditions. *Mekhanika Polimerov* **3**:393-399.

Maksimov,R.D, V.P.Mochalov, and **E.A.Sokolov**., (1975). Influence of temperature and humidity on the creep of polymer materials.Part 3.Shear,and shear and tensile strain acting together. *Mekhanika Polimerov* **4**:627-632.

Maksimov,R.D, V.P.Mochalov, and **E.A.Sokolov**., (1976). Influence of temperature and humidity on the creep of polymer materials.Part *IV* .Prediction on the basis of field test result. *Mekhanika Polimerov* **6**:982-987.

Maku,T, and **R.Hamada**., (1955). Studies on the chipboard. Part I. Mechanical properties. *Wood Research* **15**:38-52.

Meinecke, E. A, and **R.C.Clark**., (1973). Mechanical Properties of Polymeric Foams. Technomic Publishing Co., Westport, USA.

Munson, B.R, D.F.Young, and **T.H.Okiishi**., (1990). Fundamentals of fluid mechanics. Wiley, New York. 843 pp.

Nasrallah,S.B, and **P. Perre.,** (1998). Detailed study of a model of heat and mass transfer duringconvective drying of porous media. *Int. J. Heat Mass Transfer* **31(5):** 957-967.

Palka, L.C., (1973). Predicting the effect of specific gravity, moisture content, temperature and strain rate on the elastic properties of softwoods. *Wood Science and Technology* **7**: 127-141.

Pang, S., (1997). Some considerations in simulation of superheated steam drying of softwood lumber. *Drying Technology .15(2):* 651-670.

Raczkowski,J., (1969). Der Einflub von Feuchtigkeitsanderungen auf das Kriechverhalten des Holzes. *Holz als Roh-und Werkstoff* **27(6):** 232-237.

Rauch,W., (1984). Temperature und Dampfdruckverlauf bei der Herstellung von Spanplatten und ihr Einflub auf die technologischen Eigenschaften *Holz als Roh und Werkstoff* **42:** 281-286

Ren, S., (1991). Thermo- hygro rheological behaviour of materials used in the manufacture of wood-based composites. PhD. Thesis, Oregon State Univ., U.S.A. 226 pp.

Resch, H, **M.L. Hoag,** and **H.N. Rosen**., (1988): Desorption of yellow-poplar in superheated steam. *Forest Products Journal* **38(3)**: 13-18 .

Rusch, K.C., (1969). Load compression behaviour of flexible foams. *Journal of Applied Polymer Science* **13**:2297-2311.

Schulte, M, and **A. Fruhwald**., (1996). Some investigations concerning density profile, internal bond and relating failure of particleboard. *Holz als Roh-und Werkstoff* **54**; 289-294.

Scott, E.P., (1989). Estimation of the thermal and kinetic properties associated with carbon/ epoxy composite materials during curing. PhD Dissertation Michigan State University. USA.

Shao, M., (1989). Thermal properties of wood fibre networks. M.S. thesis, Oregon State Univ., U.S.A. 95 pp.

Siau, J.F., (1984). Transport processes in wood. Syracuse Univ. Press, New York. 245 pp.

Simpson, W.T., (1973). Predicting equilibrium moisture content of wood by mathematical models. *Wood fibre Sc*. **5(1):** 41-49.

Simpson, W.T, and **H.N.Rosen**., (1981). Equilibrium moisture content of wood at high temperatures. *Wood and Fibre Sci*. **13(3):** 150-158.

Skaar, C., (1972). Water in wood, Syracuse Univ. Press, New York. 218 pp.

Smith, D. C., (1982). Waferboard press closing strategies. *Forest Prod. J.* **32(3):**40-45.

Strickler,M.D., (1968). High temperature moisture relations of grand fir. *Forest Products Journal* **18(4):** 69-75.

Strickler, M.D., (1959). Effect of press cycles and moisture content on properties of Douglas-fir flakeboards. *Forest Prod.J*. **9(7):**203-215.

Suchsland, O., (1967). Behaviour of a particleboard mat during the press cycle. *Forest Prod.J.* **17 (2)**: 51-57.

Suo, S, and **J. L. Bowyer.**, (1994). Simulation modelling of particleboard density profile. *Wood Fibre Sci*. **26(3):** 397-411.

Thomen, H., (2000). Modelling the physical processes in natural fibre composites during batch and continuous pressing. PhD Dissertation, Oregon State University, USA.

Thomen, H, and **P.E. Humphrey**., (2001). Computer simulation of the continuous hot pressing process of wood-based composites: A tool for industrial and research applications. *Proceedings 3rd European Wood-Based Panel Symposium*. 1-13.

USDA Forest Products Laboratory. (1999). Wood handbook. Wood as an Engineering Material. Forest Products Society, Madison, Wisconsin (USA).

Vonhass,G., (1998). Untersuchungen zur Heibpressung von Holzwerkstoffmatten unter besonderer Berucksichtigung des Verdichtungsverhaltens der permeabilitat, der Temperaturleitfahigkeit und der Sorptionsgeschwinddigkeit. Dissertation, Univ, Hamburg, Germany. 264 pp.

Wang, S., (1992)**.** Compare the hot pressing technology of wood based panel. *Building Particleboard* **(3):**25-29 (in Chinese).

Wang, S and **P. M. Winistorfer**., (2000). Fundamentals of vertical density profile formation in wood composites Part II. Methodology of vertical density formation under dynamic conditions. *Wood Fibre Science* **32(2)**: 220-238.

Wang, S, P.M.Winistorfer, T.M. Young, and **C.M.Helton**., (2000a). Step closing pressing of medium density fibreboard. Part I. Influence on the vertical density profile. *Holz als Roh und Werkstoff*.**59**: 19-26.

Wang, S, P.M.Winistorfer, and **T.M. Young.,** (2004). Fundamentals of vertical density profile formation in wood composites. Part III. MDF density formation during hot-pressing. *Wood and Fibre Science* **36(1)**:17-25.

Winistorfer, P.M., (1992). Pressing strategies. *Proc. National Particleboard Association Pressline Technology Seminars,* Charlotte, N.C. pp 19-25.

Wolcott, M.P., (1989). Modeling viscoelastic cellular materials for the pressing of wood composites..PhD Dissertation,V.P.I & S.U.,Blacksburg,VA,USA.

Xu, W, and **P.M. Winistorfer**., (1995). Layer thickness swells and layer internal bond of medium density fibreboard and oriented strand board. *Forest Prod.J.* **45(10):**67-71.

Yin,S., (1994). Carcterization par analyses thermiques de la polycondensation d'adhesives aminoplastes et du durcissement de composites models bois-adhesif. Dissertation, Universite de Nancy I, France.

Zombori, B.G., (2001). Modelling the transient effects during the hot pressing of wood based composites. PhD Dissertation, Virginia Polytechnic Institute and State University, USA.